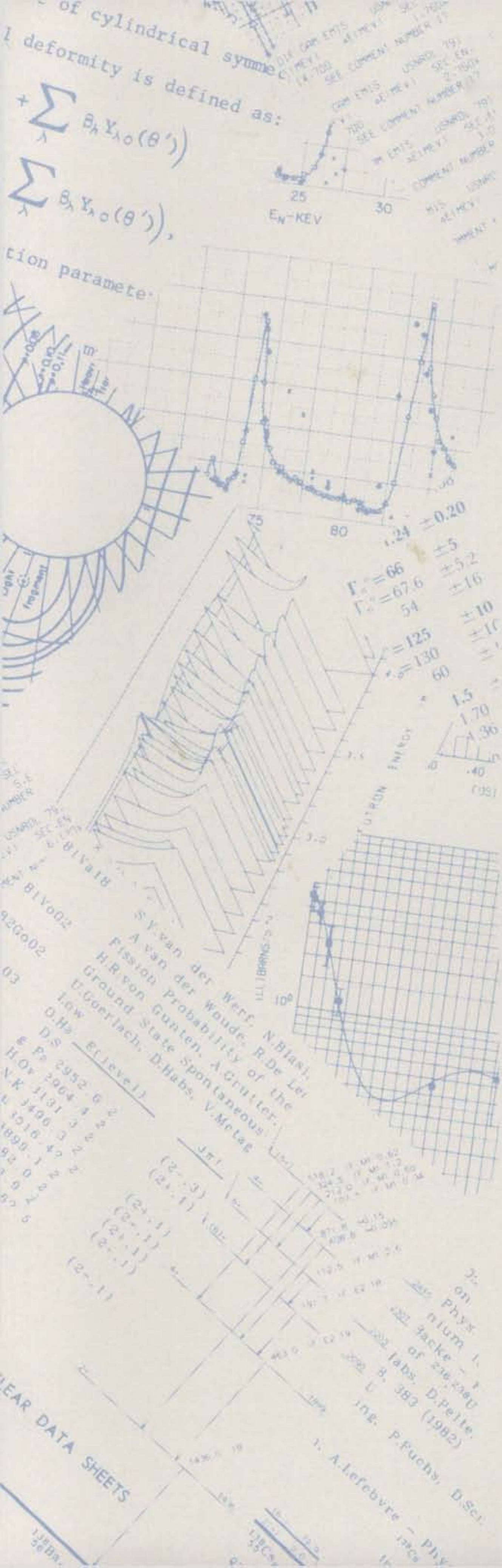

BNL-NCS-42382
DOE/NDC-49/U
NEANDC(US)-227/U
INDC(USA)-102/L
INFORMAL REPORT
LIMITED DISTRIBUTION

REPORTS TO THE DOE NUCLEAR DATA COMMITTEE

Compiled by the
NATIONAL NUCLEAR DATA CENTER
for the
U.S. Department of Energy
Nuclear Data Committee

April 1989

BROOKHAVEN NATIONAL LABORATORY
ASSOCIATED UNIVERSITIES, INC.
UPTON, LONG ISLAND, NEW YORK 11973

national
nuclear
data
Center

BNL-NCS-42382
DOE/NDC-49/U
NEANDC(US)-227/U
INDC(USA)-102/L
Informal Report
Limited Distribution

REPORTS TO

THE DOE NUCLEAR DATA COMMITTEE

APRIL 1989

national
nuclear
data
center

Compiled by the

NATIONAL NUCLEAR DATA CENTER
BROOKHAVEN NATIONAL LABORATORY
ASSOCIATED UNIVERSITIES, INC.

UNDER CONTRACT NO. DE-AC02-76CH00016 WITH THE
UNITED STATES DEPARTMENT OF ENERGY

Printed in the United States of America
Available from
National Technical Information Service
U.S. Department of Commerce
5285 Port Royal Road
Springfield, VA 22161

NTIS price codes:
Printed Copy: A10; Microfiche Copy: A01

PREFACE

The reports in this document were submitted to the Department of Energy Nuclear Data Committee (DOE-NDC) in April, 1989. The reporting laboratories are those with a substantial program for the measurement of neutron and nuclear cross sections of relevance to the U.S. applied nuclear energy program.

The authors of the Status Report contributions are responsible for collecting and editing individual contributions from their laboratory and are not necessarily the sole authors of the contributions. The scientists responsible for the work described in each individual contribution are listed at the beginning of the contribution.

The material contained in these reports is to be regarded as comprised of informal statements of recent developments and preliminary data. Persons wishing to make use of these data should contact the individual experimenter for further details. *The data which appear in this document should be quoted only by permission of the contributor and should be referenced as private communication, and not by this document number.* Appropriate subjects are listed as follows:

1. **Microscopic neutron cross sections** relevant to the nuclear energy program, including shielding. Inverse reactions, where pertinent, are included.

2. **Charged-particle cross sections**, where they are relevant to (1.) above, and where relevant to developing and testing nuclear models.

3. **Gamma ray production, radioactive decay, and theoretical developments** in nuclear structure which are applicable to nuclear energy programs.

4. **Proton and α-particle cross sections**, at energies of up to 1 GeV, which are of interest to the space program.

These reports cannot be regarded as a complete summary of the nuclear research efforts in the U.S. A number of laboratories whose research is less programmatically oriented do not submit reports; neither do the submitted reports reflect all the work related to nuclear data in progress at the submitting laboratory.

This compilation has been produced almost completely from master copies prepared by the individual contributors listed in the Table of Contents, and reports are reproduced *without change* from these master copies.

The CINDA-type index which follows the Table of Contents was prepared by Norman E. Holden and Alyce Daly of the National Nuclear Data Center, Brookhaven National Laboratory, Upton, Long Island, New York.

TABLE OF CONTENTS

NEUTRON DATA REFERENCES

Element	Quantity	Energy (eV) Min	Max	Type	Documentation Ref	Page	Date	Lab	Comments
^{1}H	Evaluation		2.0+7	Eval	DOE-NDC-49	112	Apr89	LAS	Young+ NDG. ENDF/B-VI.
^{1}H	$\sigma_{el}(\theta)$	NDG		Revw	DOE-NDC-49	132	Apr89	NBS	Carlson+ NDG. ENDF/B-VI Status RPT.
^{2}H	σ_{pol}	5.0+6	8.0+6	Expt	DOE-NDC-49	174	Apr89	TNL	Howell+ NDG. TBC.
^{2}H	$\sigma_{n,2n}$	1.2+7		Expt	DOE-NDC-49	174	Apr89	TNL	Howell+ NDG. TBC.
^{3}He	Evaluation		2.0+7	Eval	DOE-NDC-49	112	Apr89	LAS	Young+ NDG. ENDF/B-VI.
^{3}He	$\sigma_{n,p}$	1.0+0	7.5+5	Expt	DOE-NDC-49	131	Apr89	NBS	Behrens+ NDG. TBC.
^{3}He	$\sigma_{n,p}$	NDG		Revw	DOE-NDC-49	132	Apr89	NBS	Carlson+ NDG. ENDF/B-VI Status RPT.
^{6}Li	Evaluation		2.0+7	Eval	DOE-NDC-49	112	Apr89	LAS	Young+ NDG. ENDF/B-VI.
^{6}Li	$\sigma_{n,t}$	NDG		Revw	DOE-NDC-49	132	Apr89	NBS	Carlson+ NDG. ENDF/B-VI Status RPT.
^{7}Li	Evaluation		2.0+7	Eval	DOE-NDC-49	112	Apr89	LAS	Young+ NDG. ENDF/B-VI.
^{9}Be	Evaluation	NDG		Eval	DOE-NDC-49	14	Apr89	ANL	Sugimoto+ NDG. ENDF/B-VI. TBC.
^{9}Be	σ_{tot}	1.0+6	1.0+7	Expt	DOE-NDC-49	1	Apr89	ANL	Sugimoto+ NDG.
^{9}Be	σ_{el}	4.5+6	1.0+7	Expt	DOE-NDC-49	1	Apr89	ANL	Sugimoto+ NDG.
^{9}Be	$\sigma_{el}(\theta)$	4.5+6	1.0+7	Expt	DOE-NDC-49	1	Apr89	ANL	Sugimoto+ GRPH.
^{9}Be	σ_{inl}	4.5+6	1.0+7	Expt	DOE-NDC-49	1	Apr89	ANL	Sugimoto+ NDG.
^{9}Be	$\sigma_{dif.inl}$	4.5+6	1.0+7	Expt	DOE-NDC-49	1	Apr89	ANL	Sugimoto+ NDG.
^{9}Be	$\sigma_{n,X}$	4.5+6	1.0+7	Expt	DOE-NDC-49	1	Apr89	ANL	Sugimoto+ NDG.
^{9}Be	$\sigma_{n,X\gamma}$	2.0+6	1.0+8	Expt	DOE-NDC-49	183	Apr89	LAS	Gould+ NDG.
^{9}Be	$\sigma_{n,2n}$	NDG		Expt	DOE-NDC-49	172	Apr89	AI	Kneff+ NDG. TBD.
^{9}Be	$\sigma_{n,2n}$		8.0+6	Eval	DOE-NDC-49	162	Apr89	OHO	Knox+ NDG. R-MATRIX CALC.
^{10}B	Evaluation		2.0+7	Eval	DOE-NDC-4	110	Apr89	LAS	Young+ NDG. ENDF/B-VI.
^{10}B	$\sigma_{el}(\theta)$	8.0+6	2.6+7	Theo	DOE-NDC-4	118	Apr89	LRL	Hansen+ NDG.
^{10}B	$\sigma_{el}(\theta)$	3.0+6	1.2+7	Expt	DOE-NDC-4	113	Apr89	OHO	Sadowski+ NDG.
^{10}B	σ_{pol}	8.0+6	2.6+7	Theo	DOE-NDC-4	118	Apr89	LRL	Hansen+ NDG.
^{10}B	$\sigma_{dif.inl}$	3.0+6	1.2+7	Expt	DOE-NDC-4	113	Apr89	OHO	Sadowski+ NDG.
^{10}B	$\sigma_{n,X\gamma}$	1.0+5	2.5+7	Expt	DOE-NDC-4	114	Apr89	ORL	Dickens+ NDG.
^{10}B	$\sigma_{n,\alpha}$	1.0+5	3.0+6	Expt	DOE-NDC-4	118	Apr89	ORL	Schrack+ NDG. ORL+NBS.
^{10}B	$\sigma_{n,\alpha}$	NDG		Revw	DOE-NDC-4	110	Apr89	NBS	Carlson+ NDG. ENDF/B-VI Status RPT.
^{11}B	Evaluation		2.0+7	Eval	DOE-NDC-4	110	Apr89	LAS	Young+ NDG. ENDF/B-VI.
^{11}B	$\sigma_{el}(\theta)$	8.0+6	2.6+7	Theo	DOE-NDC-4	118	Apr89	LRL	Hansen+ NDG.
^{11}B	σ_{pol}	8.0+6	2.6+7	Theo	DOE-NDC-4	118	Apr89	LRL	Hansen+ NDG.
^{11}B	$\sigma_{n,\gamma}$	NDG		Expt	DOE-NDC-4	115	Apr89	KTY	.NDG. TBD.
^{11}B	$\sigma_{n,X\gamma}$	1.0+5	2.5+7	Expt	DOE-NDC-4	114	Apr89	ORL	Dickens+ NDG.

NEUTRON DATA REFERENCES

Element	Quantity	Energy (eV) Min	Max	Type	Documentation Ref	Page	Date	Lab	Comments
^{12}C	$\sigma_{n,p}$	5.0+7	2.5+8	Expt	DOE-NDC-49	38	Apr89	LAS	Sorenson+ NDG. 0-15 DEGS.
^{12}C	$\sigma_{n,p}$	5.0+7	2.5+8	Expt	DOE-NDC-49	182	Apr89	LAS	Howell+ NDG. TBD.
^{12}C	$\sigma_{n,d}$	5.6+7	6.5+7	Expt	DOE-NDC-49	37	Apr89	DAV	Romero+ NDG. 0-90 DEGS.
^{12}C	$\sigma_{n,\alpha}$		3.0+7	Expt	DOE-NDC-49	167	Apr89	LAS	Pedroni+ NDG.TBD.
^{12}C	$\sigma_{\alpha,emis}$		5.0+7	Expt	DOE-NDC-49	106	Apr89	LAS	Haight+ NDG.
^{12}C	$\sigma_{p,emis}$	5.0+7	2.5+8	Expt	DOE-NDC-49	106	Apr89	LAS	Ullmann+ NDG.
^{12}C	$\sigma_{p,emis}$	5.0+7	2.5+8	Expt	DOE-NDC-49	167	Apr89	LAS	Sorenson+ NDG. ANG. 0-15 DEGREE.
^{13}C	$\sigma_{el}(\theta)$	4.5+6	1.1+7	Expt	DOE-NDC-49	155	Apr89	OHO	Resler+ NDG.
^{13}C	$\sigma_{dif.inl}$	4.5+6	1.1+7	Expt	DOE-NDC-49	155	Apr89	OHO	Resler+ NDG.
^{13}C	$\sigma_{dif.inl}$	NDG		Expt	DOE-NDC-49	155	Apr89	OHO	O'Donnell+ NDG. TBC.
^{13}C	$\sigma_{n,p}$	5.0+7	2.5+8	Expt	DOE-NDC-49	38	Apr89	LAS	Sorenson+ NDG. 0-15 DEGS.
^{13}C	$\sigma_{n,p}$	5.0+7	2.5+8	Expt	DOE-NDC-49	182	Apr89	LAS	Howell+ NDG. TBD.
^{13}C	$\sigma_{n,\alpha}$	4.5+6	1.1+7	Expt	DOE-NDC-49	155	Apr89	OHO	Resler+ NDG.
^{13}C	Res.Params.	1.5+5		Theo	DOE-NDC-49	11	Apr89	ANL	Lynn+ WG(153 KEV RES) CALC.
^{13}C	$\sigma_{p,emis}$	5.0+7	2.5+8	Expt	DOE-NDC-49	106	Apr89	LAS	Ullmann+ GRPH. P-SPECTRA.
^{13}C	$\sigma_{p,emis}$	5.0+7	2.5+8	Expt	DOE-NDC-49	167	Apr89	LAS	Sorenson+ NDG. ANG. 0-15 DEGREE.
^{14}C	$\sigma_{n,p}$	6.5+7		Expt	DOE-NDC-49	36	Apr89	DAV	Drummond+ NDG. 0-40 DEGS.
N	$\sigma_{\alpha,emis}$	1.4+7	1.5+7	Expt	DOE-NDC-4	110	Apr89	AI	Kneff+ NDG. TBD.
^{14}N	$\sigma_{n,X\gamma}$	1.4+7		Theo	DOE-NDC-49	78	Apr89	LRL	Resler+ NDG. TBC.
^{14}N	$\sigma_{n,p}$	6.1-2	3.5+4	Expt	DOE-NDC-49	101	Apr89	LAS	Koehler+ GRPH. CFD. OTHER EXPT.
^{16}O	$\sigma_{dif.inl}$	2.0+7	2.6+7	Eval	DOE-NDC-49	163	Apr89	OHO	Mellema+ NDG.
^{20}Ne	Evaluation		3.0+7	Theo	DOE-NDC-49	82	Apr89	LRL	MacGregor+ STAT. MDL. CALC.
^{20}Ne	$\sigma_{n,\alpha}$	1.0+6	1.0+7	Theo	DOE-NDC-49	82	Apr89	LRL	MacGregor+ CALC. CFD. EXPT.
^{22}Na	$\sigma_{n,p}$	2.5-2	3.5+4	Expt	DOE-NDC-49	100	Apr89	LAS	Koehler+ GRPH. REACTION RATE.
^{22}Na	$\sigma_{n,\alpha}$	2.5-2	3.5+4	Expt	DOE-NDC-49	100	Apr89	LAS	Koehler+ GRPH. REACTION RATE.
Mg	$\sigma_{\alpha,emis}$	1.4+7	1.5+7	Expt	DOE-NDC-4	110	Apr89	AI	Kneff+ NDG. TBD.
^{24}Mg	$\sigma_{n,p}$		1.0+7	Expt	DOE-NDC-49	9	Apr89	ANL	Smith+ NDG. TBP. ANE.
^{27}Al	$\sigma_{n,\alpha}$		1.0+7	Expt	DOE-NDC-49	9	Apr89	ANL	Smith+ NDG. TBP. ANE.
^{27}Al	$\sigma_{\alpha,emis}$		5.0+7	Expt	DOE-NDC-49	106	Apr89	LAS	Haight+ NDG.
^{27}Al	$\sigma_{d,emis}$		5.0+7	Expt	DOE-NDC-49	106	Apr89	LAS	Haight+ NDG.
^{27}Al	$\sigma_{p,emis}$		5.0+7	Expt	DOE-NDC-49	106	Apr89	LAS	Haight+ NDG.
^{28}Si	$\sigma_{el}(\theta)$	8.0+6	2.6+7	Theo	DOE-NDC-49	90	Apr89	LRL	Hansen+ NDG.
^{28}Si	$\sigma_{el}(\theta)$	8.0+6	4.0+7	Eval	DOE-NDC-49	178	Apr89	TNL	Howell+ NDG.

NEUTRON DATA REFERENCES

Element	Quantity	Energy (eV) Min	Max	Type	Documentation Ref	Page	Date	Lab	Comments
^{28}Si	σ_{pol}	8.0+6	2.6+7	Theo	DOE-NDC-49	90	Apr89	LRL	Hansen+ NDG.
^{28}Si	σ_{pol}	8.0+6	4.0+7	Eval	DOE-NDC-49	178	Apr89	TNL	Howell+ NDG.
^{28}Si	$\sigma_{dif.inl}$	8.0+6	4.0+7	Eval	DOE-NDC-49	178	Apr89	TNL	Howell+ NDG.
S	$\sigma_{\alpha,emis}$	1.4+7	1.5+7	Expt	DOE-NDC-4	110	Apr89	AI	Kneff+ NDG. TBD.
^{32}S	$\sigma_{el}(\theta)$	8.0+6	4.0+7	Eval	DOE-NDC-49	178	Apr89	TNL	Howell+ NDG. TBD.
^{32}S	σ_{pol}	8.0+6	4.0+7	Eval	DOE-NDC-49	178	Apr89	TNL	Howell+ NDG. TBD.
^{32}S	$\sigma_{dif.inl}$	8.0+6	4.0+7	Eval	DOE-NDC-49	178	Apr89	TNL	Howell+ NDG. TBD.
^{32}S	$\sigma_{n,p}$	NDG		Expt	DOE-NDC-49	127	Apr89	ANL	Smith+ NDG. TBD. ANL+MHG.
^{32}S	$\sigma_{n,p}$		5.0+6	Eval	DOE-NDC-49	152	Apr89	ORL	Fu+ NDG.
^{40}Ar	σ_{tot}	1.0+4	5.0+7	Expt	DOE-NDC-49	146	Apr89	ORL	Winters+ NDG.
^{40}Ar	$\sigma_{n,\gamma}$		1.5+5	Expt	DOE-NDC-49	137	Apr89	ORL	Macklin+ CS (30 KEV)=2.79 MB.
^{40}Ar	$<\Gamma>/D$		1.5+6	Expt	DOE-NDC-49	146	Apr89	ORL	Winters+ S0,S1,S2 GIVEN.
^{40}Ca	σ_{tot}	2.5+6	8.0+7	Theo	DOE-NDC-49	145	Apr89	ORL	Johnson+ NDG.
^{40}Ca	σ_{el}	NDG		Expt	DOE-NDC-49	12	Apr89	ANL	Lynn+ NDG. COH. SCATT.LENGTHS.
^{40}Ca	$\sigma_{el}(\theta)$	2.3+6	8.0+6	Expt	DOE-NDC-49	52	Apr89	KTY	Hicks+ NDG.
^{40}Ca	$\sigma_{el}(\theta)$	5.3+6	4.0+7	Theo	DOE-NDC-49	145	Apr89	ORL	Johnson+ NDG.
^{40}Ca	σ_{pol}	9.9+6	1.7+7	Theo	DOE-NDC-49	145	Apr89	ORL	Johnson+ NDG.
^{40}Ca	$\sigma_{dif.inl}$	2.3+6	8.0+6	Expt	DOE-NDC-49	52	Apr89	KTY	Hicks+ NDG.
^{42}Ca	σ_{el}	NDG		Expt	DOE-NDC-49	12	Apr89	ANL	Lynn+ NDG. COH. SCATT.LENGTHS.
^{43}Ca	σ_{el}	NDG		Expt	DOE-NDC-49	12	Apr89	ANL	Lynn+ NDG. COH. SCATT.LENGTHS.
^{43}Ca	$\sigma_{n,\gamma}$	NDG		Theo	DOE-NDC-49	12	Apr89	ANL	Lynn+ NDG.
^{44}Ca	σ_{el}	NDG		Expt	DOE-NDC-49	12	Apr89	ANL	Lynn+ NDG. COH. SCATT.LENGTHS.
^{48}Ca	σ_{el}	NDG		Expt	DOE-NDC-49	12	Apr89	ANL	Lynn+ NDG. COH. SCATT.LENGTHS.
^{48}Ca	$\sigma_{el}(\theta)$	2.3+6	8.0+6	Expt	DOE-NDC-49	52	Apr89	KTY	Hicks+ NDG.
^{48}Ca	$\sigma_{dif.inl}$	2.3+6	8.0+6	Expt	DOE-NDC-49	52	Apr89	KTY	Hicks+ NDG.
^{48}Ca	$\sigma_{n,n'\gamma}$	NDG		Expt	DOE-NDC-49	64	Apr89	KTY	Vanhoy+. NDG. TBC.
^{45}Sc	$\sigma_{dif.inl}$	NDG		Expt	DOE-NDC-49	5	Apr89	ANL	Guenther+ NDG. DOUB. DIFF.
^{50}V	$\sigma_{n,2n}$	1.4+7		Expt	DOE-NDC-49	10	Apr89	ANL	Greenwood+ CS=258+39 MB.
^{51}V	Evaluation	NDG		Eval	DOE-NDC-49	14	Apr89	ANL	Smith+ NDG. ENDF/B-VI.
^{51}V	σ_{tot}		2.0+7	Theo	DOE-NDC-49	3	Apr89	ANL	Lawson+ NDG.
^{51}V	$\sigma_{el}(\theta)$	8.0+6		Expt	DOE-NDC-49	1	Apr89	ANL	Smith+ NDG. SIG. RATIOS,20-160 DEGS.
^{51}V	$\sigma_{el}(\theta)$	4.5+6	1.0+7	Expt	DOE-NDC-49	3	Apr89	ANL	Lawson+ NDG.
^{51}V	$\sigma_{dif.inl}$	4.5+6	1.0+7	Expt	DOE-NDC-49	3	Apr89	ANL	Lawson+ NDG.

NEUTRON DATA REFERENCES

Element	Quantity	Energy (eV) Min	Max	Type	Documentation Ref	Page	Date	Lab	Comments
^{51}V	$\sigma_{dif.inl}$	NDG		Expt	DOE-NDC-49	5	Apr89	ANL	Guenther+ NDG. DOUB. DIFF.
^{51}V	$\sigma_{n,n'\gamma}$	3.0+6	3.0+7	Theo	DOE-NDC-49	80	Apr89	LRL	Blann. NDG. HIGH EG GAM.SPECT.
Cr	$\sigma_{el}(\theta)$	8.0+6		Expt	DOE-NDC-4	111	Apr89	ANL	Smith+ NDG. SIG. RATIOS,20-160 DEGS.
Cr	$\sigma_{el}(\theta)$		1.0+7	Expt	DOE-NDC-4	114	Apr89	ANL	Smith+ NDG. TBC.
Cr	$\sigma_{dif.inl}$		1.0+7	Expt	DOE-NDC-4	114	Apr89	ANL	Smith+ NDG. TBC.
^{50}Cr	Evaluation	NDG		Eval	DOE-NDC-49	152	Apr89	ORL	Hetrick+ NDG. ENDF/B-VI.
^{52}Cr	Evaluation	NDG		Eval	DOE-NDC-49	152	Apr89	ORL	Hetrick+ NDG. ENDF/B-VI.
^{53}Cr	Evaluation	NDG		Eval	DOE-NDC-49	152	Apr89	ORL	Hetrick+ NDG. ENDF/B-VI.
^{53}Cr	$\sigma_{n,n'\gamma}$		1.0+7	Expt	DOE-NDC-49	137	Apr89	ORL	Larson+ NDG.
^{54}Cr	Evaluation	NDG		Eval	DOE-NDC-49	152	Apr89	ORL	Hetrick+ NDG. ENDF/B-VI.
Fe	$\sigma_{el}(\theta)$		1.0+7	Expt	DOE-NDC-4	114	Apr89	ANL	Smith+ NDG. TBC.
Fe	$\sigma_{dif.inl}$		1.0+7	Expt	DOE-NDC-4	114	Apr89	ANL	Smith+ NDG. TBC.
Fe	$\sigma_{n,n'\gamma}$	3.0+6	3.0+7	Theo	DOE-NDC-4	118	Apr89	LRL	Blann. GRPH. CFD. EXPT.
Fe	$\sigma_{n,X\gamma}$	7.0+5	4.0+8	Expt	DOE-NDC-4	114	Apr89	LAS	Nelson+ NDG.
^{54}Fe	Evaluation	NDG		Eval	DOE-NDC-49	152	Apr89	ORL	Hetrick+ NDG. ENDF/B-VI.
^{54}Fe	σ_{tot}	5.0+5	2.0+7	Eval	DOE-NDC-49	179	Apr89	TNL	Howell+ NDG. ENERGY DEP. OPT.POT.
^{54}Fe	$\sigma_{el}(\theta)$	8.0+6	2.6+7	Theo	DOE-NDC-49	90	Apr89	LRL	Hansen+ NDG.
^{54}Fe	$\sigma_{el}(\theta)$	5.0+5	2.0+7	Eval	DOE-NDC-49	179	Apr89	TNL	Howell+ NDG. ENERGY DEP. OPT.POT.
^{54}Fe	σ_{pol}	8.0+6	2.6+7	Theo	DOE-NDC-49	90	Apr89	LRL	Hansen+ NDG.
^{54}Fe	σ_{pol}	5.0+5	2.0+7	Eval	DOE-NDC-49	179	Apr89	TNL	Howell+ NDG. ENERGY DEP. OPT.POT.
^{54}Fe	$\sigma_{dif.inl}$	5.0+5	2.0+7	Eval	DOE-NDC-49	179	Apr89	TNL	Howell+ NDG. ENERGY DEP. OPT.POT.
^{54}Fe	$\sigma_{n,X\gamma}$	7.0+5	4.0+8	Expt	DOE-NDC-49	106	Apr89	LAS	Nelson+ NDG. TBD.
^{54}Fe	$\sigma_{n,np}$	8.0+6	1.4+7	Expt	DOE-NDC-49	159	Apr89	OHO	Saraf+ NDG.
^{54}Fe	$\sigma_{n,n\alpha}$	8.0+6	1.4+7	Expt	DOE-NDC-49	159	Apr89	OHO	Saraf+ NDG.
^{54}Fe	$\sigma_{p,emis}$	6.5+7		Expt	DOE-NDC-49	37	Apr89	DAV	McEachern+ NDG. 0-60 DEGS.
^{56}Fe	Evaluation	NDG		Eval	DOE-NDC-49	152	Apr89	ORL	Hetrick+ NDG. ENDF/B-VI.
^{56}Fe	$\sigma_{n,np}$	8.0+6	1.4+7	Expt	DOE-NDC-49	159	Apr89	OHO	Saraf+ NDG.
^{56}Fe	$\sigma_{n,n\alpha}$	8.0+6	1.4+7	Expt	DOE-NDC-49	159	Apr89	OHO	Saraf+ NDG.
^{57}Fe	Evaluation	NDG		Eval	DOE-NDC-49	152	Apr89	ORL	Hetrick+ NDG. ENDF/B-VI.
^{58}Fe	Evaluation	NDG		Eval	DOE-NDC-49	152	Apr89	ORL	Hetrick+ NDG. ENDF/B-VI.
^{59}Co	Evaluation	NDG		Eval	DOE-NDC-49	14	Apr89	ANL	Guenther+ NDG. ENDF/B-VI.
^{59}Co	$\sigma_{el}(\theta)$	8.0+6		Expt	DOE-NDC-49	1	Apr89	ANL	Smith+ NDG. SIG. RATIOS,20-160 DEGS.
^{58}Ni	Evaluation	6.5+5	2.0+7	Eval	DOE-NDC-49	15	Apr89	ANL	Smith+ NDG. ENDF/B-VI. TBC.

NEUTRON DATA REFERENCES

Element	Quantity	Energy (eV) Min	Max	Type	Documentation Ref	Page	Date	Lab	Comments
^{58}Ni	Evaluation	NDG		Eval	DOE-NDC-49	152	Apr89	ORL	Hetrick+ NDG. ENDF/B-VI.
^{58}Ni	σ_{tot}	1.0+2	2.0+7	Expt	DOE-NDC-49	137	Apr89	ORL	Perey+ NDG.
^{58}Ni	$\sigma_{el}(\theta)$	8.0+6		Expt	DOE-NDC-49	1	Apr89	ANL	Smith+ NDG. SIG. RATIOS,20-160 DEGS.
^{58}Ni	$\sigma_{el}(\theta)$	8.0+6	2.6+7	Theo	DOE-NDC-49	90	Apr89	LRL	Hansen+ GRPHS. CFD. EXPT.
^{58}Ni	$\sigma_{el}(\theta)$	1.0+4	5.0+6	Expt	DOE-NDC-49	137	Apr89	ORL	Perey+ NDG.
^{58}Ni	σ_{pol}	8.0+6	2.6+7	Theo	DOE-NDC-49	90	Apr89	LRL	Hansen+ GRPHS. CFD. EXPT.
^{58}Ni	$\sigma_{dif.inl}$		1.0+7	Expt	DOE-NDC-49	3	Apr89	ANL	Smith+ NDG. ANALYSIS TBD.
^{58}Ni	$\sigma_{n,\gamma}$	2.5+3	5.0+6	Expt	DOE-NDC-49	137	Apr89	ORL	Perey+ NDG.
^{58}Ni	Res.Params.	5.0+3	8.1+5	Expt	DOE-NDC-49	137	Apr89	ORL	Perey+ NDG.
^{58}Ni	$<\Gamma>/D$	NDG		Expt	DOE-NDC-49	137	Apr89	ORL	Perey+ S0=(3.1+-0.6)E-4.
^{60}Ni	Evaluation	NDG		Eval	DOE-NDC-49	152	Apr89	ORL	Hetrick+ NDG. ENDF/B-VI.
^{61}Ni	Evaluation	NDG		Eval	DOE-NDC-49	152	Apr89	ORL	Hetrick+ NDG. ENDF/B-VI.
^{62}Ni	Evaluation	NDG		Eval	DOE-NDC-49	152	Apr89	ORL	Hetrick+ NDG. ENDF/B-VI.
^{64}Ni	Evaluation	NDG		Eval	DOE-NDC-49	152	Apr89	ORL	Hetrick+ NDG. ENDF/B-VI.
Cu	$\sigma_{el}(\theta)$	8.0+6		Expt	DOE-NDC-4	111	Apr89	ANL	Smith+ NDG. SIG. RATIOS,20-160 DEGS.
^{63}Cu	Evaluation	NDG		Eval	DOE-NDC-4	110	Apr89	ORL	Hetrick+ NDG. ENDF/B-VI.
^{65}Cu	Evaluation	NDG		Eval	DOE-NDC-4	110	Apr89	ORL	Hetrick+ NDG. ENDF/B-VI.
Zn	$\sigma_{el}(\theta)$	8.0+6		Expt	DOE-NDC-4	111	Apr89	ANL	Smith+ NDG. SIG. RATIOS,20-160 DEGS.
Ge	$\sigma_{\alpha,emis}$	1.4+7	1.5+7	Expt	DOE-NDC-4	110	Apr89	AI	Kneff+ NDG. TBD.
^{86}Kr	σ_{tot}		2.5+7	Theo	DOE-NDC-49	146	Apr89	ORL	Johnson+ NDG.
^{86}Kr	σ_{tot}	1.5+4	2.5+7	Expt	DOE-NDC-49	147	Apr89	ORL	Carlton+ NDG.
^{86}Kr	Lvl Density		1.0+6	Eval	DOE-NDC-49	147	Apr89	ORL	Carlton+ NDG.
^{85}Rb	$\sigma_{n,\gamma}$	1.8+2	7.0+5	Expt	DOE-NDC-49	138	Apr89	ORL	Beer+ NDG.
^{87}Rb	$\sigma_{n,\gamma}$	1.8+2	7.0+5	Expt	DOE-NDC-49	138	Apr89	ORL	Beer+ NDG.
^{88}Y	$\sigma_{n,X\gamma}$	7.0+5	4.0+8	Expt	DOE-NDC-49	106	Apr89	LAS	Nelson+ NDG. TBD.
^{89}Y	$\sigma_{el}(\theta)$	8.0+6		Expt	DOE-NDC-49	1	Apr89	ANL	Smith+ NDG. SIG. RATIOS,20-160 DEGS.
^{89}Y	$\sigma_{n,p}$	NDG		Expt	DOE-NDC-49	127	Apr89	ANL	Smith+ NDG. TBD. ANL+MHG.
Zr	Evaluation	NDG		Eval	DOE-NDC-4	115	Apr89	ANL	Smith+ NDG. ENDF/B-VI. TBC.
Zr	σ_{tot}		1.0+7	Expt	DOE-NDC-4	114	Apr89	ANL	Sugimoto+ NDG. ANALYSIS TBD.
Zr	$\sigma_{el}(\theta)$	8.0+6		Expt	DOE-NDC-4	111	Apr89	ANL	Smith+ NDG. SIG. RATIOS,20-160 DEGS.
Zr	$\sigma_{el}(\theta)$		1.0+7	Expt	DOE-NDC-4	114	Apr89	ANL	Sugimoto+ NDG. ANALYSIS TBD.
Zr	$\sigma_{dif.inl}$		1.0+7	Expt	DOE-NDC-4	114	Apr89	ANL	Sugimoto+ NDG. TBC.
^{90}Zr	$\sigma_{el}(\theta)$	8.0+6	2.4+7	Expt	DOE-NDC-49	164	Apr89	OHO	Delaroche+ NDG.

NEUTRON DATA REFEFENCES

Element	Quantity	Energy (eV) Min	Max	Type	Documentation Ref	Page	Date	Lab	Comments
^{90}Zr	$\sigma_{dif.inl}$	NDG		Expt	DOE-NDC-49	164	Apr89	OHO	Wang+ NDG.
^{92}Zr	$\sigma_{dif.inl}$	NDG		Expt	DOE-NDC-49	164	Apr89	OHO	Wang+ NDG.
^{94}Zr	$\sigma_{dif.inl}$	NDG		Expt	DOE-NDC-49	164	Apr89	OHO	Wang+ NDG.
^{93}Nb	$\sigma_{el}(\theta)$	8.0+6		Expt	DOE-NDC-49	3	Apr89	ANL	Smith+ NDG. SIG. RATIOS,20-160 DEGS.
^{94}Mo	$\sigma_{n,2n}$	1.5+7		Expt	DOE-NDC-49	12	Apr89	ANL	Greenwood+ M,G PRODUCTION.
^{95}Mo	$\sigma_{n,xn}$	1.4+7		Expt	DOE-NDC-49	12	Apr89	ANL	Greenwood+ N3N, CS(M)=1.36 MB.
^{103}Rh	$\sigma_{dif.inl}$	NDG		Expt	DOE-NDC-49	5	Apr89	ANL	Guenther+ NDG. DOUB. DIFF.
Pd	$\sigma_{dif.inl}$	8.0+6		Expt	DOE-NDC-49	6	Apr89	ANL	Smith+ NDG. TBC.
Cd	$\sigma_{el}(\theta)$	8.0+6		Expt	DOE-NDC-49	3	Apr89	ANL	Smith+ NDG. SIG. RATIOS,20-160 DEGS.
In	$\sigma_{el}(\theta)$		1.0+7	Expt	DOE-NDC-49	6	Apr89	ANL	Sugimoto+ NDG. ANALYSIS TBD.
^{115}In	$\sigma_{el}(\theta)$	8.0+6		Expt	DOE-NDC-49	1	Apr89	ANL	Smith+ NDG. SIG. RATIOS,20-160 DEGS.
^{116}Sn	$\sigma_{el}(\theta)$	1.0+6	2.4+7	Eval	DOE-NDC-49	54	Apr89	KTY	Mirzaa+ NDG. SCAT. POT.
^{116}Sn	$\sigma_{el}(\theta)$	NDG		Eval	DOE-NDC-49	180	Apr89	TNL	Walter+ NDG. CC. ANALYSIS.
^{116}Sn	σ_{pol}	NDG		Eval	DOE-NDC-49	180	Apr89	TNL	Walter+ NDG. CC. ANALYSIS.
^{116}Sn	$\sigma_{dif.inl}$	1.0+6	2.4+7	Eval	DOE-NDC-49	54	Apr89	KTY	Mirzaa+ NDG. SCAT. POT.
^{116}Sn	$\sigma_{dif.inl}$	NDG		Eval	DOE-NDC-49	180	Apr89	TNL	Walter+ NDG. CC. ANALYSIS.
^{116}Sn	$\sigma_{n,n'\gamma}$	NDG		Expt	DOE-NDC-49	63	Apr89	KTY	Weil+ NDG. LVL. STRUCTURE
^{118}Sn	$\sigma_{el}(\theta)$	1.0+6	2.4+7	Eval	DOE-NDC-49	54	Apr89	KTY	Mirzaa+ NDG. SCAT. POT.
^{118}Sn	$\sigma_{dif.inl}$	1.0+6	2.4+7	Eval	DOE-NDC-49	54	Apr89	KTY	Mirzaa+ NDG. SCAT. POT.
^{118}Sn	$\sigma_{p,emis}$	6.5+7		Expt	DOE-NDC-49	36	Apr89	DAV	Hjort+ NDG. 0-40 DEGS.
^{120}Sn	$\sigma_{el}(\theta)$	1.0+6	2.4+7	Eval	DOE-NDC-49	54	Apr89	KTY	Mirzaa+ NDG. SCAT. POT.
^{120}Sn	$\sigma_{el}(\theta)$	NDG		Eval	DOE-NDC-49	180	Apr89	TNL	Walter+ NDG. CC. ANALYSIS.
^{120}Sn	σ_{pol}	NDG		Eval	DOE-NDC-49	180	Apr89	TNL	Walter+ NDG. CC. ANALYSIS.
^{120}Sn	$\sigma_{dif.inl}$	1.0+6	2.4+7	Eval	DOE-NDC-49	54	Apr89	KTY	Mirzaa+ NDG. SCAT. POT.
^{120}Sn	$\sigma_{dif.inl}$	NDG		Eval	DOE-NDC-49	180	Apr89	TNL	Walter+ NDG. CC. ANALYSIS.
^{121}Sn	$\sigma_{el}(\theta)$	1.0+6	2.4+7	Eval	DOE-NDC-49	54	Apr89	KTY	Mirzaa+ NDG. SCAT. POT.
^{121}Sn	$\sigma_{dif.inl}$	1.0+6	2.4+7	Eval	DOE-NDC-49	54	Apr89	KTY	Mirzaa+ NDG. SCAT. POT.
^{124}Sn	$\sigma_{el}(\theta)$	1.0+6	2.4+7	Eval	DOE-NDC-49	54	Apr89	KTY	Mirzaa+ NDG. SCAT. POT.
^{124}Sn	$\sigma_{dif.inl}$	1.0+6	2.4+7	Eval	DOE-NDC-49	54	Apr89	KTY	Mirzaa+ NDG. SCAT. POT.
^{124}Sn	$\sigma_{n,n'\gamma}$	NDG		Expt	DOE-NDC-49	63	Apr89	KTY	Weil+ NDG. LVL. STRUCTURE
^{134}Xe	Res.Params.	NDG		Expt	DOE-NDC-49	139	Apr89	ORL	Macklin. NDG.
^{136}Xe	$\sigma_{n,\gamma}$	NDG		Expt	DOE-NDC-49	139	Apr89	ORL	Macklin. NDG.
^{136}Xe	Res.Params.	2.2+3	1.8+4	Expt	DOE-NDC-49	139	Apr89	ORL	Macklin. NDG.

NEUTRON DATA REFERENCES

Element	Quantity	Energy (eV) Min	Max	Type	Documentation Ref	Page	Date	Lab	Comments
^{142}Nd	$\sigma_{el}(\theta)$	2.5+6	9.0+6	Expt	DOE-NDC-49	57	Apr89	KTY	.NDG. TBC.
^{142}Nd	$\sigma_{dif.inl}$	2.5+6	9.0+6	Expt	DOE-NDC-49	57	Apr89	KTY	.NDG. TBC.
^{144}Sm	$\sigma_{el}(\theta)$	2.5+6	9.0+6	Expt	DOE-NDC-49	57	Apr89	KTY	.NDG. TBC.
^{144}Sm	$\sigma_{dif.inl}$	2.5+6	9.0+6	Expt	DOE-NDC-49	57	Apr89	KTY	.NDG. TBC.
^{151}Eu	Evaluation		2.0+7	Eval	DOE-NDC-49	112	Apr89	LAS	Young+ NDG. ENDF/B-VI.
^{151}Eu	σ_{el}	NDG		Theo	DOE-NDC-49	5	Apr89	ANL	Lynn+ COH. SCATT. LENGTH (E).
^{153}Eu	Evaluation		2.0+7	Eval	DOE-NDC-49	112	Apr89	LAS	Young+ NDG. ENDF/B-VI.
^{165}Ho	Evaluation		2.0+7	Eval	DOE-NDC-49	112	Apr89	LAS	Young+ NDG. ENDF/B-VI.
^{181}Ta	$\sigma_{n,X\gamma}$	2.0+6	1.0+8	Expt	DOE-NDC-49	183	Apr89	LAS	Gould+ NDG.
W	Evaluation		2.0+7	Eval	DOE-NDC-49	112	Apr89	LAS	Young+ NDG. ENDF/B-VI.
W	$\sigma_{\alpha,emis}$	1.4+7	1.5+7	Expt	DOE-NDC-49	172	Apr89	AI	Kneff+ NDG. TBD.
^{184}W	$\sigma_{dif.inl}$	1.2+7	2.6+7	Expt	DOE-NDC-49	162	Apr89	OHO	Marcinkowski+ NDG.
^{185}Re	Evaluation		2.0+7	Eval	DOE-NDC-49	112	Apr89	LAS	Young+ NDG. ENDF/B-VI.
^{187}Re	Evaluation		2.0+7	Eval	DOE-NDC-49	112	Apr89	LAS	Young+ NDG. ENDF/B-VI.
^{189}Os	$\sigma_{el}(\theta)$	6.4+4	9.8+4	Expt	DOE-NDC-49	139	Apr89	ORL	McEllistrem+ NDG.
^{189}Os	$\sigma_{dif.inl}$	6.4+4	9.8+4	Expt	DOE-NDC-49	139	Apr89	ORL	McEllistrem+ NDG.
^{192}Os	$\sigma_{el}(\theta)$	NDG		Expt	DOE-NDC-49	54	Apr89	KTY	Hicks+ NDG.
^{192}Os	$\sigma_{dif.inl}$	NDG		Expt	DOE-NDC-49	54	Apr89	KTY	Hicks+ NDG.
^{191}Ir	$\sigma_{n,\gamma}$	2.0+3		Theo	DOE-NDC-49	85	Apr89	LRL	Gardner+ NDG.
^{191}Ir	$\sigma_{n,xn}$	NDG		Theo	DOE-NDC-49	85	Apr89	LRL	Gardner+ NDG.
^{193}Ir	$\sigma_{n,n'\gamma}$	NDG		Theo	DOE-NDC-49	85	Apr89	LRL	Gardner+ NDG.
^{193}Ir	$\sigma_{n,xn}$	NDG		Theo	DOE-NDC-49	85	Apr89	LRL	Gardner+ NDG.
^{194}Pt	$\sigma_{el}(\theta)$	8.0+6		Expt	DOE-NDC-49	54	Apr89	KTY	Hicks+ NDG.
^{194}Pt	$\sigma_{dif.inl}$	8.0+6		Expt	DOE-NDC-49	54	Apr89	KTY	Hicks+ NDG.
^{197}Au	Evaluation		2.0+7	Eval	DOE-NDC-49	112	Apr89	LAS	Young+ NDG. ENDF/B-VI.
^{197}Au	$\sigma_{dif.inl}$	NDG		Expt	DOE-NDC-49	5	Apr89	ANL	Guenther+ NDG. DOUB. DIFF.
^{197}Au	$\sigma_{n,\gamma}$	2.3+4	9.6+5	Expt	DOE-NDC-49	129	Apr89	MHG	Quang+ TBC.
^{197}Au	$\sigma_{n,\gamma}$	NDG		Revw	DOE-NDC-49	132	Apr89	NBS	Carlson+ NDG. ENDF/B-VI Status RPT.
Pb	$\sigma_{el}(\theta)$	8.0+6		Expt	DOE-NDC-4	111	Apr89	ANL	Smith+ NDG. SIG. RATIOS,20-160 DEGS.
Pb	$\sigma_{n,n'\gamma}$	3.0+6	3.0+7	Theo	DOE-NDC-4	118	Apr89	LRL	Blann. NDG. HI. EG. GAMMA SPEC.
^{204}Pb	Evaluation	NDG		Eval	DOE-NDC-49	152	Apr89	ORL	Hetrick+ NDG. ENDF/B-VI.
^{204}Pb	σ_{tot}	3.0+5	4.0+6	Eval	DOE-NDC-49	57	Apr89	KTY	.NDG.
^{204}Pb	$\sigma_{el}(\theta)$	2.5+6	8.0+6	Expt	DOE-NDC-49	53	Apr89	KTY	Hanly+ NDG.

NEUTRON DATA REFERENCES

Element	Quantity	Energy (eV) Min	Max	Type	Documentation Ref	Page	Date	Lab	Comments
^{204}Pb	$\sigma_{el}(\theta)$	2.5+6	8.0+6	Eval	DOE-NDC-49	57	Apr89	KTY	.NDG.
^{204}Pb	$\sigma_{dif.inl}$	2.5+6	8.0+6	Expt	DOE-NDC-49	53	Apr89	KTY	Hanly+ NDG.
^{204}Pb	$\sigma_{dif.inl}$	2.5+6	8.0+6	Eval	DOE-NDC-49	57	Apr89	KTY	.NDG.
^{204}Pb	$\sigma_{dif.inl}$	NDG		Exth	DOE-NDC-49	62	Apr89	KTY	Wang+ NDG. EXPT, MDL. CALC.
^{204}Pb	$\sigma_{n,n'\gamma}$	NDG		Expt	DOE-NDC-49	61	Apr89	KTY	Hanly+ NDG. PR/C 37 1840
^{206}Pb	Evaluation	NDG		Eval	DOE-NDC-49	152	Apr89	ORL	Hetrick+ NDG. ENDF/B-VI.
^{206}Pb	σ_{tot}	3.0+5	4.0+6	Eval	DOE-NDC-49	57	Apr89	KTY	.NDG.
^{206}Pb	$\sigma_{el}(\theta)$	2.5+6	8.0+6	Expt	DOE-NDC-49	53	Apr89	KTY	Hanly+ NDG.
^{206}Pb	$\sigma_{el}(\theta)$	2.5+6	8.0+6	Eval	DOE-NDC-49	57	Apr89	KTY	.NDG.
^{206}Pb	$\sigma_{dif.inl}$	2.5+6	8.0+6	Expt	DOE-NDC-49	53	Apr89	KTY	Hanly+ NDG.
^{206}Pb	$\sigma_{dif.inl}$	2.5+6	8.0+6	Eval	DOE-NDC-49	57	Apr89	KTY	.NDG.
^{206}Pb	$\sigma_{n,X\gamma}$	7.0+5	4.0+8	Expt	DOE-NDC-49	106	Apr89	LAS	Nelson+ NDG. TBD.
^{207}Pb	Evaluation	NDG		Eval	DOE-NDC-49	152	Apr89	ORL	Hetrick+ NDG. ENDF/B-VI.
^{207}Pb	$\sigma_{n,X\gamma}$	7.0+5	4.0+8	Expt	DOE-NDC-49	106	Apr89	LAS	Nelson+ NDG. TBD.
^{208}Pb	Evaluation	NDG		Eval	DOE-NDC-49	152	Apr89	ORL	Hetrick+ NDG. ENDF/B-VI.
^{208}Pb	$\sigma_{el}(\theta)$	NDG		Expt	DOE-NDC-49	57	Apr89	KTY	.NDG. TBD.
^{208}Pb	$\sigma_{el}(\theta)$	9.5+7	3.0+8	Theo	DOE-NDC-49	110	Apr89	LAS	Kozack+ NDG.
^{208}Pb	$\sigma_{el}(\theta)$		6.0+7	Eval	DOE-NDC-49	164	Apr89	OHO	Finlay+ NDG. DISPERSION CORRECTION.
^{208}Pb	$\sigma_{el}(\theta)$		2.0+7	Theo	DOE-NDC-49	148	Apr89	ORL	Jeukenne+ NDG. SEE PR/C 38(6).
^{208}Pb	$\sigma_{el}(\theta)$	4.0+6	4.0+7	Eval	DOE-NDC-49	181	Apr89	TNL	Walter+ NDG. OM. FIT.
^{208}Pb	$\sigma_{dif.inl}$	NDG		Expt	DOE-NDC-49	57	Apr89	KTY	.NDG. TBD.
^{208}Pb	$\sigma_{dif.inl}$	5.0+6	1.1+7	Eval	DOE-NDC-49	163	Apr89	OHO	Cheema+ NDG.
^{208}Pb	$\sigma_{n,X\gamma}$	7.0+5	4.0+8	Expt	DOE-NDC-49	106	Apr89	LAS	Nelson+ NDG. TBD.
^{209}Bi	Evaluation	NDG		Eval	DOE-NDC-49	14	Apr89	ANL	Smith+ NDG. ENDF/B-VI. TBC.
^{209}Bi	σ_{tot}	1.0+6	4.0+7	Eval	DOE-NDC-49	166	Apr89	OHO	Das+ NDG. OM. ANALYSIS.
^{209}Bi	σ_{tot}	1.0+6	4.0+7	Eval	DOE-NDC-49	148	Apr89	OHO	Das+ NDG.
^{209}Bi	$\sigma_{el}(\theta)$	8.0+6		Expt	DOE-NDC-49	1	Apr89	ANL	Smith+ NDG. SIG. RATIOS,20-160 DEGS.
^{209}Bi	$\sigma_{el}(\theta)$	1.5+6	2.4+7	Eval	DOE-NDC-49	166	Apr89	OHO	Das+ NDG. OM. ANALYSIS.
^{209}Bi	$\sigma_{el}(\theta)$	1.5+6	2.4+7	Eval	DOE-NDC-49	148	Apr89	OHO	Das+ NDG.
^{209}Bi	σ_{pol}	6.0+6	9.0+6	Expt	DOE-NDC-49	181	Apr89	TNL	Howell+ NDG.
^{209}Bi	σ_{pol}	6.0+6	9.0+6	Eval	DOE-NDC-49	181	Apr89	TNL	Howell+ NDG. CN. CALC. TBD.
^{227}Th	Fiss.Yield	2.5-2		Eval	DOE-NDC-49	113	Apr89	LAS	England+ NDG. ENDF/B-VI.
^{229}Th	Fiss.Yield	2.5-2		Eval	DOE-NDC-49	113	Apr89	LAS	England+ NDG. ENDF/B-VI.

NEUTRON DATA REFERENCES

Element	Quantity	Energy (eV) Min	Max	Type	Documentation Ref	Page	Date	Lab	Comments
^{232}Th	$\sigma_{el}(\theta)$		3.5+6	Expt	DOE-NDC-49	118	Apr89	LTI	Sheldon. GRPH. ANG. DIST.
^{232}Th	$\sigma_{dif.inl}$	2.3+6	3.0+6	Expt	DOE-NDC-49	116	Apr89	LTI	Beghian+ NDG. EXC. FCN.
^{232}Th	$\sigma_{dif.inl}$	1.0+5	1.5+5	Expt	DOE-NDC-49	117	Apr89	LTI	Beghian+ NDG.
^{232}Th	$\sigma_{n,X\gamma}$	7.0+5	4.0+8	Expt	DOE-NDC-49	106	Apr89	LAS	Nelson+ NDG. TBD.
^{232}Th	$\sigma_{n,f}$	1.0+6	4.0+8	Expt	DOE-NDC-49	105	Apr89	LAS	Lisowski+ NDG.
^{232}Th	Spect.fiss n	5.0+5	3.0+6	Expt	DOE-NDC-49	118	Apr89	LTI	Beghian+ NDG. TBD.
^{232}Th	Fiss.Yield	FAST		Eval	DOE-NDC-49	113	Apr89	LAS	England+ NDG. ENDF/B-VI.
^{232}Th	Fiss.Yield	1.4+7		Eval	DOE-NDC-49	113	Apr89	LAS	England+ NDG. ENDF/B-VI.
^{231}Pa	Fiss.Yield	FAST		Eval	DOE-NDC-49	113	Apr89	LAS	England+ NDG. ENDF/B-VI.
^{232}U	Fiss.Yield	2.5-2		Eval	DOE-NDC-49	113	Apr89	LAS	England+ NDG. ENDF/B-VI.
^{233}U	Fiss.Yield	2.5-2		Eval	DOE-NDC-49	113	Apr89	LAS	England+ NDG. ENDF/B-VI.
^{233}U	Fiss.Yield	FAST		Eval	DOE-NDC-49	113	Apr89	LAS	England+ NDG. ENDF/B-VI.
^{233}U	Fiss.Yield	1.4+7		Eval	DOE-NDC-49	113	Apr89	LAS	England+ NDG. ENDF/B-VI.
^{234}U	Fiss.Yield	1.4+7		Eval	DOE-NDC-49	113	Apr89	LAS	England+ NDG. ENDF/B-VI.
^{234}U	Fiss.Yield	FAST		Eval	DOE-NDC-49	113	Apr89	LAS	England+ NDG. ENDF/B-VI.
^{235}U	Evaluation		2.0+7	Eval	DOE-NDC-49	112	Apr89	LAS	Young+ NDG. ENDF/B-VI.
^{235}U	σ_{tot}	1.0+4	2.0+7	Theo	DOE-NDC-49	112	Apr89	LAS	Young+ NDG. CC OM CALC.
^{235}U	σ_{tot}	1.0+0	1.0+4	Expt	DOE-NDC-49	140	Apr89	ORL	Harvey+ NDG.
^{235}U	σ_{tot}	NDG		Eval	DOE-NDC-49	140	Apr89	ORL	Moore+ NDG. MATRIX ANAL.
^{235}U	σ_{tot}		1.1+2	Eval	DOE-NDC-49	149	Apr89	ORL	Derrien+ NDG.
^{235}U	σ_{tot}		2.3+3	Eval	DOE-NDC-49	153	Apr89	ORL	DeSaussure+ NDG. PARAMETERIZATION.
^{235}U	$\sigma_{el}(\theta)$	1.0+4	2.0+7	Theo	DOE-NDC-49	112	Apr89	LAS	Young+ NDG. CC OM CALC.
^{235}U	$\sigma_{el}(\theta)$		3.5+6	Expt	DOE-NDC-49	118	Apr89	LTI	Sheldon. GRPH. ANG. DIST.
^{235}U	$\sigma_{dif.inl}$	1.0+4	2.0+7	Theo	DOE-NDC-49	112	Apr89	LAS	Young+ NDG. CC OM CALC.
^{235}U	$\sigma_{n,\gamma}$	NDG		Eval	DOE-NDC-49	140	Apr89	ORL	Moore+ NDG. MATRIX ANAL.
^{235}U	$\sigma_{n,\gamma}$		1.1+2	Eval	DOE-NDC-49	149	Apr89	ORL	Derrien+ NDG.
^{235}U	$\sigma_{n,\gamma}$		2.3+3	Eval	DOE-NDC-49	153	Apr89	ORL	DeSaussure+ NDG. PARAMETERIZATION.
^{235}U	$\sigma_{n,n'\gamma}$	3.0+6	3.0+7	Theo	DOE-NDC-49	80	Apr89	LRL	Blann. NDG. HI. EG. GAMMA SPEC.
^{235}U	$\sigma_{n,xn}$	1.0+4	2.0+7	Theo	DOE-NDC-49	112	Apr89	LAS	Young+ NDG. CC OM CALC.
^{235}U	$\sigma_{n,f}$	1.0+6	4.0+8	Expt	DOE-NDC-49	105	Apr89	LAS	Lisowski+ NDG.
^{235}U	$\sigma_{n,f}$	1.0+4	2.0+7	Theo	DOE-NDC-49	112	Apr89	LAS	Young+ NDG. CC OM CALC.
^{235}U	$\sigma_{n,f}$	2.5-2	1.0+3	Expt	DOE-NDC-49	130	Apr89	NBS	Schrack+ NDG.
^{235}U	$\sigma_{n,f}$	1.0+6	3.5+7	Expt	DOE-NDC-49	130	Apr89	LAS	Carlson+ NDG. LAS+NBS.

Element	Quantity	Energy (eV) Min	Max	Type	Documentation Ref	Page	Date	Lab	Comments
^{235}U	$\sigma_{n,f}$	2.5+6		Expt	DOE-NDC-49	131	Apr89	NBS	Duvall+ NDG. TBD.
^{235}U	$\sigma_{n,f}$	NDG		Revw	DOE-NDC-49	132	Apr89	NBS	Carlson+ NDG. ENDF/B-VI Status RPT.
^{235}U	$\sigma_{n,f}$	NDG		Eval	DOE-NDC-49	140	Apr89	ORL	Moore+ NDG. MATRIX ANAL.
^{235}U	$\sigma_{n,f}$	NDG		Expt	DOE-NDC-49	142	Apr89	ORL	Weston+ NDG. TBC.
^{235}U	$\sigma_{n,f}$		1.1+2	Eval	DOE-NDC-49	149	Apr89	ORL	Derrien+ NDG.
^{235}U	$\sigma_{n,f}$		2.3+3	Eval	DOE-NDC-49	153	Apr89	ORL	DeSaussure+ NDG. PARAMETERIZATION.
^{235}U	ν_d	NDG		Eval	DOE-NDC-49	113	Apr89	LAS	England+ TBC. GRPH. CFD. EXPT.
^{235}U	ν_d	NDG		Expt	DOE-NDC-49	122	Apr89	LTI	Couchell+ NDG. SPECTRA.
^{235}U	Spect.fiss n	5.0+5	3.0+6	Expt	DOE-NDC-49	118	Apr89	LTI	Beghian+ NDG. TBD.
^{235}U	Fiss.Yield	FAST		Eval	DOE-NDC-49	113	Apr89	LAS	England+ NDG. ENDF/B-VI.
^{235}U	Fiss.Yield	2.5-2		Eval	DOE-NDC-49	113	Apr89	LAS	England+ NDG. ENDF/B-VI.
^{235}U	Fiss.Yield	1.4+7		Eval	DOE-NDC-49	113	Apr89	LAS	England+ NDG. ENDF/B-VI.
^{235}U	Res.Params.		1.1+2	Eval	DOE-NDC-49	148	Apr89	ORL	Leal+ NDG. AVG. RES. PAR.
^{235}U	Res.Params.		3.0+2	Eval	DOE-NDC-49	149	Apr89	ORL	Leal+ NDG. ENDF/B-VI.
^{236}U	σ_{abs}	2.0+1	1.0+6	Expt	DOE-NDC-49	141	Apr89	ORL	Macklin+ NDG.
^{236}U	Fiss.Yield	1.4+7		Eval	DOE-NDC-49	113	Apr89	LAS	England+ NDG. ENDF/B-VI.
^{236}U	Fiss.Yield	FAST		Eval	DOE-NDC-49	113	Apr89	LAS	England+ NDG. ENDF/B-VI.
^{237}U	Fiss.Yield	FAST		Eval	DOE-NDC-49	113	Apr89	LAS	England+ NDG. ENDF/B-VI.
^{238}U	Evaluation	4.5+4	2.0+7	Eval	DOE-NDC-49	15	Apr89	ANL	Smith+ NDG. PARTIAL EVL.
^{238}U	Evaluation		2.0+7	Eval	DOE-NDC-49	112	Apr89	LAS	Young+ NDG. ENDF/B-VI.
^{238}U	σ_{tot}	4.5+4	2.0+7	Eval	DOE-NDC-49	15	Apr89	ANL	Smith+ NDG. PARTIAL EVL. TBC.
^{238}U	σ_{tot}	1.0+4	2.0+7	Theo	DOE-NDC-49	112	Apr89	LAS	Young+ NDG. TBD.
^{238}U	σ_{tot}	1.0+3	1.0+5	Expt	DOE-NDC-49	140	Apr89	ORL	Harvey+ NDG.
^{238}U	$\sigma_{el}(\theta)$	1.0+4	2.0+7	Theo	DOE-NDC-49	112	Apr89	LAS	Young+ NDG. TBD.
^{238}U	$\sigma_{el}(\theta)$		3.5+6	Expt	DOE-NDC-49	118	Apr89	LTI	Sheldon. GRPH. ANG. DIST.
^{238}U	$\sigma_{dif.inl}$	1.0+4	2.0+7	Theo	DOE-NDC-49	112	Apr89	LAS	Young+ NDG. TBD.
^{238}U	$\sigma_{dif.inl}$	2.3+6	3.0+6	Expt	DOE-NDC-49	116	Apr89	LTI	Beghian+ GRPH. EXC. FCN.
^{238}U	$\sigma_{dif.inl}$	1.0+5	1.5+5	Expt	DOE-NDC-49	117	Apr89	LTI	Beghian+ NDG.
^{238}U	$\sigma_{n,\gamma}$	2.3+4	9.6+5	Expt	DOE-NDC-49	128	Apr89	MHG	Quang+ SIG=517 MB,148 MB.
^{238}U	$\sigma_{n,\gamma}$	NDG		Revw	DOE-NDC-49	132	Apr89	NBS	Carlson+ NDG. ENDF/B-VI Status RPT.
^{238}U	$\sigma_{n,\gamma}$	1.0+3	1.0+5	Expt	DOE-NDC-49	141	Apr89	ORL	Macklin+ NDG.
^{238}U	$\sigma_{n,n'\gamma}$	3.0+6	3.0+7	Theo	DOE-NDC-49	80	Apr89	LRL	Blann. NDG. HI. EG. GAMMA SPEC.
^{238}U	$\sigma_{n,X\gamma}$	7.0+5	4.0+8	Expt	DOE-NDC-49	106	Apr89	LAS	Nelson+ NDG. TBD.

NEUTRON DATA REFERENCES

Element	Quantity	Energy (eV) Min	Max	Type	Documentation Ref	Page	Date	Lab	Comments
^{238}U	$\sigma_{n,xn}$	1.0+4	2.0+7	Theo	DOE-NDC-49	112	Apr89	LAS	Young+ NDG. TBD.
^{238}U	$\sigma_{n,f}$	1.9+6	2.6+6	Expt	DOE-NDC-49	7	Apr89	ANL	Meadows+ NDG. REL. 237NP(NF).
	$\sigma_{n,f}$	1.0+6	4.0+8	Expt	DOE-NDC-49	105	Apr89	LAS	Lisowski+ NDG.
	$\sigma_{n,f}$	1.0+4	2.0+7	Theo	DOE-NDC-49	112	Apr89	LAS	Young+ NDG. TBD.
^{238}U	$\sigma_{n,f}$	NDG		Revw	DOE-NDC-49	132	Apr89	NBS	Carlson+ NDG. ENDF/B-VI Status RPT.
^{238}U	ν_d	FAST		Expt	DOE-NDC-49	120	Apr89	LTI	Couchell+ GRPHS. CFD. 239PU.
^{238}U	ν_d	NDG		Expt	DOE-NDC-49	122	Apr89	LTI	Couchell+ NDG. SPECTRA.
^{238}U	Spect.fiss n	5.0+5	3.0+6	Expt	DOE-NDC-49	118	Apr89	LTI	Beghian+ NDG. TBD.
^{238}U	Fiss.Yield	FAST		Eval	DOE-NDC-49	113	Apr89	LAS	England+ NDG. ENDF/B-VI.
^{238}U	Fiss.Yield	SPON		Eval	DOE-NDC-49	113	Apr89	LAS	England+ NDG. ENDF/B-VI.
^{238}U	Fiss.Yield	1.4+7		Eval	DOE-NDC-49	113	Apr89	LAS	England+ NDG. ENDF/B-VI.
^{238}U	Res.Params.	4.0+3	4.5+4	Eval	DOE-NDC-49	153	Apr89	ORL	DeSaussure+ NDG. UNCERTAINTIES.
^{237}Np	$\sigma_{n,f}$	1.0+6	4.0+8	Expt	DOE-NDC-49	105	Apr89	LAS	Lisowski+ NDG.
^{237}Np	Fiss.Yield	1.4+7		Eval	DOE-NDC-49	113	Apr89	LAS	England+ NDG. ENDF/B-VI.
^{237}Np	Fiss.Yield	FAST		Eval	DOE-NDC-49	113	Apr89	LAS	England+ NDG. ENDF/B-VI.
^{237}Np	Fiss.Yield	2.5-2		Eval	DOE-NDC-49	113	Apr89	LAS	England+ NDG. TBD.
^{238}Np	Fiss.Yield	FAST		Eval	DOE-NDC-49	113	Apr89	LAS	England+ NDG. ENDF/B-VI.
^{238}Pu	Fiss.Yield	FAST		Eval	DOE-NDC-49	113	Apr89	LAS	England+ NDG. ENDF/B-VI.
^{239}Pu	Evaluation		2.0+7	Eval	DOE-NDC-49	112	Apr89	LAS	Young+ NDG. ENDF/B-VI.
^{239}Pu	σ_{tot}	1.0+4	2.0+7	Theo	DOE-NDC-49	112	Apr89	LAS	Young+ NDG. TBD.
^{239}Pu	σ_{tot}	1.0+0	1.0+4	Expt	DOE-NDC-49	140	Apr89	ORL	Harvey+ NDG.
^{239}Pu	σ_{tot}		1.0+3	Eval	DOE-NDC-49	149	Apr89	ORL	Derrien+ NDG.
^{239}Pu	σ_{tot}		1.0+3	Eval	DOE-NDC-49	154	Apr89	ORL	Derrien+ NDG.
^{239}Pu	$\sigma_{el}(\theta)$	1.0+4	2.0+7	Theo	DOE-NDC-49	112	Apr89	LAS	Young+ NDG. TBD.
^{239}Pu	$\sigma_{dif.inl}$	1.0+4	2.0+7	Theo	DOE-NDC-49	112	Apr89	LAS	Young+ NDG. TBD.
^{239}Pu	$\sigma_{n,\gamma}$		1.0+3	Eval	DOE-NDC-49	149	Apr89	ORL	Derrien+ NDG.
^{239}Pu	$\sigma_{n,\gamma}$		1.0+3	Eval	DOE-NDC-49	154	Apr89	ORL	Derrien+ NDG.
^{239}Pu	$\sigma_{n,n'\gamma}$	3.0+6	3.0+7	Theo	DOE-NDC-49	80	Apr89	LRL	Blann. NDG. HI. EG. GAMMA SPEC.
^{239}Pu	$\sigma_{n,xn}$	1.0+4	2.0+7	Theo	DOE-NDC-49	112	Apr89	LAS	Young+ NDG. TBD.
^{239}Pu	$\sigma_{n,f}$	1.0+6	4.0+8	Expt	DOE-NDC-49	105	Apr89	LAS	Lisowski+ NDG.
^{239}Pu	$\sigma_{n,f}$	1.0+4	2.0+7	Theo	DOE-NDC-49	112	Apr89	LAS	Young+ NDG. TBD.
^{239}Pu	$\sigma_{n,f}$	NDG		Revw	DOE-NDC-49	132	Apr89	NBS	Carlson+ NDG. ENDF/B-VI Status RPT.
^{239}Pu	$\sigma_{n,f}$	NDG		Expt	DOE-NDC-49	142	Apr89	ORL	Weston+ NDG. TBC.

NEUTRON DATA REFERENCES

Element	Quantity	Energy (eV) Min	Max	Type	Documentation Ref	Page	Date	Lab	Comments
^{239}Pu	$\sigma_{n,f}$		1.0+3	Eval	DOE-NDC-49	149	Apr89	ORL	Derrien+ NDG.
^{239}Pu	$\sigma_{n,f}$		1.0+3	Eval	DOE-NDC-49	154	Apr89	ORL	Derrien+ NDG.
^{239}Pu	ν_d	NDG		Expt	DOE-NDC-49	122	Apr89	LTI	Couchell+ GRPH.
^{239}Pu	Spect.fiss n	5.0+5	3.0+6	Expt	DOE-NDC-49	118	Apr89	LTI	Beghian+ NDG. TBD.
^{239}Pu	Fiss.Yield	FAST		Eval	DOE-NDC-49	113	Apr89	LAS	England+ NDG. ENDF/B-VI.
^{239}Pu	Fiss.Yield	2.5-2		Eval	DOE-NDC-49	113	Apr89	LAS	England+ NDG. ENDF/B-VI.
^{239}Pu	Fiss.Yield	1.4+7		Eval	DOE-NDC-49	113	Apr89	LAS	England+ NDG. ENDF/B-VI.
^{239}Pu	Res.Params.		1.0+3	Eval	DOE-NDC-49	153	Apr89	ORL	Derrien+ NDG. ENDF/B-VI.JEF.
^{240}Pu	$\sigma_{el}(\theta)$		3.5+6	Expt	DOE-NDC-49	118	Apr89	LTI	Sheldon. NDG.
^{240}Pu	Fiss.Yield	1.4+7		Eval	DOE-NDC-49	113	Apr89	LAS	England+ NDG. ENDF/B-VI.
^{240}Pu	Fiss.Yield	FAST		Eval	DOE-NDC-49	113	Apr89	LAS	England+ NDG. ENDF/B-VI.
^{240}Pu	Fiss.Yield	2.5-2		Eval	DOE-NDC-49	113	Apr89	LAS	England+ NDG. TBD.
^{241}Pu	σ_{tot}		3.0+2	Eval	DOE-NDC-49	154	Apr89	ORL	Derrien+ NDG.
^{241}Pu	$\sigma_{n,\gamma}$		3.0+2	Eval	DOE-NDC-49	154	Apr89	ORL	Derrien+ NDG.
^{241}Pu	$\sigma_{n,f}$		3.0+2	Eval	DOE-NDC-49	154	Apr89	ORL	Derrien+ NDG.
^{241}Pu	Fiss.Yield	FAST		Eval	DOE-NDC-49	113	Apr89	LAS	England+ NDG. ENDF/B-VI.
^{241}Pu	Fiss.Yield	2.5-2		Eval	DOE-NDC-49	113	Apr89	LAS	England+ NDG. ENDF/B-VI.
^{241}Pu	Res.Params.		3.0+2	Eval	DOE-NDC-49	149	Apr89	ORL	Derrien+ NDG. ENDF/B-VI,JEF.
^{242}Pu	$\sigma_{el}(\theta)$		3.5+6	Expt	DOE-NDC-49	118	Apr89	LTI	Sheldon. NDG.
^{242}Pu	Fiss.Yield	FAST		Eval	DOE-NDC-49	113	Apr89	LAS	England+ NDG. ENDF/B-VI.
^{242}Pu	Fiss.Yield	1.4+7		Eval	DOE-NDC-49	113	Apr89	LAS	England+ NDG. TBD.
^{242}Pu	Fiss.Yield	2.5-2		Eval	DOE-NDC-49	113	Apr89	LAS	England+ NDG. TBD.
^{244}Pu	$\sigma_{el}(\theta)$		3.5+6	Expt	DOE-NDC-49	118	Apr89	LTI	Sheldon. NDG.
^{241}Am	Fiss.Yield	FAST		Eval	DOE-NDC-49	113	Apr89	LAS	England+ NDG. ENDF/B-VI.
^{241}Am	Fiss.Yield	1.4+7		Eval	DOE-NDC-49	113	Apr89	LAS	England+ NDG. ENDF/B-VI.
^{241}Am	Fiss.Yield	2.5-2		Eval	DOE-NDC-49	113	Apr89	LAS	England+ NDG. ENDF/B-VI.
^{242}Am	Fiss.Yield	2.5-2		Eval	DOE-NDC-49	113	Apr89	LAS	England+ NDG. ENDF/B-VI.
^{243}Am	Fiss.Yield	FAST		Eval	DOE-NDC-49	113	Apr89	LAS	England+ NDG. ENDF/B-VI.
^{242}Cm	Fiss.Yield	FAST		Eval	DOE-NDC-49	113	Apr89	LAS	England+ NDG. ENDF/B-VI.
^{243}Cm	Fiss.Yield	2.5-2		Eval	DOE-NDC-49	113	Apr89	LAS	England+ NDG. TBD.
^{243}Cm	Fiss.Yield	FAST		Eval	DOE-NDC-49	113	Apr89	LAS	England+ NDG. TBD.
^{244}Cm	Fiss.Yield	SPON		Eval	DOE-NDC-49	113	Apr89	LAS	England+ NDG. ENDF/B-VI.
^{244}Cm	Fiss.Yield	FAST		Eval	DOE-NDC-49	113	Apr89	LAS	England+ NDG. TBD.

Element	Quantity	Energy (eV) Min	Max	Type	Documentation Ref	Page	Date	Lab	Comments
^{245}Cm	Fiss.Yield	2.5-2		Eval	DOE-NDC-49	113	Apr89	LAS	England+ NDG. ENDF/B-VI.
^{246}Cm	Fiss.Yield	FAST		Eval	DOE-NDC-49	113	Apr89	LAS	England+ NDG. TBD.
^{246}Cm	Fiss.Yield	SPON		Eval	DOE-NDC-49	113	Apr89	LAS	England+ NDG. TBD.
^{247}Cm	$\sigma_{n,f}$	1.0-1	8.0+4	Expt	DOE-NDC-49	170	Apr89	RPI	Block+ NDG. TBD.
^{248}Cm	Fiss.Yield	SPON		Eval	DOE-NDC-49	113	Apr89	LAS	England+ NDG. ENDF/B-VI.
^{248}Cm	Fiss.Yield	FAST		Eval	DOE-NDC-49	113	Apr89	LAS	England+ NDG. TBD.
^{249}Cf	Fiss.Yield	2.5-2		Eval	DOE-NDC-49	113	Apr89	LAS	England+ NDG. ENDF/B-VI.
^{250}Cf	$\sigma_{n,f}$	1.0-1	8.0+4	Expt	DOE-NDC-49	170	Apr89	RPI	Block+ NDG. TBD.
^{250}Cf	Fiss.Yield	SPON		Eval	DOE-NDC-49	113	Apr89	LAS	England+ NDG. ENDF/B-VI.
^{251}Cf	Fiss.Yield	2.5-2		Eval	DOE-NDC-49	113	Apr89	LAS	England+ NDG. ENDF/B-VI.
^{252}Cf	ν_p	SPON		Revw	DOE-NDC-49	152	Apr89	ORL	Peele+ NDG. ENDF/B-VI STD.
^{252}Cf	Spect.fiss n	SPON		Theo	DOE-NDC-49	109	Apr89	LAS	Madland+ NDG.
^{252}Cf	Fiss.Yield	SPON		Eval	DOE-NDC-49	113	Apr89	LAS	England+ NDG. ENDF/B-VI.
^{253}Es	Fiss.Yield	SPON		Eval	DOE-NDC-49	113	Apr89	LAS	England+ NDG. ENDF/B-VI.
^{254}Es	$\sigma_{n,f}$	1.0-1	8.0+4	Expt	DOE-NDC-49	170	Apr89	RPI	Block+ NDG. TBD.
^{254}Es	Fiss.Yield	2.5-2		Eval	DOE-NDC-49	113	Apr89	LAS	England+ NDG. ENDF/B-VI.
^{254}Fm	Fiss.Yield	SPON		Eval	DOE-NDC-49	113	Apr89	LAS	England+ NDG. ENDF/B-VI.
^{255}Fm	Fiss.Yield	2.5-2		Eval	DOE-NDC-49	113	Apr89	LAS	England+ NDG. ENDF/B-VI.
^{256}Fm	Fiss.Yield	SPON		Eval	DOE-NDC-49	113	Apr89	LAS	England+ NDG. ENDF/B-VI.

ARGONNE NATIONAL LABORATORY

A. NEUTRON TOTAL AND SCATTERING CROSS-SECTION MEASUREMENTS

The following items relate to aspects of this ongoing program that have recently been completed or are nearing completion. There are many other portions of the effort that will be reported at the appropriate time. Generally, the studies are at energies of $\lesssim$ 10.0 MeV, and extend over the target mass range A = 9-240. The reader who may have a special need should contact A. B. Smith to determine if data relevant to his special requirements are available in a preliminary form.

1. Ambiguities in the Elastic Scattering of 8-MeV Neutrons from Adjacent Nuclei. (A. B. Smith, P. T. Guenther and R. D. Lawson)

Ratios of cross sections for the elastic scattering of 8-MeV neutrons from adjacent nuclei have been measured over the angular range $\approx 20^0$-160^0 for the target pairs $^{51}V/Cr$, $^{59}Co/^{58}Ni$, Cu/Zn, $^{89}Y/^{93}Nb$, $^{89}Y/Zr$, $^{93}Nb/Zr$, $^{115}In/Cd$ and $^{209}Bi/Pb$. The observed ratios vary from unity by as much as a factor of $\approx$ 2 at some angles for the lighter pairs. These experimental results are being examined in the context of the optical model, including consideration of: size effects, the Lane potential, collective effects, the dispersion relations, spin-orbit interactions, shell closures, spin-spin interactions, and nuclear structure as reflected in the imaginary-absorptive term of the potential. In some cases the observed ratios are well explained by one of these concepts. In other instances, they appear to be the consequence of a complex mixture of a number of these mechanisms, or are of a yet unindentified origin. In the latter cases the concept of a "global", or even "regional", optical potential provides no more than a qualitative representation of the physical reality. These results may be of concern in the precise prediction of neutron cross sections for applied purposes, and they imply that detailed attention must be paid to experimental measurements, making possible the derivation of explicit nuclear models. Some aspects of this work have been reported.[1]

---

[1] A.B. Smith et al., Bull. Am. Phys. Soc. 33, 1567 (1988).

2. Some Comments on the Interaction of Fast Neutrons with Beryllium.[1] (M. Sugimoto*, P. Guenther, J. Lynn**, A. Smith, and J. Whalen)

Neutron total cross sections of beryllium were measured from 1 to > 10 MeV with good precision. Differential elastic-scattering cross sections were measured from 4.5 to 10 MeV at intervals of $\approx$ 0.5 MeV and at $\approx$ 100 angular steps distributed between 18^0 and 160^0 at each incident energy. These elastic-scattering results are illustrated in Fig. 1. Concurrently, differential cross sections for the emission of a discrete inelastic-neutron group corresponding to an excited level at (2.43 ± 0.06) MeV were determined over the same incident-energy and angular range. Angle-integrated elastic-scattering cross sections were deduced from the observed differential values to accuracies of ≈ 2.5%, and angle-integrated inelastic-scattering cross sections were obtained to accuracies of ≈ 10%. The experimental results were compared with the values given in ENDF/B-V, with attention to discrepancies and implications, and large differences in the nonelastic cross sections were noted. Qualitative reaction mechanisms are proposed. This work has been published in a Laboratory report.[2]

---

* Visiting scientist. Permanent address: Japan Atomic Energy Research Institute, Tokai, Japan.

** Argonne Fellow. Permanent address: AERE, Harwell, United Kingdom.

† This work is responsive to the DOE task force addressing high-priority fusion-data issues. Report DOE/ER/02490-4, eds. D. Smith and H. Knox (1986).

[2] M. Sugimoto, P.T. Guenther, J.E. Lynn, A.B. Smith, and J.F. Whalen, ANL/NDM-108 (1988).

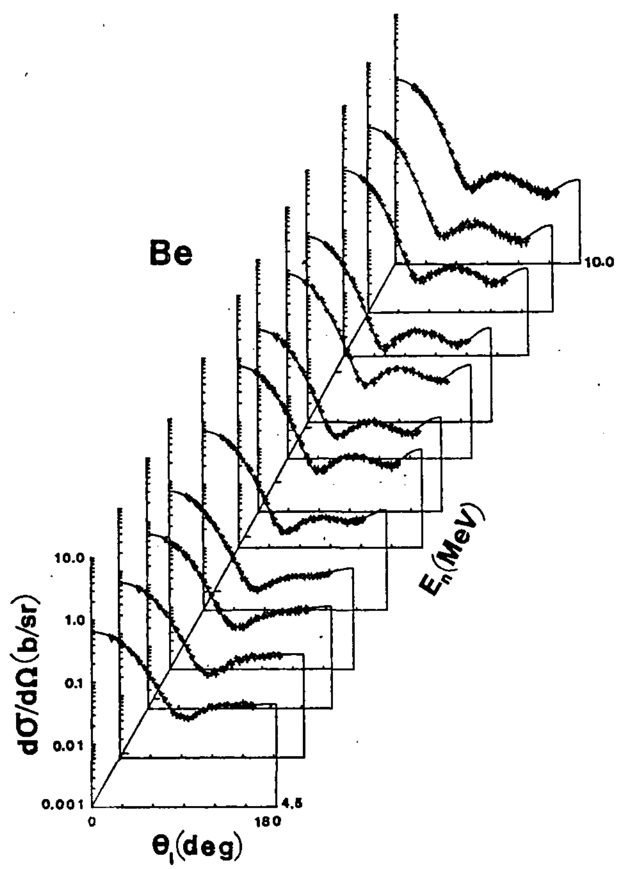

Fig. 1. Measured (symbols) differential cross sections for the scattering of fast neutrons from beryllium. The data are in the laboratory coordinate system.

3. The Fermi Surface Anomaly in ^{51}V. (R. D. Lawson, P. T. Guenther, and A. B. Smith)

This study of the interaction of fast neutrons with ^{51}V has been completed. The details are given in a Laboratory report,[1] and a corresponding manuscript has been accepted for journal publication in Nuclear Physics. Differential elastic- and inelastic-scattering cross sections of vanadium were measured from 4.5 to 10 MeV. These results were combined with previous 1.5- to 4.0-MeV scattering data from this laboratory, the 11.1-MeV elastic-scattering results from Ohio University, and the reported total cross sections to 20 MeV, to form a data base which was interpreted in terms of the spherical optical-statistical model. A good fit to the data was obtained by making both the strengths and geometries of the optical-model potential energy dependent. These energy dependencies are large below 6 MeV, but are smaller and similar to those characteristic of global models at higher energies. Using the dispersion relationship and the method of moments, the optical-model potential deduced from the 0- to 11.1-MeV neutron-scattering data was extrapolated to higher energies and to the bound-state regime. This extrapolation led to neutron total cross sections that were in good agreement with the experimental values to at least 20 MeV. For negative energies the values of the volume-integral-per-nucleon of the real potential are in excellent agreement with those needed to reproduce the observed binding energies of particle- and hole-states, and they give clear evidence of the Fermi-surface anomaly. It is argued that the use of a global optical model for interpreting low-energy data is suspect, but is probably a reasonably approximation at higher energies.

---

[1] A.B. Smith, P.T. Guenther, and R.D. Lawson, ANL/NDM-106 (1988)

4. Energy Dependence of the Optical-Model Potential for Fast-Neutron Scattering from Cobalt. (A. B. Smith, P. T. Guenther, and R. D. Lawson)

This work, cited in the 1988 DOENDC Reports, has been completed and published.[1]

---

[1] A.B. Smith, et al., Nucl. Phys. A483, 50 (1988).

5. Fast-Neutron Total and Scattering Cross Sections of ^{58}Ni. (A. B. Smith, P. T. Guenther, and R. D. Lawson)

The measurement of neutron total cross sections and elastic-scattering cross sections to 10 MeV were completed some time ago, as outlined in the 1988 DOENDC Reports. The inelastic-scattering cross sections have now been measured with good resolution, giving remarkably good definition of level structure up to excitations of ≈ 4.5 MeV. The interpretation of the experimental results is in progress, using both conventional optical-statistical and coupled-channels models. The resulting potentials are unexpectedly different from those applicable to ^{59}Co, and this discrepancy led to the ratio investigations cited above. The physical mechanisms involved are not yet clearly established. It is evident that the use of conventional size- and isovector-dependent global optical models is not suitable for quantitative description of the neutron interaction in this mass region.

6. Elastic Neutron Scattering from Indium. (A. B. Smith, R. D. Lawson, and P. T. Guenther)

Measurements are complete to ≈ 10 MeV and the model interpretations are in progress. At this point, a conventional spherical optical-statistical model appears to give a very good description of the observed cross sections. The implications of the dispersion relations are being examined.

7. Neutron Total and Scattering Cross Sections of Elemental Zirconium. (M. Sugimoto*, A. Smith, P. Guenther and R. Lawson)

The neutron total and elastic-scattering cross sections, cited in the prior report, are essentially complete. The inelastic-scattering measurements are in progress, including both good-resolution studies and measurements of continuum distributions. All of the measurements extend to 10 MeV. The physical interpretation of the experimental results is in progress. It is complicated by the elemental nature of the target which makes it impossible to explicitly fit isotopic experimental data. Various artifices have been employed, with considerable success, to circumvent this obstacle.

* Visiting scientist. Permanent address: Japan Atomic Energy Research Institute, Tokai, Japan.

8. Elastic-Scattering Cross Sections of Fe and Cr. (A. B. Smith and P. T. Guenther)

During this period, measurements of neutron elastic- and inelastic-scattering from elemental iron and chromium continued to incident energies of 10 MeV. The inelastic-scattering results include both the excitation of discrete levels and a continuum of levels.

9. Inelastic Excitation of Vibrational States in Pd. (A. B. Smith and P. T. Guenther)

Potentially large cross sections for the inelastic excitation of vibrational levels in the even isotopes of Pd are of concern in the context of the neutronics of fission products. Preliminary measurements at incident energies of ≈ 8 MeV indicate that such cross sections are indeed large. The work is being extended to lower energies.

10. Direct-excitation Contribution to Continuum Inelastic Scattering. (A. B. Smith and P. T. Guenther)

A significant high-energy direct-reaction component to continuum inelastic-neutron spectra has been reported.[1] This contribution is being examined in detail using the good resolutions obtained with the extended flight-path facility described in this report (see J.2). Preliminary results indicate a significant contribution at an incident energy of ≈ 8 MeV.

---

[1] Second Coordination Meeting of the IAEA Coordinated Research Project on Structural Materials, Vienna, February 15–17, 1988.

11. Resonance Effects in Neutron Scattering Lengths of Rare Earth Nuclides. (J. E. Lynn* and P. A. Seeger**)

Pulsed spallation neutron sources are now working far into the sub-Angstrom wavelength region for investigations into condensed matter and crystallography. It is therefore important to have detailed information on the energy variation of neutron coherent scattering lengths to facilitate accurate interpretation of the data collected on these instruments. Surprisingly, no nuclear data base of this kind exists. We have begun a program to remedy this situation. We have now completed work on the rare-earth group of nuclides. The neutron cross-section data in the literature for all the nuclides in this group that contain significant resonance effects below about 0.5 eV have been analyzed using (in most cases) a generalized single-level formalism. (The exception is ^{151}Eu, which we have analyzed using a three-level formula.) From the parameterization of these data we have deduced the complex coherent scattering lengths as a function of neutron energy (or wavelength). In a paper that we have submitted for publication in Atomic Data and Nuclear Data Tables, we have presented these computed results in the form of graphs and tables. A separate paper has been written to describe the analysis of the europium cross-sections, and has been submitted to the Journal of Applied Crystallography.

---

* Argonne Fellow. Permanent address: AERE, Harwell, United Kingdom.
** Los Alamos National Laboratory, Los Alamos, New Mexico.

B. CONTINUUM NEUTRON STUDIES

1. Double-Differential Inelastic-Neutron Emission Measurements and Analysis. (P. T. Guenther and A. B. Smith)

The underlying concepts of this investigation were outlined in the 1988 DOENDC Reports. To date, essentially all readily available monoisotopic elements suitable for an unambiguous determination of the nuclear temperature by this ratio method have been studied. During the past year Sc, V, Rh, and Au were investigated. One notable observation concerned Rh and Au, which, though quite different in mass, evinced very similar level densities.[1] On the request of other participants in an international level density research effort, the spectra of the last three years of this work are being assembled in a coherent cross-section library. This will complete the contributions to the coordinated research program, which is to conclude during the next year.[2] Experience gained in the analysis of the measurements of this work has suggested a possible means of estimating the precompound contribution to inelastic-neutron scattering from the asymptotic behavior of the nuclear temperature at lower excitation energies. This idea will be pursued in the coming months. Corraborative measurements, using the new extended-flight-path facility (see J.2), are to commence shortly.

---

[1] P.T. Guenther and A.B. Smith, Bull. Am. Phys. Soc. 33, 1567 (1988).

[2] 1988 Progress Report for Research Agreement CF/4412: IAEA Coordinated Research Programme on the Measurement and Analysis of Double-Differential Neutron-Emission Spectra in (p,n) and (α,n) Reactions.

2. Feasibility Study for ^{9}Be(n,2n)^{8}Be Neutron-Emission Cross Section Measurements in the Be(d,n) Thick-target Neutron Spectrum (D. L. Smith, J. W. Meadows, D. W. Kneff* and B. M. Oliver*)

There is considerable interest in the ^{9}Be(n,2n) reaction as a neutron multiplier for fusion reactor systems. Comparisons of integral and differential data indicate that knowledge of the basic differential cross sections for this reaction is still relatively uncertain and needs to be improved before reliable predictions can be made of neutron multiplication in engineering design studies for fusion reactors which utilize Be as a multiplier.[1]

Calculations based on the evaluated cross sections of Perkins et al.,[2] and knowledge of the Be(d,n) thick-target neutron spectrum,[3] indicate that an accurate integral cross section determination could be made at the Argonne FNG for an investment of about 100 hours of beam time. With the use of a deuteron beam energy of 7 MeV, it will be possible to produce a neutron spectrum which is sensitive to the cross section in the 2-6 MeV neutron--energy range. The production of ^{8}Be can be determined by measuring the helium (^{4}He) generated by the breakup of ^{8}Be that is trapped in samples of Be metal which are irradiated in this field. Fluence monitoring would be achieved by measuring ^{58}Co production via the ^{58}Ni(n,p)^{58}Co reaction, using foils of Ni metal in the sample packet along with Be. An agreement has been reached between Argonne National Laboratory (where the neutron irradiations will be done) and Rockwell International (where the helium measurements will take place) to pursue this experiment. Foils of high-purity Be metal have been obtained and a sample has been sent to Rockwell International for preliminary examination to insure that the unirradiated material is truly free of helium. The neutron irradiations are planned for 1989.

---

* Rocketdyne Division, Rockwell International Corporation, Canoga Park, California.

1 E.T. Cheng, "Review of the Nuclear Data Status and Requirements for Fusion Reactors", Nuclear Data for Science and Technology, ed. S. Igarasi, Saikon Publishing Co., Ltd., Tokyo, p. 187 (1988).

2 S.T. Perkins E.F. Plechaty and R.J. Howerton, Nucl. Sci. Eng. 90, 83 (1985).

3 D.L. Smith, J.W. Meadows and P.T. Guenther, ANL/NDM-90 (1985).

C. NEUTRON FISSION INVESTIGATIONS

1. A Search for Possible Structure in the $^{238}U(n,f)$ Cross Section Near 2.3 MeV. (J. W. Meadows, D. L. Smith, and L. P. Geraldo*)

This investigation was first presented in the 1988 DOENDC Reports. This work is now completed and a paper will soon be submitted to Annals of Nuclear Energy for publication. The shape of the $^{238}U(n,f)$ cross section was measured relative to the $^{237}Np(n,f)$ cross section over the neutron energy region 1.9-2.6 MeV to search for possible gross structure in the ^{238}U cross section. Forty-two measurements were made in this energy interval, with $\approx$ 24 keV energy resolution and a statistical accuracy of < 1%, using the $^{7}Li(p,n)^{7}Be$ reaction as the neutron source. No structure was observed. Absolute measurements were made at 2.150 and 2.453 MeV to normalize the shape data.

---

* Visiting scientist. Permanent address: IPEN, Sao Paulo, Brazil.

2. Adjustment of Evaluated Fission Cross Sections by Integral Data. (Y. Kanda*, Y. Uenohara, D. L. Smith, and J. W. Meadows)

Fission cross sections for ^{232}Th, $^{233,234,235,236,238}U$, ^{237}Np and ^{239}Pu, evaluated from differential experiments and compiled in JENDL-3T, have been adjusted by using integral fission cross-section ratios measured for $^{232}Th/^{235}U$, $^{237}Np/^{235}U$, $^{238}U/^{235}U$, $^{237}Np/^{238}U$, $^{232}Th/^{237}Np$, $^{236}U/^{235}U$, $^{239}Pu/^{235}U$, $^{233}U/^{235}U$, $^{234}U/^{235}U$, $^{234}U/^{238}U$ and $^{236}U/^{238}U$ in the continuum neutron spectrum produced by bombardment of a thick Be-metal target with 7 MeV deuterons. It has been demonstrated that the fission cross-section curves can be adjusted in the energy range between 1 and 10 MeV. The ratios of the calculated to experimental values for the integral fission cross-section ratios have been revised within ± 1.005, except for ^{232}Th whose result is 1.02. The original values are between 0.995 and 1.067 in JENDL-3T. The adjustment method developed in the present work is valuable to evaluate accurate and consistent cross-sections in the MeV neutron-energy region. Differential and integral data are complementary in a cross-section evaluation. The former are useful to determine shapes of the cross-section curves, and the latter serve to adjust their absolute values. The results of this investigation have been published in the proceedings for the Mito Conference, Mito, Japan, 1988.[1]

---

* Department of Energy Conversion, Kyushu University, Fukuoka, Japan.

1 Y. Kanda, Y. Uenohara, D.L. Smith and J.W. Meadows, "Adjustment of Evaluated Fission Cross Sections by Integral Data", Nuclear Data for Science and Technology, ed. S. Igarasi, Saikon Publishing Co., Ltd., Tokyo, p. 541 (1988).

3. Fifty Years of Nuclear Fission. (J. E. Lynn*)

A colloquium on this subject was given at Argonne National Laboratory, and the subject matter is to be issued as a report in the ANL/NDM report series. The abstract is given below:

The first section is an historical preamble about the events leading to the discovery of nuclear fission. This leads naturally to an account of early results and understanding of the fission phenomenon. Some of the key concepts in the development of fission theory are then discussed. The main theme of this discucssion is the topography of the fission barrier, in which the interplay of the liquid-drop model and nucleon shell effects lead to a wide range of fascinating phenomena encompassing metastable isomers, intermediate structure effects in fission cross sections, and large changes in fission product properties. It is shown how study of these changing effects and theoretical calculations of the potential energy of the deforming nucleus have led to a broad qualitative understanding of the nature of the fission process.

---

* Argonne Fellow. Permanent address: AERE, Harwell, United Kingdom.

4. The Topography of the Nuclear Fission Barrier. (J. E. Lynn*)

An invited review paper is being prepared for a special issue of the Indian journal Pramana. The abstract follows:

Fission theory first developed within the framework of the liquid drop model. Shell-model concepts were introduced into fission theory much later than they were in nuclear structure theory, but then with spectacular success in explaining striking experimental results relating to isomerism and neutron cross sections then emerging in actinide fission. In the last two decades the complex topography of the fission barrier that is the result of shell model theory has been a major theme in the expanding knowledge of fission, with most experimental data finding a natural explanation within

this theme. The development of the concept of shell-model structure in the fission barrier is outlined in this review.

---

* Argonne Fellow. Permanent address: AERE, Harwell, United Kingdom.

D. ACTIVATION CROSS-SECTION MEASUREMENTS

1. Differential Cross-section Measurements for the $^{27}Al(n,\alpha)^{24}Na$ Reaction. (D. L. Smith, L. P. Geraldo* and J. W. Meadows)

The $^{27}Al(n,\alpha)^{24}Na$ reaction is commonly used as a standard in neutron activation cross-section investigations. The cross section is very well known in the vicinity of 14 MeV, but at lower energies the uncertainties are substantially larger. A new measurement was undertaken in order to improve the knowledge of the cross section in the threshold region below 10 MeV. The data obtained in this experiment are in good agreement with the results of a 1979 evaluation,[1] and these data permit a reduction of the average uncertainty in the evaluated cross section from > 5% to ≈ 3% in the energy region below 10 MeV. The results of this work have been accepted for publication in Annals of Nuclear Energy.

---

* Visiting Scientist. Permanent address: IPEN, Sao Paulo, Brazil

[1] S. Tagesen, H. Vonach and B. Strohmaier, Physik Daten 13-1, Fachinformationzentrum Energie, Physik, Mathematik, GmbH Karlsruhe, Federal Republic of Germany (1979).

2. Measured Differential Cross Sections for the $^{24}Mg(n,p)^{24}Na$ Reaction. (D. L. Smith, L. P. Geraldo* and J. W. Meadows)

The $^{24}Mg(n,p)^{24}Na$ reaction appears on fusion nuclear data request lists because of its potential for neutron dosimetry applications. As described in the preceding contribution, the contemporary uncertainties in the evaluated cross section are too large to satisfy the requirements, particularly for neutron energies below 10 MeV. The present experiment was undertaken in order to improve upon this situation. The data obtained from this experiment agree well with the results of a 1981 evaluation,[1] and these data permit a reduction of the average uncertainty in the evaluated cross section from > 5% to ≈ 3% in the energy region below 10 MeV. The results of this work have been accepted for publication in Annals of Nuclear Energy.

---

* Visiting Scientist. Permanent address: IPEN, Sao Paulo, Brazil

[1] S. Tagesen and H. Vonach, Physik Daten 13-3, Fachinformationzentrum Energie, Physik, Mathematik, GmbH Karlsruhe, Federal Republic of Germany (1981).

3. A Search for Neutron-induced, Long-lived Activities in Copper, Silver, Hafnium, Europium and Terbium. (D. L. Smith, J. W. Meadows, L. R. Greenwood, and R. C. Haight*)

In 1988 the IAEA initiated a Coordinated Research Program aimed at developing cross section information for a select group of neutron-induced reactions which produce long-lived activities of interest to the waste disposal problem for fusion reactors. The present work was undertaken in support of this effort. Based on nuclear model calculations, it appeared feasible to investigate the production of certain activities in copper, silver, hafnium, europium and terbium which appear on the IAEA list. Two identical sample packets were prepared using chemically pure metallic and oxide materials. One packet was irradiated at the Argonne FNG accelerator in the continuum neutron field produced by the Be(d,n) thick target reaction (7 MeV deuteron energy). A second was irradiated at the Los Alamos Tandem Accelerator using tritium incident on hydrogen as a source of quasi-monoenergetic neutrons in the vicinity of 10 MeV. The components of both sample packets are in the process of being counted at Argonne. Several activities of interest are being observed, although it will be necessary to wait several months before the optimal counting conditions for measuring certain of these activities exist. Neutron fluences will be determined from the dosimeter foils that are included in the sample packets, ultimately enabling activation cross sections to be determined.

---

* Los Alamos National Laboratory, Los Alamos, New Mexico.

4. Production of ^{49}V (331 d), ^{93}Mo (3500 y), and ^{93}Nb (16.1 y isomer) near 14 MeV. (L. R. Greenwood, D. L. Bowers, and A. Intasorn*)

Measurements have been completed for the production of eight long-lived isotopes at neutron energies near 14 MeV).[1-3] The samples were irradiated at the Rotating Target Neutron Source II at Lawrence Livermore National Laboratory. Details of the neutron flux and energy distributions have been published.[1] The metallic samples of V, natural Mo, and ^{94}Mo (95%) were pressed into discs measuring 3 mm diameter by 1 mm thick. The samples were irradiated over many months to fluences as high as 10^{18} n/cm^2. We have already published results for the production of ^{91}Nb (650 y isomer) and ^{94}Nb (20,300 y).[1]

Subsequent to irradiation, the samples were analyzed following ion-exchange separations of Mo from Nb and Mn from V. Thin samples (< 1 mg/cm^2) were then deposited for x-ray counting relative to ^{55}Fe and ^{93}Nb (isomer) standards. The $^{50}V(n,2n)^{49}V$ reaction cross section was determined to be 258±39 mb at an energy of 14.3±0.4 MeV. The $^{94}Mo(n,2n)^{93}Mo$ result was 550±136 mb at 14.6±0.4 MeV. By comparison of natural and ^{94}Mo samples, we were able to determine a cross section of 5.7±0.9 mb for the production of ^{93}Nb (isomer) from ^{94}Mo and 1.36±0.27 mb from ^{95}Mo. The net production from natural Mo is then 0.75±0.11 mb. In these cases, several different reactions are involved and the average neutron energy is 14.6±0.4 MeV. There are no previously known measurements for any of these reactions.

These production cross sections are needed to predict the activation of fusion reactor materials, especially for waste material applications. For a fusion first-wall material, using the STARFIRE reactor design, calculations show that we will produce about 2.8 mCi/cc of ^{49}V in vanadium, and 28 mCi/cc of ^{93}Mo and 106 mCi/cc of ^{93}Nb (isomer) in molybdenum, assuming a fluence of 21.6 MW-y/m^2 and 3000 day cooling.

---

* IAEA fellow. Permanent address: Srinakharinwirot University, Bangkok, Thailand.

1 L.R. Greenwood, D.G. Doran, and H.L. Heinisch, Phys. Rev. 35C, 76 (1987).

2 L.R. Greenwood, ASTM-STP-956, 743 (1988).

3 L.R. Greenwood and D.L. Bowers, ASTM-STP-1001, 508 (1989).

E. NEUTRON CAPTURE STUDIES

1. Valence Capture Mechanism in Resonance Neutron Capture by ^{13}C. (J. E. Lynn* and S. Raman**)

The radiation width of the 153-keV (p-wave) neutron resonance of ^{13}C has presented problems for some time, appearing in early measurements to be remarkably large, in fact several eV in magnitude. We have undertaken a theoretical estimate of all the possible electric dipole transitions from this resonance, postulating the valence neutron capture mechanism, and using the data on the neutron width of the resonance and the single-particle spectroscopic factors of the final states in ^{14}C. We have avoided using the optical model in this calculation, basing the calculation on R-matrix formalism; the only model-dependent factors are those for representing the real well for the single-particle states postulated in the valence mechanism. The results indicate a total E1 radiation width of 0.2 eV, the bulk of this (0.16 eV) being in the transition to the 6.09-MeV state of ^{14}C.

Since these calculations were completed, Japanese colleagues (M. Igashira, Y. Dozono, H. Kitazawa at Tokyo Institute of Technology and M. Mizumoto at Japan Atomic Energy Research Institute) have completed the very difficult measurement of these radiation widths, with the results

$$\Gamma_\gamma(E1) = 0.18 \pm 0.08 \text{ eV},$$

the width to the 6.09 MeV state being 0.15 eV. It thus appears that the valence mechanism is predominant and gives an accurate description of the radiation properties for this resonance. These results will be submitted as a joint paper with the Japanese authors to Physical Review.

---

* Argonne Fellow. Permanent address: AERE, Harwell, United Kingdom.
** Oak Ridge National Laboratory, Oak Ridge, Tennessee.

2. Thermal-Neutron Scattering Lengths and Capture by Even Calcium Isotopes. (J. E. Lynn,* J. Richardson, S. Raman,** S. Kahane,** R. M. Moon,** J. Fernandez-Baca,** and J. L. Zaretsky†)

The following is the abstract of a paper accepted for publication in Physical Review.

Neutron diffraction patterns have been measured for highly enriched powder samples of calcite, using both steady-state and pulsed-neutron techniques. Greatly enhanced precision over previous work has been achieved for ^{40}Ca and ^{44}Ca, while the results for ^{42}Ca, ^{43}Ca, and ^{48}Ca represent new data. The coherent scattering lengths deduced from these measurements have been employed in a more definitive analysis of primary electric-dipole gamma-rays from thermal-neutron capture. In three cases (^{40}Ca, ^{42}Ca, and ^{48}Ca) the estimates from a spherical optical model formulation of the direct capture mechanism are in agreement with the experimental cross sections. In ^{44}Ca the theory overestimates the measured cross sections on average by about 60%; this divergence can be explained by considering the modifications to the theory due to collective vibrations of the ^{44}Ca core.

---

* Argonne Fellow. Permanent address: AERE, Harwell, United Kingdom.
** Oak Ridge National Laboratory, Oak Ridge, Tennessee
† Ames Laboratory, Ames, Iowa.

3. Analysis of Thermal Neutron Capture by ^{43}Ca. (J. E. Lynn* and S. Raman**)

The neutron coherent shattering length of ^{43}Ca has recently been measured by R. M. Moon, J. Fernandez-Baca (ORNL), J. L. Zaretsky (Ames), and J. Richardson (ANL). This allows the analysis of the capture cross section and gamma-ray spectrum of ^{43}Ca from the standpoint of the direct (potential and valence) mechanisms. The valence process is expected to be comparable with the non-resonant potential process because of the large influence of the 1.48-keV resonance, which apparently accounts for the major part of the thermal-neutron capture cross section. But earlier estimates of the valence width of this resonance have indicated that it is small compared with its measured width, the bulk of the latter being classed as more complicated compound-nucleus processes.

Our analysis shows in fact that the potential-plus-valence capture cross section accounts for as much as half of the total thermal-neutron cross section, with many of the primary transitions above 5-MeV gamma-ray energy being well explained by this mechanism. The reason for the strength of the effect is the constructive interference between the valence capture and the potential capture amplitudes.

The magnitude and spectral distribution of the compound nucleus component that is deduced from the data, after allowing for the direct capture component, is found not to be very well explained by standard models of resonance capture. We have found that a generalized valence model, which involves core states other than the ground state and which does not have the characteristics of interfering in a systematic way with potential capture or of correlating with a special set of final-state spectroscopic factors, can explain semi-quantitatively the properties of the compound-nucleus component.

---

* Argonne Fellow. Permanent address: AERE, Harwell, United Kingdom.
** Oak Ridge National Laboratory, Oak Ridge, Tennessee.

F. NEUTRON SPECTRUM INVESTIGATIONS

1. Investigation of the Low-energy Portion of the Neutron Spectrum from Bombardment of Thick Be-metal Targets with Deuterons.
(J. W. Meadows, D. L. Smith, and L.P. Geraldo*)

In 1987, time-of-flight measurements were made with a fission chamber placed about 2.7 meters from the Be-metal target at zero degrees. Data were acquired for deuteron energies between 4.0 and 7.0 MeV at 400-keV intervals. Work on this project was first described in the 1988 DOENDC Reports. During the past year, processing codes and procedures were developed, and the processing of this data set was completed. Qualitatively, the spectrum shape at energies below about 3 MeV is almost independent of deuteron energy. Most of the energy dependence is in the higher-energy portion. The spectrum appears to extend to energies below 50 keV, but the yield in this region is very small when compared to the total spectrum. Furthermore, it is uncertain because of a relatively large and poorly known background correction.

---

* Visiting scientist. Permanent address: IPEN, Sao Paulo, Brazil.

G. NUCLEAR-DATA EVALUATON ACTIVITIES

This aspect of the program is correlated with the measurement and physical-interpretation efforts, and consists of both comprehensive neutronic evaluated files and special-purpose evaluations. Much of the work is carried out in cooperation with R. Howerton and associates, Lawrence Livermore National Laboratory. The results are routinely submitted for inclusion in the ENDF/B evaluated file system. Prior submissions for ENDF/B-VI include comprehensive neutronic files for niobium and yttrium, as outlined in prior reports. A feature of the documentation provided with the comprehensive files is specification of measurements needed for improving the respective file (i.e., a request list generated from the considerations of the evaluation).

1. Vanadium. (A. B. Smith, D. L. Smith, J. W. Meadows, P. T. Guenther, R. D. Lawson, R. Howerton,* T. Djemil,** and B. J. Micklich**)

This comprehensive neutronic file has been completed and submitted for consideration as a part of ENDF/B-VI. Complete documentation has been provided.[1]

---

* Lawrence Livermore National Laboratory, Livermore, California.
** University of Illinois, Champaign, Illinois.
[1] A.B. Smith, D.L. Smith, P.T. Guenther, J.W. Meadows, R.D. Lawson, R.J. Howerton, T. Djemil, and B.J. Michlich, ANL/NDM-105 (1988).

2. Cobalt. (P. T. Guenther, R. D. Lawson, J. W. Meadows, M. Sugimoto,* A. B. Smith, D. L. Smith, and R. Howerton**)

This comprehensive neutronic file has been completed and submitted for consideration as a part of ENDF/B-VI. Complete documentation is provided.[1]

---

* Visiting scientist. Permanent address: Japan Atomic Energy Research Institute, Tokai, Japan.
** Lawrence Livermore National Laboratory, Livermore, California.
[1] P. Guenther, R. Lawson, J. Meadows, M. Sugimoto, A. Smith, D. Smith, and R. Howerton, ANL/NDM-107 (1988).

3. Bismuth. (A. B. Smith, J. W. Meadows, R. Howerton,* P. T. Guenther, R. D. Lawson, and D. L. Smith)

This comprehensive neutronic data file is very near completion and should be submitted very soon for consideration as a part of ENDF/B-VI. The new file has modest changes from the prior ENDF/B-V version, due to improved experimental information largely obtained in the associated measurement program.

---

* Lawrence Livermore National Laboratory, Livermore, California.

4. Beryllium. (M. Sugimoto,* A. B. Smith, and R. Howerton**)

Preparation of a comprehensive neutronic file is in progress, and some portions of it have already been incorporated in the proposed version of ENDF/B-VI, notably revisions of the elastic-scattering cross sections.

Changes have also been made to the total cross sections as given in ENDF/B-V. Aspects of this evaluation are discussed in a Laboratory report.[1]

---

* Visiting scientist. Permanent address: Japan Atomic Energy Research Institute, Tokai, Japan.

** Lawrence Livermore National Laboratory, Livermore, California.

[1] M. Sugimoto, P.T. Guenther, J.E. Lynn, A.B. Smith, and J.F. Whalen, ANL/NDM-108 (1988).

5. Elemental Zirconium. (A. B. Smith, P. T. Guenther, J. W. Meadows, D. L. Smith, and R. D. Lawson)

Work continues on a comprehensive evaluated neutronic file. Final results must await completion of the associated measurement and analysis program (see A.7).

6. ^{58}Ni Evaluation. (A. B. Smith, D. L. Smith, P. T. Guenther and J. W. Meadows)

This partial evaluation (from ≈ 650 keV to 20 MeV) is in progress. Completion is associated with relevant aspects of the ANL measurement program (see A.5).

7. ^{238}U Evaluation. (A. B. Smith and M. Sugimoto*)

This effort is a partial evaluation extending from the inelastic-threshold (45 keV) to 20 MeV, and including reaction channels only. The total cross section is complete (with uncertainty specification), and work is in progress on the scattering cross sections.

---

* Visiting scientist. Permanent address: Japan Atomic Energy Research Institute, Tokai, Japan.

H. NUCLEAR THEORY AND MODELS

1. Electroexcitation of 8- States in ^{52}Cr. (D. I. Sober,* L. W. Fagg,* B. Zeidman, R. D. Lawson, D. F. Geesaman, G. C. Morrison,** O. Karban,** X. K. Maruyama,*** H. de Vries,† E. A. J. M. Offermann,† C. W. de Jager,† R. A. Lindgren,†† and J. F. A. van Hienen†††)

This work has been published in Physical Review C.[1] The abstract is:

Inelastic electron scattering at incident energies between 170 and 260 MeV was used to identify and study M8 transitions in ^{52}Cr. A strong transition to an 8- state at

$$E_x = 15.47 \text{ MeV}$$

was observed, as well as number of weaker transitions. The results are compared with a single particle-hole shell-model calculation that uses a model space of the form

$$[(f_{7/2})^{11} \times g_{9/2}]_{8^-} \;.$$

The shell-model calculation and systematics in neighboring nuclei were used to determine the isospin of the observed states. The experimentally determined strengths exhaust 60.8% and 34.5% of the T = 3 and T = 2 sum rules, respectively.

---

* Catholic University of America, Washington, DC.
** University of Birmingham, Birmingham, United Kingdom.
***National Institute of Science and Technology, Gaithersburg, MD
† Nationaal Instituut voor Kernfysica en Hoge-Energiefysica, Amsterdam, The Netherlands.
†† University of Virginia, Charlottesville, VA.
†††Vrije Universiteit, Amsterdam, The Netherlands.
[1] D. I. Sober et al., Physical Review C38, 654 (1988).

2. Fragmentation of High-Spin Particle-Hole States in ^{26}Mg. (R. E. Segel,* A. Amusa,** D. F. Geesaman, R. D. Lawson, B. Zeidman, C. Olmer,† A. D. Bacher,† G. T. Emery,† C. W. Glover,† H. Nann,† W. P. Jones,† S. Y. van der Werf,†† and R. A. Lindgren†††)

This work has been accepted for publication in Physical Review C. The abstract is as follows:

The inelastic scattering of 134-MeV protons to 6- states in ^{26}Mg has been studied. Five 6- states were identified on the basis of their measured angular distributions and analyzing powers. By combining the results with those of companion electron scattering and (p,n) studies in ^{26}Mg and proton studies in ^{28}Si, it has been possible to extract isoscalar and isovector excitation amplitudes for each state. The results are compared with shell-model calculations.

---

* Permanent address: Northwestern University, Evanston, IL.
** Permanent address: Obafemi Auolowa University, Ile-Ife, Nigeria.
† Indiana University Cyclotron Facility, Bloomington, IN.
†† Kernfysisch Versneller Instituut, Groningen, The Netherlands.
†††University of Virginia, Charlottesville, VA.

2. Low-Lying States of ^{146}Tb, ^{148}Ho, and ^{150}Tm. (R. Broda,* P. J. Daly,* and R. D. Lawson)

The nuclei ^{146}Tb, ^{148}Ho, and ^{150}Tm were produced at the Argonne Tandem Linac using ^{60}Ni beams incident on ^{89}Y, ^{90}Zr, and ^{92}Mo, respectively.

In all three cases, an isomeric state was populated at an excitation energy of about 700 keV. This state, which was assigned a spin of 10+, decayed to a 7- level which subsequently depopulated to states with spins 6- and 5-. In addition to the excitation energies of these states in the various nuclei, the branching ratios for decay of the 7- states in all three cases were measured. The results for the excitation energies and decay rates were compared with the predictions of a shell-model calculation.

A paper on this work is in preparation and will be submitted to Z. fuer Phys. A.

---

* Purdue University, West Lafayette, Indiana.

4. Fitting Data from Collective Vibrators with Spherical Optical-Model Codes. (A. B. Smith)

Distortions in parameters resulting from fitting neutron data relevant to collective vibrators with conventional spherical optical-model codes have been numerically investigated in some depth. The distortions can be large and systematic. They are described in an unpublished memorandum available from the author.

I. ANALYTICAL METHODS DEVELOPMENT

1. Examination of Various Roles for Covariance Matrices in the Development, Evaluation, and Application of Nuclear Data. (D. L. Smith)

This work was undertaken in the preparation of a review paper for the Mito Conference, Mito, Japan, 1988. The abstract of this paper is as follows:

The last decade has been a period of rapid development in the implementation of covariance-matrix methodology in nuclear data research. This paper offers some perspective on the progress which has been made, on some of the unresolved problems, and on the potential yet to be realized. These discussions address a variety of issues related to the development of nuclear data, the evaluation of nuclear data, and the applications for nuclear data. Topics examined are: The importance of designing and conducting experiments so that error information is conveniently generated; the procedures for identifying error sources and quantifying their magnitudes and correlations; the combination of errors; the importance of consistent and well-characterized measurement standards; the role of covariances in data parameterization (fitting); the estimation of covariances for values calculated from mathematical models; the identification of abnormalities in covariance matrices and the analysis of their consequences; the problems encountered in representing covariance information in evaluated files; the role of covariances in the weighting of diverse data sets; the comparison of various evaluation procedures involving covariance matrices; the role of covariances in updating existing evaluations; the influence of primary-data covariances in the analysis of covariances for derived quantities (sensitivity); and the role of covariances in the merging of diverse nuclear data information.

This invited paper has been published in the proceedings of the Mito Conference.[1]

---

[1] D.L. Smith, "Examination of Various Roles for Covariance Matrices in the Development, Evaluation, and Application of Nuclear Data," Nuclear Data for Science and Technology, ed. S. Igarasi, Saikon Publishing Co., Ltd., Tokyo, p. 425 (1988).

2. Development of Activation Data Processing Codes for an IBM PC. (L. P. Geraldo* and D. L. Smith)

Work continued on implementation on an IBM PC of a complete data processing software package for the activation cross section program at Argonne. Two important codes (ACTIVE and ACTIVD) which are used in the computation of geometry and neutron source corrections were converted to the PC, and these were employed in the analysis of data from the ^{24}Mg(n,p)^{24}Na and ^{27}Al(n,α)^{24}Na experiments (see D.1 and D.2).

---

* Visiting scientist. Permanent address: IPEN, Sao Paulo, Brazil.

3. Probability Theory in Nuclear-Data Research. (D. L. Smith)

Considerable progress was made on the NEANDC monograph effort during this period. First, Report ANL/NDM-92, which is designed to serve as a basic primer on probability theory, has been sent out for reproduction. It will be ready for distribution in early March 1989. Work commenced on the actual body of the planned NEANDC monograph during this period. By the end of 1988, six chapters had been written (roughly half of the book). An agreement has been reached between the Nuclear Energy Agency (NEA) and the American Nuclear Society (ANS) concerning eventual publication of this document. It is hoped that the actual writing of the monograph will be essentially complete by the end of 1989. However, preparation of a camera-ready manuscript within a reasonable time frame following this will clearly challenge the resources of the Laboratory, as was the case for Report ANL/NDM-92.

4. A Vector Model for Error Propagation. (D. L. Smith)

A simple vector model for error propagation has been considered. It yields the same results as the more rigorous and conventional statistical approach. It also offers a convenient visualization of the nature of error propagation while, at the same time, readily demonstrating the significance of uncertainty correlations. A paper on the results of this investigation is in preparation.

5. Investigation of the Nature of Positive Definiteness for Covariance Matrices. (L. P. Geraldo* and D. L. Smith)

This investigation was discussed in the 1988 DOENDC Reports. Since then, a Laboratory report on this subject has been prepared and distributed.[1]

---

* Visiting scientist. Permanent address: IPEN, Sao Paulo, Brazil.

[1] L.P. Geraldo and D.L. Smith, ANL/NDM-104 (1988).

6. Covariance Analysis and Fitting of Germanium Gamma-ray Detector Efficiency Calibration Data. (L. P. Geraldo* and D. L. Smith)

The detailed procedures for assessing errors associated with the development of germanium detector calibration data, and the fitting of such data with parameterized calibration curves, have been investigated. A preliminary report of this work has been issued,[1] and a paper summarizing the final results is in preparation. The abstract for the draft version of this paper is as follows:

Quantitative measurements and error assessments for photon yields from neutron-induced reactions are required in the determination of many of the cross sections which are important for nuclear technology applications. This paper documents the procedures used for several years in this laboratory to determine the full-energy peak efficiency (ϵ) versus photon energy (E), and to derive estimates of the associated uncertainties, for those cross-section experiments which employ a germanium detector. The method involves the least-squares fitting of the empirical, linear, parameterized formula,

$$\ell n\ \epsilon = \sum_{k=1}^{m} p_k (\ell n\ E)^{k-1},$$

to calibration data acquired using an assortment of standard gamma-ray sources. Random and correlated (systematic) uncertainties are treated in detail through the formation and application of a calibration-data covariance matrix. The error in the derived detector efficiency at a particular energy, and its correlation to the corresponding error at any other energy, can then be deduced quite easily, within the range of applicability of the fitted curve, using conventional error propagation techniques. This approach is illustrated by presenting a detailed example.

---

* Visiting scientist. Permanent address: IPEN, Sao Paulo, Brazil.

[1] L.P. Geraldo and D.L. Smith, Bull. Am. Phys. Soc. 33, 1062 (1988).

7. Investigation into the Utilization of Advanced Statistical Methods in the Characterization of X-ray Spectra for Applications in Radiology and X-ray Fluorescence Analysis. (R. T. Mainardi* and D. L. Smith)

An investigation has been made into the utilization of advanced statistical procedures in the characterization of X-ray spectra which are produced by commercial X-ray tubes and in the analysis of X-ray fluorescence data. This work is motivated by the desire to develop reliable procedures for representing X-ray spectra, to satisfy important needs in X-ray radiology for medical and analytical applications, and to obtain improved reliability in X-ray fluorescence analysis for materials composition determinations. For X-ray spectrum characterization, the methods under consideration resemble those used in contemporary neutron dosimetry for nuclear reactors. Estimators for the essential spectral parameters are derived from least-squares adjustments, based on consideration of a variety of either direct (e.g., semiconductor diode measurements) or indirect (e.g., integrated X-ray dose measurements for collections of external absorbers) X-ray data and their uncertainties (including correlations). These procedures yield statistically unbiased mean values for the spectral parameters and their uncertainties (including correlations). This work is part of an on-going collaboration which has been established between this laboratory and the University of Cordoba, Cordoba, Argentina.

---

* Visiting scientist. Permanent address: Physics Dept., University of Cordoba, Cordoba, Argentina.

8. Implementation of Model Codes on a Small Computer. (J. F. Whalen)

The explicit fitting of extensive experimental data with model codes can be very time-consuming on even very large computational equipment. The consequent costs rule out many model approaches. Therefore, a spherical optical-statistical model code (ABAREX), a coupled-channels code (ANLECIS), and a pre-compound code (ALICE) have been implemented on a small DEC Micro-VAX computer. Computational times are 5-7 times longer than at an IBM-3033 mainframe facility, but computations can be in a background mode for essentially unlimited time, and at no cost. With this approach, extensive experimental fitting is carried out (e.g., coupled-channels fitting) in a manner that is not fiscally practicable at a mainframe facility. The converted programs have been carefully checked for computational accuracy.

9. Extension of the Neutron-Scattering Data Analysis Code SCATTER to the FNG Micro-VAX Computer. (P. T. Guenther)

The impending changeover from a CDC on-line data-acquisition computer system to one based on DEC equipment has made it desirable to revise the downstream data reduction codes to take advantage of available electronic data transfer capabilities that now link the on-line DEC systems with our Micro-VAX as well as the PCs. To this end, the code SCATTER, mentioned in the 1988 DOENDC Reports, is now being adapted to the Micro-VAX. With the completion of this conversion, the ten-channel data-handling system will be up-to-date.

J. INSTRUMENTATION DEVELOPMENT

1. Harmonic Buncher. (A. B. Smith and J. W. Meadows)

The harmonic-buncher system, cited in the previous report, has been installed at the Fast Neutron Generator. The result has been a factor of about two increase in nsec-pulse intensity at repetition rates varying from 0.1 to 2 MHz. This intensity increase is highly valued in time-of-flight measurements. It considerably extends ion-source useful life, and was achieved at very modest cost.

2. Extended Flight Path. (A. B. Smith and P. T. Guenther)

A special-purpose facility has been made operational for high-resolution time-of-flight measurements. The nsec pulsed source is situated in a heavily-shielded cave that reduces laboratory neutron backgrounds with full source intensity to no more than twice the ambient natural background. A heavily shielded scintillation detector of $\approx$ 1300 cm^2 is placed at a flight path of $\approx$ 15 m. The flight path can be varied from 8-30 m. The current measurement program uses the D(d,n) source reaction at this facility to obtain good scattered-neutron resolutions, e.g., 0.1-0.3 MeV at 8.0 MeV, depending upon the magnitude of the relevant cross sections. The practical energy resolutions are essentially governed by the energy spread of the neutron source. The facility is primarily used for the measurement of inelastically-scattered neutron groups, but it also has a very clean background and will be used for continuum-inelastic-scattering measurements consisting of both statistical and pre-compound contributions. There is an attractive potential for good-resolution nuclear-spectroscopy studies using neutrons (e.g., (d,n) measurements) that will be exploited in the future.

1. BROOKHAVEN NATIONAL LABORATORY

The reactor-based neutron-nuclear physics research at BNL is composed of two categories: the study of nuclear structure with the (n,γ) reaction, and the spectroscopy of neutron-rich, fission product nuclides. These programs use the H-1 and H-2 beam ports of the HFBR. The tailored beam facility produces beams of thermal, 2- and 24-keV neutrons. A monochromator is used for resonance neutron studies. The TRISTAN on-line mass separator is used with a U-235 target to produce fission product nuclei. These facilities are operated in collaboration with a wide variety of collaborators from national laboratories and universities. The following sections describe the recent (n,γ) and TRISTAN studies of relevance to this report.

A. p-n INTERACTION

This general topic concerns a broad variety of interrelated subjects, including nuclear phase transitions, the development of collectivity, the evolution of subshell structure, the behavior of intruder states, and the structure of the valence space. These areas have long been of interest to TRISTAN because of the access it provides to the phase transitional regions around A = 100 and A = 150 and to near semi-magic nuclei such as Cd, where intruder states are systematically observed, and because of the g-factor measurement capabilities which have been developed into a tool for rather directly counting effective numbers of valence nucleons.

1. Phase Transitions

A few years ago, the N_pN_n scheme was developed in this program. Basically, by correlating collectivity with the product of the number of valence nucleons, it achieves a great simplification of nuclear systematics, especially in transition regions. Moreover, diverse regions, which appear very different in traditional plots, actually have nearly identical behavior in the N_pN_n scheme. A refinement of this idea, the P-factor, puts the scheme on an absolute footing; nuclei become deformed in all regions of medium to heavy nuclei when $P = N_pN_n/(N_p + N_n)$ reaches a critical value, $P_{crit} \approx 4\text{-}5$. It is simple to show that the absolute value correlates well with the point at which the integrated p-n interaction begins to dominate the nuclear pairing interaction.

To achieve smooth plots in the N_pN_n or P-factor schemes, a proper accounting of subshell effects in the counting of valence nucleons is required. Following a number of TRISTAN g-factor studies, a technique was developed to integrate $g(2^+_1)$ values and $B(E2{:}0^+_1 \rightarrow 2^+_1)$ values so as to extract effective numbers of valence protons and neutrons. This work confirmed the working assumption (the Federman-Pittel picture) in the A = 150 region. This year we have begun to extend the analysis to the A = 100 region with a study of existing data and new measurements of $g(2^+_1)$ for

^{98}Sr. The basic results again show the dissolution of a shell gap (at Z = 40) as a function of neutron number but likewise show that this region is more complicated and there is a not-yet-understood Z dependence to this vibrational evolution. In particular, it was found that $g(2^+_1)(^{98}Sr) \approx g(2^+_1)(^{102}Mo)$ and that both are larger than $g(2^+_1)(^{100}Zr)$. Thus the apparently decreasing trend from ^{102}Mo to ^{100}Zr is not continued but rather ^{100}Zr now appears anomalous. Efforts to understand these phenomena continue.

2. Collectivity

Another phenomenon noticed last year was the saturation in collectivity near mid-shell in deformed regions, specifically the rare earths. This is completely contrary to normal valence models, like the Interacting Boson Approximation (IBA), which predict that $B(E2:0^+_1 \rightarrow 2^+_1) \approx N^2$, where N is the valence nucleon number. A simple explanation was proposed by calculating explicitly the integrated quadrupole p-n interaction (called S_{pn}) and observing that while it is linear in N_pN_n early in a shell, it too saturates near mid-shell. The reason is that there is poorer overlap of proton and neutron wave functions in mid-shell than earlier on, where all orbits are equatorial (downsloping in the Nilsson model). In this way it was possible to quantitatively account for the B(E2) data. Nevertheless, both the linearity of S_{pn} and its saturation are theoretical constructs.

In an important new development this year, a way was found to actually extract empirical p-n interaction strengths, ΔV_{pn}, for any given proton and neutron and the integrated valence p-n strength, V_{pn}, as well. The idea is based on a particular double difference of binding energies that estimates the T = 0 interaction of the last proton and last neutron. (Though different in detail, it is reminiscent of the mass loops of Garvey-Kelson and Sakai.) This work, inspired by and involving use of recent TRISTAN measurements of binding energies near A = 150, led to two remarkable results: V_{pn} was found to increase exactly linearly with N_pN_n early in a shell and then to slow its rate of increase near mid-shell. This empirically confirms three critical ideas about the p-n interaction. First, it provides direct empirical support for the N_pN_n scheme. Secondly, it verifies the saturation phenomena as calculated with the quadrupole p-n interaction. Thirdly, since V_{pn} slows its increase but does not become asymptotically constant, it shows that there must be another component of the p-n interaction, a monopole interaction, which is always attractive and relatively constant (it is independent of the angular orientation of the orbits), thus providing a base to the p-n strength.

3. Intruder States

An important aspect of the p-n interaction concerns intruder states. These are generally thought to involve proton 2p-2h excitations which, in effect, increase the number of valence protons. They, therefore, have a larger N_pN_n product than the normal states in the core nucleus and are both more deformed and descend faster in energy with increasing N_n so that their energies minimize near mid-neutron shell. This picture has been used to explain the Cd and Pb intruder states and systematics. In Cd, it implies that the intruder states will rise in energy in the neutron rich region. In earlier TRISTAN experiments, this was confirmed. It was shown that the normal levels left behind are the first-known good examples of near-harmonic vibrators.

In another application of the technique developed to extract empirical p-n interaction strengths, ΔV_{pn} values were obtained for both normal and intruder states in Cd. The results confirm empirically the premise of the standard model and are also sensitive to, and provide a signature of, the relative deformations of these two level systems. These states confirm the larger deformation of the intruders.

A critical test of the Cd intruder/vibrational picture involves measurements of absolute B(E2) values for key E2 transitions (that is, level lifetimes). These lifetimes are in the range up to about 50 ps and have, heretofore, been inaccessible. Now, however, with our new fast timing capabilities (see below), lifetimes as low as ≈5 ps can be measured. The first extensive experiments to actually use the technique were carried out for $^{116-120}$Cd this year. The results confirm the basic collective character of the 2^+_1 level and the two-phonon triplet levels. They show that in ^{116}Cd it is the 0^+_2, not the 0^+_3, level that is the intruder, and they are consistent with the 0^+_3 as an intruder in ^{118}Cd (although the uncertainties are large). The ^{116}Cd result shows that the 0^+_2-0^+_3 mixing amplitude is ≈0.25, in excellent agreement with our earlier estimate of 0.21 for a schematic model.

4. Coexistence

The study of the p-n interaction included other studies this year as well. We briefly note a few--the P-factor idea was extended to masses and was found to linearize their behavior in certain regions and to provide a better technique for predicting nuclear masses. In the A = 100 region, other lifetime measurements (by the slope/deconvolution method) radically revised the existing coexistence picture. Whereas the 0^+_1 (ground state) and 0^+_2 excitations were thought to be spherical and deformed in both ^{96}Zr and in ^{98}Sr and ^{100}Zr, the new data show that, in the latter two nuclei, both 0^+ excitations are deformed--one moderately, one strongly. Further theoretical work is needed to understand this surprising result. A number of TRISTAN studies, one in collaboration with other groups (Kentucky, Julich, Budapest, and Lawrence Livermore Laboratory (LLL)), have sorted out several coexisting families of levels in ^{96}Zr, a nearly doubly magic nucleus at the edge of a deformed region. This pivotal nucleus is more complex than imagined just a couple of years ago: its central role in the A = 100 region mandates urgent and serious theoretical study.

Finally, several studies of odd-A nuclei (e.g., ^{101}Y) and Coriolis coupling in the A = 100 region have further probed the development of deformation and the Nilsson structure near N = 60.

B. NUCLEAR SYMMETRIES

This has been a topic of study for many years in this program and continuing work was carried out during this year. Since the concepts are more familiar than that of our newly-evolving understanding of the p-n interaction, the discussion here can be briefer.

The IBA predicts three basic nuclear symmetries, that is, rotational SU(3), vibrational U(5), and axially asymmetric rotors (γ soft) or O(6). It has now turned out that the first known examples of all three of these symmetries, O(6), SU(3), and U(5) have been discovered in this program (in ^{196}Pt, the Yb and Hf nuclei near N = 104, and in ^{118}Cd). Also, the renowned study of ^{168}Er resulted from "complete spectroscopy" with the (n,γ) reaction. In the current time period, further studies of symmetries were carried out primarily in the Te isotopes, specifically, $^{124,126}Te$, in which ARC studies at 2 and 24 keV were done to test a recent proposal by Hamilton et al. that these nuclei also exhibit O(6) symmetry. The results, currently still under analysis, tentatively indicate that there is, in fact, virtually no solid evidence for O(6) character in these nuclei and that, rather, they more likely resemble vibrational nuclei with low lying intruder states. Other work on this theme centered on the vibrational structure of ^{118}Cd (see below) via fast-timing lifetime measurements in the few ps range. The basic vibrational character (1- and 2-phonon) of the 2^+_1 and 4^+_1 states was verified in $^{116-120}Cd$. Also, as described last year, a technique has been developed to extract effective valence proton and neutron numbers from $g(2^+_1)$ factors and $B(E2:0^+_1 \rightarrow 2^+_1)$ values. It uses a universal IBA-based formula for g factors but relies on B(E2) expressions which are only valid in nuclei near the IBA symmetries. Since most nuclei are intermediate in character, there is a need for more general B(E2) expressions. Last year, an analytic formula for the SU(3)-O(6) region was developed. This year a more general universal expression was formulated. It is currently being tested against universal calculations.

C. NEAR MAGIC NUCLEI AND TESTS OF THE SHELL MODEL

The ability of TRISTAN to access nuclei near new magic numbers provides an important test of shell model predictions.

A TRISTAN study of ^{96}Y decay, and the assignment of the Y parent as $J^\pi = 0^-$, has led to the possibility of studying a fast, first-forbidden $0^- \rightarrow 0^+$ β decay in a nearly double-magic nucleus (^{96}Zr). The result, a log ft of 5.6, is one of the fastest known. Since the wave functions of the normal states in ^{96}Zr, which has a closed proton shell at Z = 40 and a nearly-magic neutron number of N = 56 ($d_{5/2}$ subshell), are rather well known, a comparison of the empirically-measured absolute log <u>ft</u> value with one calculated in the shell model allows a sensitive test of the presence of meson exchange effects in β decay. The Zr example is comparable in quality, in fact, to those in much lighter nuclei, such as ^{16}O, and is one of the only tests available in heavy nuclei. The conclusions indicate positive evidence for meson exchange effects of the same order as found in light nuclei, and a paper is under preparation.

Weak interaction processes in nuclei normally can be assumed to arise solely from nucleonic degrees of freedom. Meson exchange currents should have a large effect on the rank-zero time-like component of the axial current, A_0, which affords a unique opportunity to test our understanding of the interplay of pions and nucleons in nuclei. The ideal process for the study of A_0 is $\Delta J = 0$ $(\pi_i\pi_f = -)$ β decay since in this process rank-zero matrix elements of the time-like and space-like components of the axial current are dominant. The expected enhancement of the time-like component in this process is 40-70 percent.

Experimental work on this issue included extraction of more accurate $\Delta J = 0$ branching ratios in ^{43}K. Theoretical work involved calculations of all known and most-possible, first-forbidden β decays in the $A = 34$-44 region. Further evidence was found for meson enhancement of the rank-zero, time-like component of the axial current. Moreover, a most interesting possible decay was pinpointed; namely $^{38}Ca(0^+{}_1) \rightarrow {}^{38}K(0^-{}_1)$, which is predicted to be 60 percent of a single-particle unit. It is also a $d_{3/2} \rightarrow p_{3/2}$ transition and, as such, will have a different dependence on the uncertainties of the calculation than the other cases studied (which are all $s_{1/2} \rightarrow p_{1/2}$ transitions). The feasibility of detecting this and other decays (near $A = 90$-100) is being surveyed.

Several other shell model studies have ensued this year. TRISTAN studies of ^{74}Cu and the $N = 83$ isotones required detailed calculations, on the one hand, to investigate effective interactions for large basis calculations and, on the other, to study the quality of the $N = 50$ shell closure.

The concept of valence mirror nuclei has recently been proposed. An example of such a pair is ${}_{60}{}^{142}Nd_{82}$ and ${}_{50}{}^{110}Sn_{60}$ which are magic in neutrons and protons, respectively, and contain 10 valence nucleons of the other type. Their excitation spectra are nearly identical. In an effort to understand this effect, shell model calculations of, first, ^{142}Nd, and, subsequently, the whole Ce, Nd, Sm, Gd $N = 82$ region and the mirror region in Sn were carried out. The ^{142}Nd core is an ideal one since, although it has 10 valence protons, it is easy to predict its structure <u>analytically</u> in the shell model/seniority scheme if one invokes the reasonable assumption that the residual interaction is short range (e.g., a delta interaction). These predictions can then be compared with relatively complex diagonalizations.

D. r-PROCESS NUCLEOSYNTHESIS

The calculation of r-process nucleosynthesis is beset with currently insurmountable difficulties because these calculations require input of both stellar and nuclear parameters, and the latter are more or less completely unknown for the neutron rich nuclei through which the r-process path flows. Therefore, the empirical characterization of any of these nuclei, and in particular those where the r-process path passes through closed shells, is extremely critical in restricting the possible stellar scenarios. The three most critical nuclei are ^{80}Zn, ^{130}Cd, and ^{195}Tm. The ^{80}Zn study was first reported a couple of years ago, and now the full level scheme has been published. An attempt to study the ^{130}Cd region has so far not been successful due to the combination of low yields and conflicting lifetimes from nearby nuclei in the 130 mass chain. The history of TRISTAN ion source development has heretofore stressed the invention of powerful, general sources capable of producing a wide array of neutron rich species. As the program has amply demonstrated, this has been a key ingredient in its success. Occasionally, however, these sources provide too much and, as in the present case, the activities of interest are obscured. Therefore, a new effort to develop element-specific sources, targets, and techniques was initiated last year. The results are promising. The first generation of these sources is specifically designed to isolate Cd so that the key r-process stumbling block can be removed. We hope for a successful experiment in the next year or two. Later this year another attempt to study ^{81}Zn will also be made. The r-process exhibits smaller mass peaks in the A = 100 and A = 160 mass regions as well. Therefore, studies of nuclei in these regions are also useful input to understanding the r-process and are planned in the next year.

E. FAST TIMING MEASUREMENTS OF SHORT NUCLEAR LIFETIMES

The measurement of absolute transition rates provides some of the most sensitive tests of nuclear models. This is particularly so in even-even nuclei where E2 transitions are the key signatures of collectivity and of vibrational and rotational structure. While E2 branching ratios can provide valuable information and test key selection rules, absolute B(E2) values are necessary to directly sample individual transition matrix elements. Near stability, absolute B(E2) values are readily available through Coulomb excitation and inelastic scattering techniques. Neutron deficient nuclei are generally produced in heavy ion reactions which bring in large amounts of angular momentum; the subsequent recoil of the residual nucleus then permits the measurement of absolute transition rates through a variety of Doppler techniques. Unfortunately, on the neutron rich side of stability, no comparable techniques are generally available. These nuclei are usually produced as a result of the fission process, induced via low energy neutrons, and hence their negligible recoil velocity renders Doppler techniques inapplicable. For this reason, until now, the confrontation of nuclear models with the data for neutron rich nuclei has been considerably more qualitative than nearer stability and for neutron deficient nuclei.

Significantly more critical tests would be possible if absolute B(E2) values and level lifetimes were available for neutron rich nuclei.

The basic idea of the method for measuring level lifetimes is the following. The decay process envisaged is one in which a β transition is followed by a sequence of γ-ray transitions cascading in parallel and series through a level scheme. The fast timing is achieved between well-shielded, precisely-positioned, thin-plastic β and BaF_2 γ detectors positioned close to the radioactive source. In general, γ decay schemes can be rather complex. Since the BaF_2 resolution is rather poor, the attendant ambiguities that could arise are minimized by the use of a large Ge detector in triple coincidence mode to define particular cascades of interest.

There are two principal advances that have led to the present improvements. The first is the use of a thin β detector in which $\Delta E_\beta \approx$ 600 keV is <u>independent</u> of incident β energy for $E_\beta \geq 1.5$ MeV. Thus, the timing response of this detector is nearly independent of the particular levels, β energies, and γ cascades involved. This is crucial to certain subtraction and calibration techniques. The second is the use of the recently-discovered, fast component in the light emission from BaF_2 crystals, along with the technique of dynode timing. This latter technique results in a $\approx$30 percent reduction in the Full Width at Half Maximum (FWHM) of the timing peak. In addition to these two factors, the use of modern, fast timing electronics, and particularly selected constant-fraction discriminators, results in a typical timing resolution for prompt transitions of 100 ps FWHM.

With such time resolution there are two techniques for the extraction of nuclear lifetimes. If the lifetime involved is $\approx$40 ps or greater, it can be deduced from the decay slope which will be visible on the "delayed" side of the time distribution time to amplitude converter (TAC) peak. The second method, applicable to shorter lifetimes, $\geq$5 ps, involves the detection of small shifts in the centroid of the TAC peak.

There are a number of corrections that must be incorporated before a lifetime is extracted from the observed centroid shift, and much of the effort this year has gone into a careful study of these corrections, their uncertainties, and systematic ways to deal with them. As a result, we now can extract half-lives of $\approx$5 ps and above with uncertainties of $\pm$4 ps. The corrections just mentioned have three principal sources: 1) the centroid position of true prompt peaks has a γ-ray energy dependence, 2) there is an energy dependent shift in the centroid of the prompt peak which depends on whether the full γ-ray energy, or a fraction of that energy from a single Compton scattering event is collected in the BaF_2 crystal, and, 3) there is a shift due to the fact that the energy gates set on the BaF_2 spectrum select both real and background events, which can have different time distributions.

In the centroid shift method all lifetimes are determined by comparison to a standard "walk" curve giving the normalized position of a true prompt centroid as a function of γ-ray energy. The walk curve is energy dependent due in part to the energy dependence of the electronics and to geometrical effects in the BaF_2 crystal. The latter are especially significant for very-short lifetime measurements because different γ rays interact, on average, at different depths in the 1 cm thick BaF_2 crystal. The walk curve is obtained from a set of calibration transitions (of various energies) that are known to be prompt.

The second correction is related to the fact that in typical spectra the BaF_2 gates are not set on the Compton plateaus but on the full energy peaks which arise, not primarily from photoelectric events, but from multiple Compton scattering within the crystal. Therefore, on average, full energy detection is a slower process. The amount of delay is also γ-ray energy dependent.

The subtraction of background gates from peak gates in normal γ-γ coincidence spectroscopy is a relatively straightforward process designed to remove accidental coincidences. However, in these fast timing experiments the background underneath a peak in the BaF_2 spectrum arises from Compton events of higher energy transitions which can, and usually do, have different lifetimes than the peak of interest. Therefore, the subtraction involves not simply a reduction in the number of counts in the spectrum but also a shift in the centroid of that spectrum.

Following a careful study of these (and other) corrections and their associated uncertainties, the fast timing technique is now capable of measuring half lives as low as 5 ps by the centroid shift technique and 20-30 ps with the slope method. The technique is now out of the developmental stage and is being used as a practical tool (although further development also continues). The first uses of it are centered on several lifetimes (mostly from a few up to 26 ps) in $^{116-120}Cd$ and of longer lifetimes near A = 100. The physics content of these studies was described above.

F. National Nuclear Data Center

1. Cross Section Evaluation Working Group (CSEWG)

CSEWG completed its 22nd year of activity with its annual meeting on May 10-12, 1988. With the work on the standards evaluations completed, emphasis is now being placed on the completion of evaluations, testing and release of ENDF/B-VI. The projected release date for ENDF/B-VI is fall of 1989. Many new and revised evaluations were reviewed at a four-day meeting held in December 1988 at ORNL. The remaining evaluations will be reviewed at the April 1989 regular CSEWG. A special CSEWG meeting will be held in September 1989 to review integral testing results for ENDF/B-VI and approve release.

Significant progress on future international cooperation in nuclear data evaluation was made during the NEANDC meeting held in September 1988 at Los Alamos. Under the sponsorship of the NEANDC and NEACRP, it was agreed that the U.S. (ENDF/B), Western Europe (JEF/EFF) and Japan (JENDL) would formalize and expand their cooperation in nuclear data evaluation. The respective data files of the participants would be freely available to the other participants. While ENDF/B-VI will be freely available throughout the world, no commitments were made by the other participants. The first planning session for the committee coordinating this cooperative effort will be held in Paris in May 1989.

Due to drastically reduced funding, the production of ENDF/B-VI has taken much longer to complete than previous releases of ENDF/B. We also recognize that all the improvements which we had hoped to make could not be completed. Nevertheless, we expect ENDF/B-VI will be a significant improvement over its predecessor. In the future CSEWG will continue to make improvements to the data file from its own resources and from the newly formed international cooperative effort.

2. Nuclear Data Sheets

The NNDC has been producing the Nuclear Data Sheets at the rate of about an issue a month. Of these, nine issues a year are devoted to nuclear structure evaluation and the remaining three to the publication of Recent References.

The Center evaluated A=69, 137, 146, 147 and 148 and submitted them for publication; A=50, 58 and 66 are being evaluated.

The U.S. is part of an international network of evaluators contributing recommended values of nuclear structure information to the Evaluated Nuclear Structure Data File (ENSDF). Publication of the Nuclear Data Sheets proceeds directly from this computerized file. In addition to the U.S., evaluations have been received or are anticipated from the Federal Republic of Germany, U.S.S.R., France, Japan, Belgium, Kuwait, Sweden, the People's Republic of China and Canada. India has joined the network and has started evaluation of mass-chains.

Use of the concise format for the published A-chains in the Nuclear Data Sheets is functioning smoothly. This format reduces the size of the publication without omitting essential information and improves its readability.

3. Online Services

For approximately 3 1/2 years, the NNDC has offered online access to several of its nuclear data bases. This service is available on the NNDC's VAX-11/780 computer via HEPNET (PHYSNET), INTERNET or over telephone lines. During the past year, the service has been used by more than 50 researchers. More than one-half of the queries have been to the NSR data base. The number of retrievals performed has increased by 60%. The NSR data base system was redesigned to improve storage and retrieval efficiency. Considerable effort has gone into correcting errors in the AUTHOR field in order to improve the author retrieval facility.

4. Neutron Data Atlas

The neutron data atlas, Neutron Cross Sections, Vol II., Book of Curves, was published in July 1988. Copies may be ordered from Academic Press for $59.50.

5. Charged Particle Reaction Data

Before the Nuclear Data Project at ORNL was reorganized in the late 1970's, it included a small charged particle reaction data compilation activity. This activity was transferred to the NNDC along with the responsibility for publishing the NUCLEAR DATA SHEETS. For several years after the transfer, as part of an international charged particle data compilation effort, we were able to continue to produce a bibliography of charged particle cross sections and thick target yields. Funding cuts forced us to discontinue that activity, but we have been able to continue the publication of the bibliography (with a reduced effort) by deriving the publication from the NSR data base.

COLORADO SCHOOL OF MINES

The main thrust of our research program continues to be the measurement of nuclear cross sections at very low energies and the application of these measurements to contemporary problems in fusion reactor diagnostics and astrophysical nucleosynthesis. In the past year, the vitality of this effort has been sustained as a result of the acquisition, in September 1987, of our low energy, high current General Ionex Model 1545 180 keV accelerator. This machine continues to operate reliably, providing controlled beams of light ions at energies up to 180 keV and currents continuously variable up to hundreds of microAmperes on a routine basis.

Since our last report to the DOE Nuclear Data Committee, we have completed a series of measurements of radiative capture reactions of protons by light nuclei. We have begun a similar series of measurements of alpha capture reactions on light nuclei. Those measurements which we have completed or are ongoing are summarized in Table 1. Our earlier measurements of light-ion capture reactions are also included in this table. Detailed results are given in the text following this table.

Table 1. Summary of radiative capture reaction measurements

Projectile	proton	deuteron	3He	Alpha
Target				
^{2}H	prev	prev	prev	prg
^{3}H		prev	fut	
^{3}He			fut	
^{6}Li	comp	fut	fut	prg
^{7}Li	comp	fut	fut	prg
^{9}Be	comp	fut		
^{10}B			fut	
^{11}B	comp	fut		

prev = previously reported or published;
comp = recently completed
prg = on going with preliminary results;
fut = to be studied in next year or so.

Radiative capture of protons by light nuclei

We have recently completed a series of measurements of the radiative capture of protons by ^{6}Li, ^{7}Li, ^{9}Be and ^{11}B for proton-target center of mass energies between 35 and 155 keV. In the case of the Lithium and Boron targets, we measured the gamma ray to charged particle branching ratios using techniques described in our earlier published results [1]. In the case of the Beryllium, we measured the thick target yields of the radiative capture gamma rays. Typical gamma ray spectra measured with the Lithium and Beryllium targets are shown in Figures 1 and 2 and the results for all four measurements are shown in Figures 3 and 4. For all four targets, angular distributions of the gamma rays were measured and found to be nearly isotropic as would be expected if the reactions are to be predominantly S-wave capture reactions. Using recent published measurements of the charged particle branches of the proton induced reactions on ^{6}Li, ^{7}Li and ^{11}B [2-4], our measurements of the gamma ray to charged particle branching ratios allowed us to infer the astrophysical S-factors for the gamma ray branches.

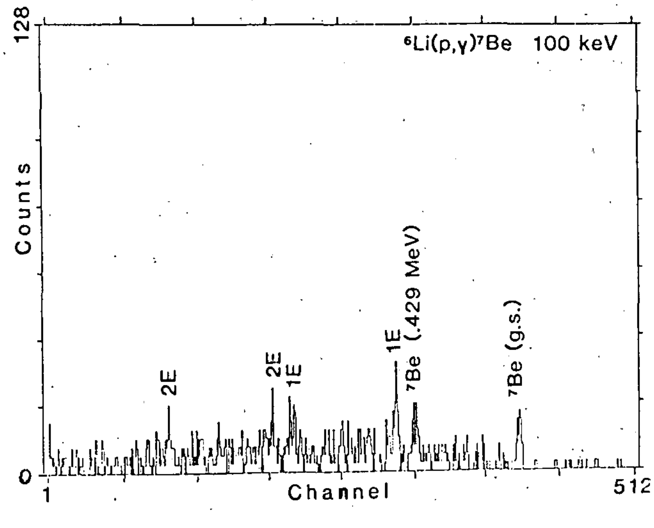

Fig 1. ^{6}Li capture gamma spectrum

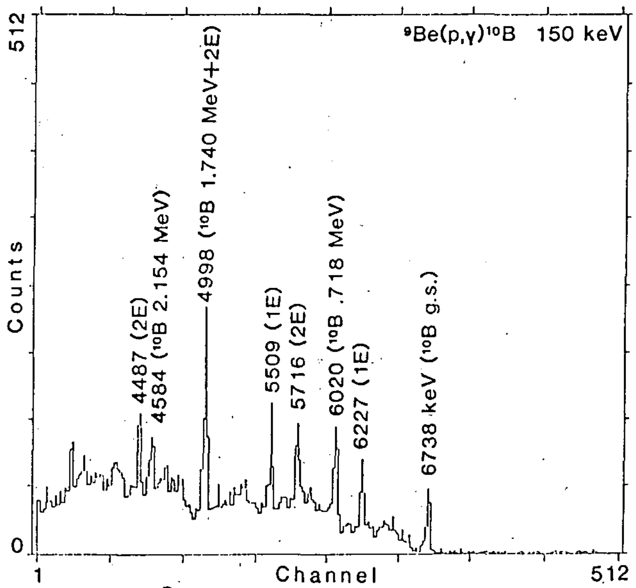

Fig 2 ^{9}Be capture gamma spectrum

Table 2 Low Energy S-factors

Target	S-Factor (keV-b)
^{6}Li	0.20
^{7}Li	0.19
^{11}B	2.1

These S-factors are given in Table 2. Assuming well accepted proton stopping powers, the S-factor for the $^{9}Be(p,\gamma)^{10}B$ reaction was deduced from the thick target yield data. The calculated yield assuming an S-factor of 0.10 MeV-b is compared to the measured total gamma ray yield in Fig 4. Except for the well known resonance in the ^{11}B reaction, all the ground state gamma ray S-factors appear to be nearly constant with energy. These reactions constitute the data base for the fusion gamma ray diagnostics of advanced fuel fusion reactors and as such we are in the process of calculating the thermonuclear reactivities.

Our measurements also allowed us to determine the branching ratios of the capture reactions to excited as well as ground states of the final nuclei. Our measured values of the first excited to ground state gamma ray branching ratios are given in Table 3. These branching ratios and the S-factors given in Table 2 are the targets of a series of direct capture calculations which are underway at this time and will be reported at a later date.

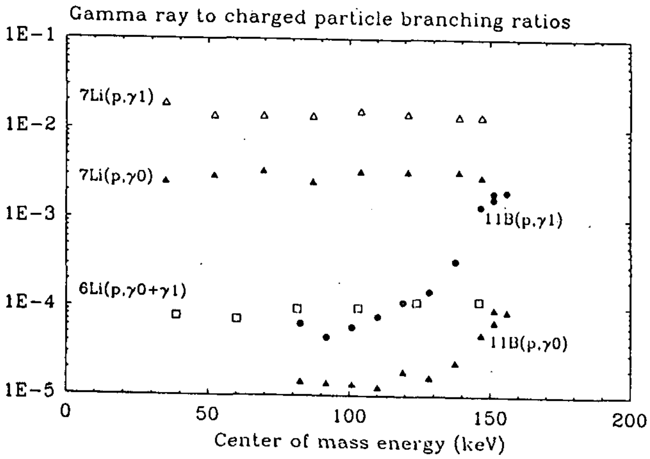

Fig. 3 Gamma ray branching ratios

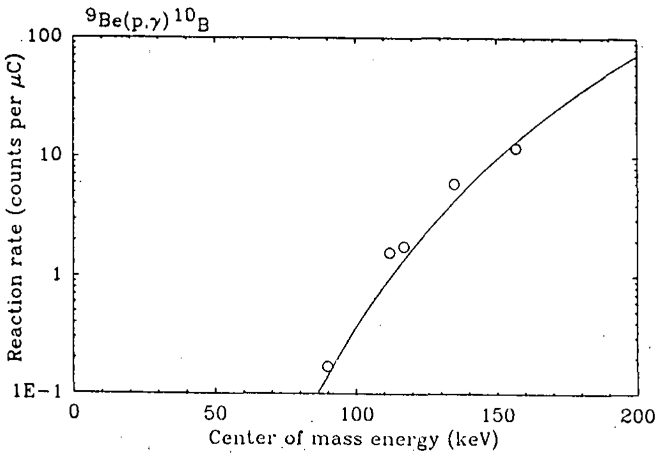

Fig 4 Reaction rate for $^{9}Be(p,\gamma)$

Table 3 Branching ratios

Target	$\gamma 1/\gamma 0$
^{6}Li	0.60±0.04
^{7}Li	5.3±0.7
^{9}Be	1.95±0.20
^{11}B	4.7±0.9

Radiative capture of alpha particles

We are in the process of carrying out a series of measurements of radiative capture of alpha particles by light nuclei. These reactions are considerably more challenging than the proton capture experiments by virtue of the lower available center of mass energies and the higher coulomb barriers. Preliminary data taken on the reactions $D(\alpha,\gamma)^6Li$ and $^6Li(\alpha,\gamma)^{10}B$ have indicated transitions to the ground state of ^6Li and to the first excited state of ^{10}B. Measured gamma ray spectra are shown in Figures 5 and 6. These reactions could play very important roles in the Big Bang nucleosynthesis of light elements and we are continuing our measurements. In addition, our measurements of these reactions will constitute a data base for gamma ray diagnostics of alpha particle confinement in present and advanced fuel fusion reactor systems.

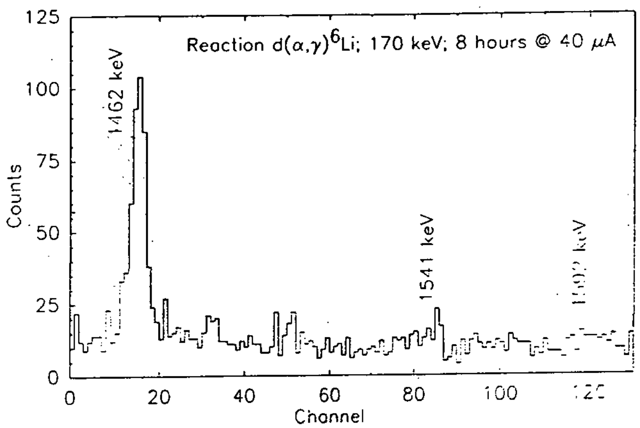

Fig. 5 Spectrum of $d(\alpha,\gamma)^6Li$ reaction

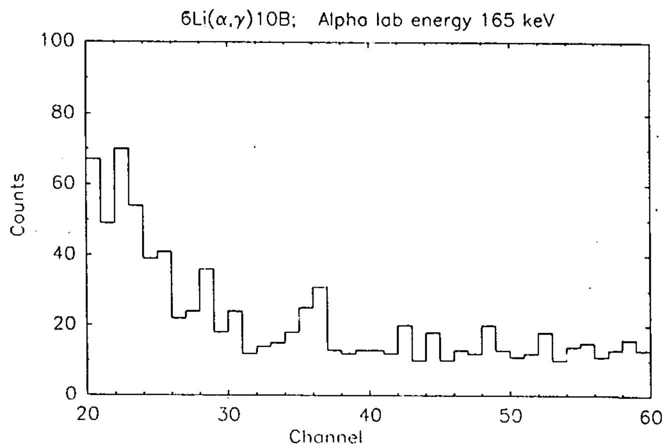

Fig.6 Spectrum for $^6Li(\alpha,\gamma)^{10}B$ reaction with the peak in channel 36 corresponding to the transition to the ^{10}B first excited state

References

1. F.E. Cecil and F.J. Wilkinson, Phys. Rev. Letts. **53** (1984) 767.
2. A.J. Elwyn, Phys. Rev. **C20**, (1979) 1984.
3. C. Rolfs and R. Kavanagh, Nucl. Phys. **A445** (1986) 179.
4. J.M. Davidson et. al., Nucl. Phys. **A315** (1979) 253.

CROCKER NUCLEAR LABORATORY AND DEPARTMENT OF PHYSICS
UNIVERSITY OF CALIFORNIA, DAVIS

A. MEASUREMENTS

1. Measurements of $^{14}C(n,p)$ at 65 MeV over a wide range of angles.* # J.R. Drummond, F.P. Brady, C.M. Castaneda, E. Hjort, B. McEachern, J.L. Romero, D.S. Sorenson;** H. Baer.†

Charge exchange reactions isolate isovector states. In particular (n,p) selects $T_0 + 1$ states for the case of $T_0 > 0$ targets. Using the Crocker Nuclear Laboratory O°(n,p) facility, the $^{14}C(n,p)$ reaction at 65 MeV was studied at angles from O° to 40°. The measurements are compared to $^{14}C(\pi, \pi^\circ)$ data from LAMPF. Theoretical calculations using DW81, and direct comparisons with $^{12}C(n,p)$ taken simultaneously are used for the interpretation of the results.

2. The (n,px) Reaction on ^{118}Sn at 65 MeV.#†† E.L. Hjort, J.L. Romero, F.P. Brady, C.M. Castaneda, J.R. Drummond, B.C. McEachern, and D.S. Sorenson.

Charge exchange reactions provide a tool to help locate the excitation of the giant isovector resonances. For $T_0 > 0$ targets (n,p) selects $T_0 + 1$ states. Evidence for the excitation of the isovector monopole and quadrupole in $^{90}Zr(n,p)$ has been obtained recently.(1) In addition, the $^{90}Zr(n,p)$ data shown substantial spin dipole strength in structure at low excitation. As a continuation of the study of such resonances on heavy nuclei, we have used our zero degree dual target facility at Crocker Nuclear Laboratory (which allow measurements from two targets simultaneously) to obtain double differential cross sections for the $^{118}Sn(n,px)$ reactions from 0 to 40 degrees.

---

* Supported by NSF grants PHY81-21003 and 84-19380.

Abstract Submitted for the Fall Meeting of the American Physical Society Division of Nuclear Physics, Santa Fe, New Mexico, October 13-15, 1988.

** Present address: Los Alamos National Laboratory.

† Los Alamos National Laboratory, Los Alamos, New Mexico 87545.

†† Supported by NSF grant PHY 84-19380.

(1) T.D. Ford et al., Phys. Lett. B195 (1987) 311.

3. Gamow-Teller Strength in ^{54}Fe (n,p) at 65 MeV.[#] [*] B. McEachern,[**] F.P. Brady, J.R. Drummond, E.J. Hjort,[**] J.L. Romero, and D.J. Sorenson; J. Rapaport.[†]

To determine the amount of missing GT strength, one compares with the non-energy-weighted sum rule, $S_- - S_+ = 3(N-Z)$, where S_- is the GT strength in the τ_- (β_-) direction and S_+ is in the τ_+ (β_+) direction. Large uncertainties in measured S values impact sum rule verification and hinder answers about GT quenching due to RPA correlations.[(1)] Recent measurement[(2)] of ^{54}Fe(p,n) should lead to an improved S_- value, providing motivation to better determine S_+ using a more precise measurement of ^{54}Fe(n,p). In addition, the GT matrix elements from ^{54}Fe(n,p), coupled with those from ^{54}Cr(p,n), are important in calculations involving $\beta\beta$-decay: processes significant in the late stages of stellar evolution.[(3)] The CNL (n,p) detector facility was used to measure ^{54}Fe (n,px), $0 \leq \epsilon < 45$ MeV, $0 \leq \alpha < 60°$; differential cross-sections for the Gamow-Teller giant resonance have been extracted and will be presented.

4. The ^{12}C (n,d) ^{11}B* Reaction at 56 to 65 MeV.[††] [♭] J.L. Romero, G.A. Needham, F.P. Brady, C.M. Castaneda, J.R. Drummond, T.D. Ford, E.H. Hjort, B.C. McEachern, D.C. Sorenson, and R. Zounes; N.S.P. King,[♮] J.L. Ullmann,[♮] and J.C. Young.[♯]

Differential cross sections are presented for the ^{12}C (n,d) ^{11}B* reaction to the g.s., 2.12 and 5.01 + 4.44 MeV excited state. The data were obtained using the neutron facility at Crocker Nuclear Laboratory. The earlier data at 56 MeV and 60 MeV cover the angular region 10° to 90°, while more recent experiments at 65 MeV extended the measurements down to 0° by using a deflecting magnet. The

---

\# Abstract Submitted for the Fall Meeting of the American Physical Society Division of Nuclear Physics, Santa Fe, New Mexico, October 13-15, 1988.

* Supported in part by NSF Grant PHY84-19380.

** Associated Western Universities Graduate Fellow.

† Physics Dept., Ohio U., Athens, OH 45701.

(1) N. Auerbach, Phys. Rev. C36 (1987) 2694.

(2) B.D. Anderson, Private Communication.

(3) H.A. Bethe, et al., Nucl. Phys. A234 (1978) 487.

†† Abstract Submitted for the Spring Meeting of the American Physical Society, May 1-4, 1989, Baltimore, Maryland.

♭ Supported by the National Science Foundation.

♮ Los Alamos National Laboratory.

♯ California State University, Chico, California.

data are compared with the corresponding (p,d) cross sections and with DWBA calculations.

5. Neutron Induced Charged Particle Reactions at 65 MeV for C, Si, and Al.* # C.M. Castaneda, J.R. Drummond, F.P. Brady, P.S. Rezentes, J.L. Romero.

Because of the practical interest in material damage due to neutron induced charged particle reactions, particularly on Si, a series of angle resolved measurements was made. Using a 3 element telescope ($\Delta E - \Delta E - E$), reaction products of isotopes of H, He, and Li have been measured. Using both time of flight and $E - \Delta E$ identification techniques exact isotope identification is possible. Three separate telescopes run simultaneously permit measurements at three angles in parallel. Results of measurements on C, Si, and Al are presented.

6. Broad Spectrum Neutron Beam (n,p) studies at LAMPF/WNR.# ** D.S. Sorenson, J.L. Ullmann,(1) F.P. Brady, J.R. Drummond, X. Aslanoglou,(2) R.C. Haight,(1) C. Howell,(3) N.S.P. King,(1) R.W. Finlay,(2) P.W. Lisowski,(1) C.L. Morris,(1) J. Rapaport,(2) J.L. Romero, W. Tornow.(3)

A facility to study the (n,p) reaction at energies between 50 and 250 MeV has been established at the LAMPF/WNR "Target-4" white neutron source. Time-of-flight is used to obtain the neutron beam energy with about 1 MeV resolution. Multiple targets are used to increase the data rate. The detection system includes four x and y multiwire drift chambers, a magnet which deflects protons out of the neutron beam, a 26 cm by 44 cm "wall" of CsI E detectors, and a large-area plastic DE detector. This arrangement allows simultaneous measurements to be made from 0 to 15 degrees, depending on beam energy. Data from ^{12}C and $^{13}C(n,p)$ will be presented.

---

* Supported by a grant from IBM and by NSF PHY-84-19380.

Abstract Submitted for the Fall Meeting of the American Physical Society Division of Nuclear Physics, Santa Fe, New Mexico, October 13-15, 1988.

** Supported by the U.S. DOE, DOD, and NSF.

(1) Los Alamos National Laboratory, Los Alamos, NM 87545.
(2) Ohio Univ., Athens, OH 45701.
(3) Duke Univ., Durham, NC 27707.

7. The Energy Dependence of the Gamow-Teller Transition for the $^{12}C(n,p)$ and $^{13}C(n,p)$ Reaction in the Neutron Energy Range 30 MeV - 200 MeV.* #

D.S. Sorenson, X. Aslanoglous,(1) F.P. Brady, J.R. Drummond, R.W. Finlay,(1) R.C. Haight,(2) C. Howell,(3) N.S.P. King,(2) A. Ling,(2) P.W. Lisowski,(2) C.L. Morris,(2) J. Rapaport,(1) J.L. Romero, W. Tornow,(3) J.L. Ullmann.(2)

Cross Sections have been extracted for the Gamow-Teller transition in $^{12}C(n,p)$ and $^{13}C(n,p)$. The cross sections were obtained simultaneously from 30 to 260 MeV using the Los Alamos National Laboratory white neutron source (W.N.R. target 4). The detection system can accommodate 3 targets and measure scattering angles from 0-15 degrees using drift chambers. Fifteen $3'' \times 6''$ CsI crystals are used to stop proton energies up to 260 MeV.

* Supported by the U.S. DOE, DOD, and NSF.

\# Abstract Submitted for the Spring Meeting of the American Physical Society, May 1-4, 1989.

(1) Ohio Univ., Athens, OH 45701.
(2) Los Alamos National Laboratory, Los Alamos, NM 87545.
(3) Duke Univ., Durham, NC 27707.

A. EXPERIMENTAL STUDIES

1. Beta Strength Functions for Fission-Product Isotopes
(R. C. Greenwood, M. A. Lee, R. G. Helmer, M. H. Putnam, C. W. Reich)

A total absorption gamma-ray spectrometer has been developed at the INEL ISOL facility for direct measurement of beta strength-function distributions of short-lived fission-product nuclides. The spectrometer consists of a large NaI(Tl) scintillator, having the dimensions 25.4-cm diameter x 30.5-cm length with a 5.1-cm diameter x 20.3-cm long axial well, together with a 300-mm^2 diameter x 1.0-mm thick Si charged-particle detector located in a thin-walled tape-transport line inside the well of the NaI(Tl) crystal. In this arrangement, the Si detector is oriented to view the bottom end of the well, with the source transport tape passing in front of the Si detector at a distance of 20 mm, giving a calculated source to detector solid angle of ~5.1%. With this arrangement, a beta-gamma coincidence requirement can be used both to minimize detection of betas in the NaI(Tl) detector and to reduce the observed background.

In our initial studies to characterize the background spectrum measured with this scintillation detector, located in a lead-shielded cave, we were particularly concerned to note that, in the energy region above 3 MeV, this background spectrum resulted primarily from neutron capture in iodine. To alleviate this problem, a modified detector shielding arrangement employing borated polyethylene, in addition to lead, has been installed at the ISOL facility. With this new shielding arrangement, the contribution to the background spectrum from neutron capture in iodine has been reduced by a factor of approximately ten.

Initial tests of the total gamma-ray absorption spectrometer, to evaluate its performance, have been conducted using radioactive sources with simple two- and three-step cascades such as ^{60}Co, ^{88}Y, ^{108m}Ag, ^{207}Bi, etc. Further tests with ^{110m}Ag, which has a somewhat more complex decay scheme, have shown that the principal levels populated in this decay, at 2480 and 2927 keV, clearly dominate the spectrum as sum peaks. Furthermore, the observed spectrum clearly shows more complete summing than that reported by the Leningrad Nuclear Physics Institute with their spectrometer (which is currently the only other operating spectrometer designed for beta-strength measurements and which is primarily used to study neutron-deficient nuclides). Following these tests, an initial series of beta strength-function measurements using the INEL ISOL facility were undertaken. Short-lived fission-product isotopes for which beta strength distributions were measured using this system were ^{140}Cs,

^{141}Cs and ^{154}Pm. Preliminary analysis of these data is currently underway.

In parallel with this activity to develop the total absorption gamma-ray spectrometer, there has been a commensurate effort to implement the analysis codes necessary to unfold the spectral distributions measured with this spectrometer to obtain beta-strength distributions. Because of the paucity of suitable monoenergetic gamma-ray sources above 3 MeV, it is difficult to obtain good quality measured response functions at these higher energies. Therefore, we have used an alternative method. We have implemented the CYLTRAN Monte-Carlo code (obtained from Sandia National Laboratory) which is able to statistically track the scattering and energy loss of gamma rays and electrons in materials. This code takes into account all of the significant physical processes that occur. By following the interactions of a large number (e.g., 30,000) of gamma rays of the same energy, the response function at this energy can be determined. This method has been used to generate response functions at 20 and 40 keV intervals over the energy range of interest.

Comparison of these computed response functions with measured response functions obtained using radioactive sources with simple one- and two-step cascades showed excellent agreement. Thus, for consistency of analysis, and in order to obtain a library of response functions at suitable energy intervals, a decision was made to use only computed response functions in the spectral unfolding routines.

As discussed above, with the source inside the NaI detector, gamma rays that are emitted from the source in sequence are observed as coincidence sum events. A computer routine has been written to convolute the response functions of 2, 3 or 4 gamma rays and thereby obtain the response function for a coincidence sum event. These response functions for single and coincidence sum events are subsequently utilized in the spectral unfolding analyses. In such spectral unfolding, it is of critical importance to have some information on the dominant cascade multiplicities contributing to various energy regions of the measured sum spectra. Thus, at this time we are exploring ways of obtaining such information from comparison of the "singles" gamma-ray spectrum (i.e., measured outside the scintillator well) with the sum-coincidence spectrum.

2. <u>IUPAP Task Group on Gamma-Ray Energies</u> (R. G. Helmer)

The task of the Task Group on Gamma-Ray Energies of the Commission on Atomic Masses and Fundamental Constants of the International Union of Pure and Applied Physics is the recommendation and publication of a consistent set of calibration energies for use in gamma-ray spectrometry, especially for use on semiconductor detectors. This group has felt that it is particularly useful if precise energies are available for gamma rays from radionuclides that are used for the calibration of detector efficiencies. Therefore, measurements were made of the energies of the strong gamma rays from the decay of ^{125}Sb and ^{154}Eu, which appear on the list of nuclides involved in a current IAEA Coordinated Research Program (see item A.3 following). This work has been described in a laboratory report[1] and the results are given in Table A-1.

TABLE A-1. Measured and deduced gamma-ray energies (in keV) for the decay of ^{125}Sb and ^{154}Eu.

^{125}Sb	^{154}Eu	
35.489(5)	123.071(1)	892.781(9)
172.719(8)	188.252(8)	904.076(6)
176.313(1)	247.930(1)	924.64(5)
178.842(5)	401.258(14)	996.262(6)
198.654(11)	444.490(6)	1004.725(7)
204.139(8)	467.84(5)	1128.560(8)
208.079(4)	591.762(5)	1140.711(9)
227.891(10)	625.254(7)	1160.37(8)
380.452(8)	676.600(12)	1188.10(4)
408.065(10)	692.425(4)	1241.38(5)
427.875(6)	715.786(18)	1246.150(9)
443.554(9)	723.305(5)	1274.436(6)
463.365(5)	756.804(5)	1290.51(10)
600.600(4)	845.423(8)	1397.35(5)
606.718(3)	850.643(12)	1494.048(9)
635.954(5)	873.190(5)	1537.80(4)
671.445(4)	880.61(3)	1542.28(4)
		1596.495(18)

1 R. G. Helmer, EGG-PHY-8256 (1988).

3. IAEA Coordinated Research Program on Decay Data for Ge Detector Efficiency Calibration:Measurement (R. G. Helmer)

A Coordinated Research Program (CRP) was convened in June, 1987 at Rome by the International Atomic Energy Agency (IAEA) to discuss the quality of the decay data for the nuclides commonly used for the efficiency calibration of Ge detectors for gamma- and x-ray spectrometry. The participants in the meeting were from nine laboratories in seven countries, including R. G. Helmer from the INEL.

A goal of this group is to get subsequent evaluators to use the values it recommends and, thereby, generate one internationally adopted set of values. The quantities evaluated are the nuclide half-life and the emission probabilities of the gamma and x-rays that can be used for Ge detector efficiency calibrations. It was also the purpose of the group to identify cases for which new measurements were needed, that is, where the data were poor or discrepant.

At an advisory group meeting in 1985, it was decided that the CRP should limit their work to the 33 radionuclides listed in Table A-2. At the CRP meeting in Rome, preliminary evaluations of the available data were presented and discussed.

In response to the needs expressed at this meeting, we have measured the relative emission probabilities for the stronger gamma rays from the decay of ^{125}Sb and ^{154}Eu. The results of these measurements are given in Tables A-3 and A-4. A description of these measurements is given in a laboratory report.[1]

TABLE A-2. Nuclides to be Considered in the IAEA Review of Decay Data

^{22}Na	^{75}Se	^{133}Ba
^{24}Na	^{85}Sr	^{134}Cs
^{46}Sc	^{88}Y	^{137}Cs
^{51}Cr	^{93m}Nb	^{139}Ce
^{54}Mn	^{94}Nb	^{152}Eu
^{55}Fe	^{95}Nb	^{154}Eu
^{56}Co	^{109}Cd	^{155}Eu
^{57}Co	^{111}In	^{198}Au
^{58}Co	^{113}Sn	^{203}Hg
^{60}Co	^{125}I	^{207}Bi
^{65}Zn	^{125}Sb	^{243}Am

1 R. G. Helmer, EGG-PHY-8250 (1988).

TABLE A-3. Measured ^{125}Sb Relative γ-Emission Probabilities

γ Energy (keV)	Relative Peak Area	Coin. Summing Corrections	Efficiency ($\varepsilon \times 10^3$)	Relative γ-emission Probability
116.6	1899(48)	1.0106	3.70	8.67(24)
172.7	1345(19)	1.0078	3.44	6.59(11)
176.3	46,661(119)	1.0034	3.41	229.6(24)
204.1	2026(39)	1.0107	3.17	10.80(23)
208.1	1538(26)	1.0078	3.14	8.25(16)
227.9	776(40)	1.0071	2.95	4.43(23)
321.1	1809(38)	1.0087	2.17	14.1(3)
380.5	5704(30)	1.0031	1.861	51.4(5)
408.1	655(19)	1.0055	1.749	6.30(19)
427.9	≡100,000	1.0017	1.675	≡1000.(8)
443.6	985(27)	1.0038	1.622	10.19(29)
463.4	32,743(80)	0.9999	1.561	350.7(28)
600.6	44,069(67)	1.0016	1.249	590.9(45)
606.7	12,358(42)	1.0016	1.239	167.0(14)
636.0	26,687(74)	1.0015	1.191	375.2(30)
671.4	4122(22)	0.9993	1.139	60.5(6)

TABLE A-4. Measured ^{154}Eu Relative γ-Emission Probabilities

γ Energy (keV)	Relative Peak Area	Coin. Sum Corrections	Efficiency ($\varepsilon \times 10^3$)	Relative γ-emission Probability
123.1	642,436(1150)	1.0062	3.70	1165(12)
188.3	3,193(13)	1.0191	3.315	6.55(7)
248.0	79,426(115)	1.0143	2.72	198(2)
401.3	1,428(10)	1.0095	1.772	5.43(6)
444.5	3,809(17)	1.0201	1.620	16.00(15)
478.3	1,454(8)	1.0083	1.518	6.44(6)
557.6	1,525(19)	1.0167	1.329	7.78(11)
582.1	4,826(6)	1.0135	1.283	25.43(21)
591.8	26,573(24)	1.0143	1.265	142.1(11)
692.5	8,378(24)	1.0114	1.110	50.9(4)
723.4	91,092(94)	1.0095	1.071	573(4)
756.8	19,771(28)	1.0162	1.032	129.9(11)
815.6	2,135(11)	0.9898	0.969	14.55(14)
845.4	2,418(20)	1.0133	0.941	17.37(20)
873.2	47,212(32)	1.0125	0.916	348.1(28)
904.1	3,341(10)	1.0130	0.890	25.37(22)
996.3	36,681(35)	1.0004	0.822	297.8(23)
1004.8	62,570(59)	1.0079	0.816	515.5(40)
1128.5	1,050(14)	1.0081	0.742	9.52(15)
1140.8	739(7)	1.0008	0.735	6.71(8)
1245.8	2,475(11)	1.0148	0.684	24.49(23)
1274.5	≡100,000	1.0074	0.672	≡1000.
1493.8	1,746(4)	1.0040	0.591	19.79(16)
1596.6	4,299(8)	0.9917	0.560	50.78(40)

4. <u>Gamma-Ray Emission Probabilities for ^{181}Hf</u> (R. G. Helmer)

Recent measurements in the Radiation Measurements Laboratory at the INEL suggested that the generally accepted emission probabilities for the gamma rays from the decay of ^{181}Hf were inaccurate. Therefore, these quantities have been re-measured. From the relative gamma-ray emission rates and the decay scheme it is possible to normalize these relative rates and determine the emission probabilities. For our measured relative rates it was possible to determine the emission probability of the strong 482-keV gamma ray to be 80.52(11)%. The emission probabilities then are

Energy (keV)	Emission probability(%)
132.9	43.3(5)
136.2	5.81(16)
136.8	0.90(18)
345.8	15.12(12)
475.8	0.703(6)
482.0	80.52(11)
614.9	0.234(18)
618.5	0.0250(12)

These measurements are described in a laboratory report.[1]

B. <u>Nuclear Data Evaluation</u>

1. <u>Mass-chain Evaluation for the Nuclear Data Sheets</u> (M. A. Lee, R. G. Helmer, C. W. Reich)

As part of our involvement in the work of the International Nuclear Structure and Decay Data Evaluation Network, which carries out the evaluation of basic nuclear-physics data for publication in the Nuclear Data Sheets, we have the evaluation responsibility for the ten mass chains in the region $153 \leq A \leq 162$. The plan for the evaluation of these mass chains has been to undertake those most out of date first.

The status of the evaluation work for our region of responsibility can be summarized as follows:

A-Chain	Status (according to currency)
160	evaluation pending; last published 1985
162	evaluation pending; last published 1985
153	submitted for publication - Sept. 1988
161	submitted for publication - Sept. 1988
158	Nuclear Data sheets <u>56</u> (1989)
157	Nuclear Data Sheets <u>55</u> (1988)
159	Nuclear Data Sheets <u>53</u> (1988)
154	Nuclear Data Sheets <u>52</u> (1987)
155	Nuclear Data Sheets <u>50</u> (1987)
156	Nuclear Data Sheets <u>49</u> (1986)

[1] R. G. Helmer, EGG-PHY-8250 (1988).

As evident from this listing, the current status of our mass-chain evaluations satisfies one of the desired objectives of the international evaluation network, namely currency of ~5 years.

As indicated in the tabulation above, the evaluations for A=160 and 162, the next ones scheduled for evaluation, are presently pending: no effort is being expended on them at this time. The reason for this temporary interruption of our mass-chain evaluation cycle is to respond to a request from the Nuclear Data Project (NDP) at Oak Ridge National Laboratory (ORNL). One of the major objectives of the International Nuclear Structure and Decay Data Evaluation Network is to have all the mass chains reasonably up to date and evaluated on a regular cycle (currently between 5 and 6 years). In many instances, however, this is not happening; and those evaluation centers whose mass chains are being satisfactorily recycled are being asked to take on, on a temporary basis, mass chains whose evaluations are greatly out of date. One such mass chain is A=206, for which the ORNL NDP has the responsibility, where the literature cut-off date for the most recent evaluation is 1978. Because of their work load and consequent inability to begin A=206 for a year or so, they have asked us if we would be willing to evaluate A=206. Since the cycle time and currency of the ten A-chains assigned to us was quite good, we agreed to accept this responsibility. Those responsible for assigning A-chain evaluations within the Network have accepted our offer. Work on A=206 got underway early this year and is presently expected to be completed this Summer. When this is done, we will return to the evaluation of those mass chains permanently assigned to us and start with the re-evaluation of those two that are the most out of date, namely, A=160 and 162.

2. <u>Evaluation of Decay Data for ENDF/B-VI</u> (C. W. Reich)

Within the framework of the Cross Sections Evaluation Working Group, we have the responsibility for the evaluated experimental decay data in ENDF/B. At present, we are involved in preparing the evaluated decay-data sets for Version VI of ENDF/B. This involves upgrading the existing data, as well as expanding the number of nuclides for which such information will be available. Three general categories of nuclides are involved, namely, those in the Actinide File, the Activation-Product File and the Fission-Product File.

In order to help avoid the proliferation of files of evaluated data--all drawn from the same base of measured information--whose contents differ only trivially from each other, we have adopted the Evaluated Nuclear Structure Data File as the starting point for this evaluation, supplementing and updating it as necessary.

At this time, our evaluation of the decay data for the Activation File (containing 149 nuclides) and the Actinide File (containing 108 nuclides) has been completed, and work on the Fission-Product File (containing ~750 nuclides) is underway. Because of the relatively large number of fission-product nuclides whose decay properties are either unknown or only incompletely known, it will be necessary to use nuclear models to calculate some of the required decay data. Toward this end, a model of the beta-strength function developed by Dr. P. Möller is being implemented in order to produce estimates of these undetermined quantities.

3. IAEA Coordinated Research Program on Decay Data for Ge Detector Efficiency Calibration:Evaluation (R. G. Helmer)

As discussed in item A.3 above, a Coordinated Research Program (CRP) was convened in June, 1987 by the International Atomic Energy Agency (IAEA) to discuss the quality of the decay data for the nuclides commonly used for the efficiency calibration of Ge detectors for gamma- and x-ray spectrometry. In response to the assignments made at this meeting we have carried out the evaluation of the gamma-ray emission probabilities for the decay of ^{94}Nb, ^{95}Nb and ^{203}Hg. These results are given below and are described in detail in a laboratory report.[1] A similar evaluation for ^{152}Eu is in progress.

Nuclide	Eγ(keV)	Pγ (%)
^{94}Nb	702	99.79(5)
	871	99.86(5)
^{95}Nb	765	99.81(3)
^{203}Hg	279	81.48(8)

4. Participation in One of the Working Groups of the ICRM (R. G. Helmer)

R. G. Helmer of INEL is Coordinator of the Gamma-and Beta-Ray Spectrometry Working Group of the International Committee for Radionuclide Metrology (ICRM), which represents metrology groups in 23 countries. In response to technical interest and leadership availability, three actions have developed. These are: the measurement of the emission probabilities of the gamma rays from ^{75}Se decay, led by R. Jedlovszky of the National Office of Measures in Hungary; a study of detection limits, led by J. E. Cline of Science Applications International, U.S.A.; and the organization of a symposium on Nuclear Decay Data: Spectrometric Methods, Measurements and Evaluations, to be held June 6-8, 1989 in Braunschweig, Federal Republic of Germany.

[1] R. G. Helmer, report EGG-PHY-8250 (1988)

AMES LABORATORY

STUDIES OF FISSION PRODUCTS WITH THE TRISTAN SEPARATOR

Neutron-rich nuclides far from stability are mass separated using the TRISTAN separator on-line to the High Flux Beam Reactor at Brookhaven National Laboratory. The nuclides are produced by thermal neutron fission of ^{235}U and their decay studied via γ-ray spectroscopy, $\gamma\gamma$ coincidences, perturbed (and unperturbed) angular correlations and lifetime measurements of nuclear excited states using triple coincidences with fast BaF detectors. The research at TRISTAN is carried out by a Participating Research Team consisting of the Ames group at Iowa State University and scientists from Brookhaven and Clark University.

1. Decay of ^{74}Zn to Levels in ^{74}Ga (Winger et al.)

Using the TRISTAN high-temperature plasma ion source, strong sources of ^{74}Zn were produced. γ-ray singles and coincidence measurements were carried out and 39 γ rays with energies ranging from 45 to 1028 keV were assigned to ^{74}Zn decay. These were placed in a level scheme for ^{74}Ga containing 11 excited stated states up to 1085 keV. This about doubles the number of placed γ rays in the level scheme. Strong β feeding (logft $\leq$ 5.8) to five of the excited levels suggested J^{π} values of 1^{+}. This work has been submitted to *Phys. Rev. C* as a brief report.

2. Decay of ^{74}Cu to Levels in Even-Even ^{74}Zn (Winger et al.)

Neutron-rich Cu nuclides are produced in fission in low yield but the high temperature plasma ion source at TRISTAN produces sufficient quantities of these nuclides to enable us to obtain useful spectroscopic information on their decay. The ^{74}Cu half-life was measured to be 1.59±0.05 s. On the basis of γ singles and coincidence measurements 22 γ rays ranging from 365 to 2363 keV were observed from ^{74}Cu decay. Of these 19 were placed in a level scheme for ^{74}Zn composed of 10 excited states up to 2969 keV. Of particular interest is the first excited 2_1^+ state at 605 keV and a triplet of states at 1164, 1418, and 1670 keV that could be interpreted as the 0_2^+, 2_2^+, and 4_1^+ levels. The only other information on excited states in ^{74}Zn is from the $^{76}Ge(^{14}C,^{16}O)^{74}Zn$ reaction. The low-lying energy levels could be reproduced in a shell-model calculation which employed a ^{66}Ni inert core. This work has been submitted to *Phys. Rev. C* for publication.

3. Decay of ^{76}Cu to Levels in Even-Even ^{76}Zn (Hill et al.)

Weak sources of ^{76}Cu were recently obtained using the plasma ion source. The experiment was more difficult than that for ^{74}Cu decay due to interference from ^{76}Zn which was very intense in the A = 76 beam. γ-ray singles and coincidence measurements were carried out and a preliminary value for the ^{76}Cu half-life of 0.39 s was obtained. So far 6 γ rays have been assigned to ^{76}Cu decay. The three strongest at 340, 598, and 697 keV were observed to be in mutual coincidence. After a complete analysis of the data a decay scheme for ^{76}Cu will be constructed and the levels in ^{76}Zn will be compared with a shell-model calculation of the type discussed in section 2.

4. <u>Decay of ^{83}Ge to Levels in the N = 50 Isotone ^{83}As</u> (Winger et al.)

The N=50 isotone ^{83}As is of interest in determining the extent to which the region around ^{83}As can be pictured as 5 active protons outside of an inert ^{78}Ni core. The ^{83}Ge half-life was measured to be 1.85±0.06 s and 51 γ rays were placed in a level scheme for ^{83}As with 28 levels up to 4841 keV. A shell-model calculation was carried out using a ^{78}Ni core. This work has been published[1] in *Phys. Rev. C*.

5. <u>Decay of ^{101}Sr and the Rotational Structure of ^{101}Y</u> (Wohn et al.)

The TRISTAN high-temperature thermal ion source was used to produce strong sources of ^{101}Sr in order to study the rotational structure of ^{101}Y. The ^{101}Sr half-life was measured to be 0.121±0.006 s and 96 γ rays were placed in a level scheme for ^{101}Y with 34 levels up to 2695 keV. The level energies and γ-decay patterns (both intraband and interband) in ^{101}Y are very accurately reproduced by simple particle-rotor calculations consisting of single quasiparticles coupled to an axially symmetric core. This work was published[2] in *Phys. Rev. C*.

6. <u>Decay of ^{101}Zr and the Rotational Structure of ^{101}Nb</u> (Wohn et al.)

Good yields of ^{101}Sr from the TRISTAN high-temperature thermal ion source made possible a study of several members of the A = 101 decay chain. A major effort of the Ames group has been to understand the nature of the single quasiproton states in the deformed A≈100 region. To that end we are studying the decay of ^{101}Zr to levels in the odd-proton nucleus ^{101}Nb. The ^{101}Zr half-life was measured to be 2.28±0.08 s. On the basis of γ singles and coincidence measurements more than 60 γ rays ranging in energy from 119 to 1013 keV have been assigned to ^{101}Zr decay. So far, three Nilsson bands have been identified in the odd-proton nucleus ^{101}Nb. The construction of a detailed decay scheme is in progress.

7. <u>Decay of ^{101}Nb and the Rotational Structure of ^{101}Mo</u> (Wohn et al.)

In the process of studying other members of the A=101 decay chain, a large amount of information was obtained on the decay of ^{101}Nb to levels in the odd-neutron nucleus ^{101}Mo. This is of interest to us as we expand our

---

[1]Winger, Hill, Wohn, Gill, Ji, and Wildenthal, *Phys. Rev. C* 38, 285 (1988).

[2]Petry, Goulden, Wohn, Hill, Gill, and Piotrowski, *Phys. Rev. C* 37, 2704 (1988).

studies from the single quasiproton Nilsson states in the A ≈ 100 region to the single quasineutron Nilsson states. The ^{101}Nb half-life was measured to be 6.57 ±0.09 s. On the basis of γ singles and coincidence measurements a total of 80 γ rays have been assigned to ^{101}Nb decay. All γ rays seen by previous observers have been identified in our spectra. Data analysis is still in progress. When the analysis is complete a level scheme for ^{101}Mo will be constructed.

8. <u>Level Lifetimes in the A≈100 Deformed Region</u> (Wohn et al.)

A method has been developed at TRISTAN for the determination, down to a few ps, of the lifetimes of excited nuclear states. The method involves $\beta\gamma\gamma$ triple coincidences obtained with plastic, BaF_2 and Ge detectors. The system was used to determine the half-lives of the 2_1^+ states in ^{98}Sr and ^{100}Zr to be 2.80±0.08 ns and 0.55±0.02 ns, respectively. A band mixing analysis using experimental B(E2) values showed that each nucleus contains a highly deformed yrast 0_1^+ state and a low-lying, weakly deformed 0_2^+ state with only weak mixing. This work has been submitted for publication to *Phys. Lett.* Using the above experimental technique, the half-lives for the 0_2^+ states in ^{100}Zr and ^{100}Mo have been measured to be 5.60±0.15 ns and 1.58±0.04 ns, respectively. We have carried out an analysis of the ρ(E0) systematics in the A≈100 region. The analysis indicated that high values of ρ(E0) from 0_2^+ states do not by themselves imply strong configuration mixing between two coexisting states. The ρ(E0) work has been submitted for publication to *Phys. Rev. C* as a rapid communication.

UNIVERSITY OF KENTUCKY

The scope of our overall research program in experimental nuclear physics is dominated by several main themes, and most of our experiments are grouped under these topics. The dominant themes are:

1. The Coupling of Target Nuclear Dynamics into Neutron Scattering Amplitudes and Cross Sections.

2. Collective Nuclear Excitations and Excited Nuclear Structures.

3. Fast Neutron and Alpha Capture Studies.

4. Specialized Nuclear Astrophysics Studies.

A. NEUTRON SCATTERING

1. Spherical Nuclei

a. Ca Isotopes Scattering Study (S.F. Hicks, S.E. Hicks, G.R. Shen, and M.T. McEllistrem)

Elastic and inelastic differential neutron scattering cross sections were measured during the past two years for the doubly magic nuclei ^{40}Ca and ^{48}Ca. Measurements were made at several energies between 2.3 MeV and 6 MeV both on and off prominent resonances observed in the ^{48}Ca total cross sections.[1] Measurements were also made at E_n = 8.0 MeV, above the resonance region in ^{48}Ca.

The ^{40}Ca + n data were taken for several reasons. Among them were to test older data sets measured at Kentucky many years ago for accuracy. These tests were eminently successful; the agreement with older Kentucky measurements for elastic scattering was excellent. A second reason was to provide a base for comparison with the neutron scattering cross sections for ^{48}Ca, which is also doubly magic. The study of neutron scattering by ^{48}Ca was of course the primary goal, and the comparison of scattering for the two isotopes shows directly that the $d_{5/2}$ scattering amplitude is much enhanced in ^{48}Ca scattering, as compared to that for ^{40}Ca. This is because the ^{48}Ca size is correct to bring the $d_{5/2}$ size resonance into the incident neutron energy interval near 2 to 4 MeV, and the absorption potential is so very weak in ^{48}Ca that the size resonance is much enhanced in the elastic scattering differential cross sections; the large d-wave amplitude for ^{48}Ca is evident in almost every elastic scattering angular distribution measured between 2 and 6 MeV; that same amplitude is not enhanced for scattering by ^{40}Ca. Only when the incident energy is near 8 MeV does the characteristic difference caused by enhanced d-wave scattering almost disappear; scattering for the two nuclei then becomes quite similar.

[1] Carlton, Harvey, Macklin, Johnson and Castel, Nucl. Phys. A465, 274 (1987).

Second, and related to this, there are quite strong core-coupled resonances in the ^{48}Ca scattering. Our analyses of the last year shows two distinct types of core-coupled resonances. The $d_{5/2}$ resonances are broad and strong, owing to their enhanced neutron escape width from the $d_{5/2}$ size resonance. A couple of core-coupled $p_{3/2}$ resonances are so narrow that they are barely visible in contrast.

The presence of these resonances in the energy interval from 0.9 to 3 MeV incident energy was well known from the phase shift analysis of the total cross sections measured at ORELA, the analysis being done by C.H. Johnson of ORNL and R. Carleton of Middle Tennessee University. We find that our measured differential cross sections, both on and off the d-wave resonances, are generally well characterized by the phase shifts provided from the total cross section analysis of Carleton and Johnson. The rapid variation of the angular distributions on and off resonance is well represented. We have also found that slight modification of the non-resonant phase shifts enables a very good fit to our differential cross sections.

A very satisfying set of results arose from the analysis of the 8 MeV incident energy differential cross section set. These elastic and inelastic scattering cross sections, together with the total cross sections near that energy, could only be fit with a model which carefully included coupling to several core excited states, including 3^-, 2^+, and other states. A combined analysis of total cross sections, elastic scattering differential cross sections, and inelastic scattering differential cross sections led to well determined strengths of the scattering potentials as well as the coupling strengths for the different core-excited states. The fixing of these parameters to describe the 8 MeV data set, together with following the potential to lower energy to maintain a good description of the general energy dependence of the total cross sections, produces a "shell-model-in-the-continuum" which then automatically generates $d_{5/2}$ resonances, or "hallway" resonances in the language of intermediate structure. These hallway resonances occur at energies close to those measured and with relative widths similar to those of the resonances observed in the total cross sections. In other words these resonances from 1 to 3 MeV incident energies are just what one needs to be consistent with the 8 MeV scattering cross sections. Much physics information about the A = 49 system is contained in the details of this description; that will be the subject of reports to be submitted for publication within the coming year. One manuscript, reporting the configurations responsible for the $d_{5/2}$ resonances and interpreting their energy distribution, has been written and will soon be published.

b. Pb Isotope Scattering Study (J.H. Hanly, S.F. Hicks, S.E. Hicks, G.R. Shen, and M.T. McEllistrem)

Measurements of differential scattering cross sections at 2.5, 4.6, and 8.0 MeV have been completed and reduced to cross sections, with all sample-size dependent and other corrections made. These measurements and data analyses have been completed for two isotopes, ^{204}Pb and ^{206}Pb. A manuscript has been prepared and is almost ready for submission reporting the measurements and their interpretations. An important aspect of that work relates to the dispersion corrections to the real scattering potential. C.H. Johnson,[2] and separately Mahaux and colleagues[3] had had great difficulty accommodating the strengths of scattering potentials, and potential geometries, which would describe low, medium, and high energy scattering as well as bound states in a single energy-dependent framework. They had a particular problem with low energy neutron scattering. This problem in $^{204,206}Pb$ has now been resolved by including the E2 excitation strengths directly in the model space, instead of letting them be part of the absorption potential. The direct coupling models provide dispersion-corrected potentials which work well for all energy regimes, low energy scattering, higher energy scattering, and negative energies or bound states.

c. Scattering Study of Five Even-A Sn Isotopes (M.C. Mirzaa, J.L. Weil, and M.T. McEllistrem)

During the past year, a start was made on the application of dispersion theory corrections to the mean field description of the interaction of neutrons with the five even-A isotopes $^{116-124}Sn$. This work was done in collaboration with M.C. Mirzaa, a former research associate and summer visitor in our lab. Included in the analysis were not only the potentials for neutron scattering at energies of 1.0, 1.63 and 4.0 MeV from the measurements at the University of Kentucky,[4] but also potentials which fit neutron measurements made at Ohio University by Mirzaa and collaborators[5] at bombarding energies of 11 and 24 MeV. We also required a fit to the neutron single hole and single particle bound state energies from various particle transfer experiments. The results were very encouraging in that with the dispersion correction there is good agreement between the calculated and experimental values of the volume integral per nucleon, J/A, for the real potential. This potential also gives fairly good agreement with the bound state binding energies. Some further work remains to be done to determine whether the use of the dispersion correction can help distinguish between the spherical and coupled channels optical models as applied to scattering from these nuclei.

2. <u>Collective, Shape-transitional Nuclei</u> (S.E. Hicks, J. Hanly, G.R. Shen, J.L. Weil, and M.T. McEllistrem)

a. Nuclear Dynamics from Coupled Elastic and Inelastic Scattering

The measurements of differential scattering cross sections and of total cross sections in the Os and Pt isotopes had been completed a year

---

[2] C.H. Johnson, D.J. Horen, and C. Mahaux, Phys. Rev. C<u>36</u>, 2252 (1987).

[3] C. Mahaux and R. Sartor, Phys. Rev. Lett. 57, 3015 (1986); C. Mahaux and R. Sartor, Nucl. Phys. <u>A458</u>, 25 (1986).

[4] R.W. Harper, J.L. Weil, and J.D. Brandenberger, Phys. Rev. C<u>30</u>, 1454 (1984).

[5] J. Rapaport, et al., Nucl. Phys. A<u>341</u>, 56(1980).

ago. The interpretations in terms of nuclear structure have also now been completed. We have learned that the Os and Pt nuclei with $A \geq 190$ are all γ-soft nuclei rather than γ-rigid. Results for ^{194}Pt have been published to date in two papers.[6,7] A third paper dealing with an extensive scattering experiment at 8 MeV neutron energy has now been submitted. This is a collaboration between investigators from three institutes, with the work largely done at two centers. The measurements of elastic and inelastic scattering were made at the Centre d'Etudes de Bruyéres-lé-Châtel (BRC).

The data were subsequently reduced to cross sections and corrected for finite sample effects at Kentucky; most of the model tests and physics interpretations were also done here. Microscopically based model calculations based on Hartree-Fock-Bogoliubov self-consistent fields were done at BRC. Happily the results of those (BRC) calculations were essentially the same as the phenomonological calculations done at Kentucky. Finally the paper now submitted was written at North Carolina and Kentucky, with revisions from BRC. This experiment and its interpretation lent support to the conclusions from our lower energy studies, completed entirely at Kentucky.[8,9]

Some of our published results were that for ^{194}Pt the neutron excitation of collective E2 strengths was much stronger than those of Coulomb excitation. These results for ^{194}Pt are made more interesting by finding that very different conclusions are provided by our interpretations for ^{192}Os. The ^{192}Os results have now been submitted for publication;[9] revisions to the manuscript will soon be complete. The ^{192}Os results show the same excitation character as found in Coulomb excitation, that is the character of a γ-soft nucleus with just the same excitation strengths as found electromagnetically, in contrast to results for ^{194}Pt.

These contrasting results for the two shape transitional nuclei are in accord with the long held prejudice here that when the nucleus becomes well deformed, the valence neutron and proton fluids of the target nucleus are strongly coupled to each other, so all hadron scattering sees the same collective excitations. Conversely when collective nuclei are not stably deformed, then the neutron and proton fluids behave separately, leading to differences in scattering by different hadrons. Thus our interpretation is that while ^{192}Os has a fairly soft shape against excitation, it is deformed, while the Pt isotopes do not have a stable deformation.

---

[6] Mirzaa, Delaroche, Weil, Hanly, and McEllistrem, Phys. Rev. C32, 1488 (1985).

[7] Hicks, Delaroche, Mirzaa, Hanly, and McEllistrem, Phys. Rev. C36, 73 (1987).

[8] Steven E. Hicks, Ph. D. Dissertation, University of Kentucky (unpubl), 1987.

[9] Hicks, Cao, Mirzaa, Sa, Weil, and McEllistrem, submitted to Phys. Rev. C.

b. Dispersion Corrections to Mean Fields

Our analyses, first of neutron scattering by ^{194}Pt and then separately by the other shape transitional nuclei, called for potentials or mean scattering fields whose strengths saturated below about 5 MeV. This "strange" saturation was systematic and unclear to us. Just at this time Mahaux and Ngo,[10] and later Mahaux and Sartor[3] and C.H. Johnson[2] were demonstrating that dispersion relations, analogous to the well known Kramers-Kronig disperson relations in optics, connect the real and imaginary (absorptive) parts of the scattering field, just as optical dispersion connects the real and imaginary parts of the index of refraction.

The application of these dispersion relations for all of our analyses, for both Pt and Os isotopes, has now been published.[11] This is the first time that dispersion corrections have been made and reported within the context of a coupled-channels model for scattering. This is an important point, since channel-coupling models result in seriously altered absorptive potentials; this is just the potential whose energy dependence gives rise to the dispersion corrections.

3. Projected Work In Neutron Scattering

a. Collective Nuclei Near A = 190

Two papers have been published, a third has been submitted, and a fourth is in revision to accommodate referee comments. All of the interpretive work on these studies is now completed. One very important result has come from recent examination of all of our results.

Examination of the neutron excess or N dependence of E2 strengths seen in bound level decays in these nuclei shows a characteristic difference in the strength patterns observed in Pt as opposed to Os nuclei. The strength patterns in the Pt isotopes nicely correlate with the observation that valence neutron bosons in these non-deformed nuclei play a significantly stronger role in the E2 excitations than do the valence proton bosons. The effective charge of the valence neutron bosons are found from examination of the neutron excess dependence of the E2 γ-ray decay strengths to be substantially larger in the Pt isotopes than in the Os isotopes. These results from the bound level decay strengths correlate very well with the excess collective strengths we have found in neutron scattering as opposed to Coulomb excitation strengths both in Pt and also in Pb nuclei. On the other hand, as noted above, in the Os nuclei all experiments consistently show that the E2 excitation strengths found in neutron scattering are just the same as those from electromagnetic excitation. We propose that in the clearly deformed Os nuclei the coupling between neutrons and protons is strong enough that the valence differences seen in Pt nuclei do not persist. These valence-boson interpretations will be developed

[10] C. Mahaux and H. Ngo, Phys. Lett. 100B, 285 (1981).

[11] S.E. Hicks and M.T. McEllistrem, Phys. Rev. C37, 1787 (1988).

and presented this coming year. As noted above, this is at least qualitatively consistent with observed γ-ray decay strengths.

b. Pb Isotope Study

Analyses of the weak collective effects in neutron scattering from the Pb nuclei with A = 204 and 206 are now in progress. These analyses are based on differential cross sections measured at three incident neutron energies, 2.5, 4.6 and 8 MeV as well as the total cross sections measured over the neutron energy interval from 0.3 MeV to 4 MeV. This extensive set of carefully measured cross sections has enabled us to separate confidently the weak collective effects of the two nuclei, and study their relationship to each other. This is very important in tracing the roles played by valence excitations, and separately, core polarization components in E2 collectivity.

c. Multi-phonon Excitations

As noted in the nuclear structure section of this proposal, many efforts are being expended to show definitively the double-phonon vibrational states through their enhanced collectivity. One of the best ways to do this would be through enhanced hadron scattering strength at incident energies high enough above the excitations to show their collective character. Several years ago we had shown very strong collective strengths at about 4.5–5.0 MeV energy in ^{208}Pb, through neutron scattering at incident energies from 7.5 to 9.0 MeV. Unfortunately our measurements for ^{208}Pb were flawed with respect to absolute normalization, and we never had been able to complete that study. However, recent calculations of 1p-1h RPA excitations built on a self-consistent field calculation using the Skyrme III force show a strong E2 fragment, split off from the giant E2 resonance, just where we had seen special strength in our scattering measurements. We propose to borrow a ^{208}Pb sample just to reexamine these excitations, and correlate new ^{208}Pb data with our recent observations for scattering from ^{204,206}Pb as well as the new theoretical calculations of E2 strength.

The isotopes ^{142}Nd and ^{144}Sm are nuclei whose character seems almost doubly magic. They have very high excited 2^+ states, and the collective 3^- levels are not much higher in excitation energy than the first excited 2^+ levels. These are prime candidates for looking at E2 strength which could arise from two phonon E3 excitations. We have begun a scattering study for these two nuclei, with data to date concentrated at lower energies. The purpose of that data is to provide a good baseline for fixing the scattering potential. Later during the next year we plan to measure scattering cross sections near incident energies of 7 to 9 MeV. We will examine these nuclei to see whether strong excitations, such as those incompletely studied but strongly observed in Pb nuclei, are present in these two nuclei. These scattering measurements will complement γ-ray measurements proposed elsewhere in this document. The combination of both neutron scattering data and γ-ray measurements should give us a powerful means of testing for collective strengths in the excitation spectra of these two nearly magic nuclei. To date scattering data have been taken for neutron energies of 2.5 MeV and 5 MeV. These data are just now being completed; the data are not yet reduced to cross sections or corrected for the many effects always present in such experiments owing to sample sizes and other experimental limitations.

Finally, the now established dispersion-corrected scattering potentials can be studied in nuclei near the region of strong collective excitations but for nuclei which are themselves rigidly spherical. We can thus address the question of whether collective excitations must be explicitly treated in order to obtain a dispersion corrected potential which works well over the entire neutron energy regime.

B. NUCLEAR STRUCTURE STUDIES

1. Collective Effects in Shape-transitional and Spherical Nuclei

We have focussed on a variety of interrelated problems. Much of this work has been performed with the inelastic neutron scattering (INS) reaction at the University of Kentucky Van de Graaff accelerator, but a healthy degree of collaborative research continues to be maintained with other laboratories where complementary nuclear probes are available.

a. Search for two-Phonon Octupole Excitations (S.W. Yates, G. Molnár, R.A. Gatenby, E.M. Baum, and E.W. Kleppinger)

Understanding the elementary degrees of freedom in complex dynamical nuclear systems is a challenge in both experimental and theoretical studies of nuclear structure. While the role of vibrational excitations in nuclei has been a subject of study for many years, our knowledge of these fundamental modes of motion of nuclei remains incomplete. One way in which vibrations in nuclei can be better understood is by the observation of multiphonon excitations. In spherical vibrators, equally spaced, degenerate quadrupole ($\lambda = 2$) phonon multiplets are expected, and there are many examples in even-even nuclei near closed shells where the $E4^+/E2^+$ ratio is near the harmonic value of two; but the expected closely spaced 0^+, 2^+, and 4^+ triplet of two-phonon states is seldom observed. Evidence for three-phonon states was sparse until recently when the identification[12] of a complete three-phonon quadrupole vibrational multiplet of levels in ^{118}Cd was reported, and candidates for higher-lying multiphonon states were proposed. However, recent measurements[13] of the lifetimes of low-lying excitations in this nucleus do not seem to be entirely consistent with this three-phonon interpretation.

Low-lying negative-parity states in many nuclei have been attributed to octupole ($\lambda = 3$) excitations, and in two heavy nuclei, ^{146}Gd and ^{208}Pb, the 3^- state lies lower than the quadrupole phonon and is the first excited state in each. Moreover, these states decay with amazingly similar E3 transition

[12] Aprahamian, Brenner, Casten, Gill and Piotrowski, Phys. Rev. Lett. 59, 535 (1987).

[13] H. Mach, private communication.

probabilities of 37 ± 2 Weisskopf units, suggesting that they are indeed collective octupole excitations. These findings have led to a number of searches (e.g., references 14 and 15) for a two-phonon quartet of states with spins and parities of 0^+, 2^+, 4^+, and 6^+ at about twice the energy of the 3^- phonon. No clear-cut identification of the members of the two-phonon quartet has emerged in either nucleus from these studies, although Curutchet et al.[16] now argue that the two 0^+ states observed near 5 MeV in ^{208}Pb, which are excited in both inelastic proton scattering and two-neutron transfer reactions, correspond to an admixture of two-phonon octupole and two-neutron pairing excitation modes. The two-proton pairing vibrational 0^+ state is predicted to lie higher in energy and is not excited by these reactions. The energies of additional members of the $(3^- \times 3^-)_\lambda$ multiplet have been calculated,[16] but none have been identified.

Despite the failure of attempts to identify two-phonon octupole excitations in ^{146}Gd, stretch-coupled states of this type have been established[17,18] in the neighboring nuclei ^{147}Gd and ^{148}Gd. The identification of these states by the characteristic cascades of two E3 transitions was possible because, serendipitously, they occur as yrast states in these nuclei and lower multipolarity decays do not occur readily. Moreover, because these states involve the coupling of one or two neutrons to the two-phonon octupole excitation ($\nu f_{7/2} \times 3^- \times 3^-$ in ^{147}Gd and $\nu f^2_{7/2} \times 3^- \times 3^-$ in ^{148}Gd), their descriptions are not as straightforward as would be the case in a doubly closed-shell nucleus. Because of these ambiguities, the identification of two-phonon octupole multiplets in even-even nuclei remains an important goal.

In closed shell nuclei, the octupole vibrations have relatively low excitation energies and compete successfully with the quadrupole mode. In recent studies[19] of ^{96}Zr in our laboratories among others, this nucleus, with a double subshell closure, has been observed to exhibit many of the properties of a doubly magic nucleus such as ^{208}Pb. Here again, the octupole excitation occurs low in energy (only 150 keV above the quadrupole phonon) with an E3

---

[14] Yates, Mann, Henry, Decman, Meyer, Estep, Julin, Passoja, Kantele, and Trzaska, Phys. Rev. C36, 2143 (1987).

[15] Julin, Kantele, Kumpulainen, Luontama, Passoja, Trzaska, Verho, and Blomqvist, Phys. Rev. C36, 1129 (1987).

[16] Curutchet, Blomqvist, Liotta, Dussel, Pomar, and Reich, Phys. Lett. 208B, 331 (1988).

[17] Kleinheinz, Styczen, Piiparinen, Blomqvist, and Kortelahti, Phys. Rev. Lett. 48, 1457 (1982).

[18] Lunardi, Kleinheinz, Piiparinen, Ogawa, Lach and Blomqvist, Phys. Rev. Lett. 53, 1531 (1984).

[19] Molnár, Belgya, Fazekas, Veres, Yates, Kleppinger, Gatenby, Julin, Kumpulainen, Passoja, and Verho, Nucl. Phys. A, submitted.

transition strength of 39^{+49}_{-15} single-particle units.[20] More recent lifetime measurements[13] indicate that the B(E3) may actually lie near the upper limit of this value, thus making it one of the strongest known octupole transitions. Associated with this octupole structure in ^{96}Zr is a higher-lying 5^- level which decays to the octupole state by a moderately collective E2 transition, suggesting coupling between the quadrupole and octupole modes.[19] At somewhat less than twice the energy of the octupole vibration is a group of states that decay to the first 3^- and 5^- states by reasonably fast (B(E1)'s = 10^{-3} W.u.) transitions. While it may be tempting to suggest[21] that these states are of two-phonon octupole character, the definitive data (i.e., from experiments such as those proposed here) required in characterizing these excitations is still lacking. Experiments designed to elucidate the possible two-phonon nature of states in ^{96}Zr are continuing, and IBM calculations with the spdf boson model[22] are in progress.[23] We should also note that the crucial lifetime information for these states was obtained with the Doppler-shift-attenuation method (DSAM) following inelastic neutron scattering (INS).[24] The development of this technique in our laboratories should make it possible to obtain lifetimes in the range from a few femtoseconds to about one picosecond for many excited nuclear states that are not accessible with other reactions. Such measurements will play a crucial role in future attempts to characterize multiphonon excitations.

If two-phonon octupole excitations are to be observed, which nuclei should be examined and what quantities should be determined? The nuclei with octupole states as the lowest excitations would appear to remain as the best candidates; however, ^{208}Pb has already been quite thoroughly studied with a variety of probes, and ^{146}Gd, which may be an even better candidate given the confirmation[17,18] of two-phonon octupole yrast excitations in neighboring nuclei and the lower energy of the one-phonon excitation, is accessible with a limited number of reactions because it is unstable. On the other hand, stable ^{144}Sm is only two protons away from ^{146}Gd, and the low energy of the one-phonon state suggests that exciting and observing two-phonon excitations is practical. We have begun studies of this nucleus and ^{142}Nd, another N = 82 nucleus, with the INS reaction at the University of Kentucky. The identification and characterization of candidates for

[20] Molnár, Ohm, Lhersonneau, and Sistemich, Z. Phys. A, in press.

[21] R.A. Meyer, et al., Proc. Int. Conf. on Nuclear Structure through Static and Dynamic Moments, Melbourne, 1987, ed. H. H. Bolotin, to be published.

[22] J. Engel and F. Iachello, Phys. Rev. Lett. 54, 1126 (1985).

[23] Henry, Meyer, Aprahamian, Maier, Mann, Kusnezov, and Roy, Bull. Am. Phys. Soc. 33, 1575 (1988).

[24] Belgya, Molnár, Fazekas, Veres, Yates, and Gatenby, Proc. Int. Workshop on Nuclear Structure of the Zirconium Region, Bad Honnef, 24-28 April, 1988, in press.

two-phonon excitations is a necessary and laborious process, but these studies are progressing well. Once candidates have been identified, we plan to measure the level lifetimes with the aforementioned DSAM technique, primarily to search for the expected fast E1 transitions to the one-phonon state. As we have shown in the case of ^{96}Zr, however, this information alone is insufficient for the characterization of two-phonon octupole states, and we must employ additional probes.

We hope to obtain new information about the role of multi-phonon vibrational excitations by combining the results of our INS measurements with those from complementary experiments. Additional studies that we will pursue (primarily during Steve Yates' planned sabbatical leave at the Nuclear Structure Facility at Daresbury, England) include detailed inelastic proton scattering, with both charged-particle and γ-ray detection, two-proton transfer reactions, and a reorientation effect measurement of the quadrupole moment of the lowest 3^- state in ^{144}Sm. The latter measurement will extend our experimental capabilities, but, without a knowledge of the quadrupole moment, it is difficult to predict the splitting of the two-phonon quartet.[25] Since E3 transitions deexciting the two-phonon states cannot be observed, inelastic proton scattering appears to be one of the few ways in which the two-phonon nature can be demonstrated.[25] The transfer experiments will assist in determining the proton contributions to the states in question. We feel that it is only through such a comprehensive set of measurements that questions about the nature of multiphonon vibrational excitations can be answered and that such complex excitations can be identified and examined.

Also available for study in these nuclei during these experiments are the low-lying negative-parity states that are superpositions of the elementary one-quadrupole and one-octupole modes.[26] These quadrupole-octupole collective states occur in the same energy region as the two-phonon quadrupole and octupole excitations, and their identification will impose stringent requirements on the theoretical description of collective vibration in nuclei.

b. Low-lying Excitations of ^{204}Pb (J. Hanly, S.E. Hicks, S.W. Yates, and M.T. McEllistrem)

The strong collective phenomena observed near A = 190 to 196 must evolve from configurations arising below neutron number N = 126. Elucidating the evolution of the weak Pb collective phenomena and their connection to hole and particle configurations depends on a good description of levels and decays in nuclei near ^{208}Pb.

Liotta and Pomar had shown, six years ago, that the few known low-lying levels of ^{204}Pb could be well described as based on the pair excitations of ^{206}Pb. Indeed, they showed a very strong overlap between single ^{206}Pb excitations and individual levels of ^{204}Pb. Thus we would expect the collective excitation amplitudes of ^{204}Pb, which are about 50% larger than those of ^{206}Pb, to be

---

[25] J. Blomqvist, Phys. Lett. 33B, 541 (1970) and private communication.

[26] P. Vogel and L. Kocbach, Nucl. Phys. A176, 33 (1971).

simply related to the amplitudes of the latter.

The knowledge of levels and decays of ^{204}Pb was rather sparse; for example, nothing was discussed in any of the early shell model calculations about unnatural parity levels. Thus as part of his dissertation on collective effects in the Pb isotopes, John Hanly completed a thorough study of levels and their γ-ray decays in ^{204}Pb. Hanly's analyses of his nuclear structure results has now been published.[27] He found that the hypothesis adopted by Liotta and Pomar, first advanced by Ko and McGrory and later developed by McGrory, that the levels of ^{204}Pb were well represented as two-boson excitations where the base bosons were ^{206}Pb levels, was supportable only for levels with excitation energies below 2 MeV. He also found a new 2^+ level, only 0.1 keV away from a previously reported 0^+ level.

There are several mysteries not discussed in the previous shell-model calculations, since the experimental information was not complete enough at that time to bring them to light. The role of the 0^+ levels is crucial to understanding configuration mixing in these isotopes, and thus collective enhancements; but as a result of this work the existence of one 0^+ level is called into question, and the character of several levels near 1.6 MeV excitation energy needs to be elucidated. These and other matters related to understanding the structure of ^{204}Pb are detailed in the published article.[27]

c. Shell Model Calculations and 0^+ Levels of ^{204}Pb (D. Wang, Y. Wang, and M.T. McEllistrem)

Hanly's γ-ray work had demonstrated conclusively that there was a 2^+ level within 0.1 keV of a reported 0^+ level, based on two different electron conversion studies. It seemed very difficult to believe that a 2^+ level could have been misassigned as 0^+ from electron conversion studies, as the conversion intensities are different by about two orders of magnitude. Nonetheless, the apparent accidental energy coincidence, to within about 0.2 keV, was so close as to raise suspicion that the 0^+ level was not really there.

A special, high resolution neutron inelastic scattering experiment was completed to test for the presence of both 0^+ and 2^+ levels, through looking for the characteristic strong forward peaking of the angular distribution of the transition to the 0^+ level. The results were, unfortunately, not conclusive; but they were consistent with the presence of both levels.

We then made shell model calculations for ^{204}Pb in a model space allowing all valence neutron-hole orbits which are relevant for that mass region. The effective interaction used was a modified surface delta interaction which had fit the spectra of many nuclei, and which fit the known level spectrum of ^{206}Pb very well. These calculations did indeed call for both the 0^+ and 2^+

---

[27] Hanly, Hicks, Weil, McEllistrem, and Yates, Phys. Rev. C37, 1840 (1988).

[28] D. Gogny, in "Nuclear Self-Consistent Fields", ed. by G. Ripka and M. Porneuf (North-Holland Press, Amsterdam, The Netherlands (1982)).

levels within about 50 keV of each other. To test the sensitivity of these conclusions, we additionally tested another effective interaction, drawn from the famed D1 interaction of D. Gogny,[28] whose interaction had been parameterized to fit level schemes and transition rates for many heavy nuclei. This calculation was not as successful for most properties of ^{204}Pb, but it did also predict both 0^+ and 2^+ levels near 1500 keV excitation energy. The neutron scattering results, now reinforced by two shell model calculations, leave little doubt that the two levels are both present. This result means that not only the expected valence orbits of $p_{1/2}$, $p_{3/2}$, and $f_{5/2}$ holes are important, but the $i_{13/2}$ orbit is also quite important for some levels at rather low excitation energy in ^{204}Pb. This orbit does not appear to play a significant role in the low-lying level scheme of ^{206}Pb. Further work will be done to complete the model description of levels and transition rates in the two Pb isotopes, ^{204,206}Pb and then the results will be published to complement the results of the earlier studies which had established the strong connection between the level schemes of these two nuclei.

d. Nuclear Structure Studies in the Sn Isotopes (J.L. Weil, R. Go, and Z. Gacsi)

The importance of and current interest in multi-phonon vibrational states has been discussed above in the section on two-phonon octupole excitations. Multi-phonon quadrupole excitations beyond two phonons are of even greater interest. An inspection of the results of an investigation of the level structure of ^{124}Sn carried out with the $(n,n'\gamma)$ reaction has revealed evidence of two and three quadrupole phonon vibrational states. We have identified the closely spaced 0^+, 2^+, 4^+ triplet of the two-phonon excitation, and also have found states with spins of 0^+, 2^+, 3^+, 4^+, and 6^+ which decay most strongly to the two-phonon states, and almost exclusively to states with vibrational character. These last we hope to establish as members of the three-phonon excitation. A more detailed comparison with the predictions of both harmonic and anharmonic vibrator models is in progress. Among other things, it involves a search for weak gamma-ray transitions that have not yet been identified in the spectra, and which are predicted by the vibrational models. If found, the decay strengths will be determined and relative B(E2)'s calculated.

In a recent annual report from the Kernfysisch Versneller Institut in Groningen there is reported a particle transfer experiment that claims to have identified many new levels in ^{116}Sn. Many of these are levels that were reported by us previously in the Proceedings of two International Capture Gamma-ray Symposia. However, there are several levels that we had not identified, and we have searched our spectra for transitions that would deexcite these levels. For the lowest-lying levels there is no evidence of any gamma decay, but for one or two higher levels there is a small possibility that we see weak decays. This information has been communicated to the Groningen lab.

On a more constructive note, the first of two papers on the level structure of ^{116}Sn is almost ready for submission. Because of the large numbers of levels of several different spin-parity combinations which have been identified in this work, it has been possible to do a statistical analysis of the level density versus excitation energy for many spins, and the results of this analysis will be included in this publication. The first paper concentrates on the establishment of the details of the decay scheme. A second paper is in preparation on the determination of the spins and parities of the levels, and a comparison to various model calculations of the level structure.

Doppler shifts have been determined for the strong transitions which were observed in the $^{116}Sn(n,n'\gamma)$ spectra. The spectra of the strong prompt transitions enabled us to remove certain gain shifts which were affecting the analysis. With these problems solved, the analysis of the Doppler shifts of the many weaker decays is ready to proceed.

2. Projected Studies

a. Sn Structure Studies (J.L. Weil and R. Go)

The analysis of the $^{116}Sn(n,n'\gamma)$ Doppler shifts will be continued to completion, and as time permits, the work on the Doppler shifts of $^{120}Sn(n,n'\gamma)$ will be started. The two papers on the structure of ^{116}Sn should be completed in the coming year. For the second paper, we are awaiting completion of new broken-pair calculations by Bonsignori and Allart with an improved effective interaction. Other calculations of a similar nature from collaborators in Hungary are also anticipated for inclusion in this paper.

The evaluation of the evidence for a multi-phonon vibrational structure in ^{124}Sn should be completed shortly, and it is anticipated that a letter will be submitted on the results to one of the letter journals. We are in the process of investigating experiments that might be used to further verify the validity of the multi-phonon interpretation. These would include the measurement of the absolute B(E2)'s of some of the highly excited states in the two-and three-phonon multiplets by Coulomb excitation, which is a very difficult task. Another possibility would be the direct measurement of the lifetimes of these states by their Doppler shift. It is estimated that most of the transitions would have lifetimes in the neighborhood of 1 to 100 picoseconds for expected values of collective enhancement of the transition strength. Such measurements would probably require going to another laboratory, in order to get into this lifetime range, and could be done during a sabbatical visit which is now being planned.

b. $^{48}Ca(n,n'\gamma)$ Cross Sections and Levels of ^{48}Ca (J. Vanhoy, S.W. Yates, and M.T. McEllistrem)

Neutron scattering experiments for target nuclei ^{40}Ca and ^{48}Ca are being studied at Kentucky to compare the collective excitations seen in these two doubly magic nuclei. It is important to see whether the extra filled shell in ^{48}Ca alters the E2 or E3 collectivity seen in electromagnetic excitation experiments, and whether excitation of these strengths in neutron scattering is the same or different than the electromagnetic excitation strengths. It is thus important to study the low-lying levels of ^{48}Ca. Several of the low-lying levels in ^{48}Ca are members of close lying doublets which cannot be separated in Sally F. Hicks neutron scattering experiment described above. Thus measuring $(n,n'\gamma)$ cross sections provides a means of achieving the separation, through high resolution γ-ray detection, which can aid the interpretation of the neutron scattering experiment. For reasons of understanding the structure of ^{48}Ca and for complementing the neutron scattering experiment, we have embarked on the present study of the $(n,n'\gamma)$ reactions.

Our results to date confirm the presence of the well known level-doublets,[29] and confirm several previous tentative spin assignments.[30,31] We expect to be able to make one or two unambiguous spin determinations to presently unassigned levels. "Low-lying" levels in a doubly magic light nucleus like ^{48}Ca means levels up to about 6 MeV excitation energy; thus the experiment must include work up to at least 8-MeV incident energy. These higher bombarding energies give quite observable Doppler shifts for the strong γ-ray decays of collective levels. Interpretation of these shifts should give us valuable information about the collective strengths seen electromagnetically. The conclusion of this experiment should occur within the next year; together with the neutron scattering experiment, a very interesting comparison of strengths will be made for these two nuclei.

C. RADIATIVE CAPTURE PROGRAM

1. $^{12}C(\alpha,\gamma)^{16}O$ Angular Distribution Measurements (J. Trice, M.A. Kovash, M. Wang and Jesse L. Weil, University of Kentucky; T.R. Donoghue and B. Luther, Ohio State University)

Despite numerous experimental attempts[32] to characterize the reaction $^{12}C(\alpha,\gamma)^{16}O$, considerable uncertainty remains in the extrapolated cross section near E_{cm} = 300 keV, i.e., at energies of stellar interest. The principal difficulties result from uncertainties in the absolute cross section in the region from 1-2 MeV, and from uncertainties in the multipole decomposition of the cross section into E1 and E2 components over the region of energy both below and above the dominant 1^- resonance near 9.5 MeV excitation. The present study is intended to provide accurate E1 and E2 cross sections over the region of center of mass energies from 1.8 to 3.2 MeV, in

---

29 Fujita, Fujiwara, Morinobu, Yamazaki, Itahashi, Ikegami, and Hayakawa, Phys. Rev. C37, 45 (1988).

30 Benczer-Koller, Seaman, Bertin, Tape, and MacDonald, Phys. Rev. C2, 1037 (1970).

31 Tape, Hensler, Benczer-Koller, and MacDonald, Nucl. Phys. A195, 57 (1972); Tape, Ulrickson, Benczer-Koller, and MacDonald, Phys. Rev. C12, 2125 (1975).

32 A. Redder et al., Nucl. Phys. A462, 385 (1987); Dyer and Barnes, Nucl. Phys. A233, 495 (1974); K.U. Kettner et al., Z. Phys. A308, 73 (1982); R.M. Kremer et al., Phys. Rev. Lett. 60, 1475 (1988).

steps of 100 keV. To this end, 6-point angular distributions of capture γ-rays to the ground state of ^{16}O have been measured at cm energies from 2.0 MeV to 2.6 MeV in 0.1 MeV steps, and at 2.9 MeV. Preliminary data have been taken at 3.1 MeV as well. Preliminary results of these measurements were presented at the most recent Spring meeting of the APS.[33]

Gamma rays are detected in a 12" diameter x 10" NaI crystal incorporating an active self-shielded design which was developed at the University of Kentucky. The detector is segmented into a central core element of 8" diameter x 10" length, which is surrounded by a 6-segment annulus also made of NaI. Each segment is instrumented with an ADC and a TDC, allowing us to reconstruct the total energy of each gamma-ray event and to actively reject cosmic rays and other backgrounds. This discrimination is based upon the distinctive signatures these events display in the annulus. As a result, time-independent backgrounds are very strongly suppressed, allowing us to observe the weak gamma-ray transitions of interest. Also, through the use of the beam-pulsing capabilities of the UK Van de Graaff, we have a very effective tool to use in discriminating against fast neutrons from the target.

In an effort to further reduce the effects of neutron backgrounds in the NaI detector we have made a detailed investigation of the scintillation response of NaI to incident gamma-rays and neutrons. The scintillation pulse shape for high-energy events from the $^{12}C(\alpha,\gamma)^{16}O$ reaction was recorded with an 8-bit transient digitizer using a 200 MHz sampling rate. The digitized pulse shape information was recorded on mag tape along with the standard signals from the ADCs and TDCs. These pulse shapes were then analyzed off-line event-by-event with sorting cuts individually placed on gamma-ray and neutron TOF. The pulse-shape spectra so determined showed clear separation of neutron and γ-ray events. The procedure has been developed now so that it can be implemented on-line as well as in the off-line replay of the event tapes. The result is a further reduction in neutron-induced backgrounds of a factor of two, well worth the development of this painstaking procedure to obtain pulse-shape discrimination.

2. Measurement of the Half-Life of ^{56}Co (K.L. Liu, M.A. Kovash)

Luminosity measurements of the remnants of collapsed stars provide tests for the models of stellar evolution, and important information on nucleosynthesis by determining the distribution of nuclear species produced during the collapse. The latter objective is realized by relating the observed exponential decay in the light output from the remnant star to the abundance distribution of the nuclear species produced. SN1987A has provided a unique opportunity to study the evolution of a star very close to the time of collapse, and numerous observations of radiation from the remnant core across the frequency spectrum now offer new tests of models of stellar collapse and of the process of nucleosynthesis.

[33] Trice, Kovash, Anderson-Pugh, Wang, Weil, Donoghue and Luther, Bull. Am. Phys. Soc. 33, 1023 (1988).

One of the largest limitations in calculating the distribution of synthesized nuclei is the present uncertainty in the half-life of ^{56}Co, which provides the dominant source of excitation of the expanding gas shell at the present time. Previous measurements of this half-life[34] exhibit a large scatter in values, although each is quoted to high accuracy. We have completed the data-taking phase of a remeasurement of this value using a Ge(Li) detector, and simultaneously collected a spectrum of γ-rays emitted by a ^{137}Cs source in close proximity to the ^{56}Co. The spectra are currently being analyzed, and we anticipate presenting a final result at the Baltimore meeting of the APS in May, 1989.

3. <u>Projected Studies</u>

The next year will see the completion of our experimental study of the ^{12}C(α,γ)16O reaction, as we exhaust the capability of the present accelerator to deliver adequately high average beam currents into adequately short beam bursts. Future studies of this process will be dependent on the ability of a new terminal to deliver 10 or more μA of beam in pulses of 1 ns duration. We have arranged with Steve Koonin that the present data set will be used to constrain his model-independent extrapolation of the cross section to 300 keV. We anticipate publishing a result during this period. Final results of the half-life mesurement of ^{56}Co will be completed and reported in this period as well.

Data collection on the reaction ^{11}B(n,γ)^{12}B will begin as the beam line is reconverted from the 'clean' line used for the α-capture measurements into the neutron-production beam line using the tritium cell. Our previous attempts to measure cross sections for this reaction in the region of excitation of 25 MeV have shown that adequate background rejection can be achieved and that several capture γ-ray transitions can be resolved. Earlier data showed these cross sections to be typically 500 nb/sr. Data collected in this study will be used to compare with our earlier measurements of cross sections for ^{11}B(p,γ)^{12}C at IUCF, where high-lying Giant Resonance excitations were observed to be built upon single-particle states of the final nucleus.

D. SPECIAL NUCLEAR ASTROPHYSICS PROJECTS

1. <u>^{81}Br(p,n)^{81}Kr Q-value Measurement</u> (Y. Wang, D. Wang, J. Vanhoy, and M.T. McEllistrem)

Neutrino capture on ^{81}Br to excited levels of ^{81}Kr has been proposed as an intermediate energy threshold solar neutrino detector. The ν-detection efficiency, and the role of excited levels in detection, depend sensitively on the ^{81}Br $-^{81}$Kr mass difference. The present uncertainty of the Q-value of the ^{81}Br(p,n)^{81}Kr reaction is about $\pm$ 4 keV. It is important to know the Q-value with an uncertainty of about 1 keV or less at the time that the ^{81}Br detector

[34] G. Emery et al., Nucl. Sci. and Eng. <u>48</u>, 319 (1972); Wright et al., Nucl. Sci. and Eng. <u>2</u>, 47 (1957); Cressy et al., Nucl. Sci. and Eng. <u>50</u>, (1974).

is taken seriously as an alternative to the presently operating ^{37}Cl ν-detector.

Measurement of neutrons in the TOF mode from the ^{81}Br(p,n)^{81}Kr reaction using a KBr target allows a direct comparison of the neutron velocities and thus energies with those from the ^{41}K(p,n) reaction. This latter reaction has a Q-value uncertainty of only ± 0.4 keV. We also plan to test the ^{81}Br(p,n) neutron energies against those from the ^{55}Mn(p,n)^{55}Fe reaction, for which the Q-value is known to within 0.3 keV. The incident energy calibration of the accelerator will be by the well known ^{7}Li(p,n) reaction, with its Q-value of -1645 ± 0.1 keV, using standard threshold techniques. We will use the threshold as determined with both monatomic and diatomic H-beams, to obtain calibration points at 1.88 and 3.76 MeV proton energy. To date our (p,n) TOF flight measurements have been made at incident energies of E_p = 3.0 and 4.0 MeV. Preliminary analysis indicates that the Q-value for the Br(p,n) reaction, which had been listed as about -1.063 MeV, may be slightly less than -1.060 MeV. Further data and analyses are necessary to test the measured Q-value through comparison to both secondary standards, to test for consistency, and to test for sensitivity or precision of the determination. Fortunately we are able to see several distinct groups from the ^{81}Br(p,n) reactions to the ground state and excited states; this gives us hope that our sensitivity will be adequate to quote an uncertainty less than 1 keV. We see two very strong transitions from the ^{55}Mn(p,n)^{55}Fe reactions, with a very well known energy difference between them. All of this information should give us an accurate calibration of the neutron energy scale derived for our TOF spectrometer.

We will certainly complete all data taking and analyses during the next six or seven months. At that time, we will have a good estimate of the accuracy attainable with these methods.

2. ^{127}I(p,n)^{127}Xe Reactions and Levels of ^{127}Xe (J. Vanhoy, D. Wang, Y. Wang, B. D. Kern, and M. T. McEllistrem)

This reaction has been recently proposed by Wick Haxton as another potentially valuable one for solar neutrino detection. Like Br, I compounds are readily available in large quantities, ^{127}I is monoisotopic, and the decay product, ^{127}Xe, is a noble gas with quite reasonable half-life of 36.4 days. Thus, unlike the ^{81}Kr, the ^{127}Xe can be counted directly.

The nucleus ^{127}Xe has previously been studied predominantly through the ^{125}Te(α,2n)^{127}Xe reactions.[35] Many levels have been located in ^{127}Xe; however definite spin assignments have only been made for a few of them. Assignments to levels of low spin, those which are of special interest for solar neutrino capture, are just the ones which have been missed. In fact, Urban et al. did not report the 411 keV state (1/2+ or 3/2+) which is reported in the Nuclear Data Sheets. This should be one of the key states for ν capture. The previous studies have suffered from γ rays arising out of the competing α + ^{125}Te reactions to ^{126}Xe and ^{128}Xe. Many unresolved doublet lines occurred in

35 Urban, Morek, Droste, Kotliński, and Srebrny, Z. Phys. A320, 327 (1985).

the singles γ-ray spectra.

We propose to use the reaction $^{127}I(p,n\gamma\gamma)$, measuring γ-ray correlations, to probe the level scheme and clarify spin assignments. Had the nucleus ^{127}I a low nuclear spin, one could have made spin determinations directly in singles γ-ray and neutron detection. However, the nuclear spin is $I = 5/2$, which precludes getting useful information about spin assignments from singles detection for any levels with spins $J \geq 5/2$. Our correlation measurements should remove ambiguities left unresolved in γ-ray singles measurements. Calculations have led to counting rate estimates for the correlation measurements which are rather low, but feasible. We will attempt this program during the coming year.

3. Optical Potential Studies (C.E. Laird[+], D.S. Sousa[+], G. Calkin[+], J. Scott[+], Q. Shen[*], T. Hooper[+], R.E. Engelhardt[*], and F. Gabbard)

This project is part of a broad study of the proton reaction strength in the mass 40 to 90 range. The study is devoted to ascertaining the validity and extent of the anomalous absorptive potential reported by Kailas.[36] The total proton strength is obtained by measuring the cross sections for proton elastic scattering, for (p,n)) reactions, and for production of gamma radiation by inelastic scattering and radiative capture. Over the past two years we have measured gamma radiation from ^{45}Sc, ^{48}Ti, ^{55}Mn, ^{59}Co, $^{58,60}Ni$, and ^{67}Zn, elastic proton yields from ^{45}Sc, ^{48}Ti, ^{55}Mn, ^{59}Co, and $^{58,60}Ni$ and (p,n) yields from proton-induced reactions on ^{45}Sc, ^{48}Ti, ^{55}Mn, and ^{59}Co. The ongoing reduction of these yields to cross sections and the optical model analyses will greatly aid in resolving the question of an anomalous absorptive potential.

---

[36] Kailas, Mehta, Gupta, Viyogi and Ganguly Phys. Rev. C20, 1272 (1979).

[+] Eastern Kentucky University

[*] Currently, Graduate Student, Duke University

A. NUCLEAR DATA EVALUATION

1. Mass-Chain Evaluation (E. Browne, R.B. Firestone, V.S. Shirley, and B. Singh)

The LBL Isotopes Project is responsible for evaluating mass chains with $167 \leq A \leq 194$ and for converting $33 \leq A \leq 44$ to ENSDF format. Responsibility for the following mass chains has been temporarily reassigned: A=170, 172 to China, A=175 to India, and A=177 to Japan. A summary of the current evaluation status of LBL mass chains is given in the table below:

Status of LBL Mass-Chain Assignments

Mass Chain	Publication Year	Status
33-44	1978	Sent to BNL (LBL)*
167	1976	Submitted 10-88 (LBL)
168	1988	Published (LBL)
169†	1982	Published (LBL)
170	1987	Published (China)
171	1984	Published (LBL)
172	1987	Published (China)
173	1988	Published (LBL)
174†	1984	Published (LBL)
175	1976	(India)
176†	1976	(India)&
177	1975	(Japan)
178	1988	Published (LBL)
179	1988	Published (LBL)
180	1987	Published (LBL)
181†	1984	Published (LBL)
182	1988	Published (LBL)
183	1987	Published (LBL)
184	1977	Submitted 5-88 (LBL)
185	1981	Submitted 9-88 (LBL)
186	1988	Published (LBL)
187†	1982	Published (LBL)
188	1981	Submitted 1-89
189	1981	Submitted 10-88 (LBL)
190†	1982	Published (LBL)
191	1980	In press (LBL)
192	1983	Published (LBL)
193†	1981	Published (LBL)
194	1989	Published (LBL)

* Radioactivity data: 7-87; Adopted Levels, Gammas: 11-87.

† To be evaluated in 1989.

& Assignment returned to LBL (9-88).

Five mass-chain evaluations were submitted by LBL between 1/1/88 and 10/27/88, one is expected to be submitted by 12-88, three are "in press", and four, submitted in 1987, have been published in 1988 (to date). "Adopted Levels, Gammas" data sets for $33 \le A \le 44$, adapted into ENSDF format from *Energy Levels of A*=21-44 Nuclei (VI), P.M. Endt and C. van der Leun, *Nucl. Phys.* **A310**, 1 (1978), were sent to BNL, November 1987. This work was done in collaboration with the French group. The Isotopes Project dedicated approximately 2.5 full-time employees (FTE) to mass-chain evaluation in 1988. This figure includes Balraj Singh, who is dividing his time between the LBL and the McMaster evaluation groups. After completion of next year's evaluation schedule, only one mass chain (*A*=192) in LBL's assignment will be as much as six years out-of-date.

2. Major Horizontal Evaluations

a. Table of Radioactive Isotopes (E. Browne, R.B. Firestone, and V.S. Shirley)

John Wiley & Sons, Inc. 1986. This book, tailored to the needs of applied users in industry, biology, medicine, and other fields, but also serving as an indispensable reference for nuclear physicists and chemists, contains 1056 pages and sells for $59.95. Sales through August, 1988 were 1869 volumes, and sales for the past year were 361 volumes.

b. Table of Isotopes, 7th edition (C.M. Lederer and V.S. Shirley, editors; E. Browne, J.M. Dairiki, and R.E. Doebler, principal authors.

John Wiley & Sons, Inc., 1978. This 1630-page book, which contains nuclear structure data not presented in the *Table of Radioactive Isotopes*, is an excellent complement to the latter. The *Table of Isotopes* was reprinted in 1986 and currently sells for $48.50. 9918 volumes were sold through August 1988, and sales for the past year were 331 volumes.

3. Evaluation Methodology (E. Browne and R.B. Firestone)

The Isotopes Project has a continuing interest in developing methods for evaluating nuclear data in order to improve efficiency and the quality of the evaluations. The group's contributions to the mass-chain evaluation effort are described below:

a. Methods and Procedures for Analyzing Nuclear Data

A recent research product of the Isotopes Project, published in *Nucl. Instrum. Methods* **A265**, 541 (1988), consists of a method for deducing uncertainties of particle-emission probabilities from decay schemes. The application of this method to mass-chain evaluations will result in more uniform and rigorous interpretation of data.

The propagation of experimental uncertainties of particle-emission probabilities into average radiation energies is important for calculating reactor decay heat. The Working Group II at the meeting on "Data For Decay Heat Predictions", Studsvik (1987), emphasized the need for uncertainties in summation calculations, which can "only be obtained from realistic uncertainties and correlations in the input data".[1] The Isotopes Project is studying this topic at the present time.

b. Computer Codes

The Isotopes Project develops computer codes for implementing new or revised methods and procedures, and maintains a library of codes for evaluating nuclear data for ENSDF. These codes are available in the *Berkeley ENSDF Evaluation Program Library* (BEEP). The code GAMUT was sent to BNL last year, and its documentation is available now.[1]
A code developed by M. Rysavy and O. Dragoun[1], which derives γ-ray multipole mixing ratios, has been implemented at LBL by the Isotopes Project. The code uses a minimization method to derive a mixing ratio (and its uncertainty) from conversion coefficients and/or electron subshell ratios. The LBL version of the code has been coupled to an existing LBL routine for interpolating the theoretical conversion coefficients required as input data for the calculation.

c. Remote Access to Databases and Computer Code Packages

Computer guest accounts are available for use of the LBL VAX/8650 computer cluster, which provides access to the LBL/ENSDF and BNL databases and to the LBL Physics Program Library (PPL). This latter is a subset of interactive programs from BEEP. There is no charge for this service, and those interested in using it may contact:

E. Browne or R.B. Firestone
Lawrence Berkeley Laboratory
Isotopes Project
Bldg. 50A, Room 6102
Berkeley, California 94720
Telephone: (415) 486-6152

26 guest accounts have been issued to remote users so far, and about 200 "logins" on these accounts were recorded during the period 1-88 to 9-88. The Isotopes Project also processes requests for data from remote users, and performed 8 database searches during the same period. Data were transmitted by both magnetic tape and via BITNET (EARNET in Europe).

4. Isotopes Project Reference Library (E. Browne and R.B. Firestone)

The Isotopes Project continues to maintain the extensive reference library it developed for production of the *Table of Isotopes*. The library consists of reference binders, ordered by mass number (A) and atomic number (Z), containing reference citations and keywords for primary nuclear structure and decay papers. Scanning was begun in 1958 and covered 42 journals issue by issue. After a thorough check of overlap with the Nuclear Data Project in Oak Ridge, the Berkeley scanning effort was discontinued for journals dated after January 1, 1970. Successive issues of *Recent References* have been incorporated into the binders so that all references for a given nucleus can be seen in one place. A second set of binders houses reprints of articles from journals which are not in the Isotopes Project's library of core journals. These reprints cover all nuclei for 1966 through about 1978. After that, they cover just the A-chain range for which the Isotopes Project has responsibility. This library is available to all LBL researchers and visitors, and limited requests for information are processed by the Isotopes Project staff.

---

[1] Proceedings of a Specialists' Meeting on *Data For Decay Heat Predictions*, Studsvik, Sweden, Sept. 7-10, 1987, p373.

[2] *GAMUT, a computer code for γ-ray energy and intensity analysis*, Report LBL-26024 (1988).

[3] *Comp. Phys. Comm.* **19**, 93 (1980).

B. SPECTROSCOPY STUDIES

1. Nuclear Penetration Effects in ^{233}U (E. Browne, B. Sur, E.B. Norman H.L. Hall, R.A. Henderson, K.T. Lesko, R.M. Larimer, and D.C. Hoffman)

The decay scheme of ^{233}Pa consists of three measured β^- transitions, populating the 5/2(633), 3/2(631), and 1/2(631) rotational bands in ^{233}U, respectively, and about fifteen γ-ray transitions between levels in these bands. Gehrke *et al.*[1] noted that their precisely measured value for the emission probability of the 312-keV γ ray (=38.6±0.5%) was inconsistent with the decay-scheme transition intensity balance, in that it allowed no β^- intensity to the ground-state rotational band. They noted an additional inconsistency, this one originating from the total K x-ray intensity measured in the decay of ^{233}Pa. This intensity was about 18% smaller than that expected from the γ-ray data and theoretical conversion coefficients.[2]

Both of these inconsistencies suggested smaller conversion coefficients than those predicted by theory,[2] leading to the decision to make precise measurements of these quantities for the 300-, 312-, and 340-keV γ rays. The conversion coefficients were determined by measuring each transition's γ-ray and conversion-electron intensities simultaneously, with a high-purity coaxial Ge detector and a lithium-drifted silicon detector, respectively. The resulting values, which are about 18% smaller than those predicted by theory,[2] were interpreted in terms of nuclear penetration effects in the conversion process. The total K x-ray intensity and the combined β^- intensity to the ground plus 40-keV levels (=6±2%), deduced from the γ-ray data and new conversion coefficients, are now consistent with the experimental data.

An independent measurement of the combined β^- intensity to the ground plus 40-keV levels (=8.8±1.4%) was made with a Au(Si) surface barrier detector shielded by a large NaI annular detector operated in anticoincidence. It is also consistent with the value deduced from the decay-scheme intensity balance. Finally, the emission probability for the 312-keV γ ray (=38.6±2.6%) was remeasured, using a ^{237}Np source with its daughter ^{233}Pa in equilibrium. This value agrees with that from Gehrke *et al.*[1]

---

[1] R. J. Gehrke, R. G. Helmer, and C. W. Reich, *Nucl. Sci. and Eng.* **70**, 298 (1979).

[2] F. Rosel, H. J. Fries, K. Alder, and H.C. Pauli, *At. Data and Nucl. Data Tables* **21**, 291 (1978).

2. <u>The Decay of ^{141}Tb by Positron Emission and Electron Capture Decay</u> (J. Gilat, R.B. Firestone, J.M. Nitschke, K.S. Vierinen, and P.A. Wilmarth)

The decay of ^{141}Tb has been investigated with at the SuperHILAC with the OASIS on-line mass separator facility. 34 γ rays were placed in a decay scheme on the basis of $\gamma\gamma$- and xγ-coincidence information and half-life. The decay scheme in fig. 1 was constructed assuming no β-feeding to the 377.7-keV $11/2^-$ level. From our analysis of 511-keV and Gd x-ray intensities, we have determined that >80% of the decay intensity has been observed in transitions feeding the 0.0- and 377.7-keV states. The spins of the first five levels have been assigned on the basis of the systematics. The other level spins have been assigned on the basis of interconnecting γ-ray transitions and allowed β-decay feeding to the indicated levels from a $5/2^-$ parent. Other consistent parent spins are $7/2^-$ and $9/2^+$, however neither is consistent with available Nilsson orbitals. For ε_2=0.17-0.28, the $\pi h_{11/2}5/2^-[532]$ level is predicted to be the ground state for nuclei near N=76[1], and ε_2=0.18 is predicted by the Grodzins' phenomenological estimate for ^{141}Tb. The establishment of $5/2^-$ spin for ^{141}Tb breaks the systematics of $11/2^-$ and $1/2^+$ isomer pairs for heavier odd-A Tb isotopes and clearly establishes a significant deformation at N=76 near the Z=64 semi-magic shell.

---

[1] J.A. Cizewski and E. Gulmez, Phys. Lett. **B175**, 11 (1986).

3. <u>Determination of Q(EC) Values for Neutron-Deficient Rare Earth Nuclei</u> (R.B. Firestone, J. Gilat, J.M. Nitschke, K.S. Vierinen, and P.A. Wilmarth)

Decay schemes of neutron-deficient rare-earth nuclei near the proton drip line have been investigated at the SuperHILAC with the OASIS on-line mass separator facility. Absolute electron capture and β^+ branching intensities have been determined for many of these decays from K x-ray intensities and 511-keV annihilation radiation intensities. Q_{EC} values for these decays can be determined from these branching intensities and the decay schemes. A limitation to determining Q_{EC} values by this method is that the decay schemes must be complete. Otherwise, unobserved statistical decay to high-lying daughter levels will lead to systematically low Q_{EC} values. For A=140 and A=142 nuclei studied with OASIS, a favorable situation for determining Q_{EC} exists because the decay schemes are strongly dominated by ground-state transitions. These high-energy, low log*ft* β-decays dominate statistical feeding and greatly reduce the uncertainty in the derived Q_{EC} value. A comparison of the experimental Q_{EC} values with the evaluated and systematic values of Wapstra *et al*[1] and the calculated values of Liran and Zeldes[2] are shown in Table I. Excellent agreement has been obtained in all cases confirming the utility of this method for these nuclei.

Table I. Comparison of experimental and theoretical Q_{EC} values

		Q_{EC}		
Isotope	$t_{1/2}$	Experiment	Wapstra *et al*[1]	Liran and Zeldes[2]
$^{140}Eu^{g}$	1.51(2) s	8.6(4)	8.4(5)	8.3
^{140}Gd	15.8(4) s	4.8(4)	4.5(7)	5.5
^{140}Tb	2.4(2) s	>11.3	10.7(11)	10.9
^{142}Pm	40.5(5) s	4.88(16)	4.87(4)	5.1
^{142}Sm	72.49(5) min	<2.1	2.10(5)	2.2
^{142}Eu	2.34(12) s	7.0(3)	7.40(10)	7.5
^{142}Gd	70.2(6) s	4.1(2)	4.2(4)	4.6
^{142}Tb	597(17) ms	10.2(4)	10.0(7)	9.9
^{142}Dy	2.3(3) s	7.00(10)	6.4(11)	7.1

[1] A.H. Wapstra, G. Audi, and R. Hoekstra, At. Data Nucl. Data Tables **39**, 281 (1988).

[2] S. Liran and N. Zeldes, At. Data Nucl. Data Tables **17**, 431 (1976).

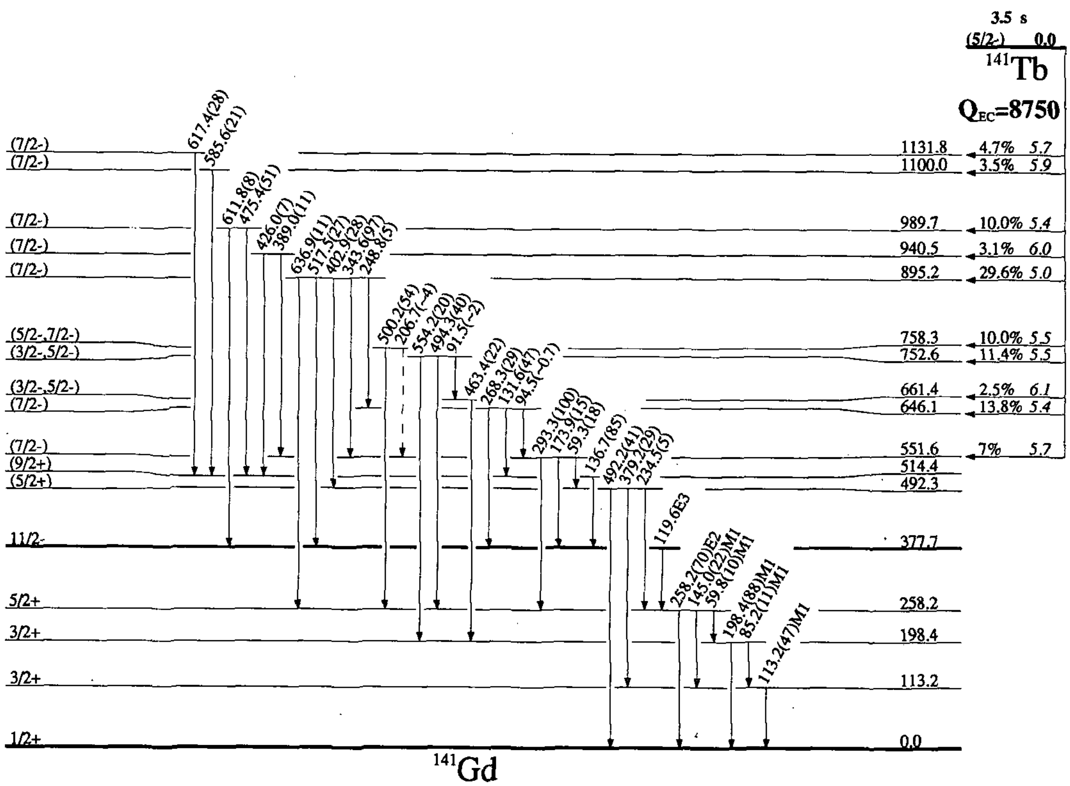

Fig. 1 ^{141}Tb decay scheme.

A. NUCLEAR DATA CALCULATIONS AND EVALUATIONS

1. Charged-particle Evaluations for Fusion Applications (R. M. White)

The Livermore Nuclear Data Group has for over 10 years maintained an evaluated charged-particle library (ECPL) for p, d, t, ^{3}He, and ^{4}He particles incident on most light isotopes through ^{16}O. We have initiated a reevaluation of this library for three reasons: (1) to provide new evaluations which include the most recent measurements of important charged-particle reaction cross sections for fusion applications; (2) to provide accurate representation of angular distributions, energy distributions, etc., of reaction products for all-particle Monte Carlo type transport calculations; and (3) to provide the most accurate possible cross section data base against which to test effective nucleon-nucleon interactions in our shell model/R-matrix calculational program (see following section). To this end we have completed new evaluations of the ^{2}H(d,p)^{3}H, ^{2}H(d,n)^{3}He, and ^{3}H(d,n)^{4}He reactions from 50 eV to 20 MeV. These evaluations include over 60 angular distributions for the d-t reaction and

over 30 angular distributions each for the ^{2}H(d,p) and ^{2}H(d,n) reaction channels. Because the ^{3}H(d,n) and ^{2}H(d,n) reactions are widely used as neutron source reactions, there exist several reviews of these reactions in the literature. For our evaluations of these reactions we have used the work of Liskien and Paulsen,[1] Drosg,[2] and the recent experimental results of Jarmie, Brown and Hardekopf[3] as well as the work of Brown, Jarmie and Hale.[4] For the ^{2}H(d,p) reaction channel, we have obtained over 70 experimental angular distributions from 10 references which span the energy range of interest. In Fig. 1 we show the integrated results of some of these angular distributions as well as our evaluation of the integrated reaction cross section over the energy range of 100 keV to 1 MeV. The evaluation angular distributions were actually obtained from an evaluated of the Legendre expansion coefficients derived from fitting the experimental angular distribution data. In the coming year, we intend to begin work on the d+^{6}Li reactions channels.

1. Nuclear Data Tables 11, (1973).
2. Nucl. Sci. Eng. 67, (1978) and Atoms and Nuclei 300, (1981).
3. Phys. Rev. C 29, (1984).
4. Phys. Rev. C 35, (1987) and private communication.

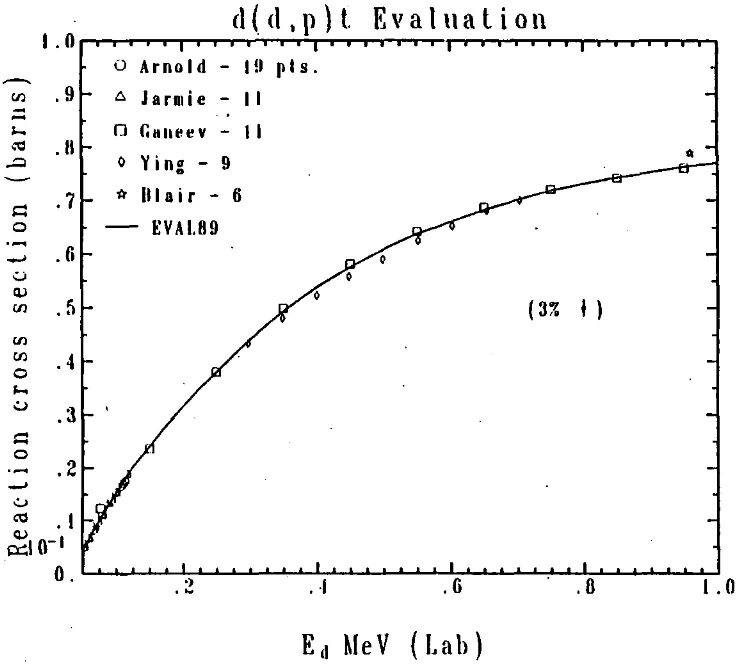

Fig. 1 Integrated results of experimental angular distributions and our evaluation of the integrated cross section for the $^2H(d,p)^3H$ reaction over the energy range 100 keV to 20 MeV.

2. Extension of the Shell Model/R-Matrix Approach to Allow the Calculation of Cross Sections Involving Multinucleon Particles (i.e., d, t, ^{3}He, α, etc.) (D. A. Resler and H. D. Knox*)

Last year we reported how the shell model/R-matrix approach was being used to calculate cross sections of interest to the nuclear data community. In the example presented of the $^{14}N(n,x\gamma)$ production for 14 MeV incident neutrons, we were unable to calculate the entire gamma spectrum since we did not have the ability to calculate gamma rays resulting from the reactions $(n,d'\gamma)$, $(n,t'\gamma)$, or $(n,\alpha'\gamma)$. The ability to calculate cross sections for reaction channels involving multinucleon particles (i.e., d, t, ^{3}He, α, etc.) requires the calculation of multinucleon spectroscopic amplitudes from shell model wavefunctions. In the shell model/R-matrix method of calculating reaction cross sections, a reaction A(k,k')B can be represented as

$$A + k \rightarrow A' \rightarrow B + k'$$

where A' is the compound nucleus of the system. In general the size of the reaction cross section is related to how much the states of the compound system which can be populated by the entrance channel "look like" A and k coupled together and "look like" B and k' coupled together. As the projectile energy is changed, the compound states populated by the entrance channel change, and the amound that A and k "look like" A' change as does the amount that B and k' "look like" A' changes. Therefore we get a cross section which changes with the projectile energy since we are populating different states in the compound nucleus.

In terms of the R-matrix theory how much a channel "looks like" the compound system is given by a reduced width amplitude γ. This can be expressed in terms of a shell model spectroscopic amplitude $S^{1/2}$. A spectroscopic amplitude indicates how much a given wavefunction "looks like" two other wavefunctions coupled together. In the case of single nucleon transfer, the spectroscopic amplitude is very simple and consists of the product of two factors. The first factor is a constant which depends on the masses of the particles and some of the quantum numbers. The second factor is simply a doubly-reduced matrix element of a compound nucleus wavefunction dotted into the result of creating a single nucleon of the proper quantum numbers onto the target/residual nucleus wavefunction.

In the multinucleon case, the spectroscopic amplitude is more complicated. The first factor is the same as before. In the second factor, the creation of a single nucleon is replaced by the creation of a multinucleon cluster which now can contain many terms as do the wave-functions for the compound, target, and residual nucleus. There is also a third factor which is for determining how much of the cluster wavefunction is in a relative s-state since we want the center-of-mass to carry all the quanta for the cluster. Finally, there can now be more than one cluster wavefunction of the required quantum numbers which can be coupled to the target/residual nucleus wavefunctions. Therefore, the final spectroscopic amplitude is a summation over these wavefunctions.

The theoretical details of these multinucleon spectroscopic amplitude calculations have been worked out for use in our m-scheme shell model code CRUNCHER. The new coding is very general--no restrictions on the number of particles in the cluster and no restrictions on the model spaces used. This is believed to be the first time such general coding has been put together for the calculation of multinucleon spectroscopic amplitudes. Extensive testing has been performed and results compared where possible with those in the literature. With the completion of this work, all sections of the coding used in our shell model/R-matrix approach to calculating nuclear reaction cross sections are general in that there are no restrictions in which two-body reaction channels can be included. Work on the complete calculation of the $^{14}N(n,x\gamma)$ production is currently underway.

---

*Ohio University, Athens, Ohio

3. Development of an Evaluated Photonuclear Library (S. Warshaw)

To provide complete coupling between neutrons, charged-particles, photons (and electrons) in a new all-particle Monte Carlo transport code being developed at Livermore, the Nuclear Data Group is creating an evaluated photonuclear data library. The data for this library are being collected from three main sources: (1) the NBS 15-volume set of photo- and electro-nuclear citations and excerpts; (2) systematic scanning of Current Contents; and (3) the Dietrich and Berman photoneutron atlas published in

1988 as Atomic and Nuclear Data Tables, Vol. 38. This atlas includes data for 181 isotopic and natural targets culled from 64 journal articles, with a few redundancies. Its chief virtue is that it is the only large collection of monoenergetic photon-induced neutron production reaction 4-pi cross section data known to cover significant photon energy and nuclear mass ranges. From these sources 400 journal references have been collected to date and photocopies and a cross-referencing index started. In Fig. 2 we show the photoneutron cross-section for ^{208}Pb and its decomposition into various reaction channel multiplicity subsets. To date data have been processed for ^{3}H, $^{3,4}He$, $^{6,7}Li$, ^{2}H, ^{9}Be, $^{10,11}B$, and ^{208}Pb. The intent is to obtain evaluated photonuclear library files for each of the isotopes (≈100) currently in the Livermore Evaluated Neutron Data Library (ENDL).

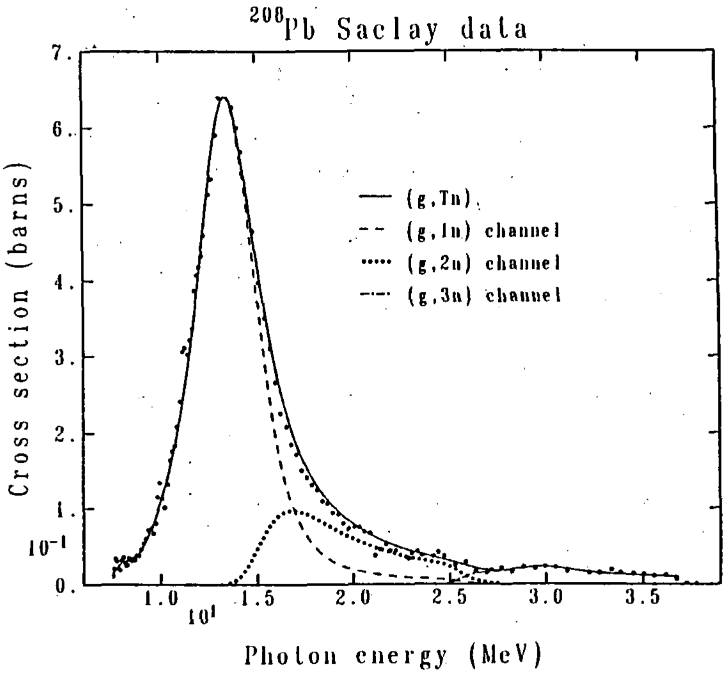

Fig. 2 Plot of total photoneutron cross section taken at Saclay in 1970, shown as a function of photon energy. The continuous curves represent a semi-analytic fit to the total (solid line) and the decomposition of the cross section into the different multiplicity channels (dashed, dotted, dot-dashed lines).

4. Calculation of Precompound Gamma-ray Spectra for Several Materials for Incident Neutrons from 3 to 30 MeV (M. Blann)

The high-energy gamma-ray spectra have been calculated for incident neutron energies from 3 to 30 MeV on natural vanadium, iron and lead, and on $^{235,238}U$ and ^{239}Pu. In this work, only gamma-rays with energies in excess of the neutron binding energy are calculated. These gamma-rays originate from a pre-equilibrium decay mechanism. Fig. 3 shows an example for iron and gives an estimate for the uncertainty in the calculations. For calculations of light isotopes such as ^{27}Al and ^{32}S the calculations do poorly. Calculated results, the physics employed in the model, and suggested alternative physical models which should work well in the light element regime are summarized in report UCRL-100324.

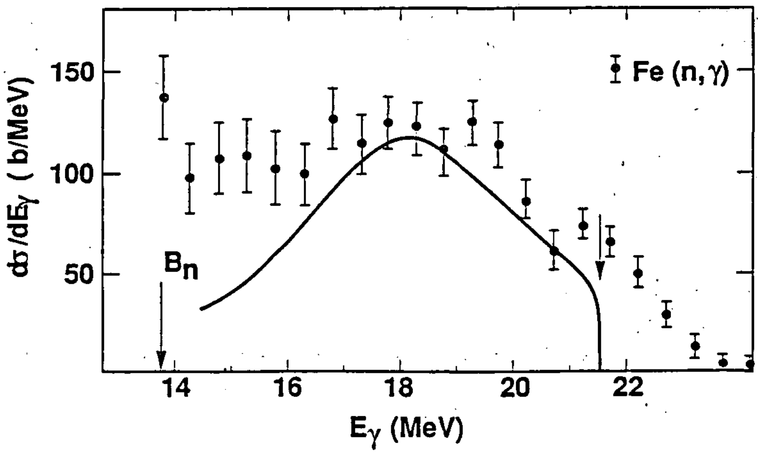

Fig. 3. Experimental and calculated (n,γ) spectra for ^{56}Fe. Experimental results are from Cvelbar, et al., Nucl. Phys. A310, 40 (1969). The arrow beneath B_n represents the energy below which γ-rays may be emitted following neutron emission. The experimental points extend beyond the maximum γ-ray energy due to experimental energy resolution.

5. Improvements of the Precompound Exciton Model in the STAPRE Code (D. Gardner and M. Gardner)

While our present precompound particle evaporation model adequately describes its total particle emission spectra, and thus its proper contribution to total reactions such as (n,n+n'), (n,2n), (n,3n), etc., the partition of such cross sections among ground and isomeric states may not be as accurately calculated. No formalism of which we are aware properly conserves spin and parity in precompound calculations. C. Y. Fu, H. Feshbach, G. Reffo, and others have attempted to follow aspects of the physics as the initial excited nucleus proceeds towards equilibrium, but there appear to be adjustable parameters that must be determined in some *ad hoc* manner. Our original version of STAPRE distributes the precompound contribution at each energy in the daughter nuclei using the same spin distributions in the continuum and over the discrete levels as in the *compound* case and disregards parity. Fu, Feshbach, Reffo, etc. have suggested the use of an exciton-dependent spin cut-off factor for the particle evaporation from each exciton configuration, as the nucleus approaches equilibrium. We implemented this approach but with some modifications.

For a given exciton state with N_p and N_h = N particles and holes, the spin cut-off factor is taken as

$$\sigma_p^2(N) = \text{const.} * NA^{2/3}.$$

The spin distribution equation is the usual one. Our modifications consist of making the precompound spin cut-off parameter dependent on the energy in each residual nucleus and on its proper normalization. The STAPRE code computes the number of exciton configurations required to "sufficiently" approach equilibrium from a given set of initial conditions. We can show that

$$\sigma_P^2(N_C) = \sigma_C^2(E_r),$$

which leads to

$$\sigma_P^2(N,E_r) = \frac{N}{N_C}\,\sigma_C^2(E_r),$$

where N_C is the particle-hole number of the final exciton configuration and

$$\sigma_C^2(E_r)$$

is the energy-dependent spin cut-off for the compound nucleus, computed in the usual way. Usually most of the precompound evaporation comes from the first exciton state, resulting in a shift in the population of the daughter nucleus to states of lower spin values. In the subsequent γ-ray cascade, for those states that do not particle decay, the lower spin isomers and/or ground state will tend to be favored over the higher spin states; the magnitude of this effect will depend on the relative amounts of the precompound and compound nucleus processes.

We have also allowed the state density and pairing gap values for the exciton model (including that of the residual nuclei) to be specified as input parameters. In many precompound models, the matrix element, $|M^2|$, for the residual interaction is taken to be excitation-energy and mass dependent, as $|M^2| = k_1 A^{-3} E^{-1}$. The new input option allows $|M^2|$ to be related to the Fermi gas level density parameter if desired. We are now conducting sensitivity studies to determine the importance of the above exciton model changes.

6. Evaluated Set of Neutron Cross Sections for ^{20}Ne from IDA Modeling Calculations (M. H. MacGregor, R. J. Howerton, and G. Reffo*)

As reported last year, the Nuclear Data Group has implemented the extensive system of nuclear modeling codes (IDA) developed by G. Reffo. These codes were used together with the very limited experimental data to obtain a complete set of evaluated neutron cross sections for ^{20}Ne from 0 to 30 MeV. The IDA codes are based on the Hauser-Feshbach statistical model formalism with width fluctuations included. In the ^{20}Ne evaluation, the IDA calculations, modified in some places to agree with experimental data, were used from 1 to 30 MeV. Below 1 MeV, cross sections were obtained from experimental neutron resonance parameters. The Livermore post-processing codes ALPHA and OMEGA were used to check energy balances for all of the reactions individually, so that the final evaluated data set accurately conserves energy. Figure 4 shows a comparison between the theoretical IDA (n,α) cross section curve and experimental data. As can be seen, the theoretical curve gives the proper threshold behavior and a good fit to the data up to 4 MeV. Above 4 MeV, the evaluated data set was modified to match experiment.

---

*ENEA, Bologna, Italy

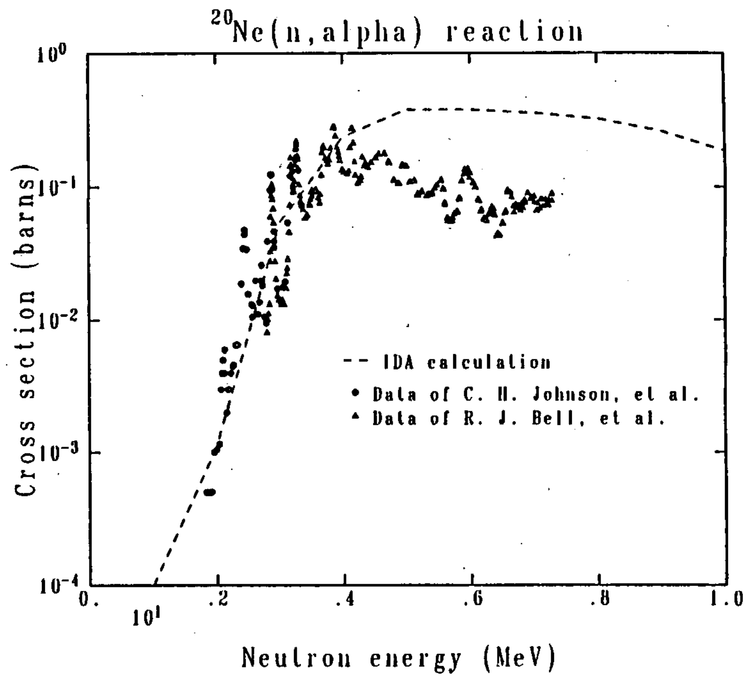

Fig. 4 Comparison between the calculated ^{20}Ne(n,α) cross section using IDA and the experimental data of C. H. Johnson, et al. Phys. Rev. 82, 117 (1951). and those of R. J. Bell, et al. Nucl. Phys. 14, 270 (1959). The calculation was subsequently altered in the evaluation to fit the experimental data.

7. Measurement and Analysis of Neutron and Gamma-Ray Spectra Leaking from Several Materials Centrally Pulsed by 14-MeV Neutrons
(E. Goldberg, L. F. Hansen, T. T. Komoto, B. A. Pohl, R. J. Howerton, R. E. Dye, W. E. Warren, and E. F. Plechaty)

Monte Carlo calculational analysis of several integral measurements have been completed with two different data bases, ENDL and ENDF/B-V. The experiments utilized spherical assemblies, pulsed centrally with 14-MeV neutrons. The measured neutron and gamma-ray leakage spectra were compared to the spectra calculated with TART and SANDYL. Preparation of the ENDF/B-V data base for use in TART proved to be a formidable task. Figures 5a and 5b showing the neutron time-of-flight and recoil electron spectra for aluminum, typify the findings of the study. Both calculated neutron spectra agree reasonably well with the measurement. However, we see the ENDF/B-V-based recoil electron spectrum to be below the experimental data while the ENDL-based spectrum is in close proximity to the experimental points.

We have chosen as a measure of gamma-ray energy deposited in the NE-213 detector the quantity $\Sigma n_i c_i$ where n_i is the number of counts in channel c_i. Ratios of these summations, evaluated with the findings from the pulsed-sphere experiments, have been applied to TART calculations of simple one-zone, one-dimensional spheres. These results may be used by the general audience as benchmark exercises. Table 1 lists our findings. We see immediately that silicon generates the largest gamma-ray element. If we rely upon the ENDL base we find that 2.008 MeV/n leaks from the centrally-pulsed sphere, while reliance on the ENDF/B-V base leaks 2.268 MeV/n. The maximum leakage is found to occur when $\rho R \simeq 35\ g/cm^2$.

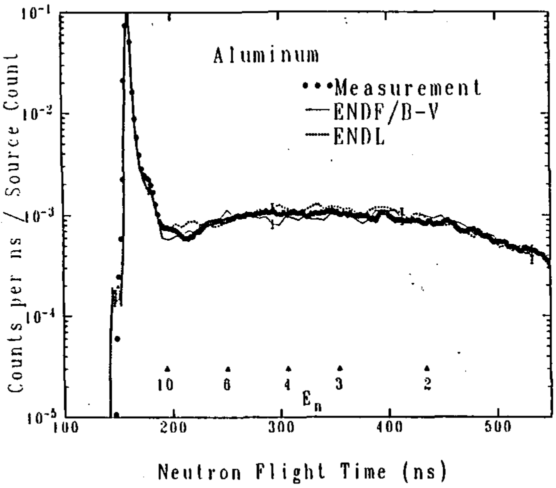

Fig. 5a

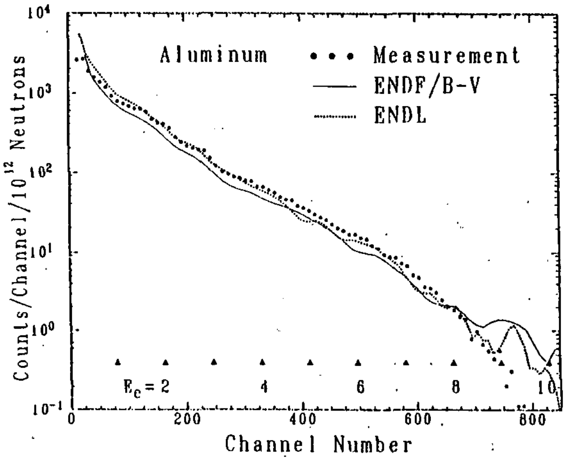

Fig. 5b

Figures 5a and 5b, showing the neutron time-of-flight and recoil electron spectra for aluminum, typify the findings of the study.

Table 1. Gamma Ray MeV Leaked/14-MeV Neutron, Normalized to Pulsed Sphere Experiments

Material	(γ MeV/n) ENDL	(γ MeV/n) ENDF/B-V	(γ MeV/n)/(C/E) ENDL	(γ MeV/n)/(C/E) ENDF/B-V	$(\rho R)Max_\gamma$ (g/cm^2)
C	0.90	0.85	0.99	1.03	40
N	1.35	1.14	1.38	1.46	40
H_2O	0.93	0.71	0.81	0.87	25
C_2F_4	0.98	0.61	0.72	0.69	35
Al	1.97	1.58	1.82	1.98	35
Si	2.15	1.67	2.00	2.26	35
Ti	1.44	1.53	1.84	1.68	45
Fe	1.49	1.25	1.37	1.49	40
Cu	0.89	0.99	0.91	0.93	45
Ta	0.51	0.43	0.56	0.55	35
W	0.42	0.39	0.52	0.48	35
Au	0.33		0.35		40
Pb	0.35	0.29	0.30	0.31	35
^{232}Th	0.34	0.29	0.35	0.34	35
^{238}U	0.38	0.32	0.37	0.38	35

8. Optical Model Calculations in the Actinide Region (H. S. Camarda*)

Phenomenological optical model calculations have been carried out which give satisfactory fits to the total and differential neutron cross sections for nuclei in the actinide region (Th-Pu) for incident neutron energies above 10 MeV. These calculations were performed by modifying one of Ohio University's global spherical optical potentials to include the nonsphericity of these target nuclei. The modified potential depends on the deformation parameter, B, which is determined by experimental data, e.g., Coulomb excitation to low-lying rotational states. With this modified potential, cross sections calculated for actinide nuclei where no experimental data exists can be carried out with some confidence.

A more sophisticated treatment of neutron interactions with actinide nuclei involves carrying out coupled-channel calculations where the rotational and vibrational degrees of freedom of the target nuclei can be taken into account more realistically. Preliminary coupled-channel calculations with the code ECIS have been performed on the Livermore Nuclear Data Group's Sun computer system. To date, equivalent calculations performed with ECIS on the Cray and the Sun computers are in good agreement.

---

*Pennsylvania State University

9. Further Developments in the Study of Our Neutron-Induced Cross-Section Library for Isotopes of Iridium. (M. Gardner and D. Gardner)

As we mentioned last year in this report, iridium is often used as a detector to measure neutron fluences in underground nuclear tests. In order to fully exploit the potential of this detector, we have completed the calculation of a preliminary set of cross sections primarily for sensitivity studies. We computed 228 excitation functions for partial and total reactions among 22 ground and isomeric states of 10 iridium isotopes, from ^{187}Ir to ^{196}Ir. The principal problems we've encountered in our calculations lie in the fact that our radiochemical diagnostic measurements involve either single isomers or sums of the ground state plus one or more isomeric populations (since portions of some of the cross sections end up in long-lived isomeric states) and that the discrete-level information required in our computations, as well as most of the experimental reaction cross-section data are presently incomplete and/or uncertain. In order to properly calculate the ground- and isomeric-state populations correctly, a complete set of reliable discrete nuclear levels and their multipole branchings must be available for each Ir isotope. Based on our initial calculations, we have been able to point out problems in the level information, particularly for the odd-odd Ir isotopes. Much new experimental and theoretical work is now under way by other members of our Nuclear Chemistry Division, primarily on the isotopes ^{191,192,193,194}Ir.

We have undertaken the evaluation of the new data and information as they become available. These include the analysis of new average resonance capture (ARC) data from 2-keV neutrons on ^{191}Ir taken by R. W. Hoff, calculated gamma-ray production information from (n,n') reactions on ^{193}Ir, and statistical analyses on spin and parity distributions, spin cut-off parameters and level densities of new theoretical discrete level sets. We have designed, and with G. Larsen, essentially completed a computer program which will search for typographical and physics errors in large level sets and their multipole branches, and which will also calculate E1, M1, and E2 transitions among single-particle intrinsic states and among rotational bandheads with K-quantum number restrictions, if desired. Additionally we are carrying out sensitivity studies on the ^{191,193}Ir(n,xn) cross-section calculations to evaluate the improvements that we made in the precompound exciton model in our version of the STAPRE nuclear reaction code.

10. R-Matrix Code Improvement (D. A. Resler)

Last year we reported that the Ohio University R-matrix code was made operational on our Sun computer network. Extensive testing has been performed to verify the correct operation of the code. During an investigation of the low-energy d+t reaction, we discovered a problem with the calculation of the Coulomb wavefunctions since the original coding was not valid in this energy region. The calculation of the Coulomb wavefuntions has been upgraded to use the coding of Bardin et al.[1] which is valid for the entire (η,ρ) plane. Published R-matrix calculations from Jarmie, et al.[2] and Brown, et al.[3] for the low-energy d+t reaction were extremely beneficial in verifying the correct operation of our coding as we have duplicated their very low-energy results to several significant digits.

1. C. Bardin, et al., Computer Physics Communications 3, 73 (1972).
2. N. Jarmie, R. E. Brown, and R. A. Hardekopf, Phys. Rev. C 29, 2031 (1984).
3. R. E. Brown, N. Jarmie, and G. M. Hale, Phys. Rev. C 35, 1999 (1987).

11. Computer Network for Nuclear Modeling Calculations (D. A. Resler, T. T. Komoto, and J. D. McGowan)

The Nuclear Data Group's network of Sun Microsystem computers, used for our nuclear modeling calculations, has been upgraded during the past year. The two Sun 3/260 servers have been replaced with Sun 4/260s. This upgrade gives us a factor of two increase in our calculational capability. In addition we have increased the memory of both machines for a total of 64 Mbytes on one and 16 Mbytes on the other. Many of the shell model/R-matrix calculations of nuclear reaction cross sections have required the full 64 Mbytes of the larger machine. We have also added a fast 8mm tape system to our network for backing up our 3 Gbytes of disk storage.

12. Upgrades to the Shell Model Code CRUNCHER (D. A. Resler and S. M. Grimes*)

Several major advances have been made to the shell model code CRUNCHER. The calculation of nuclear reaction cross sections has required the use of very large model spaces which in turn has required a large amount of computer resources. In a typical application of the shell model/R-matrix approach, the shell model part of the calculations can easily require over 95% of the total time. Therefore, it was worthwhile to better optimize the coding for these large problems. A major improvement was the use of multiparticle Hamiltonians for those problems considered "small" in terms of the computer size. Today a "small" problem can be a $2\hbar\omega$ model space description of a p-shell nucleus. Our previous method was to keep the Hamiltonian expressed in a two-body form. Now we can use the fast but large multiparticle Hamiltonian on the small problems and still use the slower but smaller two-body Hamiltonian for the larger problems. The use of the multiparticle Hamiltonian has resulted in two orders of magnitude improvement in the execution speed for these problems.

Improvements in the Ohio University version of the code have been incorporated into the LLNL version. Part of the effort at Ohio has been to improve the "unstable basis" portion of the code. This is very important for the calculation of level densities, the first stages in a diagonalization using a two-body Hamiltonian, and in the generation of a multiparticle Hamiltonian from the two-body Hamiltonian.

---

*Ohio University, Athens, Ohio

B. NUCLEAR DATA MEASUREMENTS

1. Proton and Deuteron Excitation Functions for ^{151}Eu and ^{153}Eu (H. I. West, Jr., R. G. Lanier, M. G. Mustafa, R. N. Nuckolls, J. Frehaut*, A. Adam*, and C. A. Philis*)

We have measured the proton and deuteron excitation functions for ^{151}Eu and ^{153}Eu for the reactions ^{151,153}Eu(p,n)^{151,153}Gd, ^{151,153}Eu(d,2n)^{151,153}Gd, ^{153}Eu(p,3n)^{151}Gd, ^{153}Eu(d,4n)^{151}Gd, ^{151}Eu(p,3n)^{149}Gd, ^{151}Eu(d,4n)^{149}Gd, ^{151}Eu(p,(p2n,dn,t))^{149}Eu and ^{151}Eu(d,(p3n,d2n,tn))^{149}Eu. These excitation functions are shown in Figures 1-6. In addition a new half-life of 9.282 ± 0.008 d was obtained for ^{149}Gd.

We used the stacked foil method for obtaining the data. Europium oxidizes rapidly in air bursting into flame at 150-180°C thus posing a target problem. We solved this problem by mixing Eu_2O_3 with a resin which when polymerized is the equivalent of Kapton (a DuPont trade name).

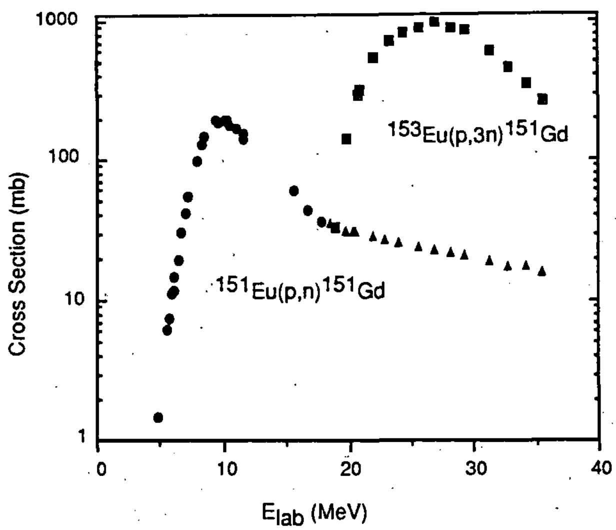

Fig. 1

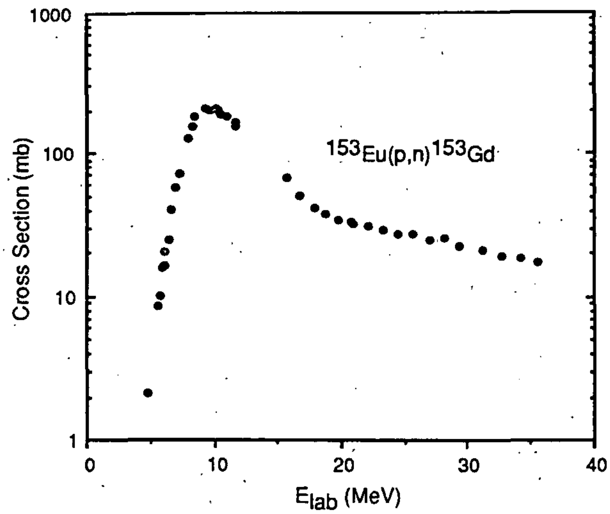

Fig. 2

The foils held up well under irradiation. Corrections were made for the charged-particle energy loss in the target foils in the rapidly varying region of the excitation functions. We plan to use a similar method in measuring the cross sections for iodine and bromine.

The measurements at less than 12 MeV were made using the Van de Graaff at Centre d'Etudes Bruyers-le-Chatel, France. The measurements at

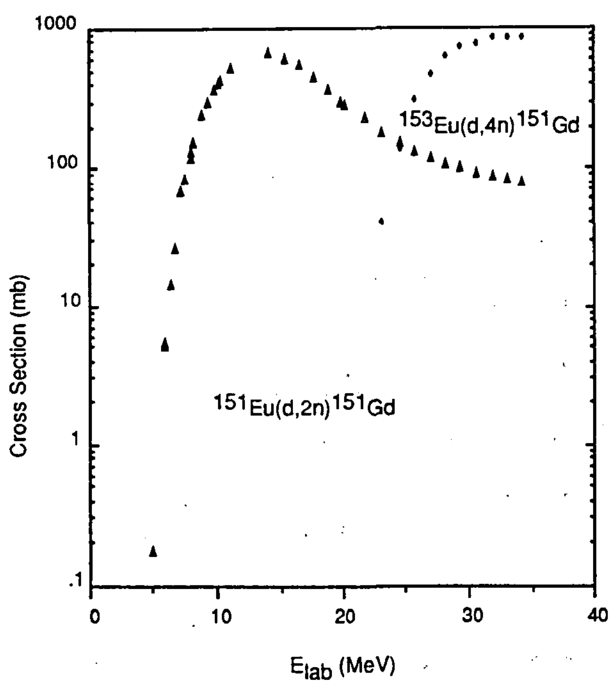

Fig. 3

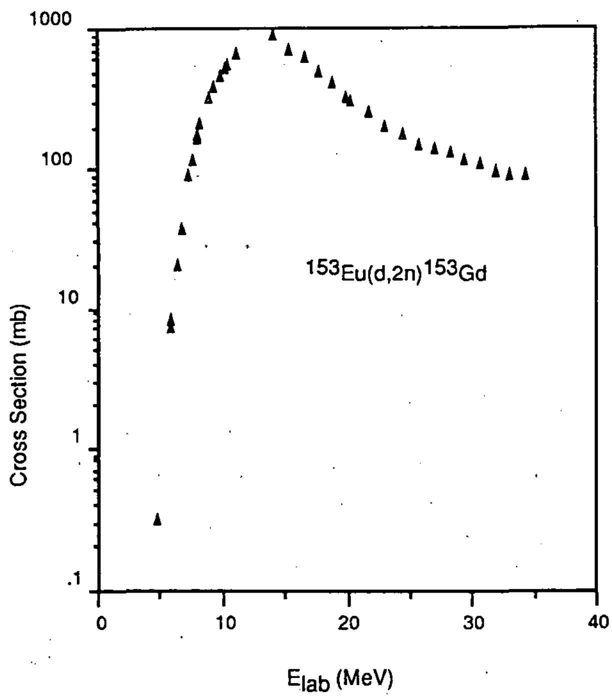

Fig. 4

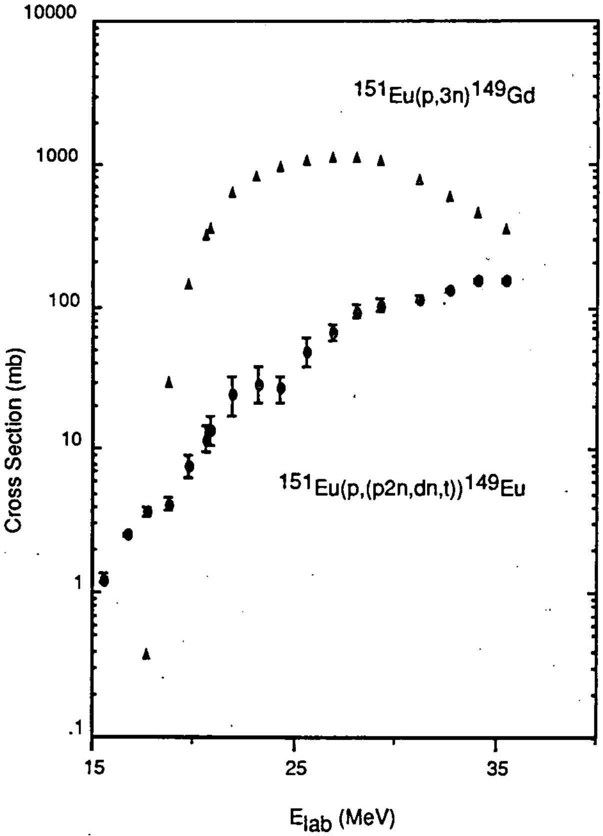

Fig. 5

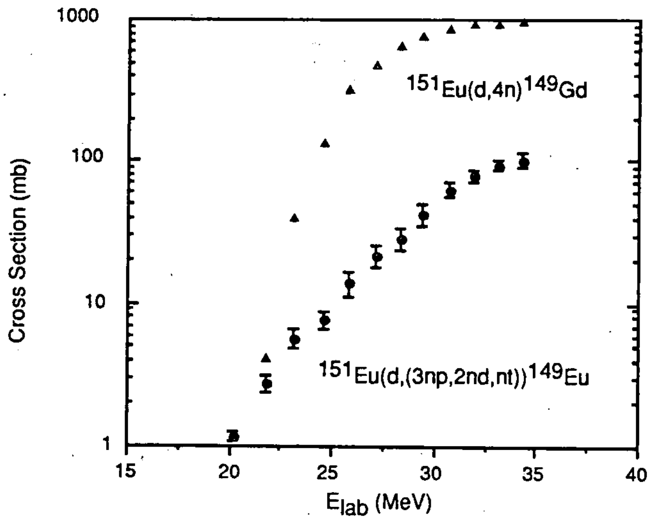

Fig. 6

the higher energies were made using the cyclotron at the Crocker Nuclear Laboratory, University of California at Davis. Although the data appeared to be of high quality we plan to make complementary measurements in the near future at 12 to 20 MeV using the Van de Graaff presently being installed at LLNL.

We have been modeling the data by means of the statistical model code STAPRE. However, one aspect of the data requires coupled-channel calculations. We find an interesting feature in the ^{151,153}Eu(p,n)^{151,153}Gd and ^{151,153}Eu(d,2n)^{151,153}Gd data; $\sigma(153)$ is enhanced at low energies relative to $\sigma(151)$. Results for (p,n) data are shown in Fig. 7. We note that the results obtained using a spherical optical potential are in poor agreement with the data. However, the results of a coupled-channel calculation, taking into account the fact that for ^{151}Eu the shape parameter $\beta_2 = 0.13$ and for ^{153}Eu $\beta_2 = 0.28$, are in reasonable agreement with the data at less than 10 MeV where the calculations are expected to be valid. Clearly, we have found a marked shape effect. The results have been prepared for submission to Physics Letters.

*Centre d'Etudes Bruyeres-le-Chatel, France

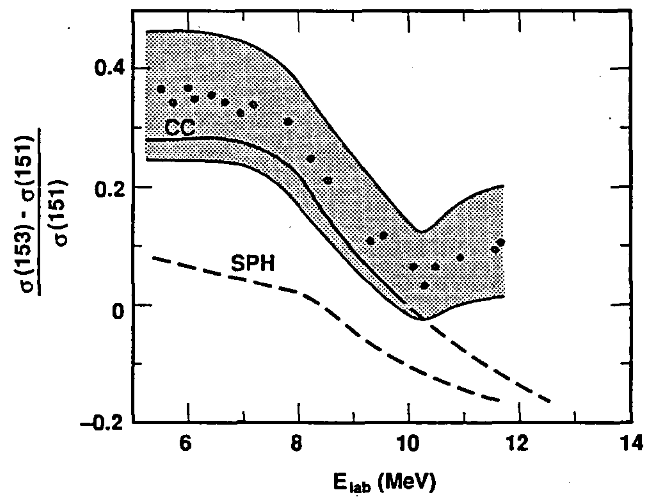

Fig. 7 Evidence of the effects of nuclear shape on reaction cross sections. The band shows the range that the data could take due to uncertainties in the Iγ's used in calculating the cross sections. SPH shows results obtained using a spherical optical potential and CC shows results for a coupled channel calculation.

2. <u>Comparative Study of Elastic Neutron and Proton Scattering and Analyzing Powers using Microscopic Optical Model Potentials in the Energy Range 8-26 MeV</u>. (L.F. Hansen, F.S. Dietrich, and R. L. Walter*)

Differential cross sections and analyzing powers for neutrons elastically scattered from $^{10,11}B$, ^{28}Si, ^{54}Fe and ^{58}Ni measured by the TUNL (8-17MeV) and Ohio (20-26 MeV) groups and the Eindhoven proton data (17-25 MeV)are compared with the predictions of microscopic optical model calculations using the JLM[1] and Yamaguchi *et al*.[2] potentials. The fits to the differential cross sections and analyzing powers (protons and neutrons) obtained with these two potentials are reasonably good using only three parameters, λ_V, λ_W and λ_{SO},(normalizing constants for the real, imaginary and spin orbit potentials respectively). The values of these parameters are given in Table 1. The value of λ_R is unity for both neutrons and protons, which reduces the number of parameters to two over the energy and mass ranges. Fig. 8-10 illustrate the quality of the fits to the data for ^{58}Ni as function of neutron and proton energy.

---

* Physics Department, Duke University.

[1] J.P. Jeukenne, A. Lejeune, and C. Mahaux, Phys. Rev. C16, 80 (1977); M3Y spin-orbit, Bertsch *et al*., Nucl. Phys. A284, 399 (1977).

[2] N. Yamaguchi *et al*., Prog. Theor. Phys. (Japan) 70, 459 (1983).

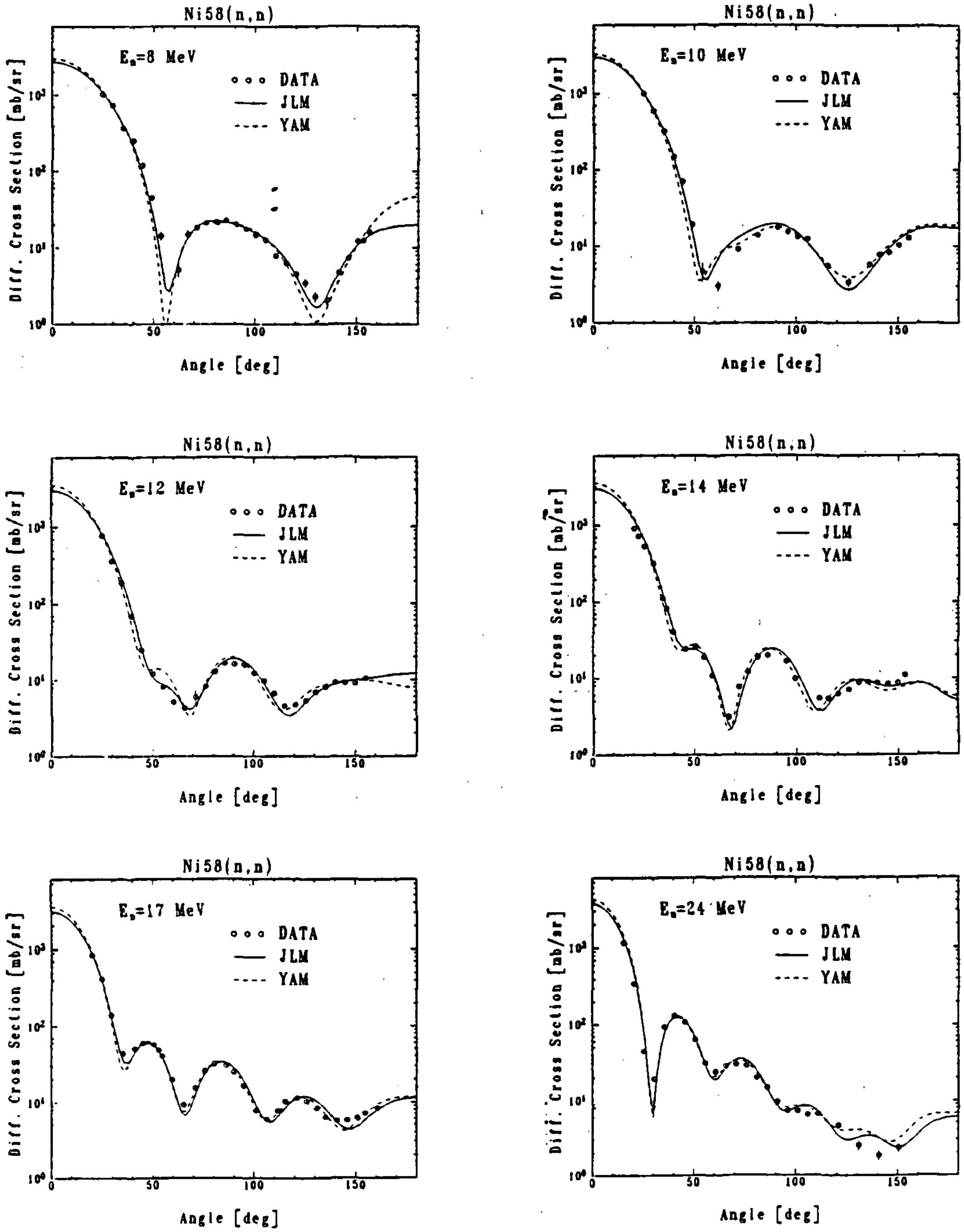

Fig. 8 Neutron elastic differential cross sections for ^{58}Ni. Calculations carried out with the microscopic OMP of Jeukenne-Lejuene-Mahaux (JLM: solid lines) and that of Yamaguchi, et al. (YAM: dashed lines).

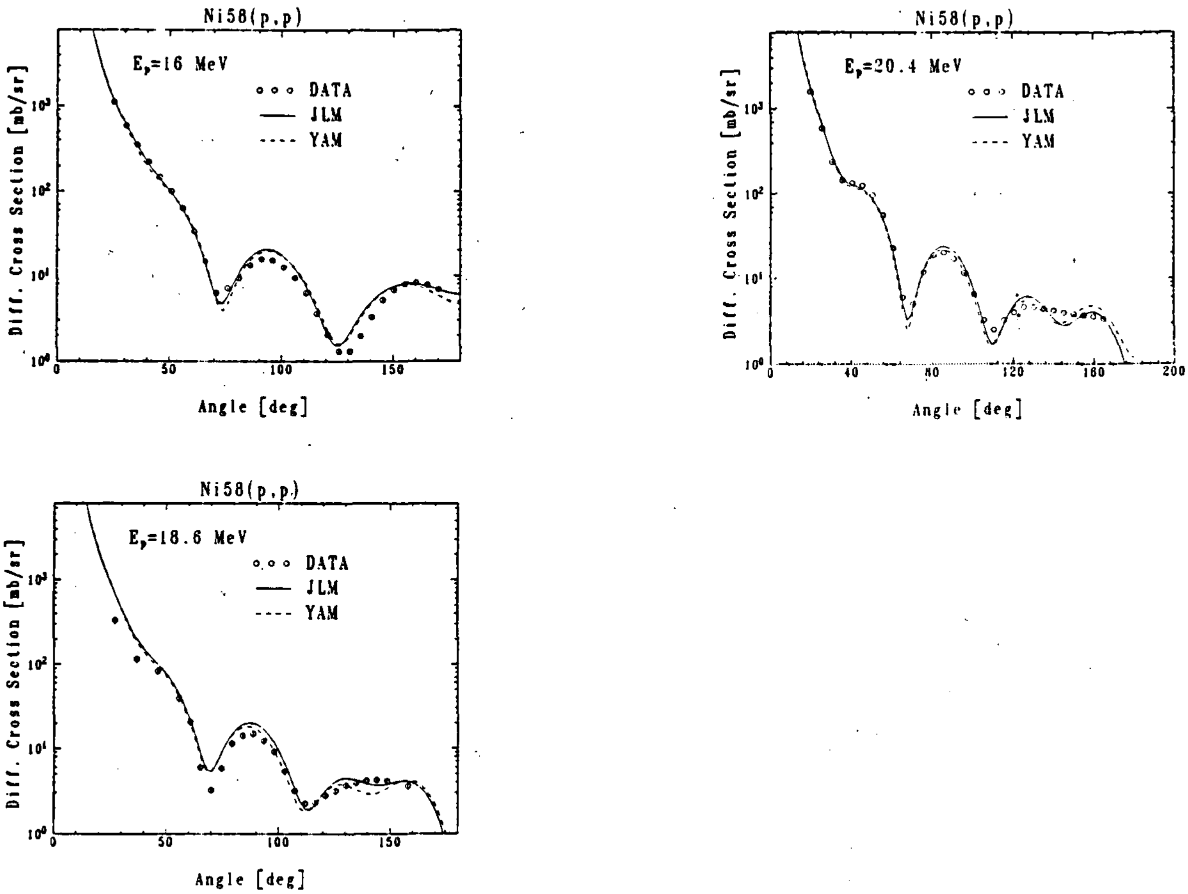

Fig. 9 Proton elastic differential cross sections for ^{58}Ni. Calculations carried out with the microscopic OMP of Jeukenne-Lejeune-Mahaux (JLM: solid lines) and that of Yamaguchi, et al. (YAM: dashed lines).

Table 1. Values of the three parameters used in the microscopic optical model calculations for all the nuclei and energies included in this report.

OMP		λ_V	λ_W	$\lambda_{S.O.}$
JLM	n	1.00±0.04	0.94±0.15	1.31±0.05
	p	1.03±0.06	0.91±0.10	1.52±0.05
YNM	n	1.00±0.06	0.70±0.10	1.45±0.06
	p	1.02±0.03	0.66±0.07	1.54±0.10

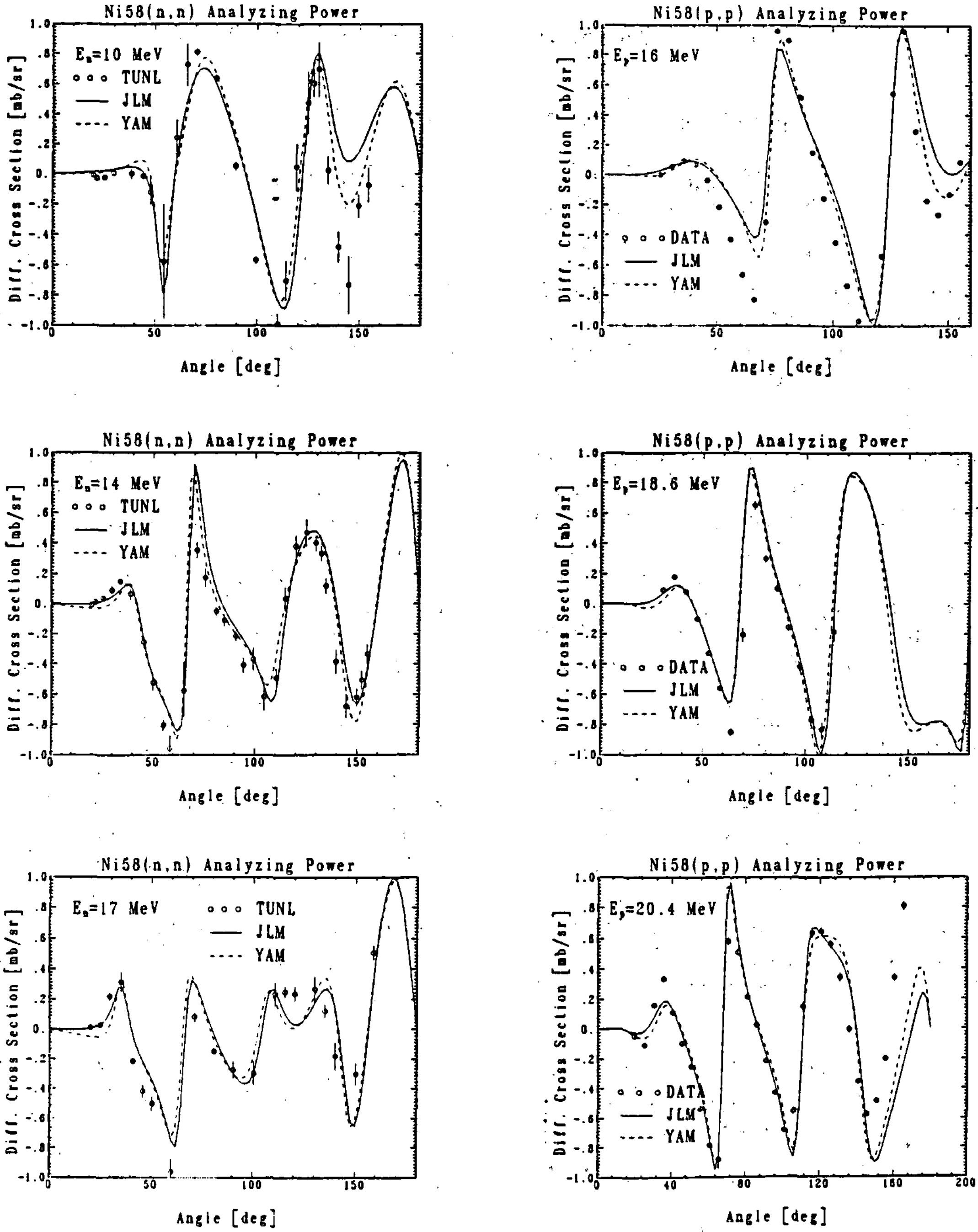

Fig. 10 Analyzing powers for neutron (left side) and proton (right side) elastic scattering from ^{58}Ni. Calculations carried out with the microscopic OMP of Jeukenne-Lejeune-Mahaux (JLM: solid lines) and that of Yamaguchi, et al. (YAM: dashed lines).

A. NUCLEAR DATA MEASUREMENTS

1. Low energy Fusion Cross Sections: Charged Particle Reactions (Nelson Jarmie and Ronald E. Brown)

The goal of this project is to determine cross sections for interactions among the hydrogen isotopes in the bombarding-energy range 10-120 keV. Such cross sections are fundamental to the operation of future controlled-fusion reactors. Experimental work with the facility constructed for this purpose [LEFCS: Low-Energy Fusion Cross Sections] is complete. Analysis and publication are continuing.

With work on the $^2H(t,\alpha)n$ reaction complete and published[1,2], the emphasis is on the $^2H(d,p)^3H$ and $^2H(d,n)^3He$ reactions. The final numerical analysis of the $^2H(d,p)^3H$ and $^2H(d,n)^3He$ data is now complete. We have measured differential cross sections for both reactions at 11 deuteron bombarding energies from 20 to 117 keV. The differential data are accurate to 2.0% over most of the energy range, with a scale error of 1.3%. Integrated cross sections are derived with total errors generally about 1.5% which greatly improves the accuracy over previous measurements. Examples were given in last year's report. See also refs. 3 and 4.

In the past, there has been considerable effort to find a meaningful way of extrapolation of the integrated cross section to very low energies for both astrophysics and fusion energy. The use of the astrophysical S function greatly simplifies the task, especially when no sharp resonance in the cross section is nearby and the S functions are slowly varying. (The S function is the result of factoring out from the cross section the energy dependences of the de Broglie wavelength and the Coulomb penetrability, which has a very steep energy dependence.) Using a least-squares fit to our data, we find the intercepts S_0 at zero energy are S_0 = 53.6 keV b (n^3He branch) and S_0 = 55.7 keV b (p^3H branch). We estimate the error in these intercepts to be few percent. An R-matrix fit using our data is expected to give similar results.

A linear least-squares fit to the S functions of Table I in the form $S = S_0(1 + aE_d)$ produces values for S_0 and a for the two branches as given in Table I. The integrated cross section σ is:

$$\sigma = 2S_0(1 + \alpha E_d)E_d^{-1} \exp[-44.402\ E_d^{-1/2}], \quad (1)$$

where E_d is the deuteron bombarding energy in keV, σ is in b (barns), and S_0 (in keV b) and α are given in Table I for each channel.

---

[1] N. Jarmie, R. E. Brown, and R. A. Hardekopf, Phys. Rev. C **29**, 2031 (1984); erratum **33**, 385 (1986);

[2] R. E. Brown, N. Jarmie, and G. M. Hale, Phys. Rev. **C 35**, 1999 (1987); erratum **36**, 1220 (1987)

[3] R. E. Brown and N. Jarmie, Radiation Effects **92**, 45 (1986); *Proceedings of the International Conference on Nuclear Data for Basic and Applied Science*, Santa Fe, 1985, edited by P. G. Young, R. E. Brown, G. F. Auchampaugh, P. W. Lisowski, and L. Stewart (Gordon and Breach, New York, 1986), p. 45.

[4] N. Jarmie and R. E. Brown, Nucl. Instrum. and Methods **B10/11**, 405 (1985).

TABLE I. Linear fit coefficients for the S function for both channels, where $S = S_0(1 + \alpha E_d)$

	p^3H branch	n^3He branch
S_0 (keV b)	55.72	53.55
α	0.001676	0.003064

In a deuterium plasma, the reactivity $<\sigma v>$ in cm^3/sec at a temperature kT (keV) is given by

$$<\sigma v> = 7.20458\ 10^{-19}\ S_{eff}\ t^2\ e^{-t}, \qquad (2)$$

where $t = 18.808(kT)^{-1/3}$, $S_{eff} = S_0[1 + \{5/(12t)\} + 2\alpha(E_0 + (35/36)kT)]$ (keV b), and $E_0 = 6.2696\ (kT)^{2/3}$ (keV). S_0 (in keV b) and α are given in Table I for each reaction channel, and E_d is the deuteron bombarding energy in keV. When using $<\sigma v>$ to calculate a reaction rate one must be careful not to double-count the deuterons. Details about these formulas and their derivation are given in Section V-B of ref. 1 and in the references given there.

A recent cross-section experiment at low energy has been performed at Münster by Krauss, Becker, Trautvetter, Rolfs, and Brand[5] whose measurements span the laboratory energy range of 6 to 325 keV. Also, new measurements are underway at Bruyère-le-Châtel, France, and at Giessen, Germany.

There have been two main forms of analysis: the Resonating Group Method (RGM), and R-matrix analyses. The RGM predictions[6,7] agree with the data fairly well considering the purity of the physical assumptions and the lack of arbitrary variables. As is often the case, the more complete a potential and physical model, the more prohibitive the computer time requirement. The actual fit of RGM theory to experiment is only fair considering the accuracy of experimental data. This accuracy remains a challenge to the RGM calculations.

The general R-matrix calculations of Hale and his collaborators[8-11] provide the best parameterization of all the data channels for the mass-4 system (up to ~29 MeV excitation in ^4He, or 10 MeV E_d); and in addition provide information about the

---

[5] A. Krauss, H. W. Becker, H. P. Trautvetter, C. Rolfs, and K. Brand, Nucl. Phys. **A465**, 150 (1987).[9] G. M. Hale and D. C. Dodder, in *Nuclear Cross Sections for Technology*, edited by J. L. Fowler, C. H. Johnson, and C. D. Bowman (National Bureau of Standards, Washington D.C., 1980), Special Publications 594, p. 650.

[6] H. M. Hofmann, G. M. Hale, and R. Wölker, in *Proceedings of Few Body Approaches to Nuclear Reactions in Tandem and Cyclotron Energy Regions*, Tokyo, 1986, p. 162, edited by S. Oryu and T. Sawada, World Scientific Publishing, Singapore (1987), and the references contained therein.

[7] H. Kanada. T. Kaneko, and Y. C. Tang, Phys. Rev. C **34**, 22 (1986).

[8] G. M. Hale and D. C. Dodder, in *Conference on Few Body Problems in Physics*, Vol. II-Contributed papers, page 433, edited by B. Zeitnitz, Elsevier Science Pub. (1984); (1983 Karlsruhe conference), and private communication. See also Nucl. Phys. **A416**, (1984).

energy levels of ^{4}He. Hale finds with an improved R-Matrix fit[11], which uses our new data and recent spin-dependent measurements, that charge symmetry between the two channels holds if proper account is taken of isospin mixing by Coulomb interaction in the internal nuclear region. This conclusion supports experiments at higher energies which also found no charge-symmetry violation indicated in earlier work. This effect of the internal Coulomb interaction is large in fitting cross sections and spin-dependent measurements.

In Figs. 1 and 2 are shown the energy dependence of the S function of the two branches and of S_a and S_b (such that $S = S_a + S_b \cos^2\theta + S_c \cos^4\theta$). S_a, S_b and S_c contain contributions from S-, P-, and D-waves. At the lower energies S_c becomes insignificant, S_b is then pure P-wave, but S_a contains both S- and P-waves. Efforts to understand the slopes, in particular using the Oppenheimer-Phillips mechanism[12] (since the deuteron has a large electric polarizability), were not very successful.

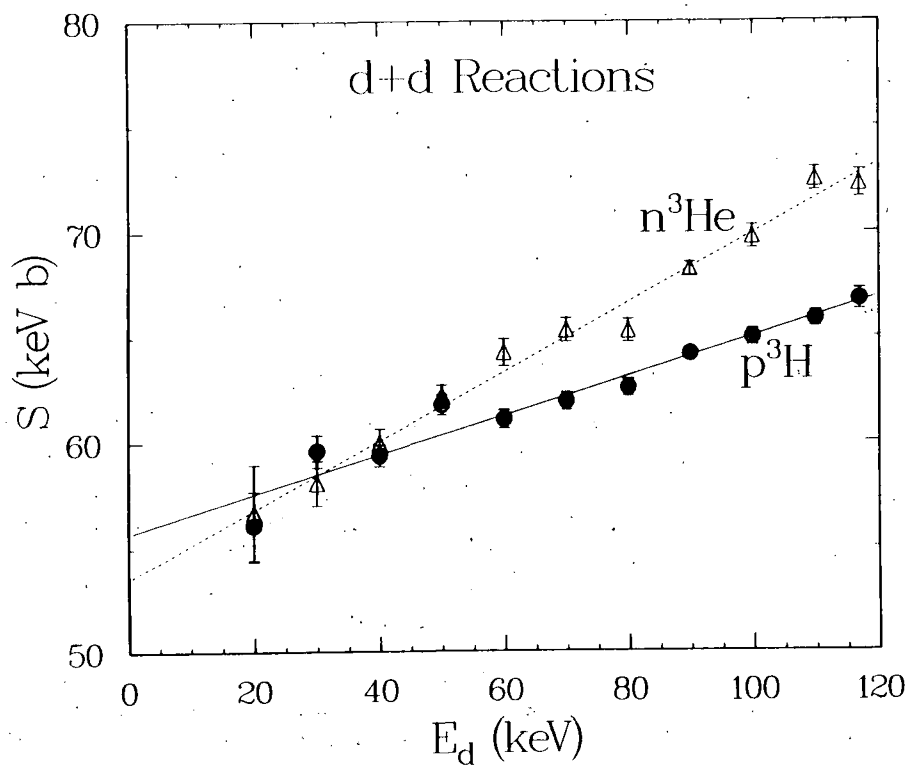

Fig. 1. The S function of Eq. (1) for both branches of the d + d reactions vs deuteron bombarding energy. Note the suppressed zero. Only relative errors are shown. The straight lines are from linear least-squares fits to the data.

---

[9] G. M. Hale and D. C. Dodder, in *Nuclear Cross Sections for Technology*, edited by J. L. Fowler, C. H. Johnson, and C. D. Bowman (National Bureau of Standards, Washington D.C., 1980), Special Publications 594, p. 650.

[10] G .M. Hale, *Status of Charged-Particle Fusion Cross Sections*, Trans. Amer. Nucl. Soc., **46**, 269 (1984) (New Orleans Conference).

[11] G. M. Hale, Bull. Am. Phys. Soc. **33**, 1571 (1988), and *Proceedings of the 1988 Annual of the Div. of Nucl. Physics* (Santa Fe). to be published.

[12] J. R. Oppenheimer, and M. Phillips, Phys. Rev. **48**, 500 (1935).

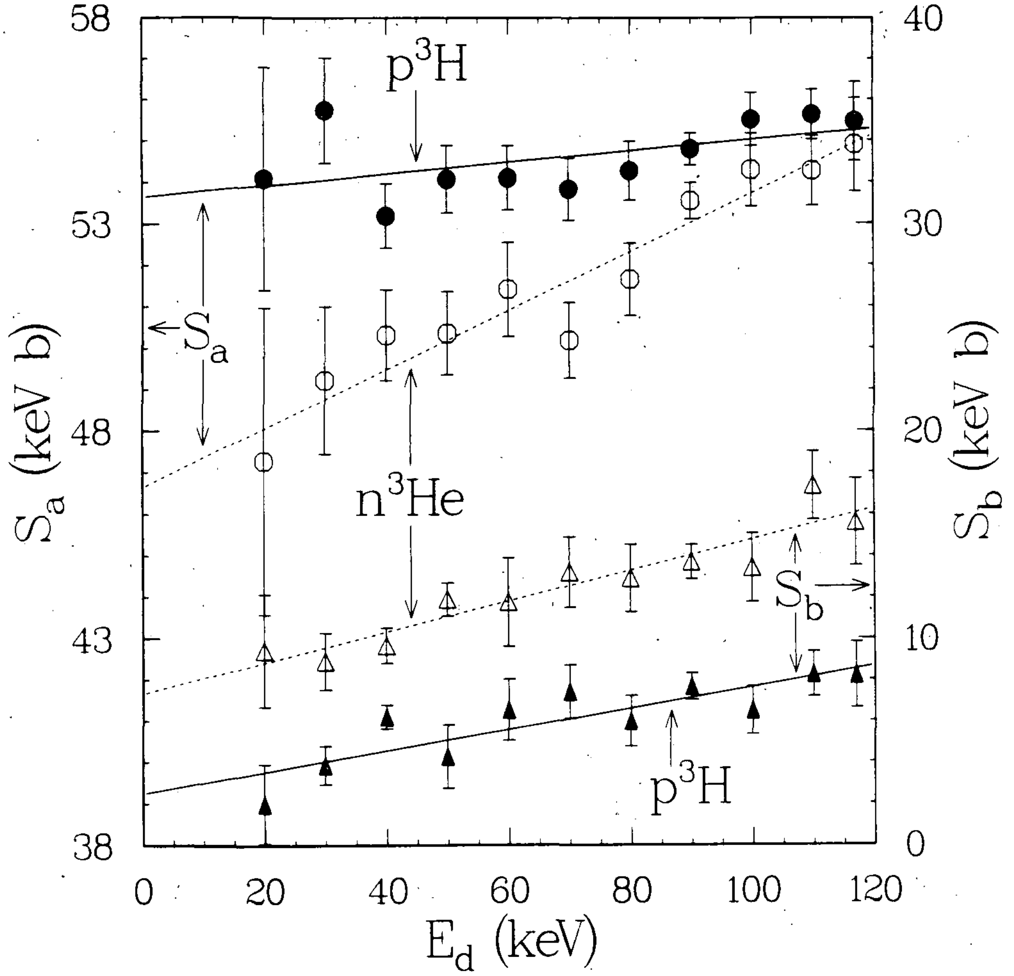

Fig. 2. Partial S functions S_a and S_b arising from the $4\pi a$ and $4\pi b/3$ contributions to the integrated cross section σ. Note the suppressed zero for S_a. The curves are linear least-squares fits to the data. Relative errors are shown.

In the analysis of the angular distributions, we find a larger D-wave reaction amplitude than previously reported. To gain more understanding of the strength of the D-wave contribution, we list in Table I the ratio c/a from the expansion coefficients ($\sigma = a + b\cos^2\theta + c\cos^4\theta$) at 100 keV, where the D-wave contribution is significant. We compare our results with those of Münster[5], Theus[13], and an R-matrix analysis[8,9] <u>not</u> containing our data. Considering only the Los Alamos data, the indication would be that the level-structure used in the R-matrix analysis does not provide sufficient D-wave strength which comes from the tails of D-wave levels higher in excitation in the ^4He compound system. An R-Matrix reanalysis[11] that includes our data does see a broadening and lowering of these levels. In Table II the data of Theus and Münster indicate conflicting results, the reason for which is unknown.

[13] R. B. Theus, W. I. McGarry, and L. A. Beach, Nucl. Phys. **80**, 273 (1966).

TABLE II. The c/a coefficient ratio at 100 keV. The R-Matrix prediction does not contain the Los Alamos or Münster data.

	p^3H branch	n^3He branch	Ref.
Los Alamos	0.27	0.19	present work
Münster	0.16	0.062	5
Theus	0.04	0.12	13
R-matrix	0.046	0.044	14

In Figs. 3 and 4 we show the angular anisotropies defined as $[\sigma(0°)\ \sigma(90°)]/\sigma(90°)$, and which can also be expressed in terms of the expansion coefficients as (b + c)/a. There we compare the LEFCS results with those of Theus *et al.*[13], the Münster work,[5] and the R-matrix calculation that does not include our data[8,9] From these

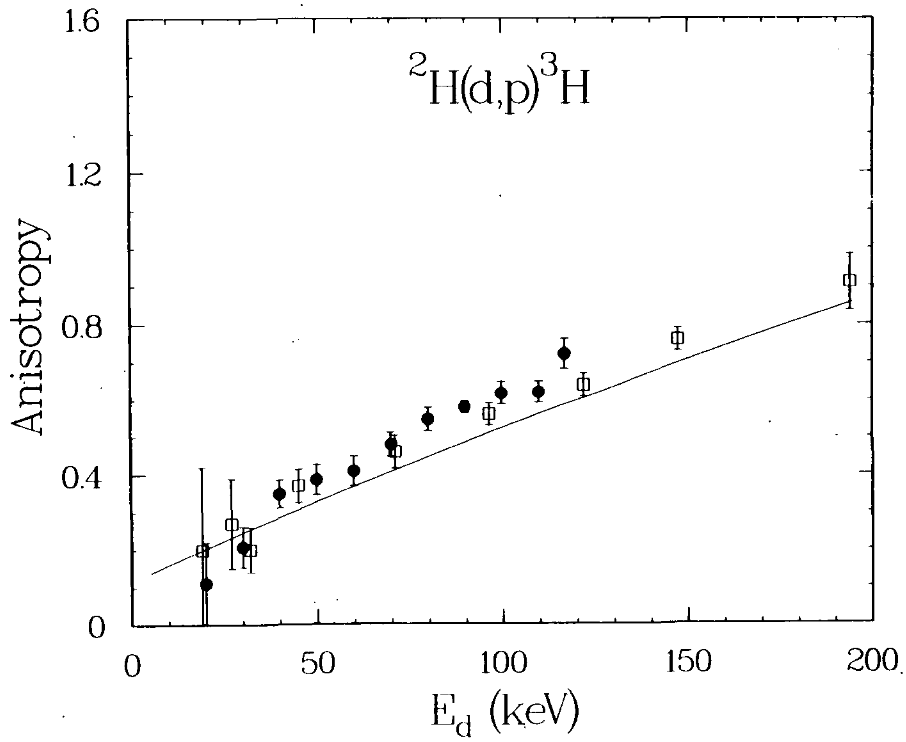

Fig. 3. $^2H(d,p)^3H$ angular anisotropy $[\sigma(0°) - \sigma(90°)]/\sigma(90°)$ vs deuteron bombarding energy. The solid circles are the present data, and the squares are the data of Theus, *et al.*[6] The curve is from a unified, mass-4, R-matrix analysis[8,9] which does not include the present data.

[14]G. M. Hale, private communication.

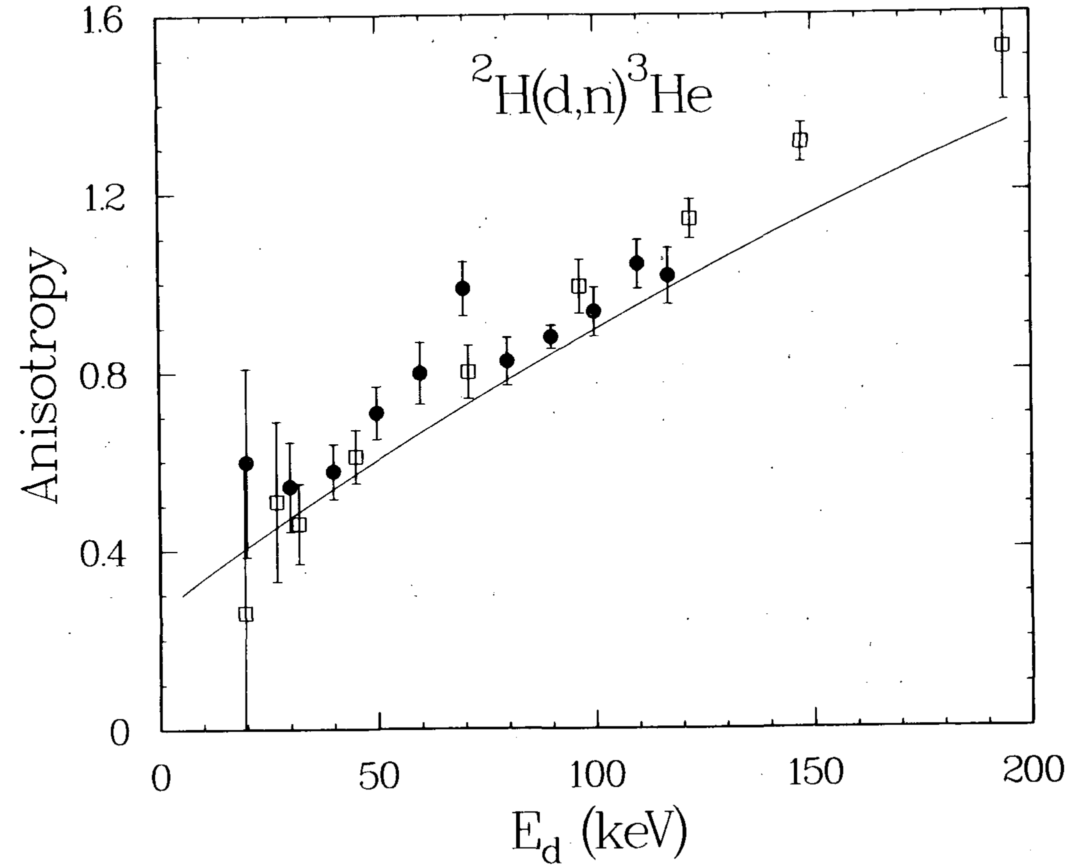

Fig. 4. $^2H(d,n)^3He$ angular anisotropy [$\sigma(0°)$ -$\sigma(90°)$]/$\sigma(90°)$ vs deuteron bombarding energy. The solid circles are the present data, and the squares are the data of Theus, et al.[13] The curve is from a unified, mass-4, R-matrix analysis[8,9] which does not include the present data.

figures, we note that the n + ^3He anisotropy is considerably larger than that of the p + ^3H branch. In evaluating the anisotropies, the results of Theus *et al.* perhaps should be given the greatest weight, since they measured $\sigma(\theta)$ at more angles than was done in the other experiments, thereby obtaining smaller errors for the anisotropies. We stress that the *absolute* cross sections from our work are the most accurate yet measured.

Calculations by G. Hale of Los Alamos extending R-Matrix phenomenology to handle 3-body breakup continue. This development is of great interest to us to help analyze the three-body breakup alpha spectra of the T(t,α)nn reaction; and, in particular, to be able to estimate the shape of the neutron spectrum, which we have found impossible to measure experimentally.

A standard "handbook" of the best evaluated fuel-cycle cross sections and reactivities is still under consideration. Some fusion-reactor designers are still using old and sometimes grossly inaccurate data, and there exists no world standard collection of charged-particle data such as exists for neutron data. Work on this idea remains dormant pending funding and manpower.

2. Low-Energy (n,charged particle) Cross Sections on Unstable Nuclei: The $^{22}Na(n,p)^{22}Ne$ and $^{22}Na(n,\alpha)^{19}F$ Cross Sections from 25 meV to Approximately 35 keV (P. E. Koehler and H. A. O'Brien)

Preliminary results of our measurements of the $^{22}Na(n,p_0)^{22}Ne$ and $^{22}Na(n,p_1)^{22}Ne^*$ cross sections to 420 eV and 35 keV respectively were reported here last year. Since that time, a paper describing these measurements and their physics implications as well as our $^{22}Na(n,\alpha)^{19}F$ measurements at thermal energy has been published.[1] As detailed in our paper, the analysis of the data has lead to; 1) a much better understanding of the structure of ^{23}Na near the neutron threshold, and 2) as shown in Fig. 1, an experimentally determined $^{22}Na(n,p)^{22}Ne$ astrophysical reaction rate which differs by almost a factor of 10 at most temperatures from the theoretical rates[2,3] used in most previous nucleosynthesis calculations. This difference could have a significant impact on the calculated production of ^{22}Na in explosive environments.

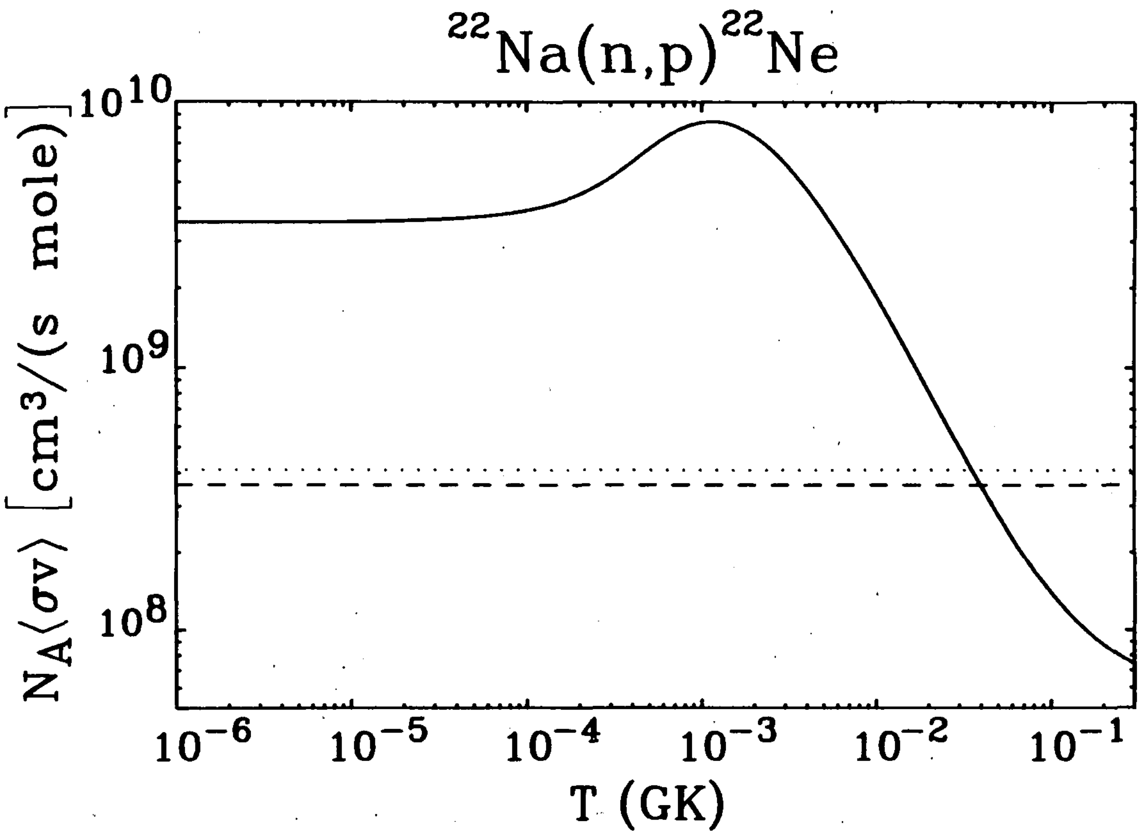

Fig. 1. Comparison of the $^{22}Na(n,p)^{22}Ne$ astrophysical reaction rate calculated from the sum of our p_0 plus p_1 data (solid curve) to the theoretical rates given in refs. 2 (dashed curve) and 3 (dotted curve).

[1] P. E. Koehler and H. A. O'Brien, Phys. Rev. C **38**, 2019 (1988).
[2] R. V. Wagoner, Astrophys. J. Suppl. **18**, 247 (1969).
[3] S. E. Woosley et al., At. Data Nucl. Data Tables **22**, 371 (1978).

During the last LANSCE run cycle we have extended our $^{22}Na(n,\alpha)^{19}F$ measurements from thermal energy to approximately 2 keV. As shown in Fig. 2, the combined yields of the α_0 through α_2 groups is dominated by the same resonance near 170 eV which is responsible for most of the p_1 cross section. Hence, as was the case for the $^{22}Na(n,p)^{22}Ne$ reaction, the astrophysical reaction rate for the combined α_0 through α_2 groups is about a factor of 10 different from the theoretical rate at most temperatures.

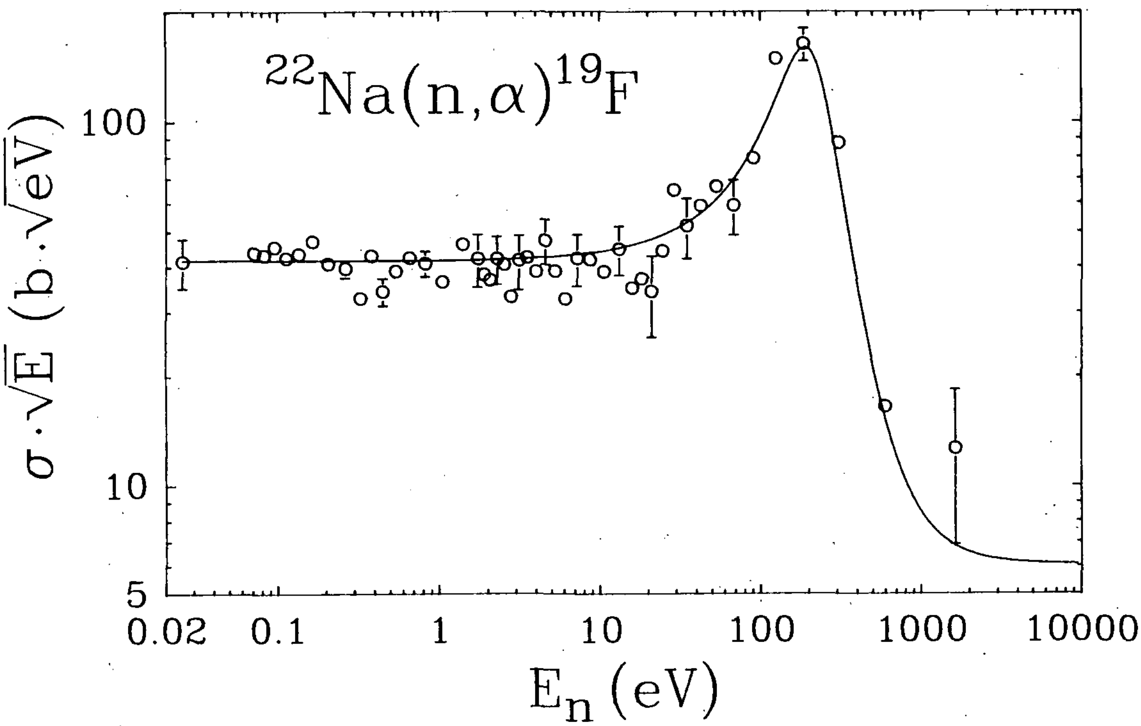

Fig. 2. Reduced cross section for the $^{22}Na(n,\alpha)^{19}F$ (α_0 through α_2) reaction (open circles). The solid curve is a fit to the data with the same Breit-Wigner shape used to fit the p_1 cross section. See ref. 1 for details.

3. <u>Low-Energy (n,charged particle) Cross Sections: The $^{14}N(n,p)^{14}C$ Cross Section from 61 meV to Approximately 34.6 keV</u> (P. E. Koehler and H. A. O'Brien)

We have measured the $^{14}N(n,p)^{14}C$ cross section from 61 meV to 34.6 keV and have submitted the results for publication to Phys. Rev. C.[1] These are the first direct measurements of this cross section between thermal energy and 25 keV to be reported. In nuclear astrophysics, this reaction is important because through it ^{14}N is potentially a strong neutron poison during the operation of the chain of reactions centered around $^{13}C(\alpha,n)^{16}O$ as a neutron source for the s-process of nucleosynthesis. If the $^{14}N(n,p)^{14}C$ cross section is large enough, then in some

[1] P. E. Koehler and H. A. O'Brien, submitted to Phys. Rev. C.

scenarios this chain of reactions can be a net neutron consumer rather than a net producer of neutrons. As shown in Fig. 1, our data are in agreement with previous measurements made via the inverse reaction[2,3], but are approximately a factor of 2.5 larger than a recent direct measurement[4]. As a result, our data support the astrophysical reaction rate[5] used in most previous nucleosynthesis calculations over the recently recommended three-fold reduction in this rate[4]. Therefore, our measurements indicate that ^{14}N would be a stronger neutron poison during the possible operation of the $^{13}C(\alpha,n)^{16}O$ s-process neutron source than the recent data of ref. 4 imply. Our results also seem to rule out the s-process as a source of significant amounts of ^{15}N if the production of this isotope is dependent upon an approximate two-fold reduction in the $^{14}N(n,p)^{14}C$ reaction rate of ref. 5 as indicated by the preliminary calculations of ref. 6.

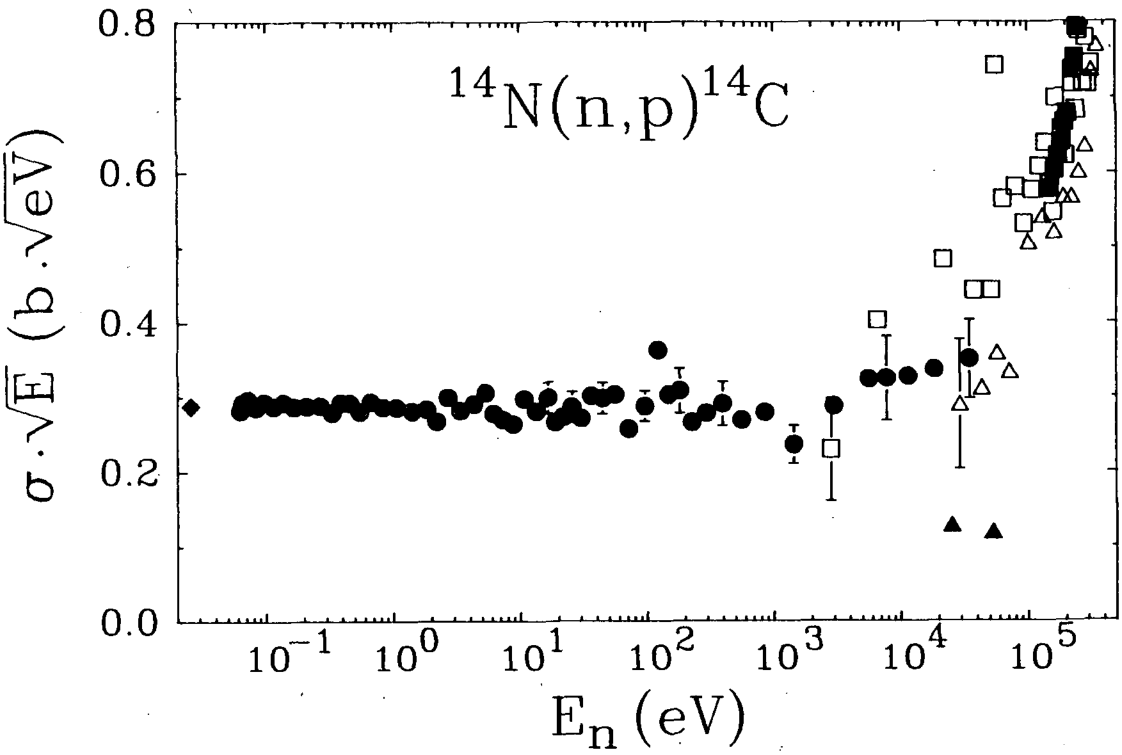

Fig. 1. The $^{14}N(n,p)^{14}C$ reduced cross section verses laboratory neutron energy. Shown are our data (shaded circles), the direct measurements of ref. 4 (solid triangles), ref. 7 (shaded diamond), and ref. 8 (shaded squares), and the inverse measurements of ref. 2 (open triangles), and ref. 3 (open squares).

---

[2] J. H. Gibbons and R. L. Macklin, Phys. Rev. **114**, 571 (1959).
[3] M. Sanders, Phys. Rev. **104**, 1434 (1956).
[4] K. Brehm, H. W. Becker, C. Rolfs, H. P. Trautvetter, F. Kappeler and W. Ratynski, Z. Phys. **A330**, 167 (1988).
[5] N. A. Bahcall and W.A. Fowler, Ap. J. **157**, 659 (1969).
[6] A. Jorissen and M. Arnould, in *Nucleosynthesis and its Implications on Nuclear and Particle Physics*, J. Audouze and N. Mathieu, eds., (Dordrecht: Reidel, 1986) p. 303.
[7] F. Ajzenberg-Selove, Nucl. Phys. **A449**, 1 (1986).
[8] C. H. Johnson and H. H. Barschall, Phys. Rev. **80**, 818 (1950).

4. <u>Direct Mass Measurements of Neutron-Rich Nuclei Using the Time-of-Flight Isochromous (TOF1) Spectrometer</u> (J. M. Wouters, D. J. Vieira)

Three years ago INC-11 commissioned the TOFI spectrometer for making systematic direct mass measurements of neutron-rich, low-Z nuclei.[1] We have successfully initiated a mass measurement program using TOFI and two sets of experimental results ranging from ^{11}Li to ^{37}P have been published.[2] In this report we present a brief description of the TOFI spectrometer and summarize the experimental results obtained to date.

The isochronicity of TOFI is the key feature which enables us to make high precision systematic mass measurements. The flight-time of an ion through the spectrometer, which consists of four identical 81 1.1 meter radius bending magnets, depends only on it's mass-to-charge ratio and is independent of energy. Since TOFI is also 1-to-1 imaging and momentum nondispersive we can use small-area, fast-timing detector (i.e. secondary electron microchannel plate detectors[3]) to get a precise measurement of the ion's mass-to-charge ratio. Currently, we can measure the flight-time to an accuracy of 180 ps (fwhm) or 1 part in 3000, which results in mass accuracies of from 100 to 1000 keV depending on statistics.

To obtain a mass, the charge state of each ion must be uniquely determined. This is done by measuring the total energy and velocity of the ion. These measurements can be of modest precision since the charge is quantized. Finally the atomic number, Z, of the ion must also be determined since the intrinsic mass-to-charge resolution of TOFI is insufficient to separate isobars directly. The total energy detector at the exit of the spectrometer is also designed to measure energy loss, dE/dx, from which the Z of the ion is determined.

Neutron-rich ions are created at the LAMPF accelerator using the 1 ma - 800 MeV proton beam which strikes a 1 mg/cm^2 thorium target. A small fraction of the ions (Ω = 2.5 msr, $\delta E/E = \pm 4\%$ E) are transported to the spectrometer using a set of four quadrupole triplet magnets arranged in a double transported to the spectrometer using a set of four quadrupole triplet magnets arranged in a double telescopic system[4]. A fast timing detector located at the intermediate focus of this transport line is used in conjunction with the first timing detector in the spectrometer to obtain the velocity of the ion. Since many more protons, deuterons, alphas and tritons are created by reactions in the target than the neutron--rich ions of interest we use a mass-to-charge prefilter consisting of an electrostatic deflector and and dipole magnet located between the first and second quadrupole triplet magnets. This prefilter reduces the unwanted ions by a factor of ~10^6 which enables us to keep the counting rates in our timing detectors to manageable level.

---

[1] J. M. Wouters, D. J. Vieira, W. Wollnik, H. A. Enge, S. Kowalski, and K. L. Brown, Nucl. Instr. and Meth., **A240** 77 (1985); J. M. Wouters, D. J. Vieira, H. Wollnik, G. W. Butler, R. H. Kraus, Jr., and K. Vaziri., Nucl. Instr. and Meth., **B26** 286 (1987).

[2] D. J. Vieira, J. M. Wouters, K. Vaziri, R. H. Kraus, Jr., H. Wollnik, G. W. Butler, F. K. Wohn, and A. H. Wapstra, Phys. Rev. **C57**, 3253, (1986); J. M. Wouters, R. H. Kraus, Jr., D. J. Vieira, G. W. Butler, and K. E. G. Löbner, Z. Phys. A 331, 229 (1988).

[3] R. H. Kraus, Jr., D. J. Vieira, H. Wollnik, and J. M. Wouters, Nucl. Instr. and Meth., **A264** 327 (1988).

[4] K. Vaziri, F. K. Wohn, D. J. Vieira, H. Wollnik, and J. M. Wouters, Nucl. Instr. and Meth., **B26** 280 (1987).

The results of our first two mass measurement experiments[2] are listed in the table. (All masses are given as mass excesses with uncertainties given in parenthesizes.)

^{A}Z	μamu	^{A}Z	μamu	^{A}Z	μamu
^{11}Li	43780(130)	^{23}F	3530(210)	^{30}Mg	-9700(230)
^{14}Be	42660(150)	^{24}F	8070(170)	^{31}Mg	-3830(220)
^{17}B	46830(180)	^{25}F	12150(130)	^{32}Mg	-800(260)
^{19}C	35080(120)	^{26}F	19820(210)	^{32}Al	-12160(220)
^{20}C	40360(240)	^{27}F	27500(700)	^{33}Al	-9490(250)
^{20}N	23350(120)	^{27}Ne	6000(600)	^{34}Al	-3800(400)
^{21}N	26750(145)	^{28}Ne	11500(400)	^{36}Si	-13900(600)
^{22}N	34340(250)	^{28}Na	-1220(190)	^{37}P	-20740(400)
^{23}O	15700(140)	^{29}Na	2820(320)		
^{24}O	20000(500)	^{30}Na	7600(500)		

In general, these measurements agree well with other recent mass measurements done in this region.[5]

Most mass models break down for light nuclei because they rely in part on methodologies that describe the nucleus as a many body (many nucleons) object. For light nuclei there simply are too few nucleons for such formalisms to work. Shell model descriptions are more successful, but fail in some cases since not all relevant components to the nuclear wavefunction can be included in describing the ground state. Thus in this mass region it is important to actually perform mass measurements to have accurate mass information. In the next year we hope to complete additional mass measurement experiments covering higher Z neutron-rich nuclei. We will also perform a new experiment to measure the half-lives of selected beta-delayed neutron emitting nuclei that relies on using TOFI to identify all recoils by their A, Z, and Q.

[5] A. Gillibert, W. Mittig, L. Bianchi, A. Cunsolo, B. Fernandez, A. Foti, J. Gastebois, C. Gregoire, Y. Schutz, and C. Stephan, Phys. Lett. **B192**, 39 (1987).

5. Status of the WNR Facility (P. W. Lisowski)

The final phase of the Weapons Neutron Research (WNR) Facility white neutron source upgrade (target-4) was completed in June of 1988. this work consisted of increasing the biological shield to the design thickness along the north, east, and west walls; shielding the beam transport line leading to the target cell; and installing personnel safety systems in all of the neutron beam-line experimental caves. The facility is shielded for up to 20 micro-Amperes of proton beam on target. Two additional neutron flight paths were installed; a 90-m flight path and detector station for 50 - 400 MeV (n,p) reaction studies; and a 15-m flight path and detector station for 0 - 50 MeV (n,charged particle) experiments. Figure 1 shows the layout of the WNR Facility.

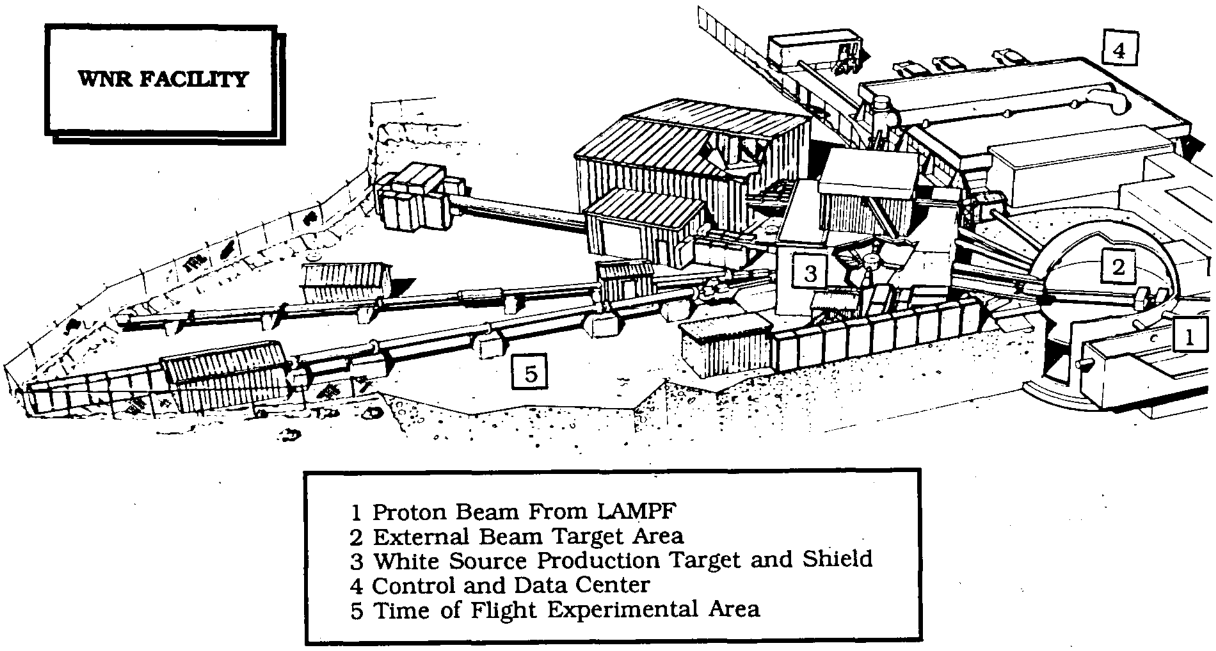

Fig. 1. WNR Facility

During the fall 1988 operating period, up to five flight paths were operated simultaneously at the white source; much of that work is reported in other Los Alamos contributions to this report. In addition, experiments were performed using the WNR target-2 facility for a variety of research, including hardened electronics damage studies for defense research, an ionizing-radiation pumped laser development project, (p,xn) angular distribution measurements, and SDI related hit-observable studies.

For the 1989 operating cycle, which will extend from May until October, the major facility improvements will consist of an upgrade to the beam delivery pulsed-magnet system for WNR and increased shielding on all of the collimators and neutron beam dumps in the time of flight experimental area. The beam delivery upgrade will increase the pulse repetition rate by as much as a factor of three, and the increased shielding will reduce scattered neutron backgrounds from the WNR white source in the neighboring LANSCE experimental area to the ambient level.

6. <u>Neutron Induced Fission Cross Section Ratios for ^{232}Th, ^{235,238}U, ^{237}Np and ^{239}Pu from 1 to 400 MeV</u> (P. W. Lisowski, J. L. Ullmann, S. J. Balestrini; A. D. Carlson, O. A. Wasson (National Institute of Standards and Technology); and N. W. Hill (Oak Ridge National Laboratory))

During the 1988 running period at WNR, final data were taken to complete the fission cross section ratio set for ^{232}Th, ^{235,238}U, ^{237}Np and ^{239}Pu. Data reduction is nearing completion. Preliminary results show better than 1% agreement with data taken the previous operating period. Addtional fission foils of ^{233,234,236}U have been procured for measurements during the 1989 running period. For the appropriate nuclei, measurements of the thermal cross sections will be made at the LANSCE Facility to verify the the foil thicknesses.

7. High Resolution (n,xγ) Measurements [R. O. Nelson, D. Drake, R. C. Haight, G. L. Morgan, H. A. O'Brien, S. A. Wender, P. G. Young (Los Alamos), H. Vonach (Vienna), and D. C. Larson (ORNL)].

As a feasibility study we measured de-excitation gamma rays from $^{nat}Fe(n,x\gamma)$ reaction products using a HPGe detector at the WNR in a 16 hr run. Gamma rays were measured in the range $0.5 < E_\gamma < 3.0$ MeV with incident neutron energies $0.7 < E_n < 400$ MeV. Comparison with previous results[1] shows that our arrangement has lower backgrounds and much higher counting rates. We are presently comparing our data with model calculations. During the next year we plan to measure (n,xγ) data for a variety of targets, including ^{54}Fe, ^{88}Y, $^{206,207,208}Pb$, ^{232}Th, ^{238}U, and a number of lighter elements.

---

[1] D.C. Larson, in Nuclear Data for Basic and Applied Science, ed. P.G. Young, R.E. Brown, G.F. Auchampaugh, P.W. Lisowski, and L. Stewart, Gordon and Breach (New York, 1986) vol. 1, p. 71.

8. (n,charged particle) Reactions at En < 50 MeV (R. C. Haight, P. W. Lisowski, S. M. Grimes*, R. Pedroni*, V. Mishra*, and N. Boukharouba*)

A 9-meter station at LAMPF/WNR was established this past year for the measurement of charged particle emission cross sections, angular distributions and spectra from reactions induced by neutrons with energies below 50 MeV. The neutron flux spectrum was measured using a ^{235}U fission chamber as well as by observing recoil protons from a CH_2 target. The neutron spectrum is in good agreement with expectations based on an intranuclear cascade code. Initial measurements were made on the ^{12}C(n,alpha) reaction and on (n,p), (n,d) and (n,alpha) reactions on aluminum. The lower energy limit for detecting alphas was 6 MeV due to the thickness of the delta-E detector in the two-counter telescope. Backgrounds were small showing good collimation of the neutron beam. Detectors of lower thresholds and larger areas will be installed this year in a continuation of these studies which are aimed at understanding (n,charged particle) reactions on light nuclides and on obtaining level density information for heavier nuclides.

---

*Ohio University, Athens, OH 45701

9. The (n,p) Reaction from 50 to 250 MeV as a Probe of Gamow-Teller Strength [J. L. Ullmann, R. C. Haight, D. S. Sorenson, A. G. Ling, P. W. Lisowski, N. S. P. King (Los Alamos), F. P. Brady, J. R. Romero, J. R. Drummond (Univ. Cal. Davis), J. Rapaport, R. W. Finlay, X. Aslanoglou, V. Mishra, W. Abfalterer (Ohio University), C. Howell, W. Tornow (Duke University)]

During the LAMPF running period during summer, 1988, a spectrometer system for measuring n-charged particle reactions was constructed, and first data taken at the WNR Target-4 White neutron source. The neutron energy was determined by time of flight over a 90 meter flight path. To study Gamow-Teller transitions, which peak at zero degrees, a magnet was used to sweep contaminant charged particles from the neutron beam. The charged particles were then detected in an E-DE detector array consisting of a plastic DE detector and 15 CsI(Tl) crystals, each 3.5 in X 3.5 in X 6 in deep. The overall solid angle of this array was 43.5 msr. The scattering angle was determined by wire chambers in front of the magnet. A multiple-target array was used to increase the count rate. All cross sections were measured relative to H(n,p). The first experiment was to study ^{12,13}C(n,p). Preliminary energy spectra, which represent about 10% of the data, are shown for ^{13}C in Fig. 1. The data are summed over 0 to 4 degrees scattering angle and the indicated incident energy range. The ground-state Gamow-teller transition (Q = -12.65 MeV) is clearly visible and separated from the first excited state at 3.48 MeV excitation. The large peak at Q = 0 indicates hydrogen in the target material.

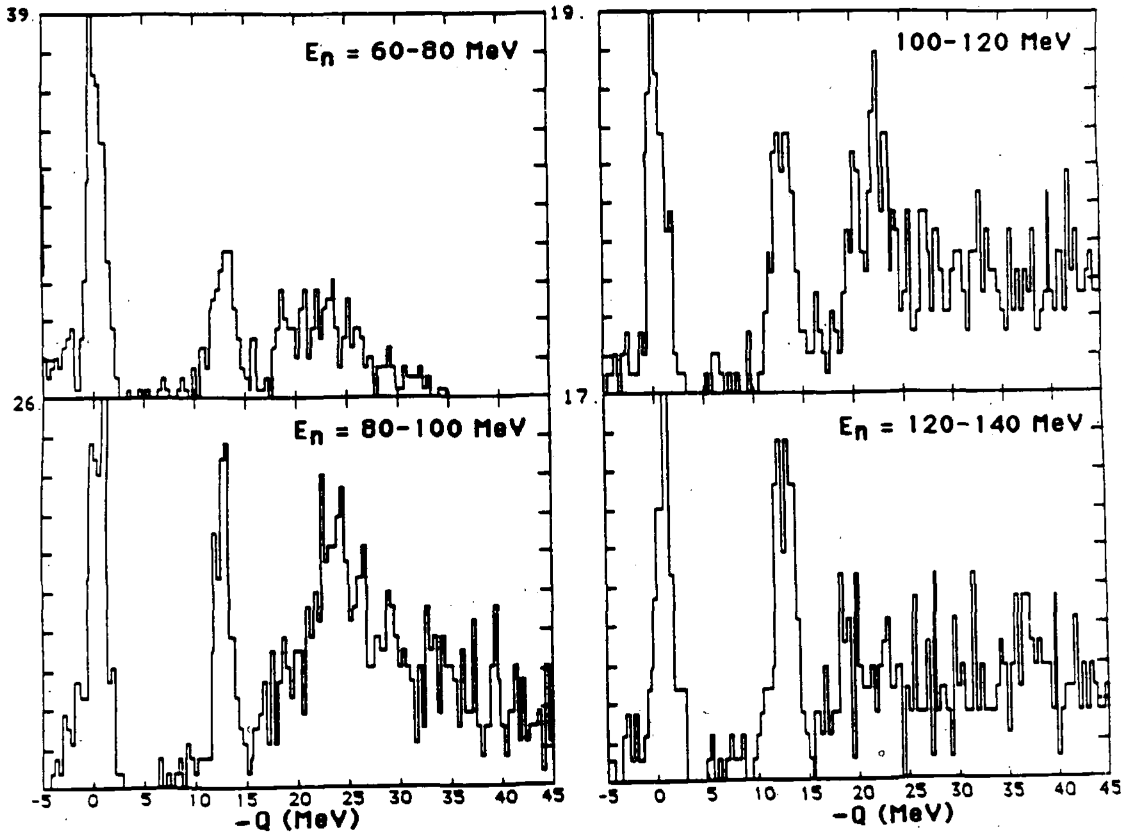

Fig. 1. ^{13}C(n,p) summed over 0 to 4 degrees.

B. NUCLEAR DATA EVALUATION

1. Charge-Independent Description of the d+d Reactions (G. M. Hale and D. C. Dodder)

Our charge-independent R-matrix description of reactions in the A=4 system accounts well[1] for the differences seen in the most recent cross-section[2] and polarization[3] measurements for the two branches of the d+d reaction at low energies. Comparisons of the calculations with experimental values of the differential cross section (a) and vector analyzing power (b) for both branches of the reaction at E_d=80 keV are shown in Fig. B-1. The rather large cross-section differences, and the more modest analyzing-power differences (including those not shown for the second-rank tensors) are reproduced by the calculation in the entire low-energy region.

Furthermore, the analysis explains the startlingly large differences that have been measured for the P-wave cross sections,

$$\left[\frac{\sigma_{d,n}^{L=1}}{\sigma_{d,p}^{L=1}}\right]_{expt} = 1.40\pm0.04, \quad \left[\frac{\sigma_{d,n}^{L=1}}{\sigma_{d,p}^{L=1}}\right]_{calc} = 1.43\ ,$$

in low-energy muon-catalyzed fusion experiments in the Soviet Union. These differences can be atttributed to the small effects of internal Coulomb isospin mixing being greatly amplified in the external Coulomb field by the proximity of broad levels having opposite isospin in the P-wave states.

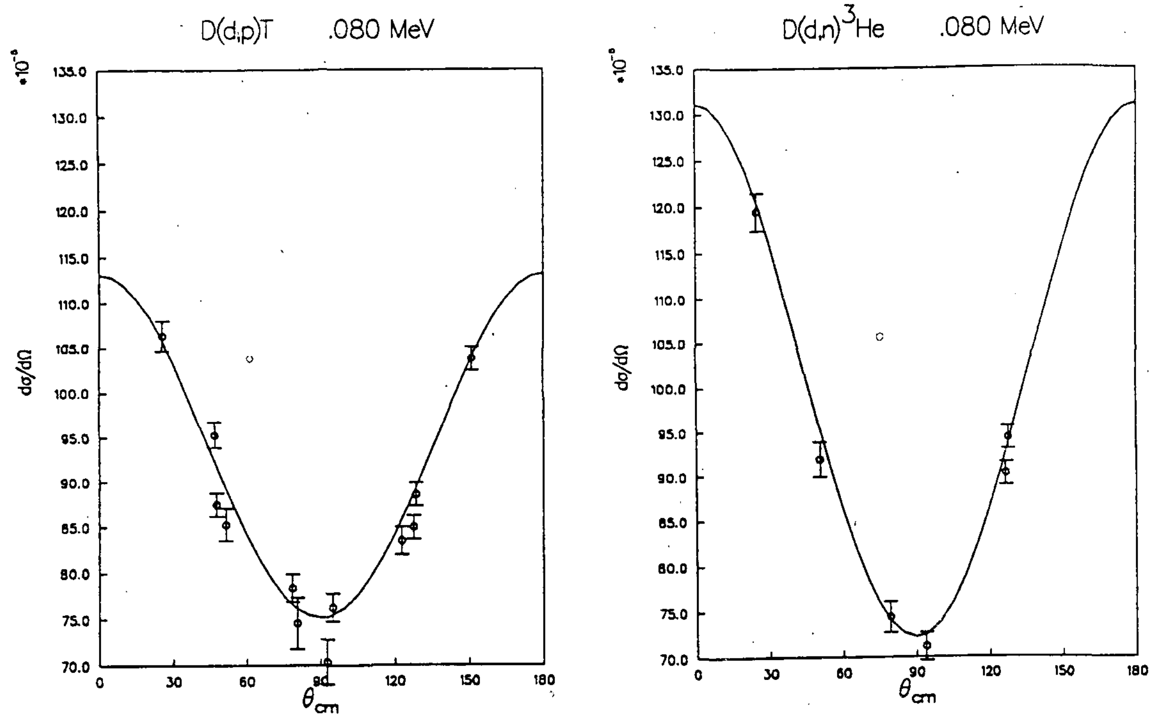

Fig. B-1(a) Comparison of the R-matrix calculations with differential cross-section[2] (a) and analyzing power[3] (b) measurements for the d+d reactions at E_d=80 keV.

[1]G. M. Hale and D. C. Dodder, Bull. Am. Phys. Soc. *33*, 1571 (1988).
[2]R. E. Brown and N. Jarmie, submitted to Phys. Rev. C (1989).
[3]E. Pfaff and G. Clausnitzer, to be published (1989).

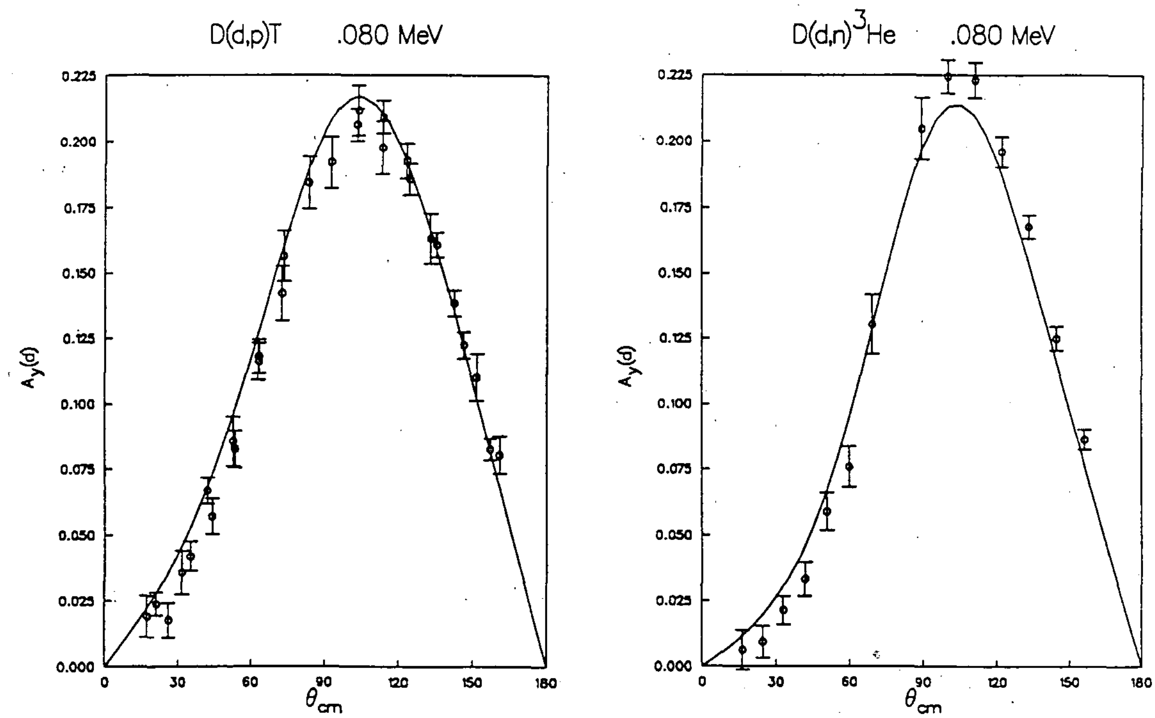

Fig. B-1(b)

2. Recent Improvements in the Calculation of Prompt Fission Neutron Spectra (D. G. Madland, R. J. LaBauve, and J. R. Nix)

An improved calculation[4] has been performed for the prompt fission neutron spectrum N(E) from the spontaneous fission of ^{252}Cf. In this calculation, the fission-spectrum model of Madland and Nix[5] is used, but with several improvements leading to a phyically more accurate representation of the spectrum. Specifically, the contributions to N(E) from the *entire* fission-fragment mass and charge distributions are calculated instead of calculating on the basis of a seven-point-approximation to the peaks of these distributions as has been done in the past. Therefore, values of the energy release in fission, fission-fragment kinetic energy, and compound nucleus cross section for the inverse process are considered on a point-by-point basis over the fragment yield distributions instead of considering averages of these quantities over the peaks of the distributions. Preliminary results have been obtained and compared with a measurement, an earlier calculation, and a recent evaluation of the spectrum.

Calculations have been performed[6] for the first time of threshold integral cross sections in the field of the fission spectrum matrix $N(E,E_n)$ for the neutron-induced fission of ^{235}U. These show a considerable sensitivity to the detail of $N(E,E_n)$ and may provide a means of testing various theoretical representations of $N(E,E_n)$.

---

[4]D. G. Madland, Proc. Int. Conf. Nuclear Data for Science and Technology, Mito,Japan,1988, Ed., S. Igarasi (Saikon Publishing, Tokyo, 1988), p. 759.
[5]D. G. Madland and J. R. Nix, Nucl. Sci. Eng. 81, 213 (1982).
[6]D. G. Madland, R. J. LaBauve, and J. R. Nix, Proc. IAEA Consultants' Mtg. on Physics of Neutron Emission in Fission, Mito, Japan, 1988 (in press).

3. Model Development for Medium-Energy Nucleon-Induced Fission: Cross Sections and Particle and Gamma Spectra (D. G. Madland)

An initial model has been completed[7] for the calculation of fission-neutron and fission gamma-ray spectra and multiplicities from medium-energy nucleon-induced fission. The model addresses both proton- and neutron-induced fission for an energy range of 10 MeV $\leq E_n, E_p \leq$ 340 MeV and for the target nucleus ^{238}U. The entire model, save the fission-fragment mass distribution representation, applies to other actinide target nuclei.

An initial model has also been developed for the barrier E_B in the simple single-humped fission-barrier model. With this model sixty-two fission barriers have been calculated for the ^{238}U(p,xnf), ^{238}U(p,pxnf), ^{238}U(n,xnf), and ^{238}U(n,pxnf) reactions. At the same time, saddle-point moments of inertia have also been calculated for the same sixty-two nuclei. These moments are used to construct the (rotational) fission transition states. The sixty-two barriers are for the most likely fissioning nuclei occurring in medium-energy multiple-chance fission.

[7]D. G. Madland, Los Alamos National Laboratory informal report T-2-IR-88-1, May 1988.

4. Neutron Scattering at Intermediate Energies from a Dirac Optical Potential (R. Kozack and D. G. Madland)

A global analysis of intermediate energy *nucleon* + ^{208}Pb scattering data has been performed[8] using the Dirac phenomenology. Proton elastic differential cross sections, analyzing powers, spins-rotation functions, and total reaction cross sections, together with neutron total cross sections, spanning an incident energy range of 80 to 800 MeV, were used in the determination of a Dirac scalar-vector global potential. Two of six energy dependencies studied were selected to construct best-fit nucleon-nucleus potentials for the reduced incident-energy interval of 95 to 300 MeV. These potentials reproduce the experimental data uniformly within the reduced energy interval. Explicit values for the isovector strengths of the nucleon-nucleus potential are given. The correlations and ambiguities among the parameters of the potentials have also been studied. Predictions have been made[9] for the elastic differential cross section and spin observables for neutron + ^{208}Pb scattering. These show remarkable differences in comparison with the corresponding proton scattering observables.

[8]R. Kozack and D. G. Madland, accepted for publication in Phys. Rev. C (January 1989).
[9]R. Kozack and D. G. Madland, submitted to Phys. Rev. Letters (December 1988).

5. Preequilibrium Exciton Model with Quasi-elastic Component[10] (R. D. Smith, M. Bozoian, and E. D. Arthur)

Standard exciton models for preequilibrium reactions cannot account for features in the spectrum due to forward-peaked direct processes such as quasi-elastic nucleon knockout. This deficiency can be removed by relaxing the assumption that each configuration possible in an n-exciton system of total energy E is equally probable, since the direct reactions must proceed from configurations where most of the energy is carried by one particle. We allow for quasi-elastic scattering in an exciton-model calculation by including in the distribution $\rho_3(E,e_p,2p1h)$ (the probability for finding a particle with energy E_p in the 3-exciton 2p1h system) a component determined by the kinematics of quasi-elastic scattering, in which configurations where one particle carries most of the energy are preferred. We also consider the effect of direct multi-nucleon knockout on the higher n-exciton probability distributions.

[10]R. D. Smith, M. Bozoian, and E. D. Arthur, Bull. Am. Phys. Soc. *33*, 1601 (1988).

6. Adaptation of the Multistage Preequilibrium Model for the Monte Carlo Method[11] (M. Bozoian and R. E. Prael)

The intranuclear cascade model, employed in the HETC Monte Carlo code, underpredicts nucleon spectra in the intermediate emission energy range of 50 to 200 MeV. In order to improve predictability in this energy range, the multistage preequilibrium nuclear model has been adapted to the Monte Carlo method using the implementation of the model in the GNASH code as a starting point. We first showed that the Monte Carlo algorithm was equivalent to the analytical solution of the GNASH exciton master equation. Other exciton model parameters were shown to be applicable to the Monte Carlo method. Calculational results from the Monte Carlo method were compared with results from the GNASH code; conclusions drawn therefrom provided us with guidelines for the implementation of the Monte Carlo multistage preequilibrium model in HETC, where it must interface with the essentially single particle interaction intranuclear cascade model.

[11]M. Bozoian and R. E. Prael, Bull. Am. Phys. Soc. *33*, 1581 (1988).

7. Quasi-Free Scattering in the Preequilibrium Region (R. D. Smith and M. Bozoian)[12]

A model for inclusive proton-nucleus scattering that covers the preequilibrium region was developed based on (1) single-step quasi-free scattering and (2) the exciton model, which describes emission from 3p2h and higher configurations. Results were compared with data for various nuclei at incident energies from 60 to 200 MeV. The systematics of angle-dependent energy spectra were well reproduced by the model, except in the large-energy-loss region at very forward angles. We found the single-step quasi-free scattering constitutes 60 to 80% of the reaction cross section in medium-heavy nuclei, and about 50% in heavy nuclei. The preequilibrium region is therefore dominated by direct reactions.

[12]R. D. Smith and M. Bozoian, submitted to Phys. Rev. C (January 1989).

8. Medium-Energy Fission Model and Libraries (E. D. Arthur, M. Bozoian, R. E. MacFarlane, P. G. Young)

The medium-energy fission model generates pre-fission and fission-fragment neutron and gamma spectra in the two cases of proton and neutron-induced fission of ^{238}U for incident energies up to 100 MeV. The model, implemented in the GNASH and FIZZIN codes, comprises fission cross-section calculations and a scission-point model[7] that follows fission fragments after scission. In particular, the FIZZIN code provides an input file of fission fragments, their yields and energetics input file to an evaporation/preequilibrium version of GNASH, which accumulates the resulting particle and gamma-ray spectra that are produced. The model has been favorably benchmarked against LANL's neutron spectra data obtained from 113 MeV $p+^{238}U$.[13] The proton-induced fission libraries include 27 incident energies ranging from 11 MeV to 100 MeV. The neutron-induced fission libraries include 20 incident energies ranging from 20 MeV to 100 MeV and are combined with the lower energy ENDF/B-V.2 evaluation at 20 MeV.

[13] M. Bozoian, E. D. Arthur, D. C. George, and D. G. Madland, Bull. Am. Phys. Soc. *35*, 1580 (1988)

9. Theoretical Analysis of n + ^{235}U Reactions (P. G. Young and E. D. Arthur)

A theoretical analysis of neutron-induced reactions on ^{235}U between 0.01 and 20 MeV has been completed . A coupled-channel optical model potential that fits total, elastic, inelastic, and low-energy resonance data was used to calculate scattering cross sections to the ground-state rotational band and neutron transmission coefficients. The transmission coefficients were utilized in a Hauser-Feshbach statistical theory analysis that includes a multiple barrier fission model as well as corrections for preequilibrium effects. Direct cross sections for higher-lying vibrational states were provided from DWBA calculations, normalized using B(Eℓ) values determined from (d,d') and Coulomb excitation data. Initial fission barrier parameters and transition state density enhancements were obtained from previous analyses, especially fits to charged-particle fission probability data. The parameters were adjusted to produce optimal agreement with experimental ^{235}U(n,f) data. The analysis is being used to calculate cross sections, energy and angle distributions of neutrons from elastic and inelastic scattering, (n,xn), and (n,xnf) reactions for the ENDF/B-VI ^{235}U evaluation. Similar analyses are in progress for ^{238}U and ^{239}Pu.

10. Data Evaluations for Version VI of ENDF/B-VI (P. G. Young, D. Dodder, G. M. Hale, R. E. MacFarlane, and D. M. Muir)

Evaluations of neutron-induced data for the upcoming issue of Version VI of ENDF/B are complete or in progress for ^{1}H, ^{3}He, ^{6}Li, ^{7}Li, ^{10}B, ^{11}B, ^{151}Eu, ^{153}Eu, ^{165}Ho, W, ^{185}Re, ^{187}Re, ^{197}Au, ^{235}U, ^{238}U, and ^{239}Pu. Additionally, proton-induced data are being analyzed for ^{1}H and ^{3}He targets. The evaluations cover the incident nucleon energy range up to 20 MeV, and in most cases new ENDF/B formats that permit precise specification of energy-angle correlations in emission spectra are used. In addition to utilizing up-to-date assessments of the available experimental data, each evaluation includes results of theoretical analyses to complement the experimental information. In the case of light elements, R-matrix analyses have been performed; for heavier materials, Hauser-Feshbach statistical calculations with supporting coupled-channel or spherical optical model, preequilibrium, direct reaction, and fission theory (for actinides) analyses are complete or in progress. All evaluations must be finalized by the fall of 1989 in order to be included in the first issue of ENDF/B-VI.

11. Neutron- and Proton-Induced Nuclear Data Libraries to 100 MeV (E. D. Arthur, M. Bozoian, D. G. Madland, R. E. MacFarlane, R. T. Perry, W. B. Wilson, and P. G. Young)

Development of a neutron- and proton-induced transport data library for incident nucleon energies to 100 MeV is continuing, with the addition of 10 new evaluations over the past year. Each data set includes specification of cross sections, energy and angular distributions of emitted neutrons, gamma rays, protons, deuterons, and alpha particles. For incident neutrons the libraries are matched below 20 MeV with more detailed ENDF/B-V evaluations. In all cases the evaluations above 20 MeV are based on combinations of deformed or spherical optical model, Hauser-Feshbach statistical and/or evaporation theory, multistage preequilibrium, and DWBA calculations, performed in the framework of the

GNASH code system. Secondary energy-angle distributions are provided with an updated formulation of the Kalbach angular distribution phenomenology. A multi-barrier fission model in GNASH is used for calculations involving fissile nuclei, coupled with our newly developed capability for calculating neutron and gamma-ray distributions from appropriately weighted fission fragments. To date, the 100-MeV library includes neutron-induced data for ^{1}H, ^{9}Be, ^{12}C, ^{16}O, ^{27}Al, ^{28}Si, ^{40}Ca, ^{56}Fe, and ^{238}U. Similarly, 100-MeV proton libraries are complete for ^{9}Be, ^{12}C, ^{16}O, ^{27}Al, ^{56}Fe, and ^{238}U.

12. Fission-Product Yield Evaluations [T. R. England and B. F. Rider (Retiree, General Electric Corp.)]

A global status report was presented in an invited paper at the Mito Conference.[14] The data have since been revised through 1988 and the evaluation for the 50 yield sets in Table B-12 is in progress. Data for ENDF/B-VI are expected to be completed in early 1989 and a report will be prepared for general distribution later in 1989. Ten additional sets listed in the footnote of Table B-12 may be included in 1989.

[14]T. R. England and J. Blachot, "Status of Fission Yield Data," Proc. of Int. Conf. on Nuclear Data for Science and Technology, May 30-June 3, 1988, Mito, Japan, Ed., S. Igarasi. [Los Alamos informal document LA-UR-88-1696.]

TABLE B-1. Fission Yields Being Evaluated for ENDF/B-VI

Fissionable Nuclide	Fissionable Nuclide
^{227}Th (T)	^{242}Pu (F)
^{229}Th (T)	^{241}Am (T,F,H)
^{232}Th (F,H)	^{42m}Am (T)
^{231}Pa (F)	^{243}Am (F)
^{232}U (T)	^{242}Cm (F)
^{233}U (T,F,H)	^{244}Cm (S)
^{234}U (F,H)	^{245}Cm (T)
^{235}U (T,F,H)	^{248}Cm (S)
^{236}U (F,H)	^{249}Cf (T)
^{237}U (F)	^{250}Cf (S)
^{238}U (S,F,H)	^{251}Cf (T)
^{237}Np (F,H)	^{252}Cf (S)
^{238}Np (F)	^{253}Es (S)
^{238}Pu (F)	^{254}Es (T)
^{239}Pu (T,F,H)	^{254}Fm (S)
^{240}Pu (F,H)	^{255}Fm (T)
^{241}Pu (T,F)	^{256}Fm (S)

Ten sets may be added, as follows: ^{243}Cm (T,F), ^{246}Cm (S,F), ^{244}Cm (F), ^{248}Cm (F), ^{242}Pu (T,H), ^{237}Np (T), ^{240}Pu (T).

S = Spontaneous, T = Thermal, F = Pooled Fast, H = 14 MeV.

13. Delayed Neutron Data [T. R. England and M. C. Brady (Oak Ridge Nat. Lab.)]

An evaluated library for 271 delayed neutron precursors has been completed[14-18] These data have been used with ENDF/B-V fission-product parameters to calculate aggregate spectra for 43 fissioning systems, and the results are compared with recent experiments at the University of Lowell. Figure B-2 shows a typical comparison of spectra following a fission pulse. All 43 systems have also been approximated with the usual six-group temporal representations and these show results that are almost identical to the calculation in Fig. B-2. Precursor and temporal group data are in 10-keV bins from 0.0 to 3 MeV and are being prepared for use in ENDF/B-VI. Table B-2 compares average energies for a ^{235}U fission pulse.

[14] T. R. England, M. C. Brady, E. D. Arthur, and R. J. LaBauve, "Status of Evaluated Precursor and Aggregate Spectra, Proc. Specialists' Mtg. on Delayed Neutrons, Birmingham, England, Sept. 15-19, 1986 [Los Alamos informal document LA-UR-86-1983].

[15] T. R. England, E. D. Arthur, M. C. Brady, and R. J. LaBauve, "Background Radiation from Fission Pulses," Los Alamos National Laboratory report LA-11151-MS (Feb. 1988). [Data summary in Trans. Am. Nucl. Soc. *54*, 349 (1987).]

[16] M. C. Brady, "Evaluation and Application of Delayed Neutron Precursor Data," doctoral dissertation, Texas A & M Univ., with research performed at Los Alamos Nat. Lab. (December 1988); [to be published as Los Alamos report (thesis series)].

[17] T. R. England and M. C. Brady, "Delayed Neutron Spectra by Decay Group for Fissioning Systems from ^{227}Th through ^{255}Fm," Proc. 1988 Int. Reactor Physics Conf., Jackson Hole, WY, Sept. 18-21, 1988.

18M. C. Brady and T. R. England, "Delayed Neutron Data and Group Parameters for 43 Fissioning Systems," submitted for publication in Nucl. Sci. Eng., December 1988 [Los Alamos informal document LA-UR-88-4118].

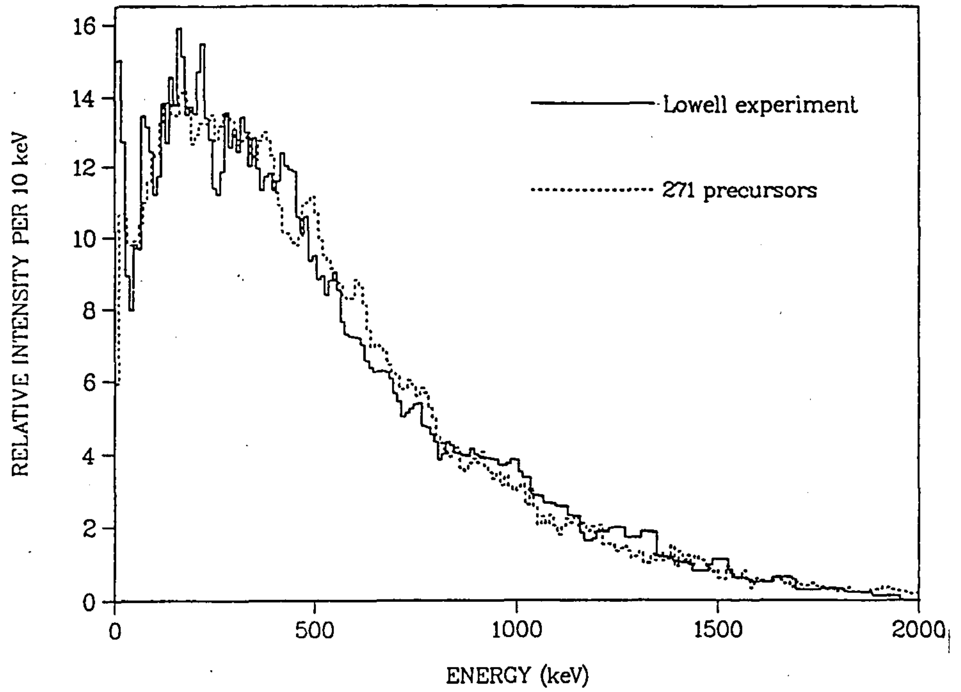

Fig. B-2. Comparisons with Lowell University spectra for delay interval 5 (2.1-3.9 s).

TABLE B-2 Average Energy Comparisons with Lowell University Data

Delay	Interval (sec)	Average Energy (keV)		
		Lowell[a]	271 prec.	6-group
1	0.17 - 0.37	473(14)	508.6	506.5
2	0.41 - 0.85	482(12)	501.0	502.2
3	0.79 - 1.25	506(12)	498.0	499.6
4	1.2 - 1.9	502(12)	496.6	498.6
5	2.1 - 3.9	491(13)	494.0	497.3
6	4.7 - 10.2	478(14)	477.7	485.2
7	12.5 - 29.0	420(12)	457.7	466.7
8	35.8 - 85.5	441(17)	476.2	468.5

[a]The values given in parenthesis following the Lowell data represent the uncertainty in the last two digits, i.e. 473(14) may be interpreted as 473 ± 14 keV.

14. The Medium-Energy Nuclear Data Library (MEDLIB): Current Status and Future Directions (D. C. George and E. R. Siciliano)

The MENDLIB project is a joint effort between T- and MP-Divisions at Los Alamos to compile medium-energy experimental data and to provide access to this data through an easy to use, menu-driven, dial-up computer program. As originally proposed, Phase I of this project had two goals: (1) to demonstrate the feasibility of such a project by constructing a database and user-friendly computer interface that would enable any user to access the database; and (2) to compile more than 50% of the available published LAMPF data, primarily from nucleon and pion induced reactions.

In the areas of design of the database and user interface the goals have been met. However, the project has only acquired about 25% (20,236) data points from our estimate of over 80,000) of the available data. Even with this limited amount of data, we decided in mid-summer of 1988 to make the library available to any user of the LAMPF/VAX cluster. Thus far, our product has been received favorably by the user. The main goal for the future is to collect more data from LAMPF and possibly some other medium-energy facilities. A secondary goal for the future is to study efficiency issues concerning data table specifications and the user interface.

University of Lowell

A. NEUTRON SCATTERING IN THE ACTINIDES
(L.E. Beghian, G.H.R. Kegel, J.J. Egan, A. Mittler, A. Aliyar, C.A. Horton, C. Jen, D. DeSimone and G. Yue)

1. Inelastic Scattering Cross Sections for States above 300 keV in ^{232}Th and ^{238}U at Energies above 2.2 MeV

During the past year we have completed our studies on high-lying states in ^{232}Th and ^{238}U at incident neutron energies in the range from 2.3 to 3.0 MeV. We have measured excitation functions at 125^{o} in 100-keV steps over this energy range. In addition we have measured angular distributions at 2.4 and 2.8 MeV over the angular range 25^{o} to 135^{o} in 10^{o}-steps. In ^{232}Th we have obtained inelastic cross sections for the following levels or level groups: 333, 714, 730, 774-785, 829, 873-889 and 960 keV. In ^{238}U we have results for levels or level groups at: 307, 680, 732, 827 and 927-988 keV.

The ^{232}Th excitation functions and the 2.4 MeV angular distributions for ^{232}Th were presented at the Mito Conference.[1] The ^{238}U results were presented at the Santa Fe meeting of the Division of Nuclear Physics of the APS.[2] Figure A-1 shows a sample of this work, the excitation function for the 732-keV, 3^{-}, state in ^{238}U. The figure shows our earlier work[3] plotted as X's and the recent work above 2.2 MeV as solid dots. For comparision we also show ENDF/B-V (dashed curve) along with the theoretical calculations of E.D. Arthur[3,4] (solid curve) in which compound nucleus statistical model cross sections were added incoherently to direct interaction cross sections obtained from DWBA calculations. The calculated cross sections are dominated by the compound nucleus component up to 2.0 MeV with the direct component becoming significant only above 2 MeV. At 3 MeV the DWBA calculations account for about half of the cross

---

1 J.J. Egan, A. Aliyar, C.A. Horton, G.H.R. Kegel and A. Mittler in Proc. Intl. Conf. on Nuclear Data for Science and Technology, May 30 - June 3, 1989, Mito, Japan, S. Igarasi, Ed., JAERI, Saikon Publishing Company Ltd., Tokyo, 1988 p. 63.

2 G.H.R. Kegel, A. Aliyar, J.J. Egan, C.A. Horton and A. Mittler, Bull. Am. Phys. Soc. 33, 1568 (1988).

3 J.Q. Shao, G.P. Couchell, J.J. Egan, G.H.R. Kegel, S.Q. Li, A. Mittler, D.J. Pullen, W.A. Schier and E.D. Arthur, Nucl. Sci. Eng. 92, 350 (1986).

4 E.D. Arthur, Private Communication.

section while at 2.0 MeV the direct component is about 10% of the cross section.

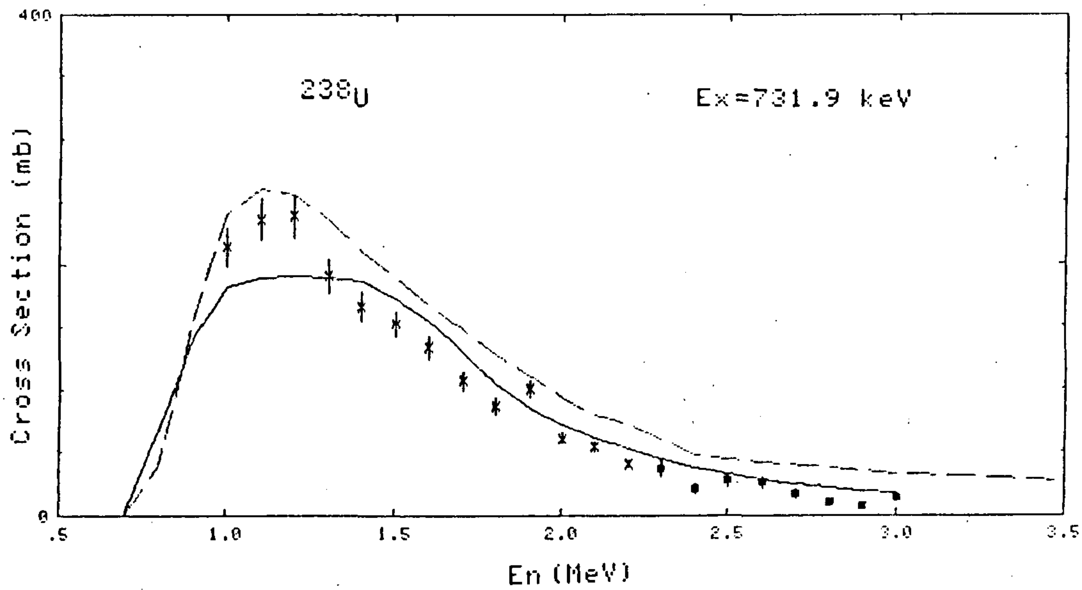

Fig. A-1 Excitation function for the 732-keV state in ^{238}U. Solid dot's, present work; x's, earlier Lowell work[3], dashed curve, ENDF/B-V; solid curve, theoretical calculations.[3,4]

The neutron time-of-flight spectra obtained in this work are very complex containing many overlapping peaks. We were able to overcome the attendant difficulties by designing an unfolding code specifically for these spectra. The unfolding procedure was the subject of a presentation at the Mito Conference.[5]

2. ^{232}Th and ^{238}U Cross Sections Below 150 keV

We are currently making neutron scattering measurements on ^{232}Th and ^{238}U at energies in the 100-150 keV region. A special detector has been assembled for this purpose consisting of a Bicron BC-418 plastic scintillator viewed by two selected low noise Amperex XP-2020 photomultiplier tubes. The detector is housed in a specially designed large low-background shield consisting of lead, paraffin and boron loaded polyethylene. With this detector we have observed inelastically scattered neutrons from the 45-keV first excited state of ^{238}U down to incident energies of 100 keV.

---

5 G.H.R. Kegel, A. Aliyar, J.H. Chang, J.J. Egan, C.A. Horton and A. Mittler, in Proc. Intl. Conf. on Nuclear Data for Science and Technology, May 30 - June 3, 1988, Mito, Japan, S. Igarasi, Ed., JAERI, Saikon Publishing Company Ltd., Tokyo, 1988 p. 399.

3. <u>Fission Neutron Spectroscopy</u>

We are planning a sequence of measurements of fission neutron spectra at incident energies in the range 0.5 - 3.0 MeV for ^{232}Th, ^{235}U, ^{238}U and ^{238}Pu using the ^{235}U fission spectrum as a standard as well as ^{252}Cf. In these studies we will use our time-of-flight spectrometer with 3-m flight path. In order to carry out these measurements we will use a set of BaF_2 detectors to signal the occurance of a fission event and thus discriminate against scattered primary neutrons. The main neutron detector will be an NE213 liquid scintillator. The BaF_2 scintillators and UV sensitive photomultiphiers have been assembled and tested. Preliminary fission neutron spectroscopy work is expected to begin within the next year.

4. <u>Improvements to the Accelerator</u>

With the impending twentieth anniversary of our CN accelerator we are commencing a refurbishing schedule. Our plans include the installation of a new accelerator tube and redesigning the post-Mobley section of the beam line entailing a relocation of vacuum pumps to obtain better pumping speed and better vacuum in the vicinity of the target.

We are also redesigning the target assembly to give flexibility in the target-goniometer center distance permitting us to work with smaller scatterers such as ^{239}Pu.

B. <u>THEORETICAL CALCULATIONS OF ELASTIC SCATTERING CROSS SECTIONS IN THE ACTINIDES</u>
(E. Sheldon)

Theoretical analyses of experimental elastic scattering cross sections in the actinides were reported at the International Conference on Nuclear Data for Science and Technology in Mito, Japan.[1] Calculated fast neutron cross sections for the 0^+ ground states of the principal even-A actinides ^{232}Th, ^{238}U, ^{240,242,244}Pu and for a "composite triad" of closely-adjacent ground-state levels of the odd-A nuclide ^{235}U were obtained in the form of excitation functions up to 3.5 MeV and angular distributions at various incident energies up to 3.4 MeV. The measurements presented were those of the Lowell group augmented where requisite by data from other laboratories. The analyses were based on the "standard" (compound nucleus plus

---

1 E. Sheldon, In Proc. Intl. Conf. on Nuclear Data for Science and Technology, May 30 - June 3, 1988, Mito, Japan, S. Igarasi, Ed., JAERI, Saikon Publishing Company Ltd., Tokyo, 1988 p. 105.

direct interaction) formalism, taking account of level-width fluctuations and extra exit-channel competition. These were contrasted with preliminary calculations in the statistical S-matrix formalism and with ENDF/B-V.

A sample set of results are shown in Fig. B-1 for angular distributions at 185 keV for ^{232}Th, ^{235}U and ^{238}U. The data are those of the Lowell group.[2,3] The solid curves represent calculations employing the "standard" approach in which the compound nucleus computations performed with the code CINDY based upon the Hauser-Feshbach-Moldauer formalism are added incoherently to the direct interaction calculations performed with the code KARJUP, the Karlsruhe variant of Tamura's[4,5] coupled channels code JUPITOR. The dashed curves represent calculations performed with the code NANCY based on the statistical S-matrix formalism of Hofmann, Richert, Tepel and Weidemuller[6,7] (HRTW). The dotted curves represent the ENDF/B-V evaluation.

The angular distribution analyses pose a challenge by entailing stringent comparisons of magnitude and structure. The results of this work feature, conceivably for the first time, the application of the HRTW formalism in its full extent to the derviation of differential elastic cross sections as a function of angle. In general ENDF/B-V and the CN/DI "standard" calculations are in accord with the data while the HRTW calculations evince rather too pronounced a variation with angle. Since the NANCY results beyond 90^{o} evoked misgivings, they have been suppressed in the figure pending further scrutiny. It bears emphasizing that as yet, these differential HRTW findings are but preliminary and tentative.

It is clear that the standard (CN+DI) approach is able to render an admirable account of neutron elastic angular distributions in the actinides. However, the more fundamental HRTW formalism continues to warrant more detailed scrutiny and development.

---

2 G. C. Goswami, J.J. Egan, G.H.R. Kegel, A. Mittler and E. Sheldon, Nucl. Sci. Eng., , 48 (1988).

3 G.C. Goswami, Ph.D. Thesis, University of Lowell (unpublished).

4 H. Rebel and G.W. Schweimer, Kernforschungszentrum Karlsruke Report KFK-1333 (1971).

5 T. Tamura, Rev. Mod. Phys. 37, 679 (1965).

6 D.W.S. Chan and E. Sheldon, Phys. Rev. C, 26, 861 (1982).

7 H.M. Hoffman, J. Richert, J.W. Tepel and H.A. Weidemuller, Am. Physics (NY) 90, 391 and 403 (1975).

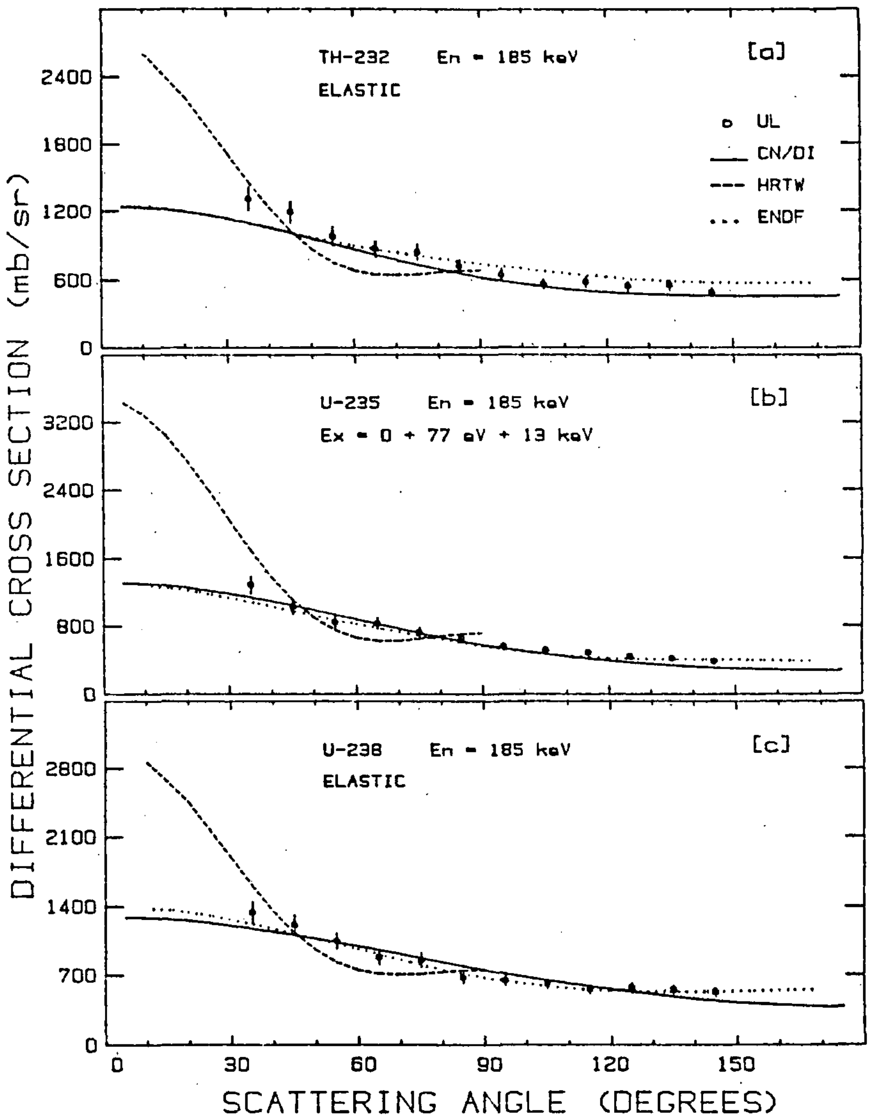

Fig. B-1 Neutron elastic scattering angular distributions at E = 185 keV for (a) ^{232}Th, (b) composite ^{235}U, and (c) ^{238}U, contrasting Lowell data with CN/DI and HRTW theory and with ENDF/B-V evaluations.

C. <u>DELAYED NEUTRON STUDIES</u>

(G.P. Couchell, D.J. Pullen, W.A. Schier, P.R. Bennett, M.H. Haghighi, E.S. Jacobs and M.F. Villani)

Measurements of the composite (aggregate) delayed neutron (DN) spectra as a function of time following the fast fission of ^{238}U were completed during this period. In addition, equilibrium DN Spectra were measured for ^{235}U, ^{238}U and ^{239}Pu.

Our method employs a helium jet to transfer the fission fragments from the fission chamber to a remote beta/neutron time-of-flight spectrometer, and during this period we also studied the fission fragment transfer efficiency of the helium jet system. Excellent progress can be reported in the extraction of 'Keepin' six-group solutions from our time-dependent spectra using a constrained least-squares decomposition technique.

1. <u>Fast Neutrons Fission of ^{238}U</u>

Our previously reported[1] measurements of the upper energy portions (0.25 - 4 MeV) of the composite DN spectra for ^{238}U have now been extended to low energies (0.01 - 0.25 MeV) for four delay time intervals, using Li-6/glass scintillators. In addition, the energy regions 1.2 - 4 MeV have been re-analyzed for six time intervals using an improved background subtraction technique. Spectra covering the full measured energy range, 0.01 - 4 MeV, are shown plotted in Fig. C-1 and are compared with our corresponding results for 239

Fig. C-1 Composite DN energy spectra from fast fission of ^{238}U (solid curves) compared with those from thermal fission of ^{239}Pu.

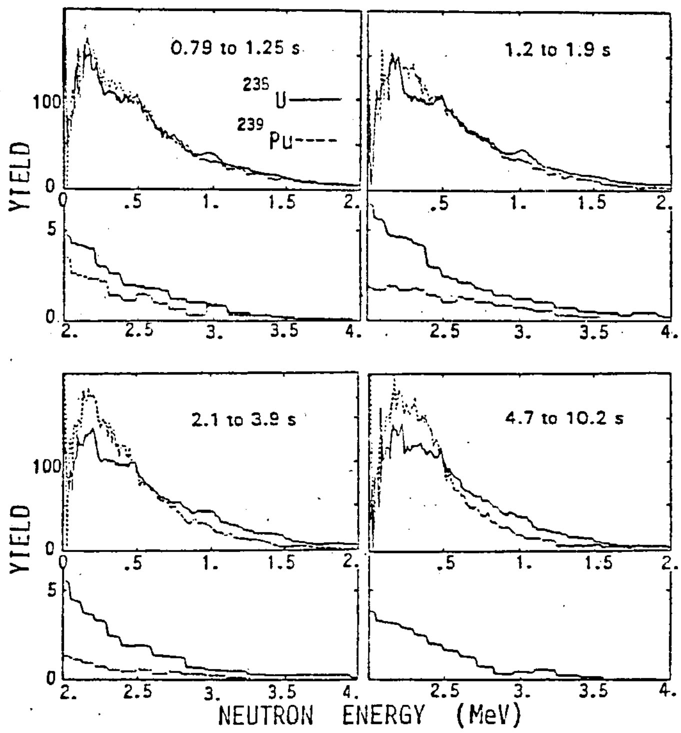

[1] DOE/NDC REPORT, 1988, p. 112.

Each spectrum is normalized to the same overall yield (10^4 counts). Although some of the same structure is evident in the two sets, the ^{238}U spectra are noticeably more energetic than those for ^{239}Pu. These spectra are currently being analyzed to extract DN spectra for groups 2-6 (Keepin six-group approximation) using our constrained least squares decomposition code (Section C-4). These results were reported in 1988 at conferences in Mito, Japan[2] and Jackson Hole, Wyoming.[3]

2. Delayed Neutron Equilibrium Spectra for ^{235}U, ^{238}U and ^{239}Pu

Delayed neutron spectra have been measured for the single time interval 0.12 - 180 s for ^{235}U, ^{238}U and ^{239}Pu. This interval encompasses >95% of all delayed neutrons emitted and essentially provides, therefore, a direct measurement of a DN equilibrium spectrum. Both BC501 liquid scintillators and Li-6/glass scintillators were used to cover the energy range 0.01 - 4 MeV. The spectra display rather similar structures. However, the average energy for the measured ^{238}U spectrum is some 60 to 100 keV higher than for ^{235}U and ^{239}Pu, respectively.

We have also calculated equilibrium spectra using the six-group spectra derived from our composite time-dependent DN measurements (Section C-4). The overall agreement between the directly measured and deduced spectra is found to be very satisfactory for all three cases. The results of this study were reported[3] [4] at conferences in 1988.

3. Helium-Jet Fission Fragment Transfer Efficiency

We have studied[5] the fission fragment transfer efficiency of the helium-jet system used in our delayed neutron energy spectrum measurements. Using a thin-window high purity germanium detector, x-ray spectra from radioactive progeny of the fission fragments were measured using the helium jet and compared with those using a pneumatic rabbit transfer system. A total of eighteen x-ray precursors were identified and comparison of the two transfer methods showed that the fission

---

[2] W.A. Schier, D.J. Pullen, G.P. Couchell, M.H. Haghighi, E.S. Jacobs, M.F. Villani and P.R. Bennett, in Proc. Int. Conf. on Nuclear Data for Science and Technology, Mito, Japan, (1988), p. 853.

[3] G.P. Couchell, et al., in Proc. Intl. Reactor Phys. Conf., Jackson Hole, Wyoming (1988), p. 111-243.

[4] D.J. Pullen, et al., in Proc. Int. Conf. on Nuclear Data for Science and Technology, Mito, Japan (1988), p. 905.

[5] G.P. Couchell, et al., Ibid., p. 415.

fragments were transferred with very little distortion in the mass distribution. The measurements did suggest a somewhat reduced efficiency in the transfer of Br, I and Xe. However, their corresponding x-ray lines were extremely weak and competed with much stronger transitions from neighboring elements. No definite conclusion could be reached concerning their transfer efficiency in the helium jet.

4. Six-Group Decomposition of Composite DN Measurements

A major goal of our delayed neutron (DN) project has been to deduce DN six-group energy spectra from our composite measurements. This can be done by fitting composite spectra $S_{\nu i}$ measured over $\nu = 1, \ldots, M>6$ time intervals with a form

$$F_{\nu i} = \sum_{\mu=1}^{6} a_{\nu\mu} \, \chi_{\nu i} \qquad i = 1, \ldots, N$$

where the index i labels the energy bins of the spectrum and $\{\chi_{\mu i}\}$ are the normalized six-group spectra to be determined. The coefficients $a_{\nu\mu}$ can be calculated from evaluated six-group parameters (β_μ, λ_μ). For the present study (β_μ, λ_μ) parameters for ^{235}U, ^{238}U and ^{239}Pu were provided us by T.R. England.[6]

It has been found, however, that six-group spectra $\{\chi_{\mu i}\}$ determined from composite spectra by standard weighted least-squares methods tend to be highly unstable, with some groups being overly oscillatory and some spectra having negative yields over certain energy regions. Nevertheless, acceptable six-group solutions can be deduced by considering least-squares methods that incorporate constraint conditions designed to exclude a large class of good mathematical fits that are physically unacceptable. An iterative constrained least-squares technique applicable to this problem has been discussed previously.[7]

The computer program SIXGP has been developed for implementing this constrained least-squares decomposition method to obtain six-group spectra from composite spectra. Because our composite measurements are insensitive to DN group 1, the spectrum is taken as known[6] in our analysis and we thus solve for the group 2-6 spectra $\{\chi_{\mu i}\}$. Six-group spectra deduced from

---

6 T.R. England, Los Alamos National Laboratory, Private Communications (1987, 1988).

7 G.P. Couchell, W.A. Schier, D.J. Pullen, L. Fisteag, M.H. Haghighi, Q. Sharfuddin and R.S. Tanczyn, Proc. Specialists' Meeting on Delayed Neutron Properties, 215 (1986), Birmingham, UK, Publ. by Univ. Birmingham, (1987).

our composite DN measurements of ^{239}Pu are shown in Fig. C-2, where they are compared with the corresponding spectra derived from individual precursor DN spectrum measurements.[6] The similarity in the two sets of group spectra is remarkable for all but group 2. Decomposition of our composite DN spectra of ^{235}U and ^{238}U has been performed in the same manner with equally satisfactory six-group solutions.

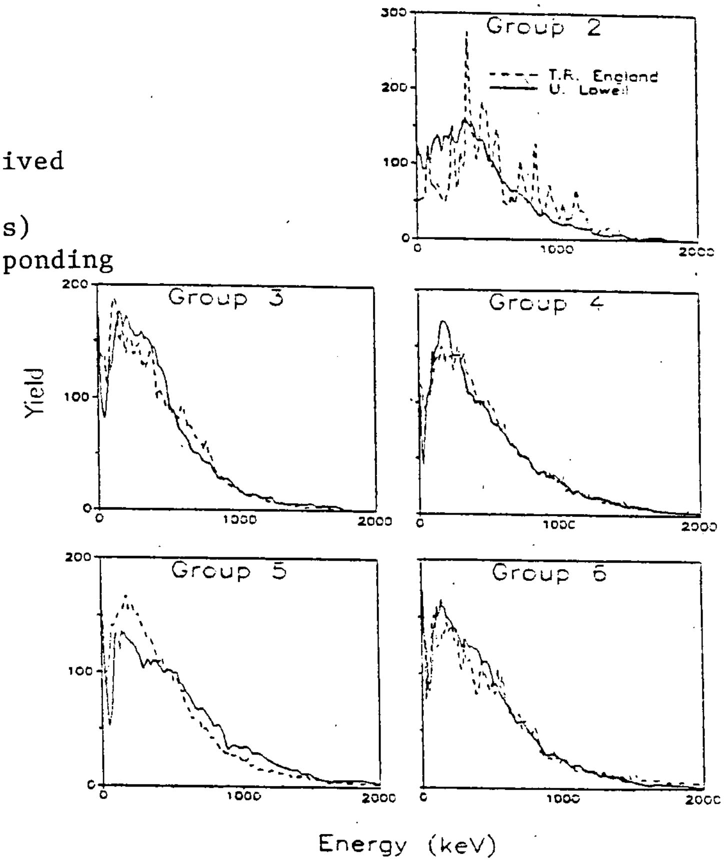

Fig. C-2 DN group spectra derived from ^{239}Pu composite studies (solid curves) compared with corresponding spectra (dashed curves) generated from evaluated individual precursor data.[6]

5. <u>Proposed Future Studies</u>

The helim jet and tape transport system developed for our study of delayed neutron energy spectra is also well suited for studying fission product decay heat by examining composite gamma-ray and beta-particle energy spectra as a function of time after fission. The helium jet is ideal for such studies due to its uniform elemental transfer efficiency, minimal finite sample effects, accurate delay time determination and the availability of beta/gamma coincidences for background reduction. A pneumatic shuttle system has also been developed which should prove useful for extending the study to long delay times.

We currently have the capability of measuring decay heat energy spectra following neutron-induced fission of ^{232}Th, ^{233}U, ^{235}U, ^{238}U and ^{239}Pu. At present there are no U.S. measurements of the decay heat from ^{238}U or ^{232}Th. Current evaluations for these two nuclides are based on theoretical estimates calculated from models deduced from studies on neighboring odd-mass nuclei, e.g., ^{235}U and ^{239}Pu. Futhermore, there are no decay heat measurements from any fissionable fuel for delay times less that 2s. Our system can extend the measurements for all five nuclides to delay times as short as 0.2s.

THE UNIVERSITY OF MICHIGAN
DEPARTMENT OF NUCLEAR ENGINEERING

A. PULSED 14 MeV NEUTRON FACILITY (J. Yang, V. Rotberg, D. Wehe, N. Tsirliganis, M. Petra, G. Knoll)

All the components of the accelerator system described in our report of a year ago have now been either acquired or fabricated in our shop facilities and have been assembled in their final configuration. These include the key pulsing components consisting of sweeper plates operating at 2 MHz, and a klystron buncher designed for a 30:1 time compression of the beam pulses. New vacuum components have been installed, and the system successfully pumped to good vacuum conditions. We are now in the process of testing the RF components that have been designed to deliver voltage to the buncher stage. We have also completed the design and construction of several other major pieces of equipment that are needed to begin fast neutron time-of-flight measurements. These include the primary proton recoil detector, and a californium fission chamber needed in the efficiency calibration of the primary detector. We have also added considerable concrete shielding designed to lower the neutron background in the experimental area.

1. Proton Recoil Scintillation Detector

The design of the primary fast neutron detector was carried out with the aid of the DETECT code[1], a Monte Carlo modeling code for light collection in scintillation detectors. The program generates individual scintillation photons in specified portions of the scintillator, follows each photon through the various components and interactions with surfaces and records the fate (absorption, escape, or detection) of each. The probabilities of these processes are derived from the results of multiple histories involving the simulation of many scintillation photons. Data are also recorded on the number of reflecting surfaces encountered and the photon flight time to detection. With this code, the length and shape of the detector and light pipe were optimized while balancing the objectives of high detection efficiency, uniform pulse height response, and minimum spread in light collection time.

The detector consists of a cylindrical aluminum cell (22 cm outer diameter, 8.6 cm height) with a 3 mm thick quartz end window. NE-213 liquid scintillator was chosen as the detector medium in order to exploit its pulse shape discrimination capabilities to suppress gamma ray pulses. The interior surface of the container is covered with a TiO_2 reflector coating. A tapered light guide made from lucite is used to connect the cell window to the smaller diameter of the Hamamatsu R1250-03 photomultiplier tube.

[1] G. Knoll, T. Knoll, and T. Henderson, IEEE Trans. Nucl. Sci. NS-35, #1, 872 (1988)

2. Fission Detector for Time-of-Flight Detector Calibration

One of the requirements in carrying out quantitative time-of-flight measurements is to calibrate the energy dependence of the efficiency of the detector described in the previous section. The method we have chosen involves the construction of a second detector containing a foil of ^{252}Cf. The principle of the method is based on assuming that the shape of the fission neutron yield from californium foil is well known. The detector with the californium foil provides a start signal from detection of the fission fragments emitted in a given fission event. While operating the time-of-flight detector under conditions that are identical to those of the actual measurement, the number of detected neutrons is recorded as a function of flight time when the two detectors are separated by a typical flight path. By comparing the recorded time-of-flight spectrum with the assumed fission spectrum, the efficiency of the detector is deduced as a function of energy.

The fission source used is a 0.5 µg ^{252}Cf electrodeposited as a spot of 0.635 cm diameter on the center of a platinum disc with 2.7 cm diameter and a thickness of 0.0127 cm. This foil is mounted in a gas-filled cylindrical chamber that functions as a scintillation detector for the emitted fission fragments. The source is positioned at one base of the cylinder while the other base is a quartz window. The quartz window is coupled to an EMI 9887B photomultiplier tube. The internal surface of the detector is covered with a TiO_2 coating which serves as a light reflector. The scintillator gas is a mixture of argon and nitrogen (85% Ar, 15% N). Nitrogen is added in order to shift the primary argon UV emission into the visible region. The gas mixture is continuously flowed through the sensitive volume of the detector to maintain gas purity.

3. Planned Measurements

We expect to devote the majority of our future effort to exploiting the new facility that has been assembled to produce nanosecond pulses of 14 MeV neutrons. Our specific objectives are: 1) Measurement of continuum neutron emission spectra induced by 14 MeV neutrons. Data of this sort are essential in the design of fusion energy systems, particularly in blanket design. 2) Determination of direct neutron inelastic scattering yields. These data are essential for complete description of neutron transport, and are also of theoretical importance in the analysis of collective rotational and vibration nuclear states. 3) Measurement of accurate angular distributions for elastic scattering. These data are important in determination of optical model parameters and in coupled channel analysis.

Once we have established the workability of the present pulsing system, we will begin to develop plans for the second phase of the development of the accelerator. This phase will involve the replacement of the current ion source and acceleration column with a new design based on a duoplasmatron ion source. We anticipate that this step will result in a significant increase in neutron intensity to permit small sample experiments in place of the ring geometry measurements planned during the initial stage.

B. MEASUREMENTS WITH PHOTONEUTRON SOURCES

1. ^{238}U Absolute Capture Cross Sections at 23 and 964 keV (E. Quang, G. Knoll)

We have completed a set of measurements of the $^{238}U(n,\gamma)$ capture cross section at 23 and 964 keV using our facilities for the activation and calibration of intense photoneutron sources. For these experiments, the antimony-beryllium and sodium-beryllium sources were employed. The preliminary results of the measurements yield values of 517 mb at 23 keV and 148 mb at 964 keV. It should be emphasized that these measurements are absolute, in the sense that the techniques employed do not depend on the precise knowledge of any other cross section values. An uncertainty analysis now near completion is expected to show an associated error of about ±2% to ±3% for the cross section values.

The neutron capture reaction in ^{238}U leads directly to ^{239}U which decays with a 23.5 minute half life to ^{239}Np. In turn, ^{239}Np decays with a 2.35 day half life to ^{239}Pu. To determine the neutron capture rate, we have used a HPGe detector to count the induced gamma ray activity of ^{239}Np. In order to produce sufficient activity levels with our sources, depleted uranium targets with masses of several hundred grams are required. Because of the large typical target mass, it is not possible to measure the activity of ^{239}Np directly, due to the limited geometric calibration of the detector and the strong interference of the background radiation from the isotopic impurities in the target itself. Therefore, chemical separation procedures have been developed in order to eliminate competing activities and to concentrate the activity of ^{239}Np to very small volumes. With ^{243}Am commercially available, it is possible to employ a gamma calibration source of high accuracy since ^{239}Np is the daughter of ^{243}Am α-decay. A ^{243}Am plated foil was obtained and its activity absolutely determined by α-counting in a low-geometry spectroscopic vacuum chamber. Using the ^{243}Am foil as the standard, the activity of the ^{239}Np separated from the uranium targets is determined by comparative counting of small-volume samples using the HPGe detector.

The depleted uranium targets of 0.5 mm thickness were fabricated in the form of hollow cylinders with 6.8 cm diameter and 10.2 cm length. After activation of the photoneutron source in the Ford Nuclear Reactor, the spherical source was remotely placed in the center of the cylinder to start the irradiation phase of the experiment. This choice of geometry helps minimize the sensitivity of the measurement to small uncertainties in the actual source position. The absolute neutron fluence during the target irradiation was calculated from the known geometry and a subsequent determination of the absolute neutron emission rate of the source in our manganese bath calibration facility.

2. ^{197}Au Absolute Capture Cross Section Measurements (S. Sakamoto [on leave from Tokai University], E. Quang)

The photoneutron facilities are now being employed to measure the absolute capture cross section in gold at 23 and 964 keV. In this case, the irradiation geometry consists of identical gold foils placed on opposite sides of the photoneutron source. In this compensating geometry, small uncertainties in the actual source position again have little effect on the summed neutron fluence in both foils. The low intensity of the induced gamma activity in the foils necessitates using high efficiency gamma ray detectors consisting of dual sodium iodide scintillators placed on both sides of the foil being measured.

As in our previous work with photoneutron sources, all irradiations are carried our in a low-albedo laboratory in which all inner surfaces have been lined with a layer of anhydrous boric acid. Measurements have been completed in which the contribution of low energy room-return neutrons to the gold activation has been determined by irradiating a series of foils at varying distance from the source. The albedo is sufficiently low so that corrections to the final irradiations for room-return activation for the 23 keV measurement are less than 2%. All measurements have recently been completed for the 23 keV case, yielding a preliminary cross section value (subject to further analysis) of 713 mb. The correction for room-return activation is near 20% for the measurement at 964 keV, which is still underway. An error analysis is expected to show an estimated uncertainty of about ±2% in the measurement at 23 keV, with a somewhat larger uncertainly for the 964 keV measurement.

C. ACTIVATION CROSS SECTION MEASUREMENTS IN COOPERATION WITH ARGONNE NATIONAL LABORATORY (D. Smith [ANL], G. Knoll)

We have begun the planning for a series of activation cross section measurements to be carried out in collaboration with Dr. Donald Smith of Argonne National Laboratory. This program will involve a University of Michigan student who will take part in the experimental procedures at both locations. Irradiations will be carried out at ANL, and samples transported to our laboratories for activity measurements. In particular, we will employ the $4\pi\beta$ counting facilities that we have developed for past measurements of induced activities for previous cross section measurements in our laboratories. Irradiations at ANL will exploit the excellent capabilities of the FNG over wide ranges of fast neutron energies. Initial measurements will likely be carried out on the ^{89}Y(n,p)^{89}Sr and ^{32}S(n,p)^{32}P reactions.

NATIONAL INSTITUTE OF STANDARDS AND TECHNOLOGY
(formerly the National Bureau of Standards)

A. NUCLEAR DATA MEASUREMENTS

1. $^{235}U(n,f)$ Cross Section from Thermal to 1 keV (R. A. Schrack, A. D. Carlson, and R. G. Johnson)

This measurement was performed in order to extend to higher neutron energies the low-energy normalization region used in many cross section shape measurements. The measurement has been completed and the results were presented at the International Conference on Nuclear Data for Science and Technology held in Mito, Japan in June, 1988. The results obtained at NIST are in good agreement with other recent measurements and show that the ENDF/B-V values are probably in error by 3 to 4% in the region between 50 eV and 1000 eV.

2. $^{10}B(n,\alpha\gamma)$ Cross Section from 100 keV to 3 MeV (R. A. Schrack, O. A. Wasson, D. C. Larson*, and J. K. Dickens*)

The data for this important cross section standard have significant uncertainties in the neutron energy region above 500 keV. The cross section is probably known now to no better than 5% in the region above 600 keV. A measurement is being planned in collaboration with Oak Ridge National Laboratory. The experiment will use the ORELA neutron source and data acquisition systems along with the NIST detector systems on the 150 m flight. Preliminary measurements of backgrounds and flight path parameters have been made and equipment is being constructed with initial linac runs to take place in the second quarter of the year. The NIST calibrated "black detector" will be used for neutron flux calibration which should provide a shape determination of the neutron-fluence energy distribution to an uncertainty of about 1%.

3. Measurements of the $^{235}U(n,f)$ Fission Cross Section in the 1-35 MeV Neutron Energy Region (A. D. Carlson, O. A. Wasson, P. W.Lisowski,** J. Ullmann,** and N. W. Hill*)

Further measurements and analyses have been done on the $^{235}U(n,f)$ cross section investigation reported in last year's status report. The experiments are being performed at the 20 m flight path of the Los Alamos National Laboratory WNR target 4 pulsed neutron source. The neutron fluence is measured with the annular proton recoil telescope developed at NIST while the fission rate is measured with a multi-plate fission chamber. Preliminary results of this work were reported at the International conference on Nuclear Data for Science and Technology in Mito, Japan last June. The most recent measurements taken during September, 1988 were made with a new improved data acquisition system with lower deadtime and many

* Oak Ridge National Laboratory
** Los Alamos National Laboratory

useful features. The large amount of data taken under different conditions is presently under analysis. These measurements should provide accurate cross sections in the MeV energy region where the present uncertainties for this standard are unacceptably high. Data is also being obtained above 20 MeV where no previous measurements of this cross section have been reported.

4. A Measurement of the $^{235}U(n,f)$ Cross Section at 2.5 MeV Neutron Energy (K. C. Duvall and O. A. Wasson)

An absolute measurement of the $^{235}U(n,f)$ cross section in the MeV neutron energy region is still required to refine the uncertainty in this important standard reaction. A measurement at 2.5 MeV neutron energy is in progress using the time-correlated associated-particle method with the $D(d,n)^3He$ reaction produced at the NIST 100 kV ion generator. Preliminary measurements of the neutron beam profile indicate that experiments with the uranium fission deposits produced at the CBNM in Geel,Belgium are feasible. Preliminary tests have been completed and cross section measurements should commence this year.

5. Measurement of the $^3He(n,p)T$ Cross Section from 1 eV to 750 keV (J. W. Behrens and A. D. Carlson)

The first measurements of this cross section have been completed. However the analysis of the data will be deferred until later due to competing manpower requirements. The first measurements used the $^{10}B(n,\alpha)$ reaction as the reference standard. The ^{10}B ionization chamber and $^3He/Xe$ gas scintillation counter were located at the 20 m flight path of the NIST linac-based pulsed neutron source.

B. NEUTRON DETECTOR DEVELOPMENT AND FACILITIES FOR NUCLEAR DATA MEASUREMENTS

1. Changes in Neutron Source Facilities

The 140-MeV electron linac at NIST which has been used as a pulsed-neutron source for over 20 years was shut down in January of this year. The remaining neutron source facilities at NIST include the 3 MV positive-ion accelerator, the 100-kV ion generator, 20-MW research reactor with cold source and recently installed neutron guide tubes, and various ^{252}Cf spontaneous fission sources. In addition to these facilities the neutron cross section standards program will also continue to use state-of-the-art neutron sources such as those located at the Los Alamos National Laboratory and Oak Ridge National Laboratory.

2. A 2.5 MeV Neutron Source for Fission Cross Section Measurements (K. C. Duvall)

A 2.5 MeV neutron source is operational at the 100-kV, 0.5-mA ion generator. Neutrons are produced by the $D(d,n)^3He$ reaction with a yield of $3x10^6$ s^{-1}. The time-correlated associated-particle method (TCAP) is used for neutron fluence determination and for neutron background elimination. A fission chamber containing six UF_4 deposits is in operation for use in the $^{235}U(n,f)$ cross section measurement at 2.5 MeV.

3. Absolute Thermal Neutron Counter Development (D. M. Gilliam, G. L. Greene and G. P. Lamaze)

An accurate neutron fluence monitor for the measurement of neutrons in the thermal energy region is being developed. A gamma-alpha coincidence is employed to make an accurate calibration of a totally absorbing ^{10}B sample and gamma-ray detector system. This detector in turn will be used to calibrate a thin ^{10}B transmission monitor. These neutron detectors have potential applications for improved thermal neutron cross section measurements, improved calibration of the NIST manganous bath, and possible implications for ^{252}Cf nubar data.

One important feature of the absolute calibration of this system is that the alpha-gamma coincidence method can be checked by intercomparisons with standard alpha-particle sources. The combination of these two methods is expected to permit uncertainties of less than 0.1%. Encouraging preliminary results have been reported (J. Radioanalytical and Nucl. Chem., 123 (1988) 551-559). A much more elaborate experimental arrangement is nearing operation. This new arrangement will include two germanium detectors to greatly reduce gamma-ray detector efficiency dependence on neutron beam position, two alpha-particle detectors to permit optimization of calibrations by both the coincidence and standard source methods, and much better boron target positioning precision. The new apparatus will be operated first at the NIST Reactor BT-7 position, and then moved to the new Cold Neutron Guide Hall as one of the first experiments to use that new facility.

C. NUCLEAR DATA COMPILATIONS AND EVALUATIONS

1. The ENDF/B-VI Neutron Cross Section Standards Evaluations (A. D. Carlson, W. P. Poenitz,* G. M. Hale,** and R. W. Peele***)

The evaluation of the standard cross sections for ENDF/B-VI, as outlined in a previous status report, has been completed. The output of the simultaneous evaluation and R-matrix analyses were combined to provide the cross sections for $^{6}Li(n,t)$, $^{10}B(n,\alpha_1)$, $^{10}B(n,\alpha_0)$, $^{10}B(n,\alpha)$, $^{197}Au(n,\gamma)$, and $^{235}U(n,f)$. Data on the $^{238}U(n,\gamma)$, $^{238}U(n,f)$, and $^{239}Pu(n,f)$ cross sections were also obtained which will be used by the evaluators of the ^{238}U and ^{239}Pu cross sections. New R-matrix evaluations for H(n,n) by Dodder and Hale and $^{3}He(n,p)$ by Hale are also now completed. These evaluations have been accepted by CSEWG for inclusion in the ENDF/B-VI standards file. The ENDF/B-VI standards are available on request from the National Nuclear Data Center at Brookhaven National Laboratory. A new evaluation of carbon by Fu et al which includes the contributions from two resonances in ^{13}C is being reviewed

* Argonne National Laboratory
** Los Alamos National Laboratory
*** Oak Ridge National Laboratory

for acceptance in the new standards file. Work is now underway to define the cross section uncertainties and establish the uncertainty (variance-covariance) files for these standards. Documentation for this evaluation effort is in progress.

2. <u>Photon Cross Section Database</u> (M. J. Berger, J. H. Hubbell, and E. B. Saloman)

Based on comparisons with measured values of photon attenuation coefficients, a comprehensive theoretical database of photon interaction cross sections has been adopted. The theoretical database covers the energy region from 1 keV to 100 GeV and atomic numbers from 1 to 100. The data include total cross sections and attenuation coefficients, and the partial cross sections for incoherent scattering, coherent scattering, photoelectric absorption, and pair production in the field of the nucleus and in the field of the atomic electrons. This database has been organized into main-frame, mini, and PC computer codes which generate the cross sections for any desired material. A new computer-readable library of these theoretical cross sections, called DLC-136/PHOTX, has been sent to the Radiation Shielding Information Center at Oak Ridge National Laboratory, and will be the basis of the data for ENDF/B-VI.

The experimental database now consists of 21000 measured data points for the total attenuation coefficient from 512 independent literature sources, spanning the photon energy range 10 eV to 13.5 GeV for 82 elements. This database has recently been organized into a PC-based code system to enable a user to easily extract selected data.

3. <u>Fifty Years with Nuclear Fission, a Conference</u> (J. W. Behrens, A. D. Carlson, B. S. Carpenter, W. A. Cassatt, E. V. Hayward, R. A. Schrack, and O. A. Wasson)

The National Institute of Standards and Technology and the American Nuclear Society will sponsor a conference entitled "Fifty Years with Nuclear Fission" to be held at the National Academy of Sciences and the National Institute of Standards and Technology from April 25-28, 1989. Joining as co-sponsors are the American Chemical Society and its division of Nuclear Chemistry along with the American Physical Society and its Division of Nuclear Physics, in cooperation with Accademia Nationale Dei Lincei, U. S. Department of Energy, Electric Power Research Institute, George Washington University Institute for Technology and Strategic Research, International Atomic Energy Agency, National Academy of Sciences, National Science Foundation, U. S. Nuclear Regulatory Commission, OECD Nuclear Energy Agency, Princeton University, and the University of California-Berkeley. Professors John Wheeler and Edoardo Amaldi will serve as honorary Co-Chairmen. Professors Glenn T. Seaborg and Emilio Segrè are general Co-Chairmen.

The conference program committee met in April, 1988 in Baltimore to define the program. The review of contributed and invited papers took place at the National Institute of Standards and Technology in November, 1988. A total of

44 invited and 96 contributed papers will be presented. The conference will open with a "Pioneers" reception on the evening of April 25 and will include a banquet on the evening of April 27. Announcements containing program and registration information were mailed in January, 1989. Additional information was provided in the various publications of the cooperating organizations. The preliminary indication is that this will be a very successful celebration of the fiftieth anniversary of the discovery of nuclear fission.

4. A Simultaneous Evaluation of Kerma in Carbon and the Carbon Cross Sections (E. J. Axton and J. J. Coyne)

Recent measurements of kerma in carbon indicate that values of this quantity calculated on the basis of cross sections taken from the ENDF/B-V file are probably too high, particularly in the energy range from 15-to 20-MeV. Measurements of the inelastic scattering cross section to the first excited state, and of the n-n'3α cross section in this energy range which have appeared since the establishment of ENDF/B-V suggest that the former should be higher, and the latter lower.

Experimental data on the total and elastic scattering, which was not used in the ENDF/B-V evaluation, is now available and has been used in the evaluation. A least squares fit was made to the available data for kerma factors and all of the cross sections in order to find the best value for these parameters. A final report will soon be available which contains tabulations of all the cross sections for carbon and the newly evaluated kerma factors. More work should be done on the separation of the n-n'3α cross section into its various possible reaction channels and the entire work should be extended up in energy to at least 60 MeV. A similar reevaluation of the cross section in oxygen should be carried out but this will move slowly due to a lack of manpower.

5. Calculated Microdosimetric Energy Distribution Spectra and Their Use to Indicate Neutron Source Quality (J. J. Coyne and H. M. Gerstenberg)

Microdosimetric energy distribution spectra, or y spectra, have been calculated for a large number of different distributed neutron sources using the analytical computer code developed at NIST. The neutron spectra used as the input for the code were obtained from calculations of the neutron fluence expected from a ^{252}Cf source, a source of neutrons from a pulsed thermal reactor with and without a lead shield, a source with a large component of high-energy neutrons up to 16.9 MeV at various distances from the source and at various points in an anthropomorphic phantom. The resulting energy distribution spectra for each of the input neutron spectra are compared and explained in terms of the proportion of low-energy neutrons to high-energy neutrons in the input neutron spectra. The variations, as well as the similarities, in shape of the resulting energy distribution spectra show that the y spectra can be a useful tool in understanding the quality of different spectra. Some calculations have also been done for neutron energy spectra which are used in radiation cancer therapy. The resulting y spectra will be used to help understand the difference in biological effectiveness of the different neutron beams.

6. Initial Spectra of Neutron-Induced Secondary Charged Particles
(J. J. Coyne, R. S. Caswell, and H. M. Gerstenberg)

Initial spectra of secondary-charged particles (such as p, α, C, N, and O) which result from neutron interactions with material such as tissue, will be tabulated in 200-keV neutron energy bin sizes from 0 to 20 MeV. Tabulations will also be made for 76 almost logarithmic bins extending from thermal energy for 2 MeV. These calculations use as input neutron cross section data in the ENDF/B format. We are in the process of putting the Axton reevaluation in the correct format to be used in our calculations. Supplementary information is also needed on the angular distribution of neutron reactions leading to charged particles and on the final excitation of residual nuclei. A problem in how to specify these spectra at low neutron energies below 100 keV have been resolved and these tabulations should soon be available. Separate spectra will be given for hydrogen, carbon, nitrogen and oxygen, along with a few examples of composite materials. These spectra should be useful in many radiation effects calculations, including biological effectiveness.

1. OAK RIDGE NATIONAL LABORATORY

Much effort has been spent this past year finalizing evaluations for ENDF/B-VI. Of the approximately 40 materials which have had major upgrades for VI, we have provided 20 full material evaluations (C, isotopes of Cr, Fe, Ni, Cu, Pb, and ^{240}Pu), and collaborated on Mn, ^{235,238}U, ^{239}Pu, and the Standards Evaluations. Except for the Big 3, evaluations have been completed and were Phase I reviewed at a December meeting held at ORELA. These evaluations have used much of the data reported in the pages of these DOENDC reports, and through the evaluation effort these experimental data will find their way into design libraries of nuclear data users. As a consequence of this evaluation effort at ORELA, there are more papers listed under heading B (theory and evaluation) than normal.

A. CROSS SECTION MEASUREMENTS

1. Capture, Total and Reaction

a. ^{10,11}B$(n, x\gamma)$ Reactions for Incident Neutron Energies Between 0.1 and 25 MeV,[1] (J. K. Dickens and D. C. Larson)

Measurements have been made of gamma-ray production due to neutron interactions with samples of boron for incident neutron energies between 0.1 and 25 MeV. For ^{11}B a 54-g sample of naturally-occurring boron in the shape of a solid cylinder was used. For ^{10}B, samples enriched to 95% in the ^{10}B isotope were used. One sample, about 49 g, was used to obtain γ-ray data following inelastic scattering; the other sample, of about 15 g, was used to delineate the production of the 478-keV gamma ray following the ^{10}B$(n, \alpha\gamma)^7$Li reaction for E_n between 0.1 and 4 MeV. The Oak Ridge Electron Linear Accelerator (ORELA), a white source, was used to provide the incident neutrons. Data were obtained using a high-purity intrinsic-germanium photon detector positioned at 125 deg with respect to the incident neutron beam. Because the peak shapes in the raw data were substantially broadened by Doppler motion, peak yields were determined with graphic-interactive methods. Except for the 478-keV gamma ray for $E_n < 1$ MeV, the γ-ray production cross sections are all small, the largest being $<$100 mb.

b. Resonance Neutron Capture by ^{20,22}Ne in Stellar Environments[2] (R. R. Winters[3] and R. L. Macklin)

[1] Nucl. Data for Sci. and Tech., Mito, Japan, 1988, pp. 213-15.

[2] The Astrophysical Journal, 329:943-950, June 15, 1988.

[3] Department of Physics, Denison University, Granville, Ohio 43023.

c. Resonance Neutron Capture by Argon-40 [1] (R. L. Macklin, R. R. Winters,[2] and D. M. Schmidt[3]3)

Neutron capture by ^{40}Ar at resonances up to 150 keV has been measured and parameterized using the single level Breit-Wigner formula. Velocity weighted Maxwellian averaged capture cross sections are presented for use in stellar nucleosynthesis calculations for stellar temperatures from kT=5 to 60 keV. The results are almost constant above kT=10 keV because most of the resonances lie at higher energies. At the conventional s-process temperature kT=30 keV the Maxwellian averaged capture cross section found is (2.79 ± 0.15) mb.

d. ^{53}Cr$(n, n'\gamma)$ Reactions and the Level Structure of ^{53}Cr[4] (D. C. Larson and J. K. Dickens)

Gamma-ray decay of levels in the stable isotope ^{53}Cr has been studied using ^{53}Cr$(n, n'\gamma)$ reactions for incident neutron energies between threshold and 10 MeV. Measured gamma-ray production cross sections have been compared with earlier measurements and with cross sections calculated using precompound-compound-nucleus theory. Some of the present results are at variance with earlier experimental or evaluated results. For example, for the decay of the $E_x = 1537$-keV level we are unable to explain variations in the measured branching ratios of the transition gamma rays as a function of incident neutron energy. The experimental data were analyzed within the framework of several theoretical model calculations of the level structure of ^{53}Cr. Quantitative discrepancies are discussed.

e. ^{58}Ni $+n$ Transmission, Differential Elastic Scattering and Capture Measurements and Analysis from 5 to 813 KeV[5] (C. M. Perey, F. G. Perey, J. A. Harvey, N. W. Hill, N. M. Larson, and R. L. Macklin)

High-resolution neutron measurements for ^{58}Ni-enriched targets were made at the Oak Ridge Electron Linear Accelerator (ORELA) from 100 eV to $\approx$20 MeV in transmission, from 10 keV to 5 MeV in differential elastic scattering, and from 2.5 keV to 5 MeV in capture. The transmission data were analyzed from 10 to 813 keV with the multilevel R-matrix code SAMMY which uses Bayes' theorem for the fitting process. This code provides energies and neutron widths of the resonances inside the 10- to 813-keV region as well as a possible parameterization for resonances external to that region to describe the smooth cross section from 10 to 813 keV. The differential elastic data at different scattering angles were compared to theoretical calculations from 30 to 813 keV using an R-matrix code based on the Blatt-Biedenharn formalism. Various combinations of spin and parity were tried to predict cross sections for the well defined $\ell > 0$ resonances, and comparison with

[1] Accepted by Astronomy and Astrophysics.

[2] Department of Physics, Denison University, Granville, OH 43023.

[3] Department of Physics, University of California at Santa Barbara, Santa Barbara, CA 93106.

[4] Accepted for publication in Phy. Rev. C, (February 1989).

[5] ORNL/TM-10841, ENDF-347 (September 1988).

the data then provided spin and parity assignments for most of these resonances. The capture data were analyzed from 5 to 450 keV with a least-squares fitting code using the Breit-Wigner formula. In this energy region 30% more resonances were observed in the capture data than in the transmission data.

From 5 to 813 keV, 477 resonances are reported. The reduced widths of the 62 s-wave resonances follow the Porter-Thomas distribution and their nearest neighbor spacings agree with the Wigner distribution. The average s-wave level spacing is equal to 13.6 ± 0.5 keV and the s-wave strength function to $(3.1 \pm 0.6) \times 10^{-4}$. The staircase plot of the s-wave reduced level widths and the plot of the Lorentz-weighted strength function show only a slight possibility of doorway states. The level densities calculated with the Fermi-gas model for $\ell = 0$ and $\ell > 0$ resonances are compared with the cumulative number of observed resonances. The average radiation widths were deduced from resonances analyzed in the three data sets below 450 keV. The mean values of the distributions of the radiation widths are equal to 2.3 eV for the s-wave resonances, 0.77 eV for the p-wave resonances, and 1.3 eV for the d-wave resonances and the standard deviations are 1.7 eV, 0.33 eV, and 0.5 eV respectively. The correlation coefficient between the s-wave reduced neutron widths and radiation widths is equal to 0.66 ± 0.11. The average capture cross section as a function of the neutron incident energy is compared to prediction based on the tail of the giant electric dipole resonance.

f. Neutron Capture by ^{79}Br, ^{81}Br, and ^{75}As[1] (Richard L. Macklin)

g. Total Cross Section and Resonance Spectroscopy for $n + {}^{86}$Kr[2] (R. F. Carlton,[3] R. R. Winters,[4] C. H. Johnson, N. W. Hill, and J. A. Harvey)

h. Measurement of the ^{85}Rb and ^{87}Rb Capture Cross Sections for s-Process Studies[5] (H. Beer[6] and R. L. Macklin)

The excitation functions for the reactions $^{85}\mathrm{Rb}(n,\gamma)$ and $^{87}\mathrm{Rb}(n,\gamma)$ have been measured over the neutron energy range of 175 eV to 700 keV. Maxwellian-averaged capture cross sections for thermal energies kT = 5–100 keV have been calculated. The data were used to carry out s-process calculations. Solar s-process abundances were reproduced with a two-component phenomenological model below mass number 90, a single-flux weak s-process, and a pulsed s-process characterized by exponentially distributed neutron exposures. The solar s-process abundances, as well as s-process abundances from Ba stars and the Murchison meteorite, were studied in the framework of the asymptotic giant branch

---

[1] Nucl. Sci. Eng. 99, 133-144 (1988).

[2] Phy. Rev. C38(4), (October 1988).

[3] Middle Tennessee State University, Murfreesboro, TN 37132.

[4] Department of Physics, Denison University, Granville, OH 43023.

[5] The Astrophysical Journal 339, (April 15, 1989).

[6] Kernforschungszentrum Karlsruhe, Institut für Kernphysik III, D-7500 Karlsruhe, Federal Republic of Germany.

models. Constraints were derived concerning the properties of the neutron pulses for a description of the empirical s-process data.

i. Search for ^{136}Xe Resonance Neutron Capture[1] (R. L. Macklin)

Evidence for neutron capture in ^{136}Xe at 2154-eV and 18.4-keV resonances is presented and quantified in terms of limits on Breit-Wigner single level parameters. Assuming the radiation width, 32 meV, found at the 18.4-keV resonance for all the reported resonances at higher energies, the Maxwellian average capture cross section is calculated for a range of stellar interior temperatures T. For $kT = 30$ keV only 0.72 mb is found. Only one-third of this comes from the resonances above 18.4 keV so an overall uncertainty at $kT = 30$ keV of ± 0.11 mb at the 68% probability level seems reasonable. Four resonances in ^{134}Xe were also found.

j. The ^{151}Sm Branching: A Probe for the Irradiation Time Scale of the s-process[2] (H. Beer[3] and R. L. Macklin)

k. Neutron Scattering in ^{189}Os for Nucleosynthesis Rates of the Odd-A Os Isotopes and Nucleochronology[4] (M. T. McEllistrem,[5] R. R. Winters,[6] R. L. Hershberger,[6] Z. Cao,[7] R. L. Macklin, and N. W. Hill)

Neutron elastic and inelastic scattering cross sections have been determined for neutrons incident on ^{189}Os at three very low energies. Cross sections for scattering to the ground state and 36.2-keV excited level have been measured for incident energies of 63.5 and 73.3 keV, and also to the 69.6-keV excited level at 97.5-keV incident energy. These measurements are combined with neutron scattering cross sections for ^{187}Os, neutron capture cross sections, and other low energy scattering observables to provide a basis for a single, consistent model of all data for both odd-A Os isotopes. The properly interpreted capture rates are important for the Re/Os nucleochronology and for s-process nucleosynthesis rates. The elastic and inelastic scattering cross sections provide a very low energy test of statistical model flux distributions; model accuracy at very low energies is an important issue for reaction rates used in nucleosynthesis estimates.

---

[1] ORNL/TM-10766 (April 1988).

[2] The Astrophysical Journal 331:1047-1057 (August 15, 1988).

[3] Kernforschungszentrum Karlsruhe, Institut für Kernphysik III, D-7500 Karlsruhe, Federal Republic of Germany.

[4] Submitted to Phy. Rev. C, (August 1988).

[5] Department of Physics, University of Kentucky, Lexington, KY.

[6] Department of Physics, Denison University, Granville, OH 43023.

[6] Nichols Research Corporation, Huntsville, AL.

[7] Institute of Atomic Physics, Beijing, Peoples Republic of China.

2. Actinides

a. High-Resolution Neutron Transmission Measurements on ^{235}U, ^{239}Pu, and ^{238}U[1] (J. A. Harvey, N. W. Hill, F. G. Perey, G. L. Tweed, and L. Leal[2])

High-resolution transmission measurements have been made on three sample thicknesses of both ^{235}U and ^{239}Pu at liquid nitrogen temperature and also on three of ^{238}U at room temperature using neutrons from the water-moderated ORELA target. The data on ^{235}U and ^{239}Pu from 1 to 10,000 eV were obtained using ^{6}Li glass scintillation detectors at 17.909- and 80.394-m flight paths. The ^{238}U data from 1 to 100 keV were obtained using a new NE 110 proton-recoil scintillation detector at a 201.558-m flight path.

b. Resonance Structure in the Fission of ($^{235}U + n$)[3] (M. S. Moore,[4] G. de Saussure, L. C. Leal,[2] R. B. Perez,[2] and N. M. Larson)

A new multilevel reduced R-matrix analysis of the neutron-induced spin-separated fission, total, and capture resonance cross sections of ^{235}U has been carried out. This analysis is the basis for the new resonance evaluation of the neutron cross sections of ^{235}U. As is well known, a two-fission-channel fit to the resonance structure in each spin state is not unique. In order to provide a parameterization that might be considered unique, as well as capable of describing scission-point variables such as the mass-distribution peak-to-valley ratio, and kinetic-energy and average neutron-emission probabilities from resonance to resonance, we used as a constraint in the analysis the angular anisotropy measurements of Pattenden and Postma, obtaining a Bohr-channel (or J, K channel) representation of the resonances in a two-fission vector space for each spin state. This parameterization gives a satisfactory description of the radiochemical measurements of the variation of peak-to-valley mass distributions from resonance to resonance.

Recently Hambsch et al. reported definitive measurements of the mass- and kinetic-energy distributions of fission fragments of ($^{235}U + n$) in the resonance region, using a Frisch-gridded ionization chamber. Hambsch et al. analyzed their results according to the fission-channel representation of Brosa et al., extracting relative contributions of the two asymmetric and one symmetric Brosa fission channels. Hambsch et al. attribute the kinetic-energy variation they observed to the variation in the contribution of the two asymmetric Brosa channels, finding that this is strongly correlated with the variation of $\bar{\nu}$, the average fission neutron emission probability. We found, however, that $\bar{\nu}$ is significantly but only weakly correlated with the Bohr channel representation of our R-matrix analysis. The variation of the symmetric Brosa channel, as deduced by Hambsch et al. is well described by our analysis in terms of Bohr channels, but the asymmetric Brosa-channel representation is not. We have explored the connection between Bohr-channel and

[1] Nucl. Data for Sci. and Tech., Mito, Japan, 1988, pp. 115-118.

[2] Oak Ridge National Laboratory and The University of Tennessee, Knoxville, TN.

[3] Submitted to International Conference Fifty Years Research in Nuclear Fission, Berlin, Germany, April 3-7, 1989.

[4] Los Alamos National Laboratory, P-15, Los Alamos, NM 87545.

asymmetric Brosa-channel representations. The results suggest that a simple rotation of coordinates in channel space may be the only transformation required; the multilevel fit to the total and partial cross sections is invariant to such a transformation.

c. Neutron Absorption Cross Section of Uranium-236[1] (R. L. Macklin and C. W. Alexander)

U-236 neutron absorption was measured as a function of neutron time-of-flight from 20 eV to 1 MeV. The neutron flux was monitored with a ^{6}Li glass scintillator. Average cross sections from 3 keV to 1 MeV were derived. Estimated uncertainties were less than 5% below 600 keV and increased to 9.5% at 1 MeV. Resonance parameterization from 20 eV to a few keV remains to be done.

d. Neutron Absorption Cross Section of Uranium-236[2] (R. L. Macklin and C. W. Alexander)

U-236 neutron absorption was measured as a function of neutron time-of-flight from 20 eV to 1 MeV. The neutron flux was monitored with a ^{6}Li glass scintillator. Average cross sections from 3 keV to 1 MeV were derived. Estimated uncertainties were less than 5% below 600 keV and increased to 9.5% at 1 MeV. From 20 eV to 4.2 keV neutron energy 293 resonance peaks were parameterized.

e. High Energy Resolution Measurement of the ^{238}U Neutron Capture Yield in the Energy Region Between 1 and 100 keV[3] (Roger L. Macklin,[4] R. B. Perez,[4] G. de Saussure, and R. W. Ingle)

A measurement of the ^{238}U neutron capture yield was performed at the 150 meter flight-path of the ORELA facility on two ^{238}U samples (0.0124 and 0.0031 atoms/barn). The capture yield data were normalized by Moxon's small resonance method.

The energy resolution achieved in this measurement frequently resulted in doublet and triplet splittings of what appeared to be single resonances in previous measurements. This resolution should allow extension of the resolved resonance energy region in ^{238}U from the present 4-keV limit up to 15 or 20 keV incident neutron energy.

Some 200 small resonances of the (^{238}U + n) compound nucleus have been observed which had not been detected in transmission measurements, in the energy range from 250 eV to 10 keV.

---

[1] ORNL/TM-10999 (November 1988).

[2] Submitted to Nucl. Sci. and Eng.

[3] Nucl. Data for Sci. and Tech., Mito, Japan, 1988, pp. 71-74.

[4] Nuclear Engineering Department, The University of Tennessee, Knoxville, TN.

f. High Resolution Fission Cross Section Measurements at ORELA[1] (L. W. Weston and J. H. Todd)

Multi-level fitting of the transmission, fission and capture cross sections have dramatically indicated the need for higher resolution and lower background fission cross section measurements of the fissile nuclides. High resolution is needed for extending the resolved resonance region to higher neutron energies, investigation of theoretical phenomena and background determination.

New measurements of the neutron fission cross sections of ^{235}U and ^{239}Pu have been carried out with the white neutron source of ORELA at a flight path of 85 meters. Fission chambers with fast current amplifiers and a parallel plate ^{10}B ionization chamber were used as detectors. These measurements have resolution more nearly comparable with recent transmission measurements and will aid in multi-level fits to higher neutron energies than previously feasible.

g. Subthreshold and Near-Subthreshold Fission Physics Measurements at the Oak Ridge Electron Linear Accelerator Facility[1] (R. B. Perez,[2] G. de Saussure, F. C. Difilippo, L. W. Weston, and J. A. Harvey)

This paper is an account of the work performed at the Oak Ridge Electron Linear Accelerator (ORELA), pertaining to the fission phenomena taking place at energies of the fissioning nucleus which are comparable to the fission barrier potential energy. In this energy region, fission cross-section measurements yield information on the physical properties of the barrier and on the nuclear states at high nuclear deformations. The ORELA facility intense pulsed neutron source and good energy resolution capabilities afford a convenient tool to carry out a program of measurements in the subthreshold and near-subthreshold regions.

Extensive and precise measurements in the actinide region were performed at the ORELA facility by an international group of researchers. These measurements were unique in many respects: fission widths and areas were determined for many previously unreported resonances in the subthreshold region and a most detailed study was performed on the physical properties of the fission barrier at high nuclear deformations.

---

[1] To be presented at the Conference on Fifty Years with Nuclear Fission, Gaithersburg, MD, April 26-28, 1989.

[2] University of Tennessee, Knoxville, TN.

3. Experimental Techniques

a. Responses of C_6D_6 and C_6F_6 Gamma-Ray Detectors and the Capture in the 1.15-keV Resonance of ^{56}Fe[1] (F. G. Perey, J. O. Johnson, T. A. Gabriel, R. L. Macklin, R. R. Winters,[2] J. H. Todd, and N. W. Hill)

We have used the electron gamma-ray transport code EGS to calculate responses of C_6D_6 and C_6F_6 gamma-ray detectors, where the geometry of the capture experiments was carefully modelled. Very good agreement was obtained with spectra from selected resonances in the capture of neutrons by ^{207}Pb. Weighting functions based upon the calculated responses were used in measuring the capture in the 1.15-keV resonance of ^{56}Fe relative to the capture in the Au 4.9-eV resonance. The neutron width was measured to be 64.5 ± 3.0 meV with C_6F_6 detectors, and 63.0 ± 2.5 meV with C_6D_6 detectors. These values are in good agreement with the value of 61.7 ± 0.9 meV found from transmission measurements.

b. SCINFUL: A Monte Carlo Based Computer Program to Determine a Scintillator Full Energy Response to Neutron Detection for E_n Between 0.1 and 80 MeV: User's Manual and FORTRAN Program Listing[3] (J. K. Dickens)

This document provides a complete listing of the FORTRAN program SCINFUL, a program designed to provide a calculated full response anticipated for either an NE-213 (liquid) scintillator or an NE-110 (solid) scintillator. The incident design neutron energy range is 0.1 to 80 MeV. Preparation of input to the program is discussed as are important features of the output. Also included is a FORTRAN listing of a subsidiary program applicable to the output of SCINFUL. This user-interactive program is named SCINSPEC from which the output of SCINFUL may be reformatted into a standard spectrum form involving either equal light-unit or equal proton-energy intervals. Examples of input to this program and corresponding output are given.

c. SCINFUL: A Monte Carlo Based Computer Program to Determine a Scintillator Full Energy Response to Neutron Detection for E_n Between 0.1 and 80 MeV: Program Development and Comparisons of Program Predictions with Experimental Data[4] (J. K. Dickens)

This document provides a discussion of the development of the FORTRAN Monte Carlo program SCINFUL (for scintillator full response), a program designed to provide a calculated full response anticipated for either an NE-213 (liquid) scintillator or an NE-110 (solid) scintillator. The program may also be used to compute angle-integrated spectra of charged particles (p, d, t, ^3He, and α) following neutron interactions with ^{12}C. Extensive comparisons with a variety of experimental data are given. There is generally overall good

[1] Nucl. Data for Sci. and Tech., Mito, Japan, 1988, pp. 379-82.

[2] Department of Physics, Denison University, Granville, OH 43023.

[3] ORNL-6462, (March 1988).

[4] ORNL-6463, (April 1988).

agreement (<10% differences) of results from SCINFUL calculations with measured detector efficiencies for the incident design neutron energy range of 0.1 to 80 MeV. Calculations of detector responses, i.e., $N(E_r)$ vs E_r where E_r is the response pulse height, reproduce measured detector responses with an accuracy which, at least partly, depends upon how well the experimental configuration is known. For $E_n < 16$ MeV and for $E_r > 15\%$ of the maximum pulse height response, calculated spectra are within $\pm 5\%$ of experiment on the average. For E_n up to 50 MeV similar good agreement is obtained with experiment for $E_r > 30\%$ of maximum response. For E_n up to 75 MeV the calculated shape of the response agrees with measurements, but the calculation underpredicts the measured response by up to 30%.

d. Covariances of Physical Constants[1] (F. G. Perey)

In many modern engineering-system studies the uncertainties in some key performance parameters are dominated by the uncertainties in the physical constants of the components of the system and are very strongly affected by the covariances of these physical constants. About 10 years ago this was realized as the case for fast nuclear reactor studies, and the data bases were modified to include covariances of the key physical constants. Experimentalists who provide nuclear data for applications are now increasingly describing the covariances in their measured data. The problems of determining and reporting the complete covariance matrix of measured data will be discussed.

e. Use of Monte Carlo Techniques to Derive Yields for $n + {}^{12}C$ Multi-body Breakup Reactions[2] (J. K. Dickens)

A computer "experiment" using Monte Carlo sampling methods has been designed to simulate the breaking up of ${}^{12}C$ by medium-energy neutrons into final reaction channels having 2, 3, or 4 outgoing charged particles. The calculational nuclear physics concept used in the "experiment" is one of a sequentially decaying highly-excited compound nucleus. Two methods of Monte Carlo sampling, the rejection method and the cumulative-distribution method, are discussed as applied to probability functions developed in the program.

f. A NE-110 Scintillation Detector for keV-Energy Neutrons[3] (J. A. Harvey and N. W. Hill)

We have developed a neutron detector with a narrow resolution function which is efficient for keV energy neutrons, has low background, and is not sensitive to overlap neutrons (<200 eV) so the pulsed accelerator can be operated at a high repetition rate (800 pps). The detector consists of a 9- by 9-cm NE 110 scintillator, 1 cm thick, mounted in a 0.025-mm mylar reflecting cylinder, and epoxy-coupled on opposite edges to two

---

[1] Invited talk, NCSL Annual Conference and Symposium, Washington, D.C., August 14-18, 1988.

[2] Submitted to Computers in Physics, January 1989.

[3] Presented at the American Physical Society Annual Meeting in Baltimore, MD, April 1988.

12.5-cm-diameter RCA 8854 photomultipliers (PMs). Each PM is biased below the single photoelectron level, and a coincidence is required between the outputs of the two PMs to eliminate counts due to PM noise. The detector has been studied down to a neutron energy of 50 eV. The observed signal-to-background ratio was 300 at 12 keV and 30 at 2 keV. The detector has an efficiency of 40% at 15 keV (ten times that of a 1-cm-thick ^{6}Li glass scintillation detector) and its efficiency equals that of the ^{6}Li detector at 4 keV. The timing resolution of the detector is 7 nsec for 10-keV neutrons, limited by the neutron flight time through the scintillator, and is less for higher energy neutrons. Results from transmission measurements on ^{238}U will be presented.

g. Calculation of the ORELA Neutron Moderator Spectrum and Resolution Function[1] (F. G. Perey and S. N. Cramer)

The yield, spectrum, and delay-time distributions (resolution function) of escape neutrons from the ORELA water-moderated and water-cooled tantalum target assembly are calculated using time-dependent, three-dimensional Monte Carlo techniques. Results are obtained for three different areas of the target that are frequently used in high resolution experiments: the full moderator, a small area of the moderator close to the tantalum target, and the tantalum target itself. The resulting spectra and delay-time distributions are compared with measured values and presented in a form suitable for use in the resonance parameter analysis code SAMMY.

h. Background Subtraction in Multiplicity Distributions[2] (F. G. Perey)

We propose an algorithm for subtracting background from neutron multiplicity distribution data which dampens the strong oscillations one frequently observes with the conventional method when the average multiplicity in the background is high and the statistics in the counting data are not very high. This algorithm, which is a constrained least-squares algorithm, produces results that converge to those of the conventional method when the statistics are sufficiently high.

B. DATA ANALYSIS

1. Theoretical

a. Neutron-^{40}Ca Mean Field Between −80 and +80 MeV from a Dispersive Optical-Model Analysis[3] (C. H. Johnson and C. Mahaux[4])

The n-^{40}Ca complex mean field is derived from a dispersive optical-model analysis of the available experimental cross sections. In this analysis the real part of the mean field contains dispersive contributions which are derived from the imaginary part by means

---

[1] In preparation for ORNL/TM

[2] In preparation for ORNL/TM.

[3] Phy. Rev. C38(6),2589 (December 1988).

[4] Institut de Physique B5, Université de Liège, B4000 Liège 1, Belgium.

of a dispersion relation. These dispersive contributions must be added to the Hartree-Fock potential which is assumed to have a Woods-Saxon shape, with a depth $V_H(\mathrm{E})$ that depends exponentially upon energy. The input experimental data are 14 differential cross sections in the energy domain (5.3, 40.0 MeV), five polarization cross sections in the domain (9.9, 16.9 MeV), and the total cross section in the domain (2.5, 80 MeV). The resulting optical-model potential is an analytic function of energy. It can thus be extrapolated towards negative energies, where it should be identified with the shell-model potential. This extrapolation yields good agreement with the experimental single-particle energies in the two valence shells of ^{40}Ca. The model also predicts the radial shape and the occupation probabilities of the single-particle orbits and the spectroscopic factors of the single-particle excitations. In order to reproduce the experimental energies of the deeply bound $1p$ and $1s$ orbits, one must use a linear rather than an exponential energy dependence of $V_H(E)$ at large negative E. It is shown that this is precisely the behavior expected from the fact that the energy dependence of $V_H(E)$ actually represents the nonlocality of the original microscopic Hartree-Fock field. The model also correctly predicts the distribution of the single-particle strength of the $1d(5/2)$ excitation in ^{39}Ca. The calculated distributions of the $1p$ strength in ^{39}Ca and the $1f(5/2)$ strength in ^{41}Ca show that the available experimental information extends over less than half the expected peak, whose energy is thus poorly known experimentally. In the energy domain (2.5, 9 MeV) the predicted total cross section deviates from the experimental data; this reflects the fact that at low energy the calculated cross section is very sensitive to small modifications of the mean field.

b. $n + {}^{40}$Ar s- and p-wave neutron resonance spacings and strength functions[1] (R. R. Winters,[2] R. F. Carlton,[3] and C. H. Johnson)

Using the ORELA we have measured the neutron total cross for $n + {}^{40}$Ar for incident neutrons in the energy range 10 keV to 50 MeV. Below 1500 keV the energy resolution of the measurement is sufficiently good to allow an R-Matrix description of the cross section with little ambiguity in the J^π assignments for the observed resonances. Our preliminary estimates for the level spacings are (63 ± 7), (33 ± 3), and (27 ± 2) keV for $J^\pi = 1/2^+$, $1/2^-$, and $3/2-$, respectively. The neutron strength functions for the same partial waves are (0.77 ± 0.25), (1.3 ± 0.3) and (0.30 ± 0.06) in 10^{-4} units.

c. Extrapolation of the Dispersive Optical Model to the Resonance Region for Neutrons on ^{86}Kr[4] (C. H. Johnson, R. F. Carlton,[3] and R. R. Winters[2])

The neutron-^{86}Kr mean field is formulated in terms of a dispersive optical model potential in which the real part contains dispersive contributions derived from the imaginary part by the dispersion relation. The dispersive contribution is added to the Hartree-Fock potential, which is assumed to have a Woods-Saxon shape and a depth that decreases

---

[1] To be presented at the American Physical Society Annual Meeting in Baltimore, Md., in May 1989.

[2] Department of Physics, Denison University, Granville, OH 43023.

[3] Middle Tennessee State University, Murfreesboro, Tennessee 37132.

[4] Phy. Rev. C39(2) (February 1989).

linearly with increasing energy. The shape parameters for all components of the potential are assumed to be independent of energy. The model is formulated in terms of the energy relative to the Fermi energy, and the imaginary potential is assumed to be symmetric about the Fermi energy, which is set equal to -7.7 MeV on the basis of the empirical level structure for $n - {}^{86}$Kr. All other parameters are taken from earlier analyses of other nuclei, particularly of ^{89}Y. The model is shown to give good overall predictions for the $n - {}^{86}$Kr mean field by comparison to the following three sets of empirical data: (i) the observed energies of the occupied and unoccupied valence levels, (ii) the energy-averaged total cross section for neutron energies up to 25 MeV, and (iii) the averaged scattering functions for s-, p-, and d-wave neutrons in the resolved resonance region from 0.015 to 0.96 MeV. The latter comparison is the unique feature of this work; the partial-wave-scattering functions that are available for s, p, and d waves in the resonance region for ^{86}Kr make possible detailed comparisons to the scattering functions from the model.

d. Level Densities from Resonance Spectroscopy for $n + {}^{86}$Kr[1] (R. F. Carlton,[2] R. R. Winters,[3] C. H. Johnson, N. W. Hill, and J. A. Harvey)

High resolution transmission measurements on a high purity ^{86}Kr gas sample were performed at the ORELA facility over the neutron energy range of 0.015–25 MeV. From R-matrix analysis of these data in the resolved resonance region below 1 MeV we have determined that $n + {}^{86}$Kr level densities for $J^\pi = 1/2^+$, $1/2^-$, $3/2^-$ reaction channels in the 1-MeV energy interval above neutron binding. The energy dependence of the $3/2^-$ level density, for which the uncertainties are smallest, is suitably modeled by a back-shifted Fermi gas model with two adjustable parameters. This model is then used to predict the level densities for $J^\pi = 1/2^+$ and $1/2^-$. Except for an unusual non-statistical behavior in the 500–600 keV region for the $1/2^-$ cumulative number of levels, the model is seen to give an excellent description of all three data sets. Parameters obtained are consistent with systematic trends in this mass region.

e. Calculations of Double Differential ^{184}W(n, xn) Cross Sections at 25.76 MeV by the TNG Code[4] (C. Y. Fu and D. M. Hetrick)

[1] To be presented that the American Physical Society Annual Meeting in Baltimore, MD, in May 1989.

[2] Middle Tennessee State University, Murfreesboro, TN 37132

[3] Department of Physics, Denison University, Granville, OH 43023.

[4] In "Results of Recent Code Comparisons" by H. Vonach, p. 265 in Proc. of Specialists' Meeting on Preequilibrium Nuclear Reactions, Semmering, Austria, Feb. 10-12, 1988, NEANDC-245'U' (1988).

f. Surface Contributions to the Complex Neutron-^{208}Pb Mean Field Between −20 and +20 MeV[1] (J. P. Jeukenne,[2] C. H. Johnson, and C. Mahaux[2])

Phenomenological analyses of the experimental n–^{208}Pb differential, total, and polarization cross sections with local optical-model potentials indicate that the radial shape of the surface absorption depends upon energy below 10 MeV: The corresponding diffuseness decreases and the radius parameter increases with decreasing neutron energy. Because of the dispersion relation that connects the real and imaginary parts of the mean field, these features imply that the real potential contains a surface component whose radial shape also depends upon energy. This radial shape is calculated numerically for typical parameterizations of the energy dependence of the surface absorption; it turns out to be quite complicated for neutron energies between 0 and 15 MeV. In this domain, the predicted differential cross sections are sensitive to the radial shapes of both the real and imaginary surface components of the mean field even though their volume integrals are exactly the same in all the investigated models. The best agreement with the experimental data is obtained for parameterizations in which the radial shape of the surface absorption depends only weakly upon energy. It is shown that good fits to the experimental data can also be obtained in the framework of models in which the radial shape of the surface absorption is independent of energy but in which the strength of the surface absorption depends upon the orbital angular momentum of the incoming neutron. Tentative physical interpretations of these features are proposed.

g. Unified Description of the n + ^{209}Bi Mean Field Between 1 MeV to 40 MeV via Dispersion Relations[3] (R. K. Das,[4] R. W. Finlay,[4] and J. A. Harvey)

The real part of the central n + ^{209}Bi mean field is the sum of a Hartree-Fock component whose radial dependence is assumed to have a Wood-Saxon shape and whose depth is energy dependent plus a dispersive component which is determined from the imaginary part of the optical model potential. Elastic neutron scattering data from 1.5 MeV to 24 MeV, along with total cross section from 1 to 40 MeV, is used for the above analysis. The energy dependence of the geometry of the optical model is also studied.

h. Analysis of the ^{235}U Neutron Cross Sections in the Resolved Resonance Range[5] (L. C. Leal,[6] G. de Saussure, and R. B. Perez[6])

Recent high resolution measurements have led to our analysis of the ^{235}U resonances to 110 eV. This paper discusses the statistical properties of the multilevel resonance

---

1 Phy. Rev. C 38(6) (December 1988).

2 Institut de Physique B5, University of Liëge, B-4000 Liége 1, Belgium.

3 Presented at the American Physical Society Annual Meeting in Baltimore, Md., in April 1988.

4 Physics Department, Ohio University, Athens, OH 45701.

5 To be presented at the Conference on Fifty Years with Nuclear Fission, Gaithersburg, MD., April 26-28, 1989.

6 University of Tennessee, Knoxville, TN.

parameters obtained from an analysis of the ^{235}U neutron cross sections. The average resonance parameters obtained from the present analysis are compared to values previously published.

i. Statistical Properties of the ^{235}U Resonance Parameters up to 300 eV[1] (L. C. Leal,[2] G. de Saussure, R. R. Winters[3] and R. B. Perez[2])

An accurate resonance analysis of the ^{235}U neutron cross sections up to 300 eV is in progress for the ENDF/B-VI files. A detailed discussion of the data base and a description of the method of resonance analysis have been given elsewhere. The purpose of this paper is to report on the statistical properties of the ^{235}U resonance parameters and compare our results with those of previous analysis. The statistical properties of nuclear levels are of both technical and theoretical interest. From the technical viewpoint these properties are the basis for an extrapolation into the unresolved resonance region, which is of relevance to the calculation of effective group cross sections for reactor design. From the theoretical viewpoint, the resonance parameters obtained from a multilevel R-matrix analysis of a consistent set of neutron cross sections should satisfy a set of statistical properties arising from general properties of the nuclear Hamiltonian.

j. R-Matrix Analyses of the ^{235}U and ^{239}Pu Neutron Cross Sections[4] (H. Derrien,[5] G. de Saussure, N. M. Larson, L. C. Leal,[6] and R. B. Perez[6])

The resonance parameter analysis code SAMMY was used to perform consistent resonance analyses of several ^{235}U and ^{239}Pu fission and capture cross section and transmission measurements up to 110 eV for ^{235}U and up to 1 keV for ^{239}Pu. The method of analysis, the measurement selection and the results are briefly outlined in this paper.

k. R-Matrix Analysis of the ^{241}Pu Neutron Cross Sections in the Energy Range Thermal to 300 eV[7] (H. Derrien[5] and G. de Saussure)

The report is a description of the analysis of the ^{241}Pu neutron cross sections in the resolved resonance region at Oak Ridge National Laboratory (ORNL) using the multilevel-multichannel Reich-Moore code SAMMY. The resonance parameters were obtained in the energy range 0 to 300 eV. The table of the resonance parameters is given with some statistical properties of the parameters. Tabulated and graphical comparison between the experimental data and the calculated cross sections are given. The results are available in

---

[1] To be presented at the American Nuclear Society Annual Summer Meeting, Atlanta, GA, June 4-8, 1989.

[2] University of Tennessee, Knoxville, TN.

[3] Department of Physics, Denison University, Granville, OH 43023.

[4] Nucl. Data for Sci. and Tech., Mito, Japan, 1988, pp. 83-86.

[5] Centre d'Etudes Nucleaires de Cadarache, Saint-Paul-Lez-Durance, France.

[6] University of Tennessee, Knoxville, TN.

[7] ORNL/TM-11123 (March 1989).

ENDF/B-V format and will be proposed for the evaluated data library JEF2 and ENDF/B-VI.

l. RFUNC – A Code to Analyze Differential Elastic-Scattering Data[1] (F. G. Perey)

The Code RFUNC is used at ORELA to analyze high resolution differential elastic scattering data from spin zero nuclides in the resonance energy region. This report presents the real R-Function formalism used in RFUNC and gives details of how the finite size corrections are currently made. Appendix A describes the input to the code RFUNC. Appendix B describes the input to a utility code MAKPA that transforms a resonance parameter file in SAMMY format into a resonance parameter file in RFUNC format. Appendix C describes the input to an adjunct code RFUNCXT that generates the contributions to the total cross section from resonances of different orbital and total angular momenta. The FORTRAN listing of the code RFUNC is given in Appendix D.

m. Resonance Parameter Analysis with SAMMY[2] (Nancy M. Larson and F. G. Perey)

The multilevel R-matrix computer code SAMMY has evolved over the past decade to become an important analysis tool for neutron data. SAMMY uses the Reich-Moore approximation to the multilevel R-matrix and includes an optional logarithmic parameterization of the external R-function. Doppler broadening is simulated either by numerical integration using the Gaussian approximation to the free gas model or by a more rigorous solution of the partial differential equation equivalent to the exact free gas model. Resolution broadening of cross sections and derivatives also has new options that more accurately represent experimental situations. SAMMY treats constant normalization and some types of backgrounds directly and treats other normalizations and/or backgrounds with the introduction of user-generated partial derivatives. The code uses Bayes' method as an efficient alternative to least squares for fitting experimental data. SAMMY allows virtually any parameter to be varied and outputs values, uncertainties, and covariance matrix for all varied parameters. Versions of SAMMY exist for VAX, FPS, and IBM computers.

n. Updated Users' Guide for SAMMY: Multilevel R-Matrix Fits to Neutron Data Using Bayes' Equations[3] (Nancy M. Larson)

In the Fall of 1985, the Oak Ridge Electron Linear Accelerator (ORELA) purchased a VAX-785 to replace her outmoded PDP10 system. SAMMY (and all other ORELA computations) thus migrated to the VAX, a move which required only slight modifications to the program. Shortly thereafter, a Floating Point System (FPS) Array Processor was obtained (jointly with the Physics Department at ORNL) for our use; the move to that machine required significant alterations in the internal structure of SAMMY, especially since we wished to produce a code which was, to as great an extent as possible, compatible for both machines. Finally, in the fall of 1987 an IBM-compatible version was

---

[1] ORNL/TM-11112 (March 1989).

[2] Nucl. Data for Sci. and Tech., Mito, Japan, 1988, pp. 573-576.

[3] ORNL/TM-9179/R2 (in preparation).

produced, again necessitating some modifications in the internal structure. These changes should not be noticeable to the casual user. IBM users should be aware of some changes in input from those needed for VAX or FPS; such changes are noted in the next.

New capabilities added to SAMMY subsequent to Revision 1 of this report include: (1) increased accuracy in calculations of Doppler-broadened cross sections; (2) the option to use an entirely new method for Doppler broadening; (3) the ability to generate energy-averaged theoretical cross sections; (4) the option to omit specified spin groups from a given analysis; (5) the use of data-reduction parameters (normalization, background, etc.) as varied parameters; (6) separate radii for potential scattering vs penetrability and shift factor; (7) different values for radii for different spin groups; (8) a "realistic" version of resolution broadening. These and other changes are documented in Revision 2 of this manual.

o. A Simplified Unified Hauser-Feshbach/Pre-Equilibrium Model for Calculating Double Differential Cross Sections[1] (C. Y. Fu)

p. Approximation of Precompound Effects in Hauser-Feshbach Codes for Calculating Double Differential (n, xn) Cross Sections[2] (C. Y. Fu)

q. On the Unresolved Resonance Region Representation of Neutron Induced Cross Sections[3] (R. B. Perez,[4] G. de Saussure, L. C. Leal,[4] and Roger L. Macklin[4])

The accurate representation of neutron cross sections in the unresolved resonance region is of interest for the calculation of the Doppler coefficient of reactivity and self-shielded group cross-section sets for fast reactors. Customarily, the cross sections in the unresolved resonance region are described on the basis of the statistical theory of nuclear reactions, by specifying average values and distribution functions for the resonance parameters. Resonance self-shielding factors can then be calculated by the appropriate statistical techniques. In this work we review the unresolved resonance region formalism in the light of the availability of new high-energy resolution measurements.

---

[1] Proc. Specialists' Meeting on Pre-Equilibrium Reactions, Semmering, Austria, February 10-12, 1988, p. 285, NEANDC 245'U' (1988).

[2] Nucl. Sci. Eng. 100, 61-76 (1988).

[3] Proceedings of the International Conference on Reactor Physics, Jackson Hole, WY, Sept. 18-21, 1988, Vol. III, p. 183, ANS ISBN: 0-89448-141-X.

[4] University of Tennessee, Knoxville, TN.

2. ENDF/B Related Work

a. Neutron Standard Data[1] (Robert Peelle and Henri Conde[2])

The neutron standards are reviewed with emphasis on the evaluation for ENDF/B-VI. Also discussed are the neutron spectrum of ^{252}Cf spontaneous fission, activation cross sections for neutron flux measurement, and standards for neutron energies greater than 20 MeV. Recommendations are made for future work.

b. A Re-Evaluation of $^{32}S(n,p)$ Cross Sections From Threshold to 5 MeV[3] (C. Y. Fu)

Two evaluations of the ^{32}S(n,p) reaction cross sections, presently being used for the Nagasaki and Hiroshima dosimetry studies, are of low quality and are in serious disagreement. The present re-evaluation of these cross sections was intended to be the most advanced possible and was based on: an exhaustive data search that uncovered an additional data set, a Bayes-theorem code for combining experimental data with uncertainties, a special procedure for including the effects of energy resolutions in data averaging, and the application of the much-improved ENDF/B-VI standards. Correlations in the experimental data were evaluated and tested for their effects but were not used for the final results because such correlations caused errors in the presence of resonances. The new results below 5 MeV (the upper limit of the present need) were combined with the ENDF/B-V dosimetry data above 5 MeV to generate a complete file, including covariances, from threshold to 20 MeV. These point data were processed into two Vitamin-E 174-group sets, one with a constant energy weighting and the other with a Maxwell-1/E-fission weighting.

c. ENDF/B-VI Evaluations for Isotopes of Cr, Fe, Ni, Cu, and Pb[4] (D. M. Hetrick, C. Y. Fu, and D. C. Larson)

Evaluations have been done for each of the stable isotopes of chromium, iron, nickel, copper, and lead. They are based on analysis of experimental data and results of nuclear model calculations which reproduce the experimental data. Evaluated data are given for neutron induced reaction cross sections, angular and energy distributions, and gamma-ray production cross sections associated with the reactions. The new file 6 formats are used to represent energy-angle correlated data and recoil spectra for the first time in ENDF. This paper reviews the structure of the evaluations, notes the major pieces of experimental data utilized, gives a summary of the model codes used, and compared calculations to measured data.

---

[1] Nucl. Data for Sci. and Tech., Mito, Japan, 1988, pp. 1005-1012

[2] Department of Neutron Research, Uppsala University, P. O. Box 535, S-751 21 Uppsala, Sweden.

[3] To be presented at the American Nuclear Society Topical Conference on Advances in Nuclear Computation and Radiation Shielding, Santa Fe, New Mexico, April 9-13, 1989.

[4] Eighth Topical Meeting on Technology of Fusion Energy, October 9-13, 1988, Salt Lake City, Utah.

d. A New Resonance-Region Evaluation of Neutron Cross Sections for ^{235}U[1] (G. de Saussure, L. C. Leal,[2] R. B. Perez,[2] N. M. Larson, and M. S. Moore[3])

This paper describes a new evaluation of the "resolved resonance range" for the neutron cross sections of ^{235}U. Up to 110 eV the evaluation is based on an R-matrix analysis of several fission, capture and transmission measurements. Above 110 eV levels are not resolved anymore so that many resonances are missed; from 110 to 500 eV most of the important resonances can be identified and analyzed so that the cross section and transmission data are well represented by the proposed parameters. From 500 to 2250 eV fictitious parameters are provided which describe fairly well the results of thick sample transmission measurements and recent fission cross-section data. We believe that such a parameterization is likely to yield a better approximation of resonance self-shielding than the current ENDF/B-V unresolved resonance treatment.

e. Uncertainties of the ENDF/B-V ^{238}U Unresolved Resonance Parameters in the Range 4 keV $< E <$ 45.18 keV (MAT = 1398, MF = 2, MT = 251)[4] (G. de Saussure and J. H. Marable).

It is a common practice in ENDF/B to represent neutron cross sections in the unresolved resonance region by specifying the average values and distribution laws of resonance parameters. This formalism allows the calculation of resonance selfshielding and of the variation of resonance selfshielding with temperature, two important reactor parameters. For many applications it is necessary to estimate the uncertainties in those model average resonance parameters. This note describes a possible approach to derive such uncertainties using as an example the ENDF/B-V representation of ^{238}U in the range from 4 to 45 keV.

f. R-Matrix Analysis of ^{239}Pu Neutron Cross-Sections in the Energy Range up to 1000 eV[5] (H. Derrien[6] and G. De Saussure)

The report is a description of the analysis of the ^{239}Pu neutron cross sections in the resolved resonance region using the multilevel-multichannel Reich-Moore code SAMMY. The resonance parameters were obtained in the energy range up to 1000 eV. The table of the resonance parameters is given with some statistical properties of the parameters. Tabulated and graphical comparisons between the experimental data and the calculated cross sections are given. The results are available in ENDF/B-V format and will be proposed for the evaluated data libraries JEF2 and ENDF/B-VI.

---

[1] Proceedings of the International Conference on Reactor Physics, Jackson Hole, WY, September 18-21, 1989, Vol. I, p. 293.

[2] University of Tennessee, Knoxville, TN.

[3] Los Alamos National Laboratory, Los Alamos, NM 87545.

[4] Nucl. Sci. and Eng. (to be published).

[5] ORNL/TM-10986 (January 1989).

[6] Centre d'Etudes Nucleaires de Cadarache, France

g. Current Plutonium Cross-Section Evaluations in the Resolved Resonance Region[1] (H. Derrien[2] and G. de Saussure)

The resonance parameter analysis code SAMMY was used to perform consistent resonance analyses of several ^{239}Pu and ^{241}Pu neutron fission and capture cross-section and transmission measurements up to 1 keV for ^{239}Pu and up to 300 eV for ^{241}Pu. The method of analysis, the measurement selection, and the results are discussed in this paper.

h. ENDF/B-VI Nuclear Data Evaluations for Fusion Applications[3] (C. L. Dunford,[4] D. C. Larson, and P. G. Young[5])

The next release of the ENDF/B data library planned for 1989 contains improved data evaluations of interest to the fusion neutronics community. New data formats permit inclusion of energy-angle correlated particle emission spectra and recoil nucleus energy spectra. Enhanced formats for covariance information have been developed. Many new isotopic evaluations will lead to improved energy conservation and kerma factor calculations. Improved nuclear model calculations will provide reliable particle emission data where experimental information is sparse. Improved Bayesian fitting codes will provide more accurate evaluations for data rich reactions such as Li(n,nt)α. All of the most important fusion material evaluations contain these new features.

i. Extended Covariance Data Formats for the ENDF/B-VI Differential Data Evaluation[6] (Robert W. Peelle and Douglas W. Muir[5])

The ENDF/B-V included cross section covariance data, but covariances could not be encoded for all the important data types. New ENDF-6 covariance formats are outlined including those for cross-file (MF) covariances, resonance parameters over the whole range, and secondary energy and angle distributions. One "late entry" format encodes covariance data for cross sections that are output from model or fitting codes in terms of the model parameter covariance matrix and the tabulated derivatives of cross sections with respect to the model parameters. Another new format yields multigroup cross section variances that increase as the group width decreases. When evaluators use the new formats, the files can be processed and used for improved uncertainty propagation and data combination.

---

[1] Proceedings of the International Conference on Reactor Physics, Jackson Hole, WY, Sept. 18-21, 1989, Vol. S, p. 65.

[2] Centre d'Etudes Nucleaires de Cadarache, France.

[3] Eighth Topical Meeting on Technology of Fusion Energy, October 9-13, 1988, Salt Lake City, Utah.

[4] Brookhaven National Laboratory, Upton, NY 11973.

[5] Los Alamos National Laboratory, Los Alamos, NM 87545.

[6] Proceedings of the Specialists' Meeting on the Application of Critical Experiments and Operating Data to Core Design Via Formal Methods of Cross Section Data Adjustments, Jackson Hole, WY, Sept. 23-24, 1988.

OHIO UNIVERSITY

A. MEASUREMENTS

1. A Study of the Higher Excitation Levels of ^{11}B via the $^{10}B(n,n)^{10}B$ and $^{10}B(n,n')^{10}B$ (0.72, 1.74, 2.15, 3.59, 4.77 MeV) Reactions*
(E.T. Sadowski**, H.D. Knox, R.O. Lane)

As part of the study of the higher energy-level structure of ^{11}B, cross sections for elastic and inelastic scattering of neutrons from isotopically enriched ^{10}B samples have been measured for incident neutron energies from 3.02 MeV to 6.45 MeV in 250 keV increments and from 7.02 MeV to 12.01 MeV in 500 keV increments. Inelastic angular distributions for scattering to the states in parenthesis in ^{10}B have been measured from the indicated energy up to 12.01 MeV: (0.718) from 3.02 MeV; (1.74) from 3.27 MeV; (2.15) from 3.77 MeV; (3.59) from 5.52 MeV; (4.77) from 7.02 MeV. The measurements at 3.02, 3.51, 4.02 and 4.51 MeV were done at nine laboratory angles from 20° to 158° in 17.5° increments with a sample that is isotopically 95.86% ^{10}B. All other distributions measured scattering at 11 laboratory angles from 18° to 158° in 15° increments from a sample that is isotopically 99.49% ^{10}B. The data are corrected for air scattering, sample attenuation, minor isotope impurity, multiple scattering, and elastic and inelastic scattering from the sample of the neutron source continuum and contaminants. An eight-channel, multi-level R-matrix analysis was performed on the data. Level energies, spins and parities were deduced for twelve levels above 13 MeV excitation in ^{11}B. Only two definite and three tentative assignments for T = 1/2 levels had been made previously above 13 MeV. The two definite levels were confirmed. Good agreement between the data and the R-matrix calculation in all analyzed channels was obtained for the proposed structure.

2. Structure of ^{14}C via Elastic and Inelastic Neutron Scattering from ^{13}C: Measurement and R-Matrix Analysis*
(D.A. Resler***, H.D. Knox, P.E. Koehler+, R.O. Lane and G.F. Auchampaugh+)

Differential cross sections for neutrons elastically scattered from ^{13}C and inelastically scattered to the first three excited states of $^{13}C^*$ (3.09, 3.68 and 3.85 MeV) were measured at 69 incident energies for $4.5 \leq E_n \leq 11$ MeV. A multiple scattering code provided a simulation of the experimental scattering process allowing accurate corrections to the small measured inelastic cross sections. The integrated $^{13}C(n,\alpha)^{10}Be$ cross section was determined by subtracting the sum of the measured integrated

---

* Work supported by U.S. Department of Energy.

** Permanent address: Savannah River Plant, Aiken, SC.

*** Permanent address: Lawrence Livemore National Laboratory, Livemore, CA.

\+ Permanent address: Los Alamos National Laboratory, Los Alamos, NM.

cross sections from the total. Shell-model calculations were used to generate the R-matrix parameters for the elastic and first three inelastic channels of $^{13}C+n$, and, after some minor adjustments, the predicted structure generally agreed with experiment for $E_n < 4$ MeV. Previous elastic $^{13}C+n$ data were refitted to replace constant R_0 R-matrix background terms by more realistic broad states and to achieve better agreement with model calculations and the data. R-matrix fitting of the full data set produced new ^{14}C level information. For $E_n > 4$ MeV ($E_x > 12$ MeV), five states were given definite J^{π} assignments and three states tentative assignments.

3. <u>Neutron Inelastic Scattering from ^{13}C*</u> (J.E. O'Donnell, R.O. Lane and H.D. Knox)

Currently under study are the properties of highly excited levels in ^{14}C at energies of $15 \lesssim E_x (^{14}C) \lesssim 19$ MeV. The excitation energies, J^{π} assignments, reduced-width amplitudes, etc. for levels in ^{14}C will be deduced from inelastic neutron scattering to levels in ^{13}C of $6.86 \lesssim E_x \lesssim 10$ MeV. A dynamic form of pulse-shape discrimination has been developed which, together with dynamic bias on TOF measurements, should improve the observational capabilities for the low energy neutrons from deep inelastic scattering to highly excited levels of ^{13}C. Initial measurements are now in progress. Final results for level properties deduced from R-matrix fitting of the data will be compared with shell model predictions to aid in the determination of the model properties.

4. <u>The (p,n) Reaction as a Probe of Beta Decay Strength**[1]</u> (T.N. Taddeucci***, C.A. Goulding***, T.A. Carey***, R.C. Byrd+, C.D. Goodman+, C. Gaarde++, J. Larsen++, D. Horen+++, J. Rapaport and E. Sugarbaker#)

The evidence for a useful proportionality relationship between 0° (p,n) cross sections and the corresponding Gamow-Teller and Fermi beta-decay transition strengths is examined in detail. A simple parameterization for small momentum transfer L = 0 transitions is developed and used in

---

* Work supported by the U.S. Department of Energy.
** Work supported in part by U.S. Department of Energy and the National Science Foundation.
*** Permanent address: Los Alamos National Laboratory, Los Alamos, NM.
\+ Permanent address: Indiana University Cyclotron Facility, Bloomington, IN.
++ Permanent address: Niels Bohr Institute, Copenhagen, Denmark.
+++ Permanent address: Oak Ridge National Laboratory, Oak Ridge, TN.
\# Permanent address: Ohio State University, Columbus, OH.
1 Published in Nucl. Phys. <u>A469</u>, 125 (1987).

the analysis of (p,n) data in the bombarding energy range 120—200 MeV. The parameterization describes the (p,n) differential cross section in terms of momentum transfer, energy loss, mass number and bombarding energy and provides a straightforward way of extrapolating to zero momentum transfer. It is found that a single proportionality constant can serve to relate all Gamow—Teller transitions originating from the same target nucleus. The target dependence of this proportionality constant, however, is found to be unpredictable at the 20%—50% level, even within isotopic chains. Such large variations cannot be easily explained in the context of the standard single—step direct—reaction distorted—waves impulse approximation model.

5. Ratio of Gamow—Teller to Fermi Strength Observed in ^{13,14}C(p,n) at 492 and 590 MeV.*[1] (J.L. Ullmann**, J. Rapaport, P.W. Lisowski**, R.C. Byrd**, T. Carey**, T.N. Taddeucci**, J. McClelland**, L. Rybarcyk**, R.C. Haight**, N.S.P. King**, G.L. Morgan**, D.A. Lind***, R. Smythe***, C.D. Zafiratos***, D. Prout***, E. Sugarbaker+, W.P. Alford++ and W.G. Love+++)

It has been recognized for a number of years that certain spin—isospin components of the nucleon—nucleus effective interaction can be inferred from (p,n) reactions to states of known nuclear structure. For L = 0, S = 0 and L = 0, S = 1 transitions, the 0—degree (p,n) cross section can be related respectively to Fermi and Gamow—Teller beta decay matrix elements. If these transitions occur in the same nucleus, the ratio of isovector spin—flip to non—spin—flip effective interactions can be measured without regard for absolute normalization. The best reaction to measure this is ^{14}C(p,n) which goes by a pure Gamow—Teller transition to the 1^+ state at 3.95 MeV in ^{14}N, and Fermi transition to the 2.31 MeV 0^+ state. This work extends the ratio measurements made at lower energies (Ref. 1, 2 and 3) to 492 and 590 MeV.

We also report on the ^{13}C(p,n) reaction which goes by a pure GT transition to the 3.51 MeV $3/2^-$ state in ^{13}N, but by a mixed Fermi plus Gamow—Teller transition to the $1/2^-$ ground state.

---

* Work supported by the U.S. Department of Energy and the National Science Foundation.
** Permanent address: Los Alamos National Laboratory, Los Alamos, NM.
*** Permanent address: University of Colorado, Boulder, CO.
+ Permanent address: Ohio State University, Columbus, OH.
++ Permanent address: TRIUMF, Vancouver, B.C., Canada.
+++ Permanent address: University of Georgia, Athens, GA.
1 Presented at Telluride Conference, March 1988.

6. Fermi and Gamow–Teller Strength in p–Shell Nuclei from (p,n) Reactions at 492 MeV and 590 MeV*[1] (J. Rapaport, P.W. Lisowski**, J.L. Ullmann**, R.C. Byrd**, T.A. Carey**, J.B. McClelland**, L.J. Rybarcyk**, T.N. Taddeucci**, R.C. Haight**, N.S.P. King**, G.L. Morgan**, D.A. Clark**, D.E. Ciskowski***, D.A. Lind+, R. Smythe+, C.D. Zafiratos+, D. Prout+, E.R. Sugarbaker++, D. Marchlenski++, W.P. Alford+++ and W.G. Love#)

Zero–degree (p,n) cross sections, measured with approximately 1 MeV energy resolution at E_p = 492 MeV, are reported for ^{7}Li, ^{11}B and ^{12,13,14}C. Measurements for ^{11}B(p,n) and ^{13}C(p,n) were also obtained at 590 MeV. The cross sections for Gamow–Teller and Fermi type transitions are used to estimate the strengths of the isovector spin–dependent ($J_{\sigma\tau}$) and spin–independent (J_{τ}) terms of the effective interaction. The measured zero–degree cross sections for the ^{14}C(p,n)^{14}N transitions to the 2.31 MeV isobaric analog state and the 3.95–MeV $J^{\pi} = 1^{+}$ state are compared with calculated values. Values for the unit cross section ratio $R^2 = \sigma_{GT}/\sigma_F = (J_{\sigma\tau}/J_{\tau})^2\ (N_{\sigma\tau}/N_{\tau})$ obtained from the present data are compared with results for other energies.

7. Spectroscopy of Unbound Isobaric Analog States via ^{28}Si(d,n)^{29}P and ^{32}S(d,n)^{33}Cl Reactions##[2] (Paul M. Egun###, C.E. Brient, S.M. Grimes, S.K. Saraf† and H. Satyanarayana††)

Proton transfer to unbound states was studied within the framework of the standard distorted–wave Born approximation formalism by using the form factors of their bound isobaric analog states. The results of the present analyses have shown that the spectroscopic factors obtained by substituting the form factors of the parent analog states for the unbound

---

* Work supported by the U.S. Department of Energy and the National Science Foundation.
** Permanent address: Los Alamos National Laboratory, Los Alamos, NM.
*** Permanent address: University of Texas, Austin, TX.
+ Permanent address: University of Colorado, Boulder, CO.
++ Permanent address: Ohio State University, Columbus, OH.
+++ Permanent address: University of Western Ontario, London, Ontario, Canada.
# Permanent address: University of Georgia, Athens, GA.
Work supported in part by the U.S. Department of Energy.
Present address: Institut für Mittelenergiephysik, Zürich, Switzerland.
† Present address: Brookhaven National Laboratory, Upton, NY.
†† Present address: 1221 Cambia Drive, Apt. 1218, Schaumburg, IL.
1 Submitted to Phys. Rev. C.
2 Published in Phys. Rev. C38, 2495 (1988).

states in the distorted—wave Born approximation calculations are frequently not reliable.

8. The $^{52,54}Cr(p,n)^{52,54}Mn$ and $^{57,58}Fe(p,n)^{57,58}Co$ Reactions at E_p = 120 MeV*[1] (D. Wang**, J. Rapaport, D.J. Horen***, B.A. Brown+, C. Gaarde++, C.D. Goodman+++, E. Sugarbaker# and T.N. Taddeucci##)

Differential cross sections for the (p,n) reaction on ^{52,54}Cr and ^{57,58}Fe have been measured for angles up to θ_{lab} = 10.5° and 14.6°, respectively, using 120 MeV protons. The observed angular distributions are used to evaluate the location and strength of Gamow—Teller resonances. A shell—model calculation of this strength distribution is presented and compared with the experimental results. The M1 strength for ^{52}Cr is also calculated and compared with available results from (e,e') and (p,p') experiments. A comparison is made with other $1f_{7/2}$ nuclei.

9. Multi—Step Compound Nuclear Reactions Induced by Neutrons of 8 to 14 MeV in Iron 54 and 56 Isotopes### (S.K. Saraf†, C.E. Brient, P.M. Egun††, S.M. Grimes, S. Long†††, V. Mishra and R.S. Pedroni)

Neutron—induced charged—particle emission cross sections have been measured using a TOF spectrometer. Total emission cross sections for proton and alpha show an enhancement in the low energy region. A two—step compound nuclear reaction mechanism of the type (n,n'p) and (n,n'α) has been investigated. Enhancement in cross sections for low energy protons is due to the fact that in ^{54}Fe the last proton is 4.5 MeV less bound than the last neutron, resulting in many reactions where sub—Coulomb barrier proton decay competes only with gamma decay. In ^{56}Fe the binding energy difference

---

* Work supported by the U.S. Department of Energy and the National Science Foundation.

** Present address: Department of Physics, University of Kentucky, Lexington, KY.

*** Permanent address: Oak Ridge National Laboratory, Oak Ridge, TN.

+ Permanent address: Michigan State University, East Lansing, MI.

++ Permanent address: Niels Bohr Institute, Copenhagen, Denmark.

+++ Permanent address: Indiana University Cyclotron Facility, Bloomington, IN.

Permanent address: Ohio State University, Columbus, OH.

Permanent address: Los Alamos National Laboratory, Los Alamos, NM.

Work supported by the U.S. Department of Energy.

† Present address: Brookhaven National Laboratory, Upton, NY.

†† Present address: Institut für Mittelenergiephysik, Zürich, Switzerland.

††† Summer intern at Ohio University.

1 Published in Nucl. Phys. A480, 285 (1988).

between last proton and neutron is only 1.0 MeV and so the multi–step emission shows up at higher excitation energies than in ^{54}Fe. Calculations have been performed using Hauser–Feshbach model, and level density parameters for residual nuclei have been inferred. Measured data along with the fits of the theory will be presented.

10. Level Densities of ^{57}Co from $^{57}Fe(p,n)^{57}Co$ at $E_p = 5.5, 6.5, 7.5$ and 8.5 MeV and $^{56}Fe(d,n)^{57}Co$ at $E_d = 4, 5, 6, 7, 8$ and 9 MeV* (V. Mishra, C.E. Brient, N. Boukharouba, S.M. Grimes, M. Hoque, R. Pedroni and S.K. Saraf**)

Spectra from $^{57}Fe(p,n)^{57}Co$ and $^{56}Fe(d,n)^{57}Co$ have been measured at $\theta = 0°, 25°, 50°, 75°, 100°, 125°$ and $150°$ at $E_p = 5.5, 6.5, 7.5$ and 8.5 MeV and $E_d = 4, 5, 6, 7, 8$ and 9 MeV, respectively. Level densities in the continuum have been deduced from comparisons with Hauser–Feshbach calculations. These will be compared with information from level counting at low energies and from Ericson fluctuations at high energies.

11. Level Density of ^{57}Co and Reaction Mechanism in $^{56}Fe(d,n)^{57}Co$* (V. Mishra, S.M. Grimes, C.E. Brient, N. Boukharouba, S.K. Saraf** and R.S. Pedroni)

Continuum spectra from $^{56}Fe(d,n)^{57}Co$ have been measured between deuteron energies of 3.5 and 8.1 MeV for a 2 mg/cm^2 thick target. Relative contributions of compound nuclear and direct interaction mechanisms in the obtained cross sections will be deduced from fits with the Hauser–Feshbach formalism by fitting $^{57}Fe(p,n)^{57}Co$ data and the level density of ^{57}Co, thus obtained, has previously been compared with other sources.

12. Continuum Measurements for the Reaction $^{56}Fe(\alpha,n)^{59}Ni$ at $E_p = 9$, 11 and 13 MeV* (R.S. Pedroni, C.E. Brient, N. Boukharouba, S.M. Grimes, M. Hoque, V. Mishra and S.K. Saraf**)

As part of an ongoing study of continuum measurements for reactions forming the compound nucleus ^{60}Ni, spectra for the $^{56}Fe(\alpha,n)^{59}Ni$ reaction have been measured at bombarding energies of 9, 11 and 13 MeV. Data for the $^{59}Co(p,n)^{59}Ni$ reaction have already been measured,[1] and future measurements are anticipated for the $^{57}Fe(^3He,n)^{59}Ni$ reaction. The data

---

* Work supported in part by the U.S. Department of Energy.

** Present address: Brookhaven National Laboratory, Upton, NY.

1 R.S. Pedroni, C.E. Brient, P.M. Egun, S.M. Grimes, V. Mishra and S.K. Saraf, Bull. Amer. Phys. Soc. 33, 1048 (1987).

will be compared with Hauser–Feshbach calculations for both resolved states and the continuum in order to deduce level density information. The data were measured using the Ohio University tandem and beam swinger facilities.

13. Analog (p,n) Cross Sections of the Zirconium Isotopes at 18 and 25 MeV*[1] (J.D. Anderson**, R.W. Bauer**, V.R. Brown**, S.M. Grimes, V.A. Madsen***, B.A. Pohl**, C.H. Poppe** and W. Scobel+)

The differential cross sections for the (p,n) reaction to the ground–state analogs of the lightest four stable zirconium isotopes (90, 91, 92 and 94) have been measured at proton energies of 18 and 25 MeV. Integrated cross sections are found to deviate from the expected linear dependence on neutron excess as was previously found for the molybdenum isotopes. The observed dependence is in quantitative agreement with calculations, including inelastic couplings used to explain the molybdenum results. The energy dependence of the zirconium analog cross sections confirms the resonant–type enhancement of the low energy (p,n) excitation function observed previously for the molybdenum isotopes.

14. Pre–Equilibrium Neutron Emission in (p,nx) Reactions with 80–160 MeV Projectiles++[2] (M. Trabandt+++, H.M. Blann**, R. Bonetti#, R.C. Byrd##, C.C. Foster##, S.M. Grimes, B.A. Pohl**, B.R. Remington** and W. Scobel+)

The reactions ^{90}Zr, ^{208}Pb(p,xn) have been studied in the neutron continuum $E_n \geq 20$ MeV and the angular range $0° \leq \theta \leq 145°$ for projectile energies of 80, 120 and 160 MeV. Results are compared to predictions of phenomenological parameterizations, a semi–classical precompound and a quantum statistical multi–step model.

---

* Work supported in part by the U.S. Department of Energy.

** Permanent address: Lawrence Livermore National Laboratory, Livermore, CA.

*** Permanent address: Department of Physics, Oregon State University, Corvallis, OR.

\+ Permanent address: Institut für Experimentalphysik, University of Hamburg, Federal Republic of Germany.

++ Supported by the BMFT (Vorhaben 06HH175) and by the DOE under contract No. W–7405–ENG48.

+++ Permanent address: I. Inst. für Experimentalphysik, University of Hamburg, Federal Republic of Germany.

\# Instituto di Fisica Generale Applicate dell'Università Milano, Italy.

\## Permanent address: Indiana University Cyclotron Facility, Bloomington, IN.

1 Published in Phys. Rev. C38, 1601 (1988).

2 Contribution to the 5th International Conference on Nuclear Reaction Mechanisms (Varenna, 1988).

15. Neutron Emission Cross Sections on ^{184}W at 11.5 MeV and 26.0 MeV and the Neutron–Nucleus Scattering Mechanism* (A. Marcinkowski**, R.W. Finlay, J. Rapaport, P.E. Hodgson*** and M.B. Chadwick***)

Inelastic neutron emission at 11.5 MeV and 26 MeV incident energies has been studied for monoisotopic sample of ^{184}W. Time–of–flight spectra were taken at several angles between 12° and 160° using the beam swinger spectrometer. The data are averaged over 1 MeV energy bins and compared with the quantum–mechanical statistical multi–step calculations.

B. MODEL CALCULATIONS AND ANALYSES

1. A Study of the $^{9}Be(n,2n)$ Reaction Cross Section+ (H.D. Knox)

Techniques developed earlier at this laboratory for using shell model predictions in R–matrix calculations are being used in studies of the $^{9}Be(n,2n)$ reaction. It is assumed that the $^{9}Be(n,2n)$ reaction proceeds through sequential reactions involving either a) inelastic neutron scattering to states in ^{9}Be which subsequently decay by n–emission, b) the $^{9}Be(n,\alpha)$ $^{6}He^* \rightarrow 2n+\alpha$ reaction, or c) $^{9}Be+n$ reactions leading to the production of two ^{5}He (either in the ground or first excited state) which subsequently decay by n–emission. Shell model calculations for the ^{10}Be system have been carried out for $E_x \leq 20$ MeV and spectroscopic factors for the $^{9}Be+n$, $^{9}Be^*+n'$, $^{6}He+\alpha$ and $^{6}He^*+\alpha'$ channels have been obtained. Preliminary R–matrix calculations for $E_n \lesssim 8$ MeV have been carried out. Codes are currently being developed for the calculation of spectroscopic factors for the ^{5}He channels. As these codes are developed, the remaining ^{5}He channels will be added to the R–matrix calculation and the calculation of all relevant cross sections will be extended to $E_n \approx 14$ MeV.

2. Spectral Distribution Calculations of the Level Density of ^{20}Ne+[1] (B. Strohmaier++ and S.M. Grimes)

A recent paper compared moment method and Lanczos method calculations of the level density of ^{20}Ne. The present work extends this comparison to include a new type of Lanczos method expansion. This

---

* Supported in part by the National Science Foundation and the Atomic Energy Agency of Poland.

** Permanent address: Soltan Institute for Nuclear Studies, 00–681 Warszawa, Hoza 69, Poland.

*** Permanent address: Nuclear Physics Laboratory, Oxford, UK.

+ Work supported by the U.S. Department of Energy.

++ Permanent address: Institut für Radiumforschung und Kernphysik, Wien, Austria.

1 Published in Z. Phys. A329, 431 (1988).

expansion procedure shares the advantage of the traditional Lanczos method of a positive definite level density, but unlike the latter, may be used in an essentially infinite basis. Calculations utilizing dsdf and ppdsd bases have been compared with experimental values for the level density, parity ratio and spin cutoff parameters to determine the appropriateness of the input parameters and the model, while calculations in a dsd basis are compared with exact calculated results to test the accuracy of representation provided by the expansion technique.

3. Microscopic DWBA Analysis of Nucleon Scattering from ^{16}O* (S. Mellema**, D. Kadrmas**, R.W. Finlay, M.S. Islam*** and F.S. Dietrich+)

Measurements of inelastic neutron scattering to several low-lying states in ^{16}O at incident energies from 20–26 MeV have been analyzed consistently with existing proton-scattering measurements for these states using a microscopic folding model with an energy- and density-dependent effective interaction. Transition densities were obtained from inelastic electron-scattering measurements, and three different effective interactions were compared. Results for the first three 2^+ states (E_x = 6.917, 9.845 and 11.52 MeV) are in good agreement with the data and demonstrate the sensitivity of the model to the shapes of the transition densities. Results for the 3^- state (E_x = 6.130 MeV), while not agreeing as well with the data, demonstrate possible energy-dependent effects in the model as well as differences between the effective interactions.

4. Evidence for Dispersion Relation Corrections in Inelastic Nucleon Scattering to the 3^- State in ^{208}Pb++[1] (T.S. Cheema+++ and R.W. Finlay)

Inelastic scattering of 5–11 MeV neutrons to the 3_1^- state in ^{208}Pb is reanalyzed in the distorted wave Born approximation using phenomenological potentials and form factors that explicitly reflect the "threshold anomaly" effects observed in the elastic scattering channel. A previously reported energy dependence of the deformation length δ_3 is largely removed by this analysis. We conclude that dispersion corrections to the one-

---

* Work supported in part by a Northwest Area Foundation grant of Research Corporation, by National Science Foundation Grant PHY-8507137, and by the Department of Energy under contract number W-7405-ENG-48.

** Permanent address: Gustavus Adolphus College, St. Peter, MN.

*** Present address: Ohio State University, Columbus, OH.

\+ Address: Lawrence Livermore National Laboratory, Livermore, CA

++ Work supported in part by the National Science Foundation.

+++ Permanent address: Punjab University, Chandigarh, India.

[1] Published in Phys. Rev. C37, 910 (1988).

channel optical potentials are important in the off–diagonal elements of the potential matrix.

5. Neutron–^{90}Zr Mean Field from a Dispersive Optical Model Analysis*[1] (J.P. Delaroche**, Y. Wang*** and J. Rapaport)

Elastic scattering cross sections have been measured for 8, 10 and 24 MeV neutrons incident on ^{90}Zr. These measurements, together with other neutron elastic scattering and total cross sections data available up to 29 MeV, are used in grid searches to obtain an optical model potential which contains a dispersion relation term. This potential is then extrapolated toward negative energies to predict bound single–particle state properties. An overall good description of the data at positive and negative energies is achieved.

6. Nucleon Scattering Analysis from ^{90,92,94}Zr and Isospin Decomposition of Transition Matrix Elements for Low–Lying Collective Transitions*[2] (Y. Wang*** and J. Rapaport)

Simultaneous analysis of neutron and proton inelastic scattering to low–lying collective states in ^{90,92,94}Zr are used to derive an isospin decomposition of the corresponding transition matrix elements. The deduced (M_n/M_p) ratios for the strongest transitions are in sharp disagreement with values derived from Coulomb–nuclear interference observed in 35.4 MeV inelastic α–scattering from even Zr isotopes.

7. Dispersion Correction for the p+^{208}Pb Optical Potential Reconsidered* (R.W. Finlay, J. Wierzbicki+ and R. Das++)

Elastic scattering of protons and neutrons from ^{208}Pb up to ~ 60 MeV is analyzed with attention to energy–dependent geometries and other "anomalies" that might be taken as evidence for a dispersion theory correction to the optical potential at low energy. Emphasis is placed on reliable estimates of the uncertainties in optical model parameters. While the low–energy (4–24 MeV) neutron scattering data do show clear evidence for dispersion effects, no such effects are observed in proton scattering down to the lowest energy (9 MeV) for which precision proton data are available. We conclude that early reports of large dispersion corrections in the p+^{208}Pb potential were not correct. Further conclusions concerning the behavior of the imaginary potential near the Coulomb barrier are presented.

---

* Work supported in part by the National Science Foundation.
** Permanent address: Centre d'Etudes de Bruyères–le–Châtel, P.O. Box 12, 91680 Bruyères–le–Châtel, France.
*** Address: Indiana University Cyclotron Facility, Bloomington, IN.
+ Address: Medical Center, University of Kentucky, Lexington, KY.
++ Present address: University of North Carolina, Chapel Hill, NC.
1 To be published in Phys. Rev. C (1989).
2 Published in Z. Phys. A331, 305 (1988).

8. Unified Shell Model and Optical Model Potential for p+^{208}Pb* (R.W. Finlay, J. Wierzbicki**, R.K. Das*** and F.S. Dietrich+)

Construction of the shell model potential for single quasi-particle states from elastic scattering data and the dispersion connection is considered for ^{208}Pb+p. Following the procedures developed by Mahaux and Sartor, the radial moments of the real potential for $-20 < E_p < 100$ MeV are constructed from a dispersion relationship involving the radial moments of the imaginary potential. Special attention is paid to the uncertainties in the phenomenological input parameters and to the quality and range of the input scattering data. Comparison of the present results with existing analyses of the n+^{208}Pb potential provides a basis for discussion of the Coulomb correction term and the Coulomb barrier effects.

9. The Fermi Energy Anomaly in the Nucleon—Nucleus Potential++[1] (R.W. Finlay)

Careful comparisons of the parameters of the nucleon—nucleus optical potential at low energy ($E < 10$ MeV) with those at higher energies ($E > 20$ MeV) have revealed discrepancies. Commonly used "global optical models" tend to fail in one energy region or the other. Improved agreement with the data can be restored in phenomenological models in which certain geometrical parameters of the model are allowed to depend explicitly on neutron energy. The origin of this effect in the n+^{208}Pb system has been explained in terms of the dispersion correction to the real part of the standard local optical potential. In dispersion theory, the magnitude of this correction is obtained from the energy dependence of the phenomenological imaginary potential. In the present work, we re—examine the phenomenological parameters for n and p on ^{208}Pb. The dispersion theory explanation of the low energy behavior of the neutron potential is supported by the present analysis, but no similar effect is observed for protons in the range of available data ($E_p > 9$ MeV). The present analyses suggest that the Fermi energy anomaly for the p+^{208}Pb potential is located at energies well below the Coulomb barrier.

10. Dispersion Correction for the n+^{209}Bi Mean Field* (R.D. Das***, R.W. Finlay, J. Wierzbicki** and F.S. Dietrich+)

The nucleus ^{209}Bi provides an excellent testing ground for calculation of the dispersion correction to the optical model for spherical

---

* Supported by NSF Grant PHY—8507137 and by DOE Contract Number W—7405—ENG—48.
** Address: Medical Center, University of Kentucky, Lexington, KY.
*** Present address: University of North Carolina, Chapel Hill, NC.
+ Address: Lawrence Livermore National Laboratory, Livermore, CA.
++ Work supported by the National Science Foundation.
1 Published in "Proceedings of the International Conference on Neutron Physics", Kiev, USSR, October 1987, Vol. 1, p. 41.

nuclei. Shape elastic scattering can be confidently extracted from the data down to 1–2 MeV thus allowing a very short extrapolation to negative energies. In the present work, we compare the moment method of Mahaux and Sartor with the "energy–dependent potential model" of Johnson, Horen and Mahaux. Energy dependence of the shape of the real potential is obtained from the analysis and compared with the results of phenomenological Fourier–Bessel analysis of the scattering data.

11. <u>Unified Description of the n+^{209}Bi Mean Field Between 1 MeV and 40 MeV via Dispersion Relations*</u> (R.K. Das**, R.W. Finlay and J.A. Harvey***)

The real part of the central n+^{209}Bi mean field is the sum of a Hartree–Fock component whose radial dependence is assumed to have a Wood–Saxon shape and whose depth is energy dependent plus a dispersive component which is determined from the imaginary part of the optical model potential. Elastic neutron scattering data from 1.5 MeV to 24 MeV, along with total cross section from 1 to 40 MeV, is used for the above analysis. The energy dependence of the geometry of the optical model is also studied.

12. <u>Spin–Isospin Response in Nuclei and Nuclear Structure Implications*[1]</u> (J. Rapaport)

Charge–exchange reactions are used to obtain the spin–isospin response of nuclei. Results are presented of data obtained at intermediate energies which have shown to be very specific to probe the spin response. This is an effect of the free nucleon–nucleon interaction ratio of the spin–transfer and non–spin–transfer channels. Data are presented characterizing the response function in three regions: a) the nuclear region, small energy loss; b) the quasifree peak region, energy loss of 50–150 MeV; and c) the Δ–region with an energy loss of 200–400 MeV. Nuclear structure implications of the data are discussed.

13. <u>Problems in Calculating Parity Ratios for Nuclear Level Densities with the Fermi Gas Model+[2]</u> (S.M. Grimes)

The Fermi gas model is widely used in calculating nuclear level densities. With the use of modern computers, calculations can be made including both pairing and shell effects. Despite these improvements, there are indications that the model fails to properly predict the parity

---

* Work supported by NSF Grant PHY 8507137.
** Present address: University of North Carolina, Chapel Hill, NC.
*** Permanent address: Oak Ridge National Laboratory, Oak Ridge, TN.
+ Work supported by the U.S. Department of Energy.
1 To be published in "Proceeding of Workshop on Nuclear Structure with Medium Energy Probes", Santa Fe, NM, October 12, 1988.
2 Published in Phys. Rev. <u>C38</u>, 2362 (1988).

ratio even in situations where the level density itself is correctly described. A detailed examination of the discrepancies for some specific systems is presented.

14. The Nuclear Shell Model Code CRUNCHER*[1] (D.A. Resler** and S.M. Grimes)

A new nuclear shell model code CRUNCHER, patterned after the code VLADIMIR, has been developed. While CRUNCHER and VLADIMIR employ the techniques of an uncoupled basis and the Lanczos process, improvements in the new code allow it to handle much larger problems than the previous code and to perform them more efficiently. Tests involving a moderately-sized calculation indicate that CRUNCHER running on a SUN 3/260 workstation requires approximately one-half the central processing unit (CPU) time required by VLADIMIR running on a CRAY-1 supercomputer.

C. TECHNIQUES AND FACILITIES

1. A Facility for Measuring Charged Particles Emitted in Neutron-Induced Reactions up to 30 MeV* (R.S. Pedroni, N. Boukharouba, S.M. Grimes, V. Mishra and R.C. Haight***)

A new beam line is being developed at WNR at LAMPF for the measurement of neutron-induced charged-particle reactions. The WNR white neutron source at Target-4 will be used to make simultaneous measurements for neutrons up to 30 MeV. Silicon detector telescopes with 30 micron ΔE-detectors and 1000 micron E-detectors will be used. The first reaction to be studied will be the $^{12}C(n,\alpha)$ reaction. The status of the facility and measurements will be described.

2. Broad Spectrum Neutron Beam (n,p) Studies at LAMPF/WNR+ (D.S. Sorenson++, J.L. Ullmann+++, F.P. Brady++, J.R. Drummond++, X. Aslanoglou, R.C. Haight+++, C. Howell#, N.S.P. King+++, R.W. Finlay, P.W. Lisowski+++, C.L. Morris+++, J. Rapaport, J.L. Romero++ and W. Tornow#)

A facility to study the (n,p) reaction at energies between 50 and 250 MeV has been established at the LAMPF/WNR "Target-4" white neutron

---

* Work supported by the U.S. Department of Energy.
** Address: Lawrence Livermore National Laboratory, Livermore, CA.
*** Permanent address: Los Alamos National Laboratory, Los Alamos, NM.
\+ Supported by the U.S. Department of Energy, U.S. Department of Defense, and the National Science Foundation.
++ Permanent address: University of California, Davis, CA.
+++ Permanent address: Los Alamos National Laboratory, Los Alamos, NM.
\# Permanent address: Duke University, Durham, NC.
1 Published in Computers in Physics 2, 65 (1988).

source. Time–of–flight is used to obtain the neutron beam energy with about 1 MeV resolution. Multiple targets are used to increase the data rate. The detection system includes four x and y multiwire drift chambers, a magnet which deflects protons out of the neutron beam, a 26 cm by 44 cm "wall" of CsI E–detectors and a large–area plastic DE–detector. This arrangement allows simultaneous measurements to be made from 0 to 15 degrees, depending on beam energy. Data from ^{12}C and $^{13}C(n,p)$ will be presented.

3. Longitudinal Linac Beam Focusing for Neutron Time–of–Flight Measurements*[1] (J.B. McClelland**, D.A. Clark**, J.L. Davis**, R.C. Haight**, R.W. Johnson**, N.S.P. King**, G.L. Morgan**, L.J. Rybarcyk**, John Ullmann**, Paul Lisowski**, W.R. Smythe***, D.A. Lind***, C.D. Zafiratos** and Jack Rapaport)

A method is described in which 805 MHz acceleration cavities in the LAMPF LINAC are used to form a nearly isochronous beam of particles for use in high–resolution neutron time–of–flight spectroscopy at energies less than 800 MeV.

---

* Work supported by the U.S. Department of Energy and the National Science Foundation.

** Permanent address: Los Alamos National Laboratory, Los Alamos, NM.

*** Permanent address: University of Colorado, Boulder, CO.

UNIVERSITY OF PENNSYLVANIA

A. INTRODUCTION

The principal thrust of the work deals with the compilation of the information on the energy levels and on the structure of the nuclei with mass numbers A = 5-20. Approximately 1500 papers are published every year on these nuclei.

B. PUBLICATIONS

1. "Energy Levels of Light Nuclei A = 5-10", Nuclear Physics A490 (1988) 1 - 225

2. "Of DHW and the Light Nuclei", Proceedings of the Conference on Interactions and Structures in Nuclei, Sussex, U.K., September 7-9, 1987, published by Adam Hilger (IOP Publishing Ltd.) (1988) p. 181-189

C. ACCEPTED FOR PUBLICATION

"The Light Nuclei: What is Known and What is Not", presented at the Twentieth Masurian School, September 3, 1988, Mikolajki, Poland, and will be published in 1989 by IOP (Adam Hilger)

D. VADE MECUM

In 1981 the AIP Vade Mecum of Physics, edited by Herbert Anderson, was published by the AIP at the time of its Fiftieth Anniversary. During the past year H. H. Barschall (University of Wisconsin) and I have been helping to direct the revision of this volume. The revisions are nearly complete and the Vade Mecum will be republished in 1989.

E. COMMITTEE

Member, Physical Sciences Panel, Associateship Programs, National Academy of Sciences, National Research Council, 1988-

F. WORK IN PROGRESS

We prepared preliminary versions of the reviews on A = 11 (sent out as preprint 4-88 in October 1988) and A = 12 (sent out as preprint 1-89 in February 1989).

F. Ajzenberg-Selove; with
G. C. Marshall

RENSSELAER POLYTECHNIC INSTITUTE

A. NUCLEAR DATA

1. "Measurement of the Neutron-Induced Fission Cross Section of Cm-247, Cf-250 and Es-254" R.C. Block, R.E. Slovacek, Y. Danon and R.W. Hoff (LLNL)

The neutron-induced fission cross section of microgram quantities of Cm-247, Cf-250 and Es-254 will be measured over the neutron energy range 0.1 eV to 80 keV. The Rensselaer Intense Neutron Spectrometer (RINS), a 70-ton lead spectrometer driven by the RPI electron linear accelerator, will be used for these measurements. This will be the first set of fission measurements for Cm-247 and Es-254 over this energy range; Cf-250 will be measured to correct for its presence (from Es-254 alpha and subsequent beta decay) in the Es-254 sample. It is anticipated that in addition to obtaining the fission cross section over this energy range for Cm-247 and Es-254, new resonances will be observed (from which resonance parameters can be extracted) and information be obtained on subthreshold fission. In particular, this will be the first measurement of this type on such a heavy actinide as Es-254 and any results should be both interesting and unique.

2. "Technique for Fission Measurements of Highly Active Actinides" R.C. Block, R.E. Slovacek and R.W. Hoff (LLNL)

RINS (Rensselaer Intense Neutron Spectrometer) is a large lead slowing down time spectrometer coupled to a powerful source of pulsed neutrons that is well suited for fission cross section measurements of highly active actinides over the neutron energy range 0.1 eV to 100 keV. Measurements on microgram quantities of actinides with halflives as short as half a year have been successfully measured with this technique. The RINS method is the only technique available at this time that can make fission measurements on such active nuclei over this energy range. This paper describes the RINS system and the nuclei it is uniquely capable of measuring.

This paper has been accepted for presentation at the Conference on Fifty Years with Nuclear Fission, April 25-28, 1989, National Institute of Standards and Technology, Gaithersburg, MD.

3. "A Multiplicity Detector for Accurate Low-Energy Neutron Capture Measurements" R.C. Block, R.E. Slovacek, P. Marano, J.A. Burke (KAPL), N.J. Drindak (KAPL), F. Feiner (KAPL) and K.W. Seemann (KAPL)

The 16-segment 20-liter NaI multiplicity detector is now located in its permanent position at the 25-m flight station inside a 15-cm-thick lead shield. Multiplicity data have been taken in time of flight and signal-to-background ratios greater than 100:1 have been observed for multiplicities between 2 and 4 in strong resonances in the tens of eV range. For a LINAC run of only a few hours duration, the statistical precision of the net resonance capture signal (summed over all multiplicities) is on the order of 0.5%. We thus conclude that this multiplicity detector has the capability to provide the accuracy required for low energy capture cross sections measurements. An automatic 8-sample computer-controlled sample changer is under construction.

A. NEUTRON PHYSICS

1. Helium Generation Cross Sections for Fusion Applications
(D. W. Kneff and B. M. Oliver)

Neutron-induced helium generation is a major consideration in the development of materials for fusion reactor environments. Rockwell International is engaged in the measurement of helium production in fusion-energy neutron environments and in other neutron environments used for fusion reactor materials testing. Current emphasis is on the measurement of the cross sections of pure elements and separated isotopes for fast (~8-15 MeV) monoenergetic neutrons, and of helium production rates of pure elements irradiated in mixed-spectrum (comparable fast and thermal neutron flux) fission reactors. Most of this work is performed as a collaborative effort with L. R. Greenwood of Argonne National Laboratory (ANL) and is sponsored by the Department of Energy's Office of Fusion Energy. Additional work has been performed in cooperation with Lawrence Livermore National Laboratory (LLNL) and with Los Alamos National Laboratory (LANL).

Current work includes the analysis of several materials irradiated in three experiments using 13.8- to 15-MeV T(d,n) neutrons, and one using ~10-MeV $^{1}H(t,n)$ neutrons. The T(d,n) experiments were performed at the Rotating Target Neutron Source-II (RTNS-II) facility at LLNL. They include one primary-volume high-flux experiment, and two lower-flux irradiations at 75^{o} and 110^{o} angles relative to the neutron source axis. The $^{1}H(t,n)$ irradiation was a joint Rockwell-LANL experiment performed using the LANL tandem Van de Graaff accelerator.

The high-flux T(d,n) analyses include helium concentration measurements for the helium accumulation neutron dosimeters incorporated in the irradiation, and for several platinum-encapsulated samples (for Be, N, O, and Mg cross section determinations). Neutron fluence mapping is in progress using a combination of radiometric and helium accumulation neutron dosimetry. The lower-flux T(d,n) analyses to date include the measurement of several Cu, Al, Mn, and Be samples in a low-background constant temperature furnace. Those analyses established the measurement techniques for the subsequent analysis of the low-flux $^{1}H(t,n)$ samples.

The $^{1}H(t,n)$-irradiated materials were exposed to ~10^{3} times smaller neutron fluences than the RTNS-II high-flux measurements, and thus represent significantly more difficult measurements. Samples of Al, Cu, Mn, and Be have been successfully analyzed to date using the constant temperature furnace, with helium generation concentrations ranging from about 1 to 250 appt (atomic parts per trillion, 10^{-12} atom fraction). These measurements have uncertainties of about 2-5% for concentrations greater than about 5 appt; at the 1-3 appt level (Mn) the uncertainties are considerably greater (10-15%). The analyses provided a demonstration of our ability to perform low-level helium production measurements using monoenergetic neutron sources based on reactions other than T(d,n). Final cross section determinations will require neutron fluence mapping for the irradiation volume, which has not been completed.

Planned future work includes the completion of the neutron fluence mapping for the various experiments, and the completion of the helium generation analyses for several materials. This will provide initial total helium production cross sections for ~10-MeV neutrons, and a number of new cross sections in the 14- to 15-MeV neutron energy region. The latter will include N, Mg, S, Ge, and W. The planned future work also includes a joint experiment with D. L. Smith and L. R. Greenwood of ANL to determine the $^{9}Be(n,2n)^{8}Be \rightarrow 2\alpha$ cross section by measuring the total helium production. Characterization of the unirradiated beryllium sample material has been initiated.

A. INTRODUCTORY COMMENT

The report for nuclear data activities given here has been excerpted from the annual progress report of the laboratory (TUNL XXVII) by R. L. Walter. Significant additional details, such as experimental methods, references, and graphs of the data and calculations can be found there. Alternatively, additional information can be obtained by contacting the first author for each project.

B. NUCLEAR SYSTEMS WITH A ≤ 6

1. Neutron-Deuteron Elastic Analyzing Powers below 10 MeV (C. R. Howell, W. Tornow, R. L. Walter, P. D. Felsher, M. Al Ohali, Z. P. Chen, J. M. Hanly, G. Mertens*, I. Slaus)

Recently the first results of rigorous Faddeev three-nucleon n-d continuum calculations using meson based two-nucleon interactions became available.[1] In these calculations all partial-wave components of the Paris and the new Bonn (OBEPQ) potential with two-body total angular momenta $j \leq 3$ are included. Definite discrepancies between these calculations and our elastic n-d analyzing power $A_y(\theta)$ data at 10, 12 and 14.1 MeV are found in the region of the maximum of $A_y(\theta)$. For instance, our data at 10 MeV is about 25% higher than a Paris potential calculation. The Bonn OBEPQ potential prediction is even lower than the Paris potential prediction due to its larger $^3P_0$ phase shift. It seems that the discrepancy between data and calculation cannot be explained in the framework of the Paris and Bonn nonrelativistic meson based two-nucleon forces. In order to increase the energy range of these studies and to reduce the influence of higher partial waves, we extended our elastic n-d $A_y(\theta)$ measurements to 5.0, 6.5 and 8.0 MeV. Our data are presently being corrected for finite-geometry, multiple-scattering and other small instrumental effects.

2. Studies of $^2H(n,np)n$ Scattering Using Polarized Neutron Beams (C. R. Howell, T. Cornelius+, P. D. Felsher, W. Glöckle+, I. Slaus, W. Tornow, R. L. Walter, H. Witala+)

Recent advances on the theoretical front of the three-nucleon (3N) problem have placed new demands on both the accuracy and variety of 3N data needed to examine the on-energy-shell and off-energy-shell behavior of

---

*Physikalisches Institut, Universität Tübingen, FRG

[1] H. Witala, W. Glöckle and T. Cornelius, Suppl. to Few Body Systems 2 (1987) 555 , and H. Witala, private communication.

+ Ruhr-Universität Bochum, FRG

potential models. It has been demonstrated that polarization observables for neutron-deuteron (n-d) scattering stringently test the nucleon-nucleon (N-N) potentials used in 3N calculations. It has also been suggested that such data might be sensitive to 3N force effects.

Measurements of the vector analyzing power $A_y(\theta)$ for the $^2H(\vec{n},n_1p_2)n_3$ breakup reaction were performed with an incident neutron energy of 12 MeV. Detailed comparisons between the data for elastic scattering and exact 3N calculations, which used separable equivalents to the meson-exchange-based Paris and Bonn potentials, reveal new information about the sensitivity of the data and calculations to the triplet P-wave N-N interactions. The data are providing benchmarks for future 3N calculations. We have recently reported some of the above comparisons.[2]

3. Nuclear Data Compilations for A = 3 and 4 (D. R. Tilley, H. R. Weller, H. Hasan)

The compilation of data on the A = 3 system was published in Nuclear Physics A474 (1987) 1. The previous compilation on A = 4 was carried out by Fiarman and Meyerhof in 1973. At the request of the National Nuclear Data Center, work on a data compilation for the A = 4 system was begun in spring 1988 and is expected to extend over about two years.

4. $^2H(d,\gamma)^4He$ Reaction at Low Energies (H. R. Weller, D. R. Tilley, J. L. Langenbrunner, M. Balbes, L. Kramer, G. Feldman, J. R. Riley, R. M. Whitton, J. Z. Williams)

The sensitivity of the $^2H(d,\gamma)^4He$ reaction to the D-state of ^4He was first demonstrated by TUNL measurements of the tensor analyzing power at E_d = 10 MeV. Since the reaction is dominated by E2 radiation at this energy, the tensor analyzing power arises from d-wave capture (S=0) leading to the L=S=0 component of the 0+ ^4He ground state interfering with s-, d- and g-wave capture (S=2) leading to the L=S=2 ground-state component (the D-state). The presence of s-wave capture implied that the effects of the D-state of ^4He could be more readily observed at lower deuteron beam energies, since the angular momentum barrier should suppress the d-wave capture to the S-state relative to the s-wave capture to the D-state. We are completing our analysis of the $^2H(\mathbf{d},\gamma)^4He$ reaction with tandem beam energies. Data were obtained for $\sigma(\theta)$ at $\langle E_d \rangle$=0.4, 1.2, 2.3, 9.7 and 14.7 MeV ($\langle E_d \rangle$ is the center-of-target energy). Our results for absolute cross section agree well with previous results. Angular distributions of the tensor and vector analyzing powers $A_{yy}(\theta)$, and $A_y(\theta)$ were obtained at 0.4, 1.2, 9.7 and 14.7 MeV and as a function of energy with $\theta_{lab}=130^\circ$ from 0.4 to 14.7 MeV.

Our study of these observables has interesting implications. The symmetrical nature of two-deuteron capture implies that $\Delta S=0$ isovector E1 transitions are forbidden and that isoscalar M1 transitions are inhibited. $\Delta S=0$, E2 capture strength is expected to dominate. The interference of capture

---

[2] C. R. Howell et al., Phys. Rev. Lett. 61 (1988) 1565

amplitudes with channel spin S=0 and S=2 can show a signature of the D-state component in the ground state of ^4He. The tensor analyzing powers $A_{yy}(\theta)$ and $T_{20}(\theta)$ are sensitive to this interference. However, the vector analyzing power $A_y(\theta)$ is mainly sensitive to interference between amplitudes with S=1 and S=0, which indicates the presence of isoscalar spin-flip ($\Delta S=1$) E1 strength and/or M2 strength (both involve p-wave capture). This is interesting, as these multipoles are generally buried by the dominant transition strengths; but near E_d=1.2 MeV, these spin-flip terms (E1 and M2) could account for more than 50% of the capture strength compared to the E2 strength.

These data seem to indicate that the character of the reaction changes over this energy range. At 9.7 and 14.7 MeV, the data are consistent with dominance of the E2 multipole with very little E1 and M2 strength. At lower energies the magnitude of the vector analyzing power $A_y(E)$ shows a strong energy dependence peaked near 2.5 MeV with a width on the order of 2 MeV. This region is affected by the onset of p-wave capture and the presence of p-wave resonances (both 1^- and 2^-).

5. Analyzing Powers of the $\vec{d}$+d→d+p+n Breakup Reaction (C. R. Howell, R. L. Walter, W. Tornow, M. Al Ohali, P. D. Felsher, J. M. Hanly, J. M. Lambert*, M. L. Roberts, I. Slaus, P. A. Treado*, G. Weisel)

Continual advances in parameter-free four-nucleon (4N) calculations make the d+d→d+p+n breakup reaction a good starting place for studying 4N unbound systems. From a theoretical perspective, the deuteron-neutron (d-n) and deuteron-proton (d-p) quasi-free scattering (QFS) processes are the most convenient 4N breakup reactions to investigate for two reasons. First, these processes are essentially free of contamination from final-state interactions (FSI). The formation of the neutron-proton (n-p) FSI in the $^1S_0$ state is isospin forbidden, and the $^3S_1$ n-p FSI has a very low and structureless formation cross section as a function of relative nuclear momentum. Second, since the deuteron-nucleon (d-N) QFS processes are three-body breakup reactions, the data for these processes should resemble, within the validity of the impulse approximation, that for d-N elastic scattering.

Measurements of the vector and tensor analyzing powers A_y, A_{yy}, and A_{zz} have been made at 12 MeV for the d+d→d+p+n breakup reaction at angle pairs suitable for observing d-n and d-p QFS. Each two dimension spectrum was projected onto the kinematically allowed locus. Since 4N calculations are not yet available, the data are compared to 3N calculations for d-n elastic scattering. The d-n QFS data substantially differ from the calculations for d-n elastic scattering. These differences probably indicate that the contributions from multiple-scattering terms in this 4N scattering process are large at this low energy. A complete analysis of the present data is underway and more measurements of d-p QFS are being planned at angles compatible with the d-n QFS data.

---

* Georgetown University, Washington, DC

6. Radiative Capture of Tensor- and Vector-Polarized Deuterons by ^3H at 250 keV (H.R. Weller, D.R. Tilley, J.C. Riley)

The radiative capture of polarized deuterons by tritium at 8.6 MeV and on the $3/2^+$ "fusion" resonance at E_d(lab)=107 keV has been measured. For the measurement at $\langle E_d \rangle$ = 250 keV, we expected only S-wave capture and thus an isotropic angular distribution of cross section and $A_y(\theta)$ = 0.0. We have measured an unpolarized angular distribution which was found to be isotropic to within 0.6%, and angular distributions of $A_{yy}(\theta)$ and $A_y(\theta)$. The A_y is consistent with zero at all angles, as predicted; however, A_{yy} indicates the presence of S=1/2. A simultaneous fit to the unpolarized cross section, $A_{yy}(\theta)$, and $A_y(\theta)$ yields a 5.5% admixture of S=1/2 in the d-T capture cross-section of ^5He and a relative phase of 180 degrees between $^2S_2$ and $^4S_4$ transition matrix elements. This is in contrast to the previous analysis of the $^3H(d,n)^4He$ cross-section data which indicates that essentially no S=1/2 background was present in the energy region below 250 keV. Comparison of the present results and R-matrix calculations is underway.

7. Ground State Widths of ^5Li and ^5He (H. R. Weller, D. R. Tilley, M. J. Balbes, G. Feldman, L. H. Kramer, J. L. Langenbrunner, J. C. Riley, R. M. Whitton, J. Z. Williams)

The ground states of ^5Li and ^5He are unbound to particle decay. We have measured their ground-state widths using the $^3He(d,\gamma)^5Li$ and $^3H(d,\gamma)^5He$ reactions, respectively. Our measured values are $\Gamma_{^5Li}$ = 1.6 ± 0.2 MeV and $\Gamma_{^5He} \approx$ 0.6 MeV. The previously obtained values were $\Gamma_{^5Li} \approx$ 1.5 MeV and $\Gamma_{^5He}$ = 0.60 ± 0.02 MeV. We hope to improve our preliminary value for $\Gamma_{^5He}$ to an accuracy on par with or better than this value.

The data were fitted using the spectrum fitting routine MULCCFIT, which allows the convolution of a Breit-Wigner resonance (including energy-dependent width effects) with the measured lineshape of the NaI detectors. The Breit-Wigner resonance width was varied to give the best χ^2 fit to the data. We are presently using a direct-capture cluster model in order to better understand the relative values of these widths.

C. REACTIONS FOR A ≥ 6

1. Microscopic Folding Model of the Nucleon-Nucleus Interaction (R. L. Walter, L. F. Hansen*, F. S. Dietrich*)

New constraints are placed on microscopic folding models when the requirement to fit analyzing power data is also applied. During the last few years polarized-beam measurements by the neutron group at TUNL have provided a large body of analyzing power $A_y(\theta)$ data for (n,n) scattering for

* Lawrence Livermore National Laboratory

nuclei ranging from ^{6}Li to ^{209}Bi in the energy range from 6 to 17 MeV. We have initiated a project at LLNL to investigate the accuracy with which microscopic folding models can describe the new $A_y(\theta)$, along with $\sigma(\theta)$ and σ_T data for neutrons, and $\sigma(\theta)$ and $A_y(\theta)$ data for (p,p) scattering. Calculations are underway for nucleon-nucleus scattering for about ten nuclei from A = 6 to A = 208. A status report was given at the Santa Fe meeting of the Nuclear Physics Division. The calculations use the JLM effective interaction[3] based on the Reid hard-core interaction and the YNM effective interaction[4] based on the Hamada-Johnson interaction. In fitting the data the strengths of the real, imaginary, and real spin-orbit potentials have been allowed to vary. The dependences upon A and E_n for these three normalizing constants are being investigated to obtain systematic trends, so that the weaknesses in the models and ranges of applicability may be recognized.

2. Scattering of Polarized and Unpolarized Nucleons from ^{28}Si (C. R. Howell, R. C. Byrd*, R. S. Pedroni**, R. L. Walter)

As reported last year, measurements of differential cross sections $\sigma(\theta)$ and analyzing powers $A_y(\theta)$ have been made at TUNL for ^{28}Si(n,n_0) and ^{28}Si(n,n_1) for incident neutron energies between 8 and 17 MeV. These data were combined with $\sigma(\theta)$ and total cross section σ_T data from other laboratories to form the most complete data set for neutron scattering from ^{28}Si over the 8- to 40-MeV energy range. The data have been described within the framework of a symmetric rotational model using the coupled-channels method. Values for the quadrupole and hexadecapole nuclear moments were extracted. The systematic analysis of the $A_y(\theta)$ data enabled the determination of the deformation length for the spin-orbit potential. Comparisons between neutron- and proton-scattering data and calculations were made to test the sensitivity of this type of data to charge symmetry breaking (CSB) in the nuclear force and to investigate the isospin dependence of the absorptive part of the nucleon-nucleus scattering potential for ^{28}Si. The results of these comparisons strongly suggest that the observed differences between ^{28}Si+n and ^{28}Si+p scattering can be accounted for without introducing CSB. This comparison was recently reported.[5] A detailed analysis concentrating on the differences in the imaginary potentials for neutron and proton scattering from ^{28}Si is continuing. A similar study is underway using ^{32}S + nucleon scattering data over the 8- to 40-MeV energy range.

---

[3] J. P. Jeukenne, A. Lejeune and C. Mahaux, Phys. Rev. C16 (1977) 80

[4] N. Yamaguchi, S. Nagata and T. Matsuda, Prog. Theor. Phys. (Japan) 70 (1983) 459

* Los Alamos National Laboratory, Phys. Div., Los Alamos, NM

** Present addess: Physics Department, Ohio University, Athens, OH

[5] C. R. Howell et al., Phys. Rev. C38 (1988) 1552

3. Description of the p-^{40}Ca Nuclear Mean Field Using Dispersion Relations (W. Tornow, Z. P. Chen, J. P. Delaroche)

As shown recently,[6] the Coulomb correction term ΔV_C to the optical model real central potential consists of energy dependent volume and surface components. This new result, obtained from the dispersion relation between the real and imaginary parts of the mean field, is expected to modify estimates on the upper limit of charge-symmetry breaking effects in the nucleon-nucleus interaction.[7]

In order to study Coulomb correction and possible charge-symmetry-breaking effects in the nucleon-^{40}Ca interaction in the framework of the dispersion relation, we derived the p-^{40}Ca complex mean field from a dispersive optical model analysis of experimental cross-section and analyzing-power data. To correctly describe the experimental bound-state energies, a linear rather than an exponential energy dependence was required for the Hartree-Fock component of the real term of the optical potential for energies below ε_F. This feature reflects the nonlocality of the microscopic Hartree-Fock field. Presently we are concentrating on a similar analysis for the n-^{40}Ca system. The comparison of both results is expected to give accurate information on Coulomb correction terms and better estimates of possible charge-symmetry-breaking effects.

4. Energy Dependence of Optical Potential Geometry for n+^{54}Fe Scattering (C. R. Howell, J. P. Delaroche, R. L. Walter)

There is evidence that the geometry parameters of the optical potential for neutron-nucleus scattering at low energies are energy dependent. This energy dependence was noted by Mahaux and Sartor[8] as the signature of the dispersion relationship between the real and imaginary parts of the potential. In light of these findings, we are extending our previous analysis of neutron scattering from ^{54}Fe, which covered the energy range from 8 to 80 MeV, down to 0.5 MeV. The new analysis was divided into two energy intervals. The upper energy interval of the analysis extends from 20 to 80 MeV and all these data could be described well using a SOM with the energy independent geometry of Pedroni et al.[9] The resulting potential strengths varied smoothly with energy.

From 0.5 to 20 MeV good descriptions of the $\sigma(\theta)$ and $A_y(\theta)$ data can be achieved by using the fixed geometry parameters, but fits to the σ_T data

---

[6] W. Tornow and J. P. Delaroche, Phys. Lett. B210 (1988) 26

[7] J. S. Winfield et al., Phys. Rev. C33 (1986) 1

[8] C. Mahaux and R. Sartor, Phys. Rev. C34 (1986) 2119

[9] R. S. Pedroni, Ph.D. dissertation, Duke University (1986); see also Phys. Rev. C38 (1988) 2052

require an energy dependent radius for the real potential. The radius varies smoothly with energy, indicating the need to apply dispersive corrections to the real part of the scattering potential. The SOM calculations will be corrected for compound nucleus (CN) formation at energies less than 10 MeV. A more detailed analysis, which includes dispersion correction terms, is planned.

5. Deformed Optical Potential for Neutron Scattering from ^{54}Fe and ^{58}Ni
(R. L. Walter, R. S. Pedroni*, R. C. Byrd**, J. P. Delaroche+, G. M. Honoré, C. R. Howell, H. G. Pfützner)

A paper describing the re-analysis of elastic and inelastic neutron scattering from ^{54}Fe and ^{58}Ni was published.[10] This coupled channels analysis extends from 10 keV (strength functions) up to the 30- to 80-MeV region, where only total cross section data are available. New $A_y(\theta)$ obtained at TUNL at 17 MeV are included in this analysis. The surface and volume parts of the absorptive potential are allowed to take on complicated but meaningful energy dependences. Good agreement with the data was obtained with a deformed potential obtained through fitting with a vibrational model in the coupled-channels formalism.

6. Coupled-Channels Analysis of Nucleon Scattering from ^{116}Sn and ^{120}Sn
(R. L. Walter, P. P. Guss++, R. C. Byrd**, J. P. Delaroche, C. R. Howell, R. S. Pedroni*, G. Tungate+++)

The isospin dependences of potential and deformation parameters for medium-mass nuclei are of long-term interest. We have submitted to Phys. Rev. C a report that describes a coupled-channels analysis of neutron and proton scattering from ^{116}Sn and ^{120}Sn. The calculations, which use the formalism for vibrational nuclei, were made for scattering to the 0^+, 2^+ and 3^- states of the Sn isotopes. Cross-section and analyzing-power data obtained at TUNL, as well as total cross-section data from 10 keV to 80 MeV, were fit with a deformed potential that has the customary energy-dependent surface and volume components of the absorption term. Deformation parameters obtained from fitting (n,n') are compared to those from (p,p) and

---

* Present address: Dept. of Physics, Ohio University, Athens, OH

** Present address: Physics Division, Los Alamos National Laboratory, Los Alamos, NM

+ Centre d'Études de Bruyères-le-Châtel, France

10 R. Pedroni et al., Phys. Rev. C38 (1988) 2052

++ Present address: E.G.&G. Energy Measurements, Andrews AFB, Washington, DC

+++ Present address: Dept. of Physics, University of Birmingham, Birmingham, England to the core polarization model predictions of Brown and Madsen.[11] The potentials derived were able to describe the (n,n) and the (p,p) data quite adequately when customary magnitudes were used for the real and imaginary components of the isovector potential. The s-wave strength functions and the potential radii for E_n = 10 keV, which were reported in the BNL compilation, were also well described by our model.

7. Nature of the Neutron-Nucleus Interaction for ^{208}Pb (R. L. Walter, W. Tornow, C. R. Howell, M. L. Roberts, P. D. Felsher, D. J. Horen*)

Recently completed measurements at TUNL for the ^{208}Pb(n,n)^{208}Pb differential cross section at 8 MeV and analyzing power at 6, 7, 8, 9, and 10 MeV should allow a critical assessment of recently published "unified" or "systematic" n+^{208}Pb models.[12,13]

Our data have been combined with previous TUNL cross-section and analyzing-power data, as well as cross-section data measured at Ohio University and Michigan State University, to obtain a detailed and high-accuracy data set for neutron elastic scattering from ^{208}Pb from 4 to 40 MeV. Optical model fits have been performed with both constant geometry and energy-dependent geometry. In both cases, while the average fits were quite good, no optical model solution based on conventional Woods-Saxon form factors was found that could perfectly describe all of the details seen in the data. To relax the constraint of a Woods-Saxon form factor, each term in the optical potential was modified using a Fourier-Bessel expansion. Successful fits could be obtained by expanding the real central part of optical potential and letting all other terms in the potential retain their Woods-Saxon shapes. Unfortunately, the Fourier-Bessel solution is not unique and the shape obtained for the real central potential depends upon the number of terms used in the Fourier-Bessel expansion and a geometrical Fourier-Bessel cutoff radius.

Currently, we are modifying our optical model to include contributions from dispersion relations connecting the real and imaginary parts of the optical potential. This method allows us to extrapolate the potential to negative energies to compare to single-particle bound-state energies.

8. Interaction of 6- to 24-MeV Neutrons with ^{209}Bi (C. R. Howell, W. Tornow, R. L. Walter, G. Weisel, M. Al Ohali, Z. M. Chen, P. D. Felsher, J. M. Hanly, M. L. Roberts)

In order to test the nucleon-nucleus models and CN calculations for ^{208}Pb and ^{209}Bi, we are also investigating neutron scattering from ^{209}Bi.

---

[11] V. R. Brown and V. A. Madsen, Phys. Rev. C11 (1975) 1298; V. A. Madsen, V. R. Brown and J. D. Anderson, Phys. Rev. C12 (1975) 1205

* Oak Ridge National Laboratory, Oak Ridge, TN

[12] C. H. Johnson, D. J. Horen, and C, Mahaux, Phys. Rev. C36 (1987) 2252

[13] J.R.M. Annand, R.W. Finlay, and F.S. Dietrich, Nucl. Phys. A443 (1984) 249

It is known that above 8 MeV $\sigma(\theta)$ for n+^{208}Pb and n+^{209}Bi are nearly identical. Our aim is to make comparisons below 8 MeV where differences are evident in $\sigma(\theta)$ for these two nuclei. For n+^{209}Bi the level density is greater than for the ^{208}Pb case, so the CN elastic scattering contribution is appreciably reduced on an absolute scale. We have performed high accuracy $A_y(\theta)$ measurements at 6 and 9 MeV to complement the same measurements for ^{208}Pb. Values for $\sigma(\theta)$ are available from experiments of Annand et al.[13] The CN calculations are to be made using the code OPSTAT obtained from R. Finlay. Preliminary spherical optical model (SOM) fits with Woods-Saxon form factors are being pursued to obtain starting parameters for successive SOM calculations that will include either the Fourier-Bessel expansion method or the dispersion relation.

9. Measurements of A(n,p) Reaction Cross Sections at Intermediate Energies (C. R. Howell, W. Tornow, X. Aslanoglou*, F. P. Brady**, J. R. Drummond**, R. W. Finlay*, R. C. Haight+, N. S. P. King+, P. W. Lisowski+, C. L. Morris+, J. Rapaport*, J. L. Romero**, D. S. Sorenson**, J. L. Ullmann+)

A collaboration is measuring A(n,z) charge-exchange reaction cross sections near 0°. The measurements use the continuous energy neutron beam of the LAMPF/WNR facility. The initial experiments will concentrate on the A(n,p) reaction and are planned to span an incident neutron energy range from 50 to 250 MeV for reaction angles between 0° and 15° in the lab system. Much of the scientific motivation for this project stems from our lack of understanding about the nature of the isoscalar and isovector parts of the nucleon-nucleus interaction.[14] The first measurements of the ^{12}C and ^{13}C(n,p) reactions were conducted in early autumn.

10. Spin-Spin Dependence of Total Cross Sections and Static Nuclear Deformation (C. R. Gould, N. R. Roberson, W. J. Thompson)

Hnizdo and Kemper[15] recently investigated the effect of static deformation of polarized target nuclei on total cross sections for polarized neutrons. They showed that coupling through the spin-orbit interaction leads to transfer of orbital angular momentum in elastic scattering if the

---

[13] J.R.M. Annand, R.W. Finlay, and F.S. Dietrich, Nucl. Phys. A443 (1984) 249

* Physics Department, Ohio University, Athens, OH

** Physics Department, University of California, Davis, CA

\+ Los Alamos National Laboratory, Los Alamos, NM

[14] C. Gaarde, J. S. Larsen and J. Rapaport, *Spin Excitations in Nuclei*, ed. F. Petrovich et al. (Plenum Press, New York, 1984) p. 65

[15] V. Hnizdo and K. W. Kemper, Phys. Rev. Lett. 59, (1987) 1892

polarized target nucleus is deformed and has spin I > 1/2. This quadrupole reorientation (QR) effect gives rise to a spin-spin cross section, σ_{SS}, and they stated that QR alone, without any spin-spin potentials, leads to differences in n_{pol} + $^{27}Al_{pol}$ total cross sections having the magnitudes observed by us.[16] We recently pointed out[17] that it does not account for the spin-spin dependence we observed in the TUNL polarized target, polarized beam measurements, and is also not as large as they estimated.

11. Neutron-Induced Photon Production Cross Sections (C. R. Gould, G. E. Mitchell, S. A. Wender*, P. K. Ramakrishnan, G. F. Auchampaugh*, R. C. Little*)

Neutron-induced photon production cross sections and the spectra of the secondary gamma rays are needed in a variety of applications. Recently, intense beams of neutrons have become available at WNR, the white neutron source at the Los Alamos Meson Physics Facility. This source has excellent characteristics for γ-ray production cross section studies. Measurements were made using an array of five bismuth germanate (BGO) detectors. The good detection efficiency of BGO at high γ-ray energy, combined with the ability to measure complete angular distributions, provides a unique capability for performing neutron-induced γ-ray production cross section measurements. The energy dependence of the spectral shapes and of the angular distributions can be used to infer changes in the dominant reaction channel.

Our first continuum gamma-ray production measurements were performed for ^{181}Ta and ^{9}Be. The Be data were used to simulate the background. The Ta(n,xγ) cross section (integrated over γ-ray energy) was obtained from E_n = 2 to 100 MeV. The cross section agrees qualitatively with earlier data below E_n = 20 MeV and seems to increase slowly with energy above 20 MeV. The angular distributions are approximately isotropic at all neutron energies. The photon cross section for various γ-ray energy ranges shows much more energy dependence, but the angular distributions are still approximately isotropic.

D. INSTRUMENTATION AND FACILITY IMPROVEMENTS

1. Installation of a New NaI Gamma Ray Detector (H. R. Weller, D. R. Tilley, M. Balbes, G. Feldman, L. H. Kramer, J. L. Langenbrunner, J. C. Riley, R. M. Whitton, J. Z. Williams)

A new Bicron 10" x 10" NaI(Tl) detector was installed this year. The detector it replaced consisted of two 5"-long segments which had partially separated, giving a distorted lineshape response. The new crystal

---

[16] C. R. Gould et al., Phys. Rev. Lett. 57 (1986) 2371

[17] C. R. Gould, N. R. Roberson and W. J. Thompson, Phys. Rev. Lett. 60 (1988) 2335

* Los Alamos National Laboratory

is viewed by seven 3" Hamamatsu R1911 phototubes arranged with six tubes surrounding a central tube on the detector axis. The gain of the detector and associated electronics is stabilized by an LED pulser feedback system. The response of the detector to γ rays is $(3.0 \pm 0.2)\%$.

2. Neutron Detector Efficiency Calibration (R. L. Walter, C. R. Howell, W. Tornow, J. Hanly, A. Aksoy*, M. Al Ohali, Z. P. Chen, A. Coban*, G. Dietze**, P. D. Felsher, R. Setze, G. Weisel)

A project to determine the efficiency $\varepsilon(E_n)$ of several sizes and types of organic scintillators has been undertaken for the neutron energy range 2 MeV $< E_n <$ 17 MeV. The measurements use the calibrated neutron source reaction $^2H(d,n)^3He$ at $\theta = 0^\circ$ for 5 MeV $< E_n <$ 18 MeV and at $0^\circ < \theta < 120^\circ$ for 2 MeV $< E_n <$ 9 MeV, using E_d = 6 MeV for the latter. Data have been obtained for a 12.5-cm diameter, 5-cm thick scintillator manufactured by Nuclear Enterprises (NE). The $\varepsilon(E_n)$ was obtained in fine steps (50- to 100-keV) in order to explore the effect of the presence of ^{12}C in the scintillator and local enhancements to the efficiency caused by n-^{12}C resonances. Additional preliminary data were obtained for a 25-cm diameter NE detector and a 12.5-cm diameter Bicron detector. The data are stored in event-by-event format on magnetic tape so that a map of $\varepsilon(E_n)$ as a function of detector bias energy could be obtained. Five bias settings are fixed in the on-line data collection.

3. Low Energy Beam Accelerator Facility (E. J.Ludwig, K. Fletcher)

The installation of the new atomic beam polarized ion source at TUNL provides opportunities for experiments at low energies. The new source is being installed such that beam may be directed into the Tandem Van de Graaff accelerator for the higher energy experiments, or directly out of the source to low energy experimental stations with no additional acceleration. The latter setup will permit investigations of polarization phenomena with a 30 to 150 keV beam and currents on the order of 100 µA. A collaborative investigation with T. R. Donoghue (University of Pittsburgh) to study the D(d,p) and D(d,n) tensor analyzing powers, utilizing a supersonic deuterium gas jet target is being designed.

---

* Dept. of Physics, King Fahd University of Petroleum and Minerals, Dhahran, Saudi Arabia

** Physikalisch-Technische Bundesanstalt, Braunschweig, FRG